Decision Support System for Floodwater Spreading Site Selection in Iran

Mirmasoud Kheirkhah Zarkesh

Promotor:

Prof. Dr. Ir. L. Stroosnijder
Professor of Erosion and Soil & Water Conservation

Co-promotors:

Prof. Dr. A.M.J. Meijerink
Professor in Water Resources Surveys and Watershed Management, ITC, Enschede

Dr. M.A. Sharifi
Associated Professor in Urban and Regional Planning and Geo-Information Management, ITC, Enschede

Examining committee:

Prof. Dr. A. Stein (Wageningen Universiteit)

Dr. Ir. E. Seyhan (Vrije Universiteit Amsterdam)

Dr. Ir. C.M.M. Mannaerts (ITC, Enschede)

Dr. B. Saghafian (Soil Conservation & Watershed Management Research Institute (SCWMRI), Tehran, Iran)

This research was carried out within the C.T. de Wit research school PE & RC

Decision Support System for Floodwater Spreading Site Selection in Iran

Mirmasoud Kheirkhah Zarkesh

Thesis
To fulfil the requirements for the degree of Doctor on the authority
of the rector magnificus of Wageningen University,
Prof. Dr. Ir. L. Speelman,
to be publicly defended on Thursday 26 May 2005 at 15:00 hours
in the auditorium of ITC, Enschede

ISBN: 90-8504-256-9
ITC Dissertation Number: 122
International Institute for Geo-information Science & Earth Observation,
Enschede, The Netherlands

To my Parents

Table of Contents

ACKNOWLEDGMENTS

Thanks to the Merciful God Who Brought Me to This Stage

The work reported in this thesis was made possible in the present shape with the support and contribution from many organizations and individuals to whom I feel indebted and wish to express my gratitude.

I would like to express my profound gratitude to Soil Conservation and Watershed Management Research Institute (SCWMRI) for permitting me leave to study and to ITC through the Water Resources Survey (WRS) department for the PhD fellowship.

I gratefully acknowledge my gratitude to my university promoter, Prof. Leo Stroosnijder and thank him for his inspiring guidance and valuable support especially during the last year of the research period. I appreciate him for his critical reading and comments on the drafts of different chapters and the adjusting his schedule.

I would like to pay my kind regards to my ITC promoter Prof. Allard M.J. Meijerink. My dream for further study could never come true if he did not kindly accept to supervise me. His never-ending support, excellent guidance and outstanding advice accompanied me through the whole period of my Ph.D. research as well as my MSc. I heartedly appreciate his professional view on research issues, critical comments, intellectual opinion, and the way he put them in simple and straightforward argument and suggestion. He was always there to help me. What I learned from him was far beyond my imagination and for that, I greatly owe him. I feel proud of the honour I got of working under the guidance of Prof. Meijerink. Unfortunately, words fall short when I try to reciprocate honestly to all that he has done for me. I respectfully acknowledge the scientific and moral support received from you and the most importantly for being a great teacher, friend and guide for me. I would like also to thank your wife for helping me to translate the English summary of the thesis to Dutch language.

I am also gratefully indebted to my second ITC promoter Dr. M.A. Sharifi for his invaluable contribution, support, guidance and encouragement through the duration of this work, but I would especially like to thank him for being such a great friend. I gained a lot from him while working under his supervision. I owe a great debt to Dr. Sharifi for his keen interest in the subject, for his unfailing willingness to discuss and constructively criticise my effort, for his persistence in exhorting me to make a quality work. Dr. Sharifi, words are not enough to express my gratitude to you. I also acknowledge the endless hospitality and brotherhood extended by Dr. Sharifi and his wife to me and my family. Thanks a lot.

Thanks are due to Prof. Dr. A. Stein, Dr. Ir. E. Seyhan, Dr. Ir. C.M.M. Mannaerts and Dr. B. Saghafian who honoured me by accepting to be in my graduation committee.

My very special thanks go to Dr. Aminipouri, Dr. Shoaei, Prof. Dr. Kowsar, Mr. Amanpoor, Dr. Telvari, Dr. Rajabbigi, Mr. Vahabi, Dr. Abbasi, Dr. Nikkami, Dr. Ghayoumian, Dr. Rahmati, Dr. Piri, Mr. Sanjani, Mr. Aghtoman, Mr. Bandarabadi, Mr.

Lotfollahzadeh Mr. Hassanzadeh, Mr. Karami and Mr. Noorozi for their invaluable help and support during all period of my research.

I extend my deepest gratitude to a number of ITC staff: Prof. Dr. Ir. K. Harmsen (ex-rector), Prof. Dr. Ir M. Molenaar rector of ITC, Prof. Dr. A.K. Skidmore, Prof. Dr. Martin Hale, Dr. M. Sharif, Dr. A. Farshad, Sjaak Beerens, Arno Van Lieshout , Jan Schipper, Bas Retsios, Dr. B. Maathuis, Dr. R. Becht, Dr. Z. Vekerdy, Dr. M. Lubczynski, Dr. A. Gieske, Dr. T. Rientjes and Mark Noort for their support and contribution. Loes Colenbrander, Marion Pierik, Bettine Geerdink, Thea De Kluijver and the late Riet Allessie for the excellent administrative and financial arrangements. I also appreciate Loes Colenbrander for helping to format this book. I am grateful to the ITC Library staff, in particular to Carla Gerritsen, computer cluster managers Gerrit Polman and Aiko Mulder, secretaries Anke Walet and Tina Butt Castro, Publication office manager Ronnie Geerdink, Technical assistants Job Duim and Benno Masselink, ITC Hotel staff Saskia Tempelman, Bianca Haverkate, Marjolein Woerlee and Johan Lippold, Mail office Anne van der Linde, Desk top publishing office Andries Menning, Reception desk Roelof Schoppers and Hans Verdam for their logistic and technical support during all period of my research.

I have been fortunate in having a number of Iranian friends and colleagues here in the Netherlands. I am thankful to all of them in particular to Mr. Hossein Shammaei, Mrs. Fatemeh Shamaei, Dr. Saadi Mesgari and family, Dr. Ali Abkar and Family, Mr. Majid Daftari and family, Mr. Bahman Farhadi and Family, Dr. Nirvana Meratnia, Mr. Banihashemi, , Mr. Farhang Sargordi, Mr. Mohsen Zebarjadi, Mr. Mohammad Hossein Mokhtari, Miss Katayoun Mesgaryan Zanjani, Dr. Masoud Sharif and family. I also would like to acknowledge the endless hospitality extended by Dr. Sharif and his wife to me and my family. I deeply appreciate considerable support and friendship received from my colleagues Dr. Ivan Bacic, Dr. Mobin-ud-Din Ahmad, Diana Chavarro, Obed Obakeng, Arta Dilo, Dr. Martin Yemefack, Dr. Grace Nangendo and Dr. Alfred Duker.

Finally, a special note of thanks and a profound gratitude to all of my family members. I owe a lot to my mother and my father who has been very ill since a year ago, my sisters and brothers, who tolerated my absence for a long time. They have been a constant source of sacrifice, encouragement, prays, good wishes and support throughout my life. I am very grateful to them. As a reminder of all this, the thesis dedicated to my loving and affectionate parents. Lastly, I express my gratefulness to my wife and my son for their support and care during the period of my Ph.D. study. Without her support as a wife and friend, I would not have been able to finish. My only son Sayyed Amir Abbas who made my busy and sometimes difficult life an easy one, from whom I get the soul of motivation and success. My son, thank you very much.

Mirmasoud Kheirkhah Zarkesh
May 2005, Enschede, The Netherlands

Abstract

Kheirkhah Zarkesh, M. 2005. Decision Support System for floodwater spreading site selection in Iran. Ph.D. Thesis, Wageningen University, the Netherlands.

Most aquifers of semi-arid Iran suffer from over-exploitation of groundwater for irrigation. It is therefore important to augment the groundwater resource by artificial recharge, using flood waters that flow into salt lakes or in the sea. The recharge schemes consist generally of diversion of part of the flood discharges of ephemeral rivers in small to medium sized catchments onto infiltration basins.

Apart from recharge of groundwater, supporting food production and drinking water supplies, the schemes have other benefits, such as mitigation of flood damages and 'greening of the desert'. Many governments, including the one of Iran, place now much emphasis on increasing the number of floodwater spreading schemes.

A large number of factors play a role in the selection of the most suitable sites for deciding on investment in a scheme. These factors pertain to earth science (geology, geomorphology, soils), to hydrology (runoff and sediment yield, infiltration and groundwater conditions) and to socio-economic aspects (irrigated agriculture, flood damage mitigation, environment, job creation and so on). Hence, the decision depends on criteria of diverse nature.

This thesis deals with developing a Decision Support System (DSS) to assist decisions as to where the most suitable catchments and associated infiltration areas are and to work out options of types of schemes, which are adjusted to the characteristics of the selected infiltration area (the site available).

After discussion of the bio-physical setting for flood spreading schemes in the Introduction (Chapter 1), attention is given to the selection of the desired approach for multi-criteria evaluation in Chapter 2. The Analytical Hierarchical Processes (AHP) approach was considered to be appropriate for the problem at hand and use was made of the spatial extension of this approach in a GIS environment, after structuring all the major criteria for a flood spreading scheme.

Of key importance is of course the expected infiltration of flood water diverted. For such an a-priori estimate the effect of soil textures in a soil column on infiltration and percolation have to be made, as well as an estimate of the effects of sedimentation of clay and sand in a scheme, as well as effect of inundation depth and flooding frequency. One-dimensional soil modelling was done with the SWAP model, Chapter 3, using two pedo-transfer functions for the hydraulic parameters based on textures. It was found that for coarse textured soils there was reasonable agreement between functions used, but quite some differences were found for the soils containing clay and silt. As expected, recharge efficiency was positively affected by inundation depth and by rapid succession of inundations.

Because simulation results differed, the recharge of the complex and large Sorkhehesar scheme was analysed, by developing a spreadsheet programme to work out depths, areas and duration of inundation, Chapter 4. It was found that the Mualem-van Genuchten transfer function was the most appropriate one.

Given the large number of ephemeral rivers draining hilly catchments and passing through alluvial areas, is necessary to first use a rapid screening method to obtain zones which contain promising areas, for which the main criteria are applicable. The screening depends heavily on interpretation of remotely sensed images, which have the advantage that various aspects are presented in a synoptic view. The interpretation has to have a firm footing in earth science because runoff and sediment delivery processes have to be estimated in qualitative terms, as well as aquifer properties. A number of examples from Iran have been described in Chapter 5, highlighting the importance of transmission losses.

In order to select the most suitable area among the promising ones, the spatial AHP was applied in the Varamin zone under consideration of a multitude of criteria, in Chapter 6. The difficulty in the application was to develop and specify the preferences that are the base of the relative importance values for all the decision criteria involved at different levels, once the various factors had been estimated using standard hydrological and other methods. The use of the linguistic measures of preferences in the pair-wise comparisons made it possible to implement the full procedure, even though data differed much in nature, consistency and quality. In the Varamin zone, the Chandab catchment and infiltration area came out as the "most satisfying" area; it had the highest sum of utilities for three of the four objectives and the highest score in a combination scenario.

For the Chandab infiltration site, a spreadsheet model was developed to work out various options with regard to type of scheme (shallow basin or deep basin type) and size of scheme, resulting in the expected volumes of recharge during the lifetime of the scheme by assuming desilting operations. Of the additional benefits, the flood damage mitigation could be expressed in monetary terms, and that benefit had a profound effect on the cost per unit volume of recharge water if one opts for the two large sized scheme designs.

To our knowledge, this study presents for the first time information on costs and benefits of a flood water spreading scheme in Iran in a structured manner of various designs adjusted to a particular site.

The final conclusion (Chapter 8) states that the DSS described here, with its three stages of increasing focus and associated data requirements and with the approach for evaluation using a multitude of criteria of diverse nature, has proven to be applicable and an efficient way to select the most appropriate alternatives for making a choice for investment in a flood spreading scheme. Although the emphasis was on Iranian conditions, the DSS is essentially of generic nature and may be applied – *mutatis mutandis*- to other semi arid regions.

Keywords: DSS, remote sensing, GIS, spatial multi-criteria evaluation, analytical hierarchy process, floodwater spreading, groundwater recharge, Iran.

CHAPTER 1
Introduction

1.1 Why floodwater spreading schemes in Iran?

Water is becoming an increasingly scarce commodity because most of Iran is located in semi-arid regions with a high population growth. This is leading to a rising demand for water for agricultural, industrial and drinking purposes. According to recent studies on water resource development in Iran, the total amount of annual precipitation is about 430 billion m^3, of which about 20% is lost in the form of flash floods to the playas and seas. From the geological point of view, about 87 million hectares of the total geographical area of Iran are occupied by mountainous lands, and 78 million hectares are plain lands, about three quarters of which are Quaternary formation, mostly in the form of alluvial plains. Many areas of these plains are suitable for diverting flash floods from small to medium-sized catchments to infiltration areas in order to augment groundwater resources for the maintenance or expansion of irrigation, for the drinking water supply and for the improvement of ecology.

One main reason for considering floodwater spreading schemes is the declining groundwater level in most of the aquifers exploited for irrigation in the semi-arid parts of the world (Seckler et al., 1998) – and Iran is no exception in this (Kowsar,1995). In order to increase agricultural production and rural income, a rapid expansion of tubewells in hundreds of local aquifers took place in Iran after the revolution in 1979. The majority of the local aquifers are situated in the semi-arid parts, where rainfall is less than 350 mm annually, rendering rainfed agriculture impossible or marginal. To keep the groundwater irrigation in place or even increase it, artificial recharge is needed. An overview of artificial recharge is given by Bouwer (2002), who points out the major factors to be considered. The success of artificial groundwater recharge via surface infiltration is discussed by Fennemore et al. (2001) and Haimerl (2001), among others.

An additional reason for diverting at least part of the flash flow is the damage that the episodic flows cause to human life, settlements and agriculture. It is difficult to know the damage done by floods of the small to medium-sized catchments because damage statistics are aggregated over larger administrative units (such as provinces in Iran) and the damage includes that of the major river basins. Furthermore, the frequency distribution of flood damage for the small to medium-sized catchments is not known. However, in one of the areas considered in more detail in this thesis, the local flood damage was reported to be 860 million rials (about 860,000 euros) for a flood event with a water volume between 500,000 and 1,000,000 m^3 during the year 1995 (Khalilpour, 2003; Chandab area), indicating that such damage is substantial.

Ecological considerations are gaining importance in Iran, particularly the desire to have more green vegetation and trees in the vast dry areas that suffer from overgrazing. Visits of leading politicians to the Gareh Baygan floodwater spreading scheme in south Iran, where forest lots and grass areas have been included in the

design and provide a sharp contrast to the barren surroundings of the scheme, precipitated the act of 1995, calling for additional schemes in all the provinces.

The construction of many floodwater spreading schemes with relatively low initial investment forms a diversion from the past development in Iran emphasizing building large dams with high initial capital costs. Such large reservoirs have been constructed on rivers with perennial flows or flows that last for longer periods of time during the year. Keller et al. (2000) discuss the various forms of storage to mitigate water scarcity. Large dams score low in operational flexibility and reliability, but high in adequacy and conservation potential because the capacities usually far exceed the annual inflow. They consider groundwater storage as having high conservation potential, operational flexibility and reliability, but low adequacy because of the limited volume of water stored during its lifetime in comparison with the large dams. On a worldwide basis, large dams have comparatively low costs per 1000 m^3 water stored: up to US$ 32 for large dams, but US$ 110 for small to medium-sized surface water storage projects owing to shorter lives and greater evaporation. Data from Gleick (1993) put the costs of artificial groundwater recharge per 1000 m^3 at US$ 190 for low storage capital costs, ranging up to US$ 230 for the high end.

In Iran, additional suitable sites for dams and reservoirs are limited, the rate of sedimentation is much higher than that on a worldwide basis, and the costs of conveyance systems from dam to fields are often very high. The conveyance costs for recharge projects, however, are low or non-existent because the infrastructure for delivering water to the fields by pumping or by qanats is usually in place. Increased awareness of the environmental impact of large dams has increased the costs: Keller et al. (2000) mention US$ 346 for a dam in California in the last decade. Therefore, the artificial recharge schemes have become most cost-effective.

1.2 The problem

In Iran, many floodwater spreading schemes have been constructed and many additional ones are planned. Remarkably, there are no published documents to our knowledge that deal with the selection of the sites or the performance of existing schemes. Quite a few of the schemes do not function well or could be regarded as superfluous. For example, in the eastern Zanjan Valley a reservoir was created to feed infiltration wells. However, it can be shown (Chapter 5) that all the runoff infiltrates by natural causes. Hence the effect of the considerable investment is that the induced recharge now takes place in a more concentrated manner a little more upstream. In an area near the city of Yazd, long dikes were built across the lower part of a large alluvial fan to recharge the aquifer. However, it has been shown that the drop in the level of water stored behind the dike after a runoff event equalled precisely the drop attributable to evaporation, indicating no recharge. Other schemes suffer from strong sedimentation in the conveyance and infiltration channels, raising maintenance costs. In other cases, the magnitude of river shifts was underestimated and therefore expensive adjustments to the intake structures were required. In the Chandab scheme, most of the infiltration area is located on the steeper part of an alluvial fan, causing gully formation in the shallow infiltration

basins and reducing the efficiency of the scheme because of reduced infiltration area and infiltration time.

As many more floodwater spreading schemes will be constructed and the best sites have already been used, determining suitable areas for such schemes – taking into consideration the many factors that play a role in the functioning of floodwater spreading schemes for recharging groundwater – poses a problem.

1.3 Objectives and research questions

The main objective is to develop and evaluate a decision support system (DSS) for the site selection and conceptual design of floodwater spreading schemes in the semi-arid regions of Iran. The sub-objectives are:

1 to develop and evaluate a method for screening larger areas or zones for feasible areas under conditions of data scarcity as a component of the DSS
2 to develop and evaluate a DSS for finding a 'suitable area' within a zone
3 to work out a method (integrated into a DSS) to arrive at options for decision makers with regard to type and size of scheme that honours the site-specific characteristics of the 'suitable area'.

The sub-objectives lead to the following research questions:

1 What are the main factors for a floodwater spreading scheme that have to be considered in the screening process, and how should they be structured?
2 What is an efficient way of identifying areas where schemes are feasible, in view of the fact that relevant data for the screening process may not be readily available?
3 Induced infiltration of water is the key process, but how can the infiltration be estimated on an a priori basis during the initial stage of a scheme and during its lifetime when sedimentation in the scheme will take place?
4 How well do the a priori estimates of infiltration compare with observed infiltration in an existing large and complex scheme?
5 What method is suitable for evaluating the 'suitable area' in view of the many factors and criteria of various (biophysical and socio-economic) nature and different degrees of quantification?
6 Since gauged data for the ephemeral small to medium-sized catchments are generally lacking, how can estimates for runoff and sediment load be evaluated?
7 In working out a conceptual design at a given site, what are the main cost factors in relation to the estimated efficiency of the scheme?
8 Which options, and in what form, should be presented to the decision makers?

1.4 Structure of the thesis

Chapter 1, the introduction, discusses particularly the factors pertaining to runoff, infiltration areas, aquifers and sediment that steer the screening of zones and areas that have sufficient promise for further scrutiny, with reference to the literature.

Chapter 2 is devoted to a review of the method adopted for the DSS. The range of biophysical and socio-economic aspects is structured in Chapter 3, and, in order to compare and weigh the various factors of different nature, the multi-criteria evaluation method (MCEM) is used as an important component for the DSS. Since floodwater spreading schemes take place in given areas, diverting water from catchments, a spatial component has been added.

Since the efficiency of a floodwater spreading scheme much depends on the infiltration (and little specific information could be found in the literature), one-dimensional soil moisture modelling was carried out for a range of textures, inundation depths and frequencies for a scheme at the initial stage, as well as for simplified conditions after sediment accumulation in a scheme, and this is dealt with in Chapter 3. Since the computer simulations using various pedo-transfer functions (PTFs) may not represent the true field conditions, a major recharge event in the Sorkhehesar scheme is analysed in Chapter 4.

Part of the DSS is a hierarchical approach for finding suitable zones containing potential areas, first at reconnaissance level (termed screening) whereby use is made of image interpretation of remotely sensed data, and this is handled in Chapter 5. With regard to the importance of the fate of recharged water, conceptual groundwater aspects are discussed in this chapter too.

The screening is followed by an analysis at semi-detailed level of the most promising area(s) within a suitable zone. Chapter 6 describes the application of the multi-criteria evaluation model (MCEM), including the Spatial multi-criteria evaluation (SMCE), to find a suitable area.

Once the boundary conditions, such as expected runoff and sediment are known, the specific conditions of the identified area or site make it necessary to work out for the decision makers the options as to the size and type of the scheme in relation to global costs and estimated benefits in terms of recharged amount of water and flood damage mitigation. This stage is described in Chapter 7. Once type and size have been decided, then comes the stage for engineering designs (not discussed here).

The conclusions and recommendations are outlined in the final chapter, Chapter 8.

1.5 Outline of the applied approach

This work concentrates on the types of scheme that divert water from flash flows in ephemeral rivers, partly or fully, onto a nearby area overlaying an aquifer in order to recharge groundwater, particularly to maintain irrigated agriculture. Therefore, runoff and sediment delivered by the catchment upstream of the diversion have to be considered, the suitability of the area for infiltration, the aquifer properties, and certain environmental aspects such as the implication of increased groundwater

level for soil salinity. The various aspects related to artificial recharge, including floodwater spreading schemes, have been presented by EWRI/ASCE (2001).

The flow of ephemeral rivers draining semi-arid hilly or mountainous terrain is discussed by Cooke et al. (1982). It consists of small to medium-sized catchments that are of interest in this study of a rapid, near-instantaneous rise of the hydrograph and a steep initial recession limb followed by a relatively long slow fall towards dry conditions. The fast rise represents the overland and semi-concentrated flow that is retarded somewhat in the channel by the large amount of debris that is picked up and by transmission loss. The wave-like advance of the flow has led to the terms 'flash flood' or 'flash flow'. The prolonged recession part is due to the depletion of surface storage and the leaking out of shallow permeable deposits close to the surface. Flow occurrence is variable because of the irregular distribution in time of rainfall events large enough to surpass the high initial abstraction in semi-arid catchments. Hence there can be years with few or no flash floods of sufficient volume to have an effect on groundwater recharge and there can be years with one or more large floods.

The most common locations for floodwater spreading schemes are the middle to upper parts of alluvial fans. These are landforms that owe their existence to fluvial deposition at a break in the river gradient between a mountain catchment and a plain. Typical of an alluvial fan is the decrease in slope in the downstream direction, which is associated with a decrease in grain size but an increase in the sorting of deposits. Their sizes and gradients reflect the catchment geology (Gregory and Walling, 1973). In semi-arid regions, the upper parts of the fans consist of a mixture of fluvial deposits, unsorted and debris flow deposits, and unstratified mudflow deposits (Cooke et al., 1982).

Generally, the break in gradient can be attributed to faulting along the mountain front. Uplift of the mountain and subsidence in the plain over periods of time explain why alluvial fan deposits, or fanglomerates, can attain considerable thickness. Variable tectonic movements in time and climatic changes can complicate the stratigraphy of the fanglomerates and their hydrogeological properties. In many parts of Iran, Late Pleistocene tectonism or neo-tectonism has affected the vertical and horizontal stability of the rivers on the fans and the sedimentation. A number of examples will be given in a later chapter.

From a hydrogeological point of view, the upper parts of the fans have phreatic conditions and are permeable, with the groundwater occurring at depths usually exceeding 20 m or more. The lower parts of the larger fans have semi-confined conditions owing to the presence of layers with clay and silt and reduced permeability, and, depending on local geological conditions, groundwater levels can be shallow. Because of the heavier textures, the lower parts are used for agriculture using groundwater recharged in the upper parts, chiefly by channel bed infiltration, termed 'transmission loss'.

As mentioned, there are various factors and criteria to be evaluated in the selection process leading to the best sites and options regarding size and type of scheme. These will be dealt with later, but first the major biophysical factors will be discussed.

1.6 Major biophysical factors to be considered

1.6.1 Water: flash flood volumes and occurrences

Of interest for the design of a floodwater spreading scheme are the frequencies of flash flows, their corresponding volumes, and the instantaneous peak flows, in order to estimate the total volume of water that is available for a floodwater spreading scheme and the dimensioning of the diversion intake structures, conveyance channels, and infiltration channels and basins.

A major problem in the screening is the estimation of the flow characteristics of ungauged catchments in semi-arid regions. This can be illustrated by comparing rainfall and peak discharges and volumes of a 56 km^2 gauged catchment in the Fasa region at a distance of 27 km from one of the cases discussed below. The data set of daily rainfall from a station 3 km outside the catchment and of daily discharge, including maximum instantaneous peak discharge, pertained to 11 years of records. Most of the catchment geology is made up of limestone. As shown in the plots of Figure 1.1, neither the peak flow response (Figure 1.1a) nor the flood volume (Figure 1.1b) response to daily rainfall has a clear pattern, even when antecedent soil moisture (ASM) is considered. These erratic responses show the uncertainty when runoff is estimated from rainfall.

The major cause of uncertainty in estimation runoff is poor knowledge of the spatial rainfall. Area-depth curves derived from rainfall fields with substantial rainfall in southern Iran show a reduction in maximum point rainfall of about 70 to 80% only for areas of 3500 km^2 in size (Sarlak, 1994;Oroumieh, 1994). Such rainfall associated with large depressions will result in large flow volumes, but not necessarily high peak flows in the small to medium-sized catchments. Intensities of convective rainfall are usually higher than those of the widespread depressional rainfall and can cause high peak flows, but the temporal and spatial rainfall patterns are not known in most cases because of the low density of rain gauges.

Therefore, a good alternative to rainfall-runoff estimation is to use flood frequency curves of partial series obtained from gauged catchments, as described for an arid area by Meirovich et al. (1998). Runoff from an ungauged catchment could then be estimated using similarity in lithology and relief to the gauged ones. However, this method requires a sufficient number of small to medium gauged catchments in a given climatic region – a condition not encountered in Iran.

In the absence of gauging data, the relative volume of the runoff is assessed in the screening by catchment size and the permeability of the catchment. Variation in catchment permeability has been shown to substantially affect peak flows – up to some 20 times in small to medium-sized catchments (e.g. Meijerink, 1985) – and for an area in south Iran the peak flow magnitude was inversely related to the percentage of limestone in the catchments (Sarlak, 1994). For the Sahel region in the 100 to 300 mm annual rainfall zone, runoff coefficients of catchments of 85 to 400 km^2 turned out to vary from a few percent to some 14% of the annual rainfall, depending on catchment permeability (Rodier, 1975). Permeable catchments are those that consist predominantly of limestone, sandstone and alluvial deposits

within the catchment. Shentsis et al. (1999) used a method they termed as 'hydrological-stratigraphical analogy' for transposing runoff data in an arid region.

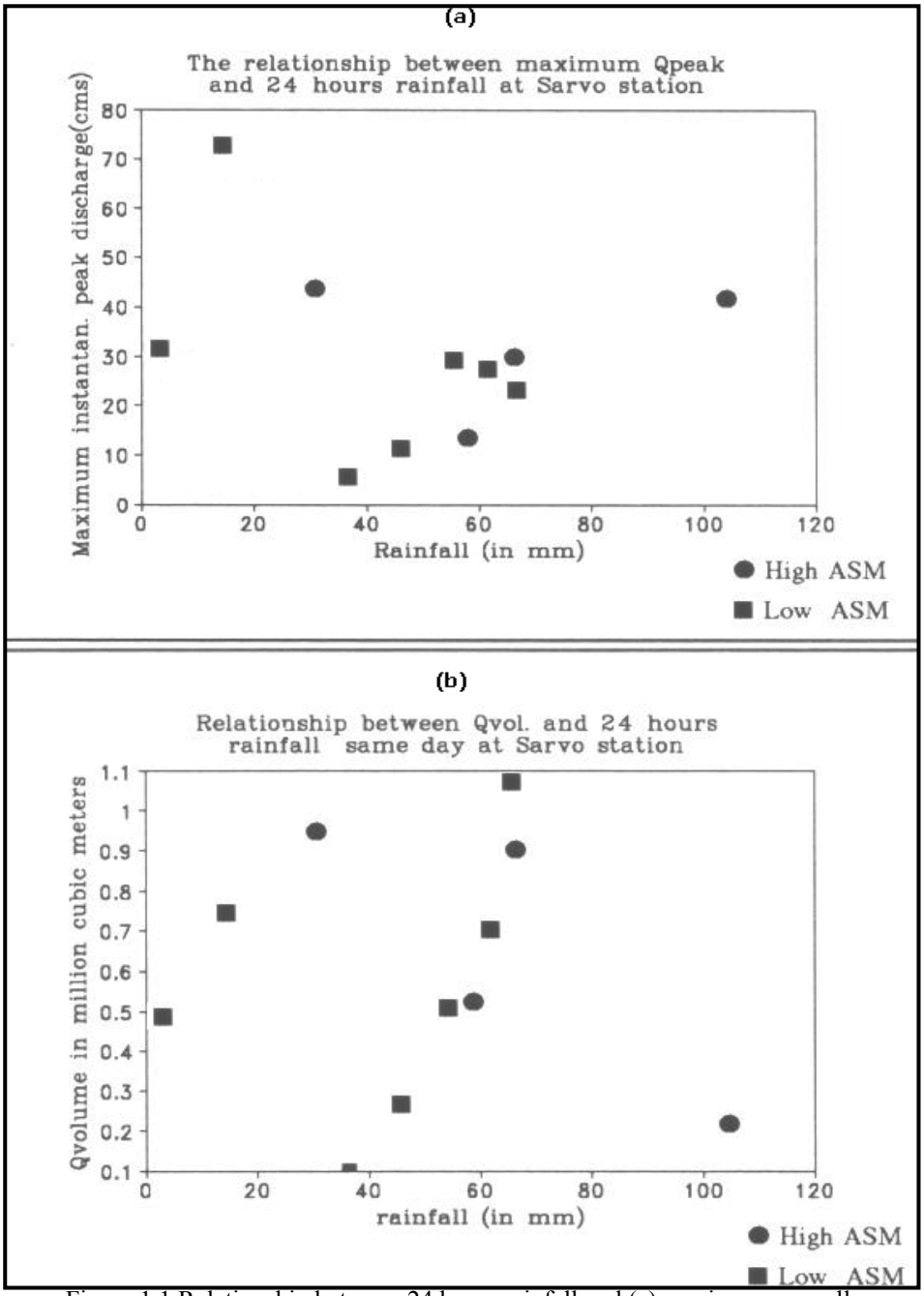

Figure 1.1 Relationship between 24 hours rainfall and (a) maximum annually instantaneous peak discharge, (b) maximum annually volume of runoff

The size of a catchment is a major determinant of the runoff volume. Catchments with a size of at least several square kilometres are considered, because, as a rule of thumb, 1 km^2 with 200 mm annual rainfall generates only 1000 to 5000 m^3 of recharged water, and the aim of floodwater spreading schemes is to recharge aquifers that benefit an agricultural community. By considering catchment sizes of at least a few square kilometres, the rapid decrease in specific runoff noticed in micro-catchments (Wood et al., 1988) has stabilized, although much variation in runoff coefficients remains, owing to variations in catchment characteristics in relation to spatial rainfall properties.

For area selection at the semi-detailed scale, current hydrological methods such as the SCS curve number method or unit hydrograph method (Soil Conservation Service, 1972) may be used to estimate flood occurrences and volumes for ungauged catchments, but the accuracy remains to be seen, as will be discussed in Chapter 7 (Chandab area). Considering the difficulty of predicting runoff, it is wise to gather runoff data by interviewing local inhabitants as to the frequency of occurrences and corresponding water levels, and then survey the river sections near the intended intake point and construct a hydrodynamic model and hydrograph convolution to estimate discharges.

1.6.2 Chemical water quality

The water to be used for recharge for irrigation should fall in the class of low to medium salinity, having electrical conductivity values <250 mhos cm^{-1} or <750 mhos cm^{-1} at 25ºC (Withers et al., 1988). However, on permeable soils the water quality may exceed the 750 mhos cm^{-1} limit, as is often the case in Iran. Because flash flows are a rapid response to rainfall, the floodwaters usually have low total dissolved solids (TDS) values, barring exceptional situations when, for example, rock salt outcrops are present.

The catchments generating the flash flows usually have a cover of sparse rangeland vegetation and no settlements or industry, and the waters are free from chemical contamination apart from suspended loads.

It is assumed that during percolation to groundwater and flow in the saturated zone the chemical quality does not change much, although some temporary quality deterioration may occur owing to washout of the unsaturated zone (Hionidi et al., 2002). This assumption is reasonably safe for the upper and middle parts of alluvial fan deposits. However, in the lower parts of the fans there could be interbedded playa or saline coastal plain deposits. These parts are not used for artificial infiltration but soil salinity due to capillary rise from shallow groundwater may require attention if upstream artificial recharge is carried out.

Geochemical reactions in the aquifer are more difficult to predict, but so far no adverse effects have been reported from the artificial floodwater spreading schemes in Iran.

1.6.3 Sediment amount

Any floodwater spreading scheme in a semi-arid environment using the turbid floodwaters will experience sedimentation in the infiltration basins or areas.

As is well known, deposition of coarse materials may not lower infiltration much, contrary to what is reported for clays and silts (see Chapter 3). However, a high coarse-natured sediment load is undesirable because it can choke the conveyance canals and reduce the capacity of the infiltration basins or areas, shortening the lifetime of the scheme or increasing the maintenance costs.

Assessing the sediment yield of ungauged rivers with flash floods is notoriously difficult. Even when suspended load records are available, the accuracy is low because most sampling is done on a routine basis and few, if any, samples are taken during the flash floods, when suspended load concentrations are the highest (Hadley et al., 1985) and the sand fraction is transported as saltation load.

Cooke et al. (1982) comment on the paucity of useful sediment yield data and discuss the large variation noted in the suspended load concentration in dry lands. Data summarized in a table show no upper limit of the concentration, which is in agreement with the observation that debris flows and mudflows occur in the arid and semi-arid catchments, where the concentration reaches >200,000 ppm.

Sediment surveys in reservoirs are preferred but they are generally limited to the major reservoirs of Iran. Using worldwide data, Jansson (1988) discusses the sharp reduction in sediment yield with increasing catchment area. In Jansson's overview of the semi-arid climates, the yields for six medium-sized catchments in west Iran ranged from 500 to >1000 ton km^2 y^{-1}. Averaged data from the USA (Langbein and Schumm, 1958) indicated a maximum for the semi-arid climate, which was 520 $km^2.y^{-1}$ if reservoir data were used. The yields from large catchments in Iran cannot be used for the smaller ones because the effects of local conditions average out in the larger catchments and the sediment delivery ratio decreases with increasing catchment size. Unfortunately, few data are available for the smaller catchments in Iran, but the following examples are indicative for the variation. Sediment yields ranging from 108 to 1002 ton km^2 y^{-1} were measured in small reservoirs in sub-catchments (1.8 to 10.1 km^2) with hard marls but extensive glacis of the Gorgak catchment in central Iran (Raeisi Nafchi, 2000). During the wettest year in a period of 15 years of recording rainfall, discharge and suspended load, the Sorkhab catchment (327 km^2) in the mountains of central-west Iran had a sediment yield of about 25,000 ton km^2 y^{-1}, against 3900 ton km^2 y^{-1} for a year with normal rainfall and 800 ton km^2 y^{-1} for the driest year. Some 20% of that catchment consists of shale and mudstone that have been uplifted and deeply dissected (Mobarakian, 1998). The sediment yields from the Maghreb countries, where geology and climate are similar to those of large parts of Iran, ranged from 12,000 to 15,000 ton km^2 y^{-1}, while for the Zeroud river in 1969, when a flood with a recurrence interval of >1000 years took place, the estimate was 25,000 ton km^2 y^1 against an average of 492 ton km^2 y^{-1} for that river (Heusch et al., 1971). These authors demonstrated that median values of suspended load varied from 1.2 mg l^{-1} for catchments with resistant rocks, such as sandstones and micaschists, to 31 mg l^{-1} for catchments composed of soft marls, with other lithologies taking an

intermediate position. They presented regression equations that related rainfall to runoff and runoff to turbidity for three groups of catchment lithology.

It is likely that in catchments that are vulnerable to erosion events excessive amounts can be produced, including the transport of very large boulders that cause much damage to the infrastructure of a scheme. Inbar (1972) reports an event in an arid catchment with a yield of 60,000 ton km^2 against a normal yield of 6000 to 8000 ton km^2 y^{-1}. That amount can be surpassed in the case of large mudflows, which can fill valleys with deposits of several tens of metres. Although catastrophic events have low return periods, vulnerable catchments should be regarded with caution in the screening process.

At the semi-detailed level, the sediment yield can be estimated by the PSIAC (Pacific Southwest Interagency Committee, 1974) method, preferably using local sediment yield data for calibrating the weighting factors.

1.6.4 Sediment type

The type of solid load of the river affects floodwater spreading schemes. Much suspended load means much deposition of clays and silts in the infiltration basins, reducing the effectiveness (Bouwer et al., 2002; Schuh, 1990). In addition, inflow of turbid water in a fresh scheme leads to clogging of the pore space of the original soil surface and eluviation. The type of clay plays a role in the infiltration, because swelling types such as montmorillonite can make the clay layer of an infiltration basin impervious when wetted. Unfortunately, few data are available on the clay mineralogy of suspended load deposits and the effect on infiltration during the lifetime of the schemes in Iran – or elsewhere for that matter – apart from very general observations.

Much bedload requires careful design to prevent the filling of the intake and conveyance channels. Estimating the amount of bedload is a problem because hydrodynamic equations pertain to transport, not to the supply of coarse sediment to the river system by landsliding, gullying and bank erosion.

The relative magnitude of the suspended load and the bedload is a reflection of the catchment lithology and drainage network characteristics, as will be discussed in Chapter 5.

1.6.5 Topography of the infiltration area

The type of scheme whereby water is spread over the soil surface requires gently sloping, non-dissected land. If the erosivity of the soil is low, the maximum slope for floodwater spreading is 5% according to Vallentine (1971). In the older literature, low slope gradients for floodwater spreading are recommended: 0.05 to 1% with a maximum of 3% (Matson, 1961). Furthermore, Stokes, et al. (1954) mentioned that, if the suspended load of the flood is insignificant, slopes between 1 and 2% are suitable and a maximum of 3%. However, as most infiltration areas will be located on the middle to upper parts of alluvial fans, it should be remembered that for fluvial sediments the grain size is related to the slope. In other words, coarse materials with high permeability are found on the upper parts of the fans, where the gradient is the steepest.

If higher construction costs are accepted (e.g. for the deep basin type), steeper slopes than those mentioned above can be considered. The FAO (AGL, 2000) recommends slope steepness less than 10% for floodwater harvesting projects. In the Jongan floodwater spreading scheme near Mamasani city in Iran, the slope of the site is about 10% and the project has had satisfactory results, although the costs were very high (Kowsar, 1995).

The cost aspects are worked out in Chapter 7, which deals with conceptual site design.

1.6.6 Aquifers

As mentioned earlier, most aquifers to be considered consist of fanglomerates, and the general hydrogeological properties of coarse-grained alluvial aquifers are described by Freeze at al. (1979) and Todd (1980), among others.

The hydrogeological study of the large Varamin alluvial fan and plain, southeast of Tehran, described by De Ridder and Erez (1977), used transmissivities (T) that ranged from >6000 $m^2 d^{-1}$ in the upper fan to <500 $m^2 d^{-1}$ in the lower fan. These values were upheld in later groundwater modelling (Ministry of Energy, 2002). For the floodwater spreading scheme of Gareh Bygan, Fatehi-Marj (1994) used T values that ranged from 85 to 790 m^2/day for the upper and lower parts respectively. The groundwater model was calibrated on an initial condition with head data from the mother wells of qanats and the 1994 situation with head data from wells. For the alluvial fan complexes in the eastern Zanjan Valley, deposited by smaller catchments than those mentioned above, Bani Hashemi (1994) used T values of 16 to 20 m d^{-1} for upper fanglomerates and 1 to 4 m d^{-1} for the deposits of the lower fan. The model was calibrated on heads and outflow. For the fanglomerates of steep alluvial fans deposited by rivers draining mountain catchments with highly resistant rocks, T values are likely to exceed 10,000 $m^2 d^{-1}$.

Such permeable conditions increase the efficiency of recharge, particularly since the storage coefficient or specific yield is highest in the upper parts of the fans and decreases in the downstream direction (e.g. from >15% to <5% in the Varamin area).

Although the data show quite a range in the T values adopted by various authors, all the authors agree that permeable conditions of the upper alluvial fans are necessary to make artificial recharge by floodwater spreading feasible. However, loss of recharged water by outflow should be avoided and the increase in head should not stimulate soil salinity. Therefore, conceptual groundwater modelling was carried out to study pumping schemes to avoid such unwanted effects.

1.6.7 Permeability of the infiltration area as assessed by transmission losses

Data on transmission losses provide information on the natural recharge in riverbeds that are not dissimilar to those in floodwater spreading schemes in the vadose zone. Furthermore, if the transmission is so high that no water leaves the fan

except during floods with a high recurrence interval – and that is the case in some fans in Iran – the usefulness of an artificial recharge scheme can be questioned.

Cooke et al. (1982) mention the 'sieve deposits' and associated irregular topography on alluvial fans in semi-arid terrain that result from rapid loss of water in permeable deposits, leading to the sieving out of the coarse material. Transmission loss is the most important process of natural recharge in semi-arid regions and has been studied by many (e.g. Sorman, et al., 1993), but only some studies were supported by field data from ephemeral wadis (of interest here). The studies are indicative of the permeable conditions for the fluvial coarse-grained alluvium in semi-arid regions.

Walters et al. (1990) presents data showing that the loss varies exponentially (exponent is 1.22) with the width of the river and with the root of the volume of the inflow. A maximum of some 20% of the low inflow volumes can infiltrate in the first 1.6 km, but less than 2% of the high inflow volumes over the same distance. Hughes and Sami (1992) found that in two events 22% to 75% of the stream flow of a wadi was lost in the alluvial materials. Shentsis et al. (1999) mention that runoff from tributary catchments measuring 35% and 25% of the total catchment area (about 308 km^2 and 490 km^2 respectively) did not contribute to the runoff of the main river in the arid Negev because of large transmission losses, except perhaps during extreme floods. Haimerl (2001) found that the recharge increased from 38% of the water flowing in a wadi to 94% when low dams were constructed in the wadi bed.

Sorman, et al. (1993) mention the large temporal variations in the transmission loss in a wadi bed, and an agreement was found between the recharge to the shallow groundwater, as determined in three wells, and the transmission loss based on hydrometry. The loss could be related to flow width or stage height and the duration of flow. They found a relation between groundwater recharge and inflow volume, as well as with transmission loss. During 27 flow events, groundwater recharge along the wadi varied from 0 m to a maximum of 0.77 m, which corresponds to a rise of 2.85 m because they adopted an effective porosity of 27%. In two of the examples from Iran discussed below (Sargon and Zanjan), groundwater rises attributable to transmission loss were sometimes more than a few metres. The presence of impeding layers, or shallow depth to an impermeable base in the unsaturated zone, can limit transmission loss of infiltration in general. Schwartz et al. (1990) noted that transmission loss in alluvium on the impermeable granite of an ephemeral river in an arid climate was positively related to the time elapsed since the last runoff event. Apparently, the rise of the groundwater in the area studied and increased moisture reduced infiltration.

In their field and laboratory experiments for a wadi in Namibia, Crerar et al. (1987) found the formation of an impermeable silt layer during flood events to be an extremely important factor in the recharge, a factor not noticed by earlier researchers.

The sorting and packing of riverbed materials, as influenced by catchment geology, play a role, as was observed by Bani Hashemi (1994) in the ephemeral riverbeds of the eastern Zanjan Valley. The infiltration of clear water (snowmelt and base flow) in the mixtures of boulders, pebbles and sands with some clay and

silt present in the beds of the upper alluvial fans, determined as loss of discharge over the wetted area, varied from 1.15 to 1.77 m d^{-1} (n=4) for bed materials with a mixed granite provenance, and from 0.5 to 5 m d^{-1} (n=4) for a volcanic rock provenance only.

These studies show the complexity of the river recharge process. In this thesis, one-dimensional soil moisture modelling was carried out to study the effects of textures, water depths and inundation frequencies. Since computer simulations represent only a part of reality, an actual recharge scheme in Iran was included in the analysis.

CHAPTER 2
Decision Support Systems (DSS)

2.1 Theory

2.1.1 Decision making

To make a decision on the suitable site of a floodwater spreading scheme with matching suitable design options is complex because many factors of diverse nature have to be considered. Data or information available varies in quality and detail and various stakeholders are involved. Therefore, in this chapter the decision-making process is explored and a formal approach is selected.

Decision-making processes transform information into instructions that are intended to affect system behaviour in such a way that they improve system performance (Sharifi and Herwijnen, 2003). Mintzberg et al. (1976) defined a decision process as a set of actions and dynamic factors that begins with the identification of an incentive for action and ends with a specific commitment to action. Decision making starts by examining the environment in order to identify problem or opportunity situations. Next, the individual or group of decision makers should generate alternative courses of action and be able to set priorities among these alternatives in order to solve the problem. In this process, the decision makers (individuals or groups of people with a common problem) directly or indirectly provide value judgments on the decision making, to define and choose between alternative courses of action (Chankong and Haimes, 1983).

2.1.2 Planning and decision-making framework

In his model, Simon (1960) suggests that the decision-making process can be structured into three major phases: intelligence, design and choice. Based on this model, Sharifi and Rodriguez (2002) defined a framework for planning and decision-making processes as described below (see Figure 2.1).

The intelligence phase
'Is there a problem or opportunity for change?' This phase includes inspecting the environment to identify problems or opportunities demanding a decision.

The design phase
'What are the available alternatives?' This phase relates to initiating, developing and analysing the possible courses of action. This includes the processes of understanding the problem, applying planning models that generate alternative solutions, and testing their feasibility and applicability.

The choice phase
'Which line of action will return the most perceived benefits?' This involves selecting a course of action from the alternatives available.

2.1.3 Decision support systems (DSS)

The decision support concept originated probably in the late 1950s and early 1960s from studies on organizational decision making at the Carnegie Institute of Technology by Herbert Simon and Allen Newell, and on interactive computer systems at the Massachusetts Institute of Technology by Tom Gerrity (Power, 1999). Gorry and Morton (1971) define the term 'DSS' as an interactive computer-based system that helps decision makers to utilize data and models to solve semi-structured or unstructured problems. A system that makes some contribution to decision making is defined by Sprague and Watson (1986), while Stuth and Lyons (1993) explain the term as contemporary jargon for an integrated approach to the age-old problem of helping people to make better decisions. Computerized tools to analyse large amounts of data and complex relations for making rational decisions are proposed by Makowski (1994). Klosterman (1997) explains the term 'DSS' as a system or methodology that assists in poorly or ill-structured decisions by facilitating interactive and participatory decision processes.

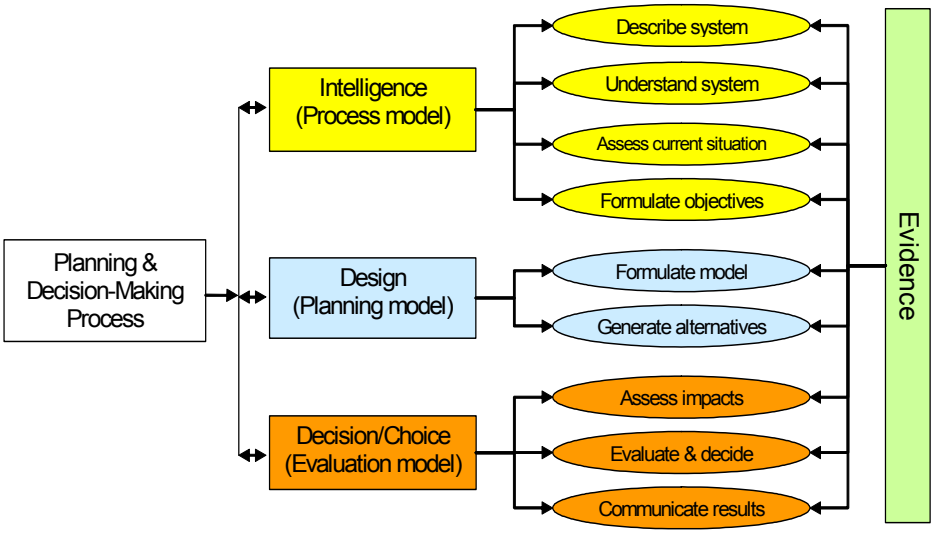

Figure 2.1 Planning and decision-making processes explained by Sharifi and Rodriguez (2002) based on Simon's (1960) model

An important point in relation to DSS' is that the decision maker is responsible for the decision and the DSS is a tool to provide a larger window of opportunity. Hence, the user is the central part of the system and the DSS is analogous to a hand-held calculator in that it supplements, rather than supplants, the

decision-making process (Stuth and Lyons, 1993). DSS' are models that use flexible data as inputs, and give alternative solutions as outputs. Their primary objective is to assist specific decision makers, individually or as groups. This allows custom design of the system, in which the decision maker can develop the DSS interactively, thus providing the opportunity to adapt the analytical models used in the decision-making process. DSS' are interactive, as they allow the decision maker to systematically generate and evaluate a number of alternative solutions (Klosterman, 1997). They are integrative in the sense that they incorporate substantive knowledge of the decision maker, along with quantitative data and formalized existing knowledge of processes, to create solutions and evaluate all alternatives across a range of pertinent criteria. They are also participatory in permitting decision makers to examine the consequences of applying different information and modelling approaches and to select alternative decision criteria, objectives and constraints.

Classic DSS tool design is comprised of components for (i) sophisticated database management capabilities with access to internal and external data, information and knowledge (database part); (ii) powerful modelling functions accessed by a model management system (processing part); and (iii) powerful, yet simple, user interface designs that enable interactive queries, reporting and graphing functions. All three components should have the flexibility to accommodate different types of software and techniques. For data management, many options are available, from simple tables to sophisticated user-friendly databases such as Excel. Many tools are also available for the model base of the system, such as simulation models, physical models, and linear and nonlinear models. The level of sophistication is determined by the complexity of the problem at hand and the availability of information.

2.1.4 Planning and planning support system (PSS)

Planning is a continuous process that involves decisions or choices about alternative ways of using available resources with the aim of achieving particular goals at some time in future (Conyers and Hill, 1989). According to this definition, planning consists of choosing and allocating resources to achieve goals and to plan for the future. Furthermore, planning is a specific type of decision making. Therefore, Sharifi and Rodriguez (2002) conclude that it should comply with the definition and phases of decision-making and problem-solving processes as mentioned above. In this context, they define PSS as a class of geoinformation system composed of data/information, models and visualization tools that are primarily developed to support different phases of the planning process and its functions. PSS contributes to rationalization planning and related decision-making processes by providing the necessary support to systematically structure and formulate problems, develop alternative plans or policy scenarios, assess and evaluate their impact (considering the objectives of the relevant stakeholders), and select a proper policy or plan. Therefore, planning support systems are very similar to DSS. They also provide interactive, integrative and participatory procedures for dealing with poorly structured problems. However, as a planning system, PSS also pays attention to

planning problems and strategic issues, and explicitly facilitates group interaction and discussion (Klosterman, 1997). According to Klosterman (1995), the difference between these two is one of degree and purpose. In DSS, the role of the model is to support semi-structured decision making; in PSS the role of the model is taken further and is not only to aid semi-structured decision making, but also to promote interaction, communication and dialogue. It must also combine continuous and interactive processes of analysis, design and evaluation with open and accessible processes for public feedback, interaction and dialogue.

Sharifi and Rodriguez (2002) distinguish between the planning and decision-making components (see Figure 2.2) of PSS as a specific type of decision support system as follows:

- **A database management system:** To accommodate and organize the basic spatial and thematic data, and provide facilities for selecting and manipulating data, as well as interrelating data from various sources.
- **A model base management system:** This includes quantitative and qualitative models that support resource analysis, and the assessment of potential and capacities of resources at different levels of management. It is a knowledge base that provides information on data and existing processing capacity and models, which can be used to identify problems, generate solutions, evaluate and appraise their impacts, and finally communicate the results to the decision makers.
- **A user-friendly interface:** This allows smooth and easy communication with the system, and visualization and communication of the analysis result to the decision makers in a manageable and understandable form.

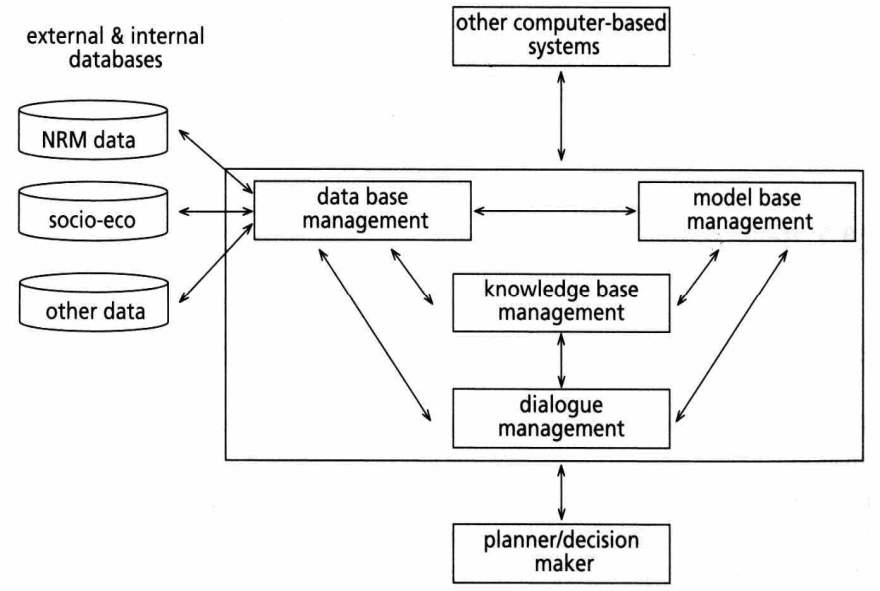

Figure 2.2 Overall architecture of a planning support system (adapted from Turban (1995) and Sharifi et al. (2002))

2.1.5 Multiple criteria decision analysis (MCDA)

MCDA is a transparent way of systematically collecting and processing objective information, and expressing and communicating subjective judgments concerning choice from a set of alternatives affecting several stakeholders. Such systematic, rational and transparent judgments most probably lead to more effective and efficient decisions by individuals or groups of decision makers (Sharifi et al., 2004). The main goal of MCDA is to generate a gauge to compare possible alternatives or solutions. These methods integrate multiple criteria in order to combine all the relevant concerns in the decision problem as a gauge for comparison.

Traditionally, the evaluation of decision criteria consists of two major forms: objective or subjective. In objective analysis, efforts are made to present a functional assessment of the decision event by identifying all the potential effects and the significance of such impacts based on the market value of the events and criteria involved. Subjective analysis of decision events comprises various approaches, which share the common purpose of helping decision makers to express consistent judgment and choose rationally. The techniques adopted in the various approaches of objective and subjective analysis are called multicriteria decision methods (MCDMs).

Decision analysts (DA) distinguish two types of utility (the relevant transformation functions that convert the facts (data) related to each selected criterion to a value judgment[1], the so-called 'utility' or 'value'). Value preferences are made between choices when no uncertainty is present. Utility functions are used to address risk preference in the decision maker's attitude towards risk taking under uncertainty. Value judgment is essentially comparing two or more alternatives/criteria. Such value judgment in MCDA is also expressed in the form of a value function when handling criterion performance, besides setting appropriate weights.

2.1.6 Decision-making paradigms

There are two main paradigms for decision-making[2] and their related decision models.

Objective rationality (substantive rationality)

The decision process results in the selection of the best solution (i.e. the selection of an optimal course of action). It is also known as multi-objective decision making (MODM). It is sometimes viewed as a natural extension of mathematical programming, where single or several objective functions are considered simultaneously. The objective and procedural rationalities can be related to two

[1] Values are subjective evidence specific to the problem. These are opinions, views, attitudes, prejudices, assumptions and interpretations that are difficult to measure but have important influences on the decision-making process. They are often used to test desirability and answer the question 'Is the decision right?' Research on improving the assessment techniques for the value function are still in progress (Van Herwijnen, 1999).

[2] Failing to differentiate such understanding will result in users applying MCDM within a cookbook paradigm. Relevant expert knowledge in translating such criterion thresholds into a value function curve is a requirement (Sharifi et al., 2003).

types of decision model, i.e. normative (prescriptive) models and descriptive models (Figure 2.3). Normative models (as in MODM) indicate how to make a class of decisions – for example, engineering and economic criteria for selection among alternatives are handled through optimization. Decision makers seek to maximize profit or utility and are sensitive to differences in outcomes. MODM problems involve designing alternatives and searching for the 'best' decisions among infinite or very large sets of feasible alternatives. These problems can be defined and solved by several alternative optimization models, such as compromising programming, constraint method, goal programming, and fuzzy multi-objective programming.

Procedural rationality (bounded rationality)
This procedure aims at searching for a satisfying alternative rather than for an optimal alternative. Therefore, the objective is the selection of a course of action that is 'good enough'. This is supported by simulation and multi-attribute decision making (MADM). The descriptive models (as in MADM) indicate how a decision maker, through a limited search for a few alternatives, actually makes a decision that satisfies the decision maker's aspiration level (satisfied). This thesis essentially focuses on such satisfying concerns and thus deals with MADM methods.

MADM includes a finite number of alternative solutions described by several attributes in the decision-making process. Colson and Bruyn (1989) define an attribute as the characteristic of an option/object that can be evaluated objectively or subjectively by one or several persons according to a measurement scale. Based on the value of these attributes and the priorities that the decision maker allocates to each (weight), the alternative options are evaluated to reject bad ones or recognize good ones, in order to better understand the pros and cons and their impacts, and to identify the most appealing option and rank the alternatives. The main aim of any MADM technique is the evaluation of the impact of each alternative on every criterion after the production of a discreet set of alternatives and the formulation of a set of criteria. Most of the methods build an aggregation from the evaluation, or preferences associated with each attribute, so that a unique preference structure can be derived for the whole set.

Because of the uncertainty in determining criteria for the problem addressed in this study, and the limited number of alternatives, the objective rationality paradigm is not appropriate. Therefore, in this study the second paradigm (procedural rationality), which searches for a satisfying alternative rather than an optimal alternative, will be used. This paradigm will be supported by simulation and multi-attribute decision making (MADM).

2.1.7 Decision-making approaches

According to Keeney (1992), two major approaches can be distinguished: the alternative-focused and the value-focused approaches. The alternative-focused approach starts with the development of alternative options, and specification of values and criteria, and then proceeds to the evaluation and recommendation of an option. The value-focused approach considers the values as the fundamental element in the decision analysis. Therefore, it focuses on the specification of values,

after which feasible options (also known as alternative options) are developed and evaluated based on the predefined value and criteria structure for floodwater spreading schemes. In this approach, the order of thinking is focused on what is desired rather than on the evaluation of alternatives. In fact, alternatives are considered as means to achieve the more fundamental values, rather than being an end. Naturally, in decision problems where alternative options have to be developed and then evaluated, the value-focus approach can be much more effective. However, if the decision problem starts with choice of option, the alternative-focused is more relevant (Sharifi et al., 2004).

In this study, the value-focused approach will be explored for developing and evaluating alternative options.

Having chosen the value-focused approach, the next choice pertains to the aggregation procedure. Out of the existing options mentioned in the literature – (i) compensatory methods, (ii) outranking methods, and (iii) non-compensatory methods – the compensatory method is the most attractive for the problem at hand in this study. This method aggregates criteria to form unique meta-criteria (i.e. criteria aggregated to one unique or single value) and permits tradeoffs between attributes. This approach is based on the assumption that the low performance of an alternative on one or more criteria can be compensated for by the high performance of the same alternative on other criteria. Examples of this approach are the weighted summation, the multi-attribute method (Jankowski, 1995; Janssen, 1992) and the analytical hierarchy process method (AHP) (Saaty, 1980).

Analytical hierarchy process (AHP)

The AHP approach is a crucial method in this study and therefore essential aspects are mentioned.

In the late 1960s, Thomas Saaty, a world-renowned mathematician and one of the pioneers of operations research (OR), was motivated to attempt to develop a simple way to help ordinary people in complex decisions. The result was AHP. The meaning of each of the three words ‘analytical’, ‘hierarchy’ and ‘process’ is given below.

Analytical

Analytical comes from the word ‘analysis’, which means the separating of any material or abstract entity into its constituent elements. Analysis is the opposite of synthesis, which involves putting together or combining parts into a whole. Many organizations have departments or divisions with the words ‘analysis’ and ‘process analysis’ in their titles. Organizations have become quite good at doing analysis. Few organizations, however, know how to synthesize! In a sense, AHP should really be called the *synthesis* hierarchy process because at its core AHP helps us to measure and synthesize the multitude of factors involved in complex decisions.

Hierarchy

Discussing how to deal with complexity, Herbert Simon, father of the field of artificial intelligence (AI), makes the analogy with large organizations: ‘Large organizations are almost universally hierarchical in structure. That is to say, they

are divided into units which are subdivided into smaller units, which are, in turn, subdivided and so on.' He mentions that hierarchy is the adaptive form for finite intelligence to assume in the face of complexity.

Process

A process is a series of actions, changes or functions that bring about an end or result. AHP is not a magic formula or model that finds the 'right' answer, rather a process that helps decision makers to find the possible 'satisfying' answer. AHP is based on criteria that are measured on a ratio scale. In AHP, the decision maker has to make a comparison for every pair of criteria, first qualitative and then quantitative on a scale from 1 to 9, to make the method operational. This scale is presented in Table 2.1. The method then creates a matrix containing the pairwise comparison judgments for the criteria, from which a priority vector is derived of relative weights for these elements. Moreover, due to the fact that more information than is necessary is retrieved from the decision maker, the method can deliver an inconsistency measure.

Table 2.1 Linguistic measures of preference (Saaty, 1980)

Linguistic Expression of Relative Importance of One Member of Comparison Pair Relative to Another	**Number Assigned to Linguistic Expression**
Equal preferences of indifference	1
Weak preference	3
Strong preference	5
Demonstrated preference	7
Absolute preference	9
Intermediate Values	2, 4, 6, 8

This measure can be used to verify in what measure the judgments supplied are consistent. AHP is specially designed to assess weights within a hierarchical structure of the criteria.

Weights or priorities are not arbitrarily 'assigned'

By using the AHP pairwise comparison process, weights or priorities are derived from a set of judgments expressed either verbally, numerically or graphically. While it is difficult to justify weights that are arbitrarily assigned, it is relatively easy to justify judgments and the basis (hard data, knowledge, experience) for the judgments. These weights or priorities are ratio-level measures, not counts. Furthermore, the priorities that are derived from judgments automatically incorporate the necessary nonlinearities in measuring utility. For example, when considering a vehicle for city driving, the preference for a vehicle with a top speed of 40 miles per hour is probably more than twice that for a vehicle with a top speed of 20 miles per hour. But the preference for a vehicle with a top speed of 100 miles per hour would be much less than twice the preference for a vehicle with a top speed of 50 miles per hour (Forman, 1999).

Inconsistency

The theory of AHP does not demand perfect consistency. AHP allows inconsistency but provides a measure of inconsistency in each set of judgments. This measure is an important by-product of the process of driving priorities based on pairwise comparisons. It is natural for people to want to be consistent. Being consistent is often thought of as a prerequisite for clear thinking. However, the real world is hardly ever perfectly consistent, and we can learn some things simply by allowing for some inconsistency in what we already know. If we are perfectly consistent (as measured with an AHP inconsistency ratio of zero), we cannot say that our judgments are good, just as we cannot say that there is nothing wrong with us physically if our body temperature is 98.6º Fahrenheit. On the other hand, if our inconsistency is say 40 or 50% (an inconsistency ratio of 100% is equivalent to random judgments), we can say there is something wrong, just as we can say that there is something wrong if our body temperature is 104º Fahrenheit. An inconsistency ratio of about 10% or less is usually considered acceptable, but the particular circumstance may warrant the acceptance of a higher value. For example, a body temperature of 100º Fahrenheit (about 38ºC) may be taken as normal if we know that the person has just completed a 26-mile marathon on a hot sunny day (Forman, 1999).

Principles of AHP

AHP is built on a solid yet simple theoretical foundation. AHP is based on three basic principles: decomposition, comparative judgment, and hierarchical composition or synthesis of priorities (Saaty, 1994). The decomposition principle is applied to structure a complex problem into a hierarchy of clusters (see Figure 2.4), sub-clusters, sub-sub-clusters, and so on. The principle of comparative judgment is applied to construct pairwise comparisons of all combinations of elements in a cluster with respect to the parent of the cluster. These pairwise comparisons are used to drive 'local' priorities of the elements in a cluster with respect to their parent (Forman, 2000). The principle of hierarchical composition or synthesis of priorities is the last step. The comparisons are synthesized to get the priorities of the alternatives with respect to each criterion and the weights of each criterion with respect to the goal. The local priorities are then multiplied by the weights of the respective criterion. The results are summed to get the overall priority of each alternative.

The simplest form (see Figure 2.3) used to structure a decision problem is a hierarchy consisting of different levels. The goal of the decision for which a solution is needed forms the top of the hierarchy, followed by the problem decomposed into smaller parts that state pertinent concerns of the problem. A proper decision can be made based on these smaller parts, which are called the evaluation criteria. The evaluation criteria consist of two major types, which are also represented by different hierarchical levels, namely objectives and attributes. The desired condition of the system, which an individual or a group of individuals would like to achieve, is expressed by objective or main criteria, while attributes or sub-criteria are used to characterize the respective objective. To make it clear, imagine a floodwater spreading area. An objective could be the increase in social safety or benefits, explained by control of the damage created by floods in the study

region. For each objective/main criterion, a hierarchical decomposition into attributes is made, where the lowest level of attributes needs to represent measurable entities, which are called indicators.

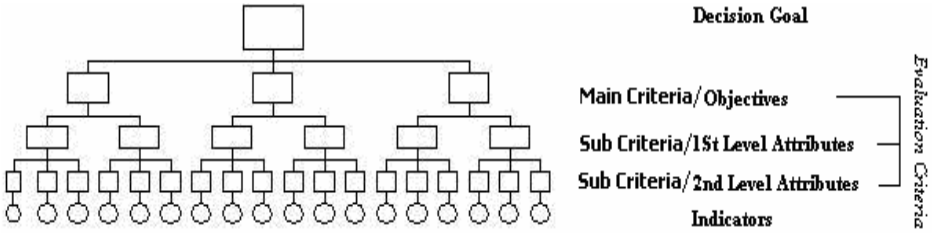

Figure 2.3 Systematic decomposition of the decision problem into main/objectives, attributes/sub-attributes and indicators using analytical hierarchy process (adapted from Saaty, 1980).

For example, referring to the example above, a measurable entity could be the number of persons that could be saved after the operation of floodwater spreading schemes. In order to provide an indication of the achievement of the related objective, a meaningful integration of the underlying indicators is necessary.

2.1.8 Spatial multi-criteria evaluation (SMCE)

There are four analytical function groups present in most GIS models: selection, manipulation, exploration and confirmation. These four functions can be considered as a logical sequence of spatial analysis. Further integration of the maps/results from spatial analysis is an important next step in supporting decision making, and is called evaluation (Anselin and Getis, 1992).

Conventional multicriteria decision-making (MCDM) techniques have been largely non-spatial. They use average or total impacts that are deemed appropriate for the entire area under consideration (Tkach and Simonovic, 1997). The most significant difference between spatial multicriteria decision analysis and conventional multicriteria decision analysis is the explicit presence of a spatial component. Spatial multicriteria decision analysis therefore requires data on the geographical locations of alternatives and/or geographical data on criterion values. To obtain information for the decision-making process, the data are processed using MCDM as well as GIS techniques. Spatial multicriteria decision analysis is a process that combines and transforms geographical data (the input) into a decision (the output). This process consists of procedures that involve the utilization of geographical data, the decision maker's preferences, and the manipulation of the data and preferences according to specified decision rules. In this process, multidimensional geographical data and information can be aggregated into one-dimensional values for the alternatives.

The combination of multicriteria evaluation methods and spatial analysis is referred to as spatial multiple criteria evaluation (SMCE). SMCE is an important way of producing policy-relevant information about spatial decision problems for decision makers. An SMCE problem can be visualized as an evaluation table of

maps or as a map of evaluation tables, as shown in Figure 2.4 (Sharifi and Herwijnen, 2003). If the objective of the evaluation is a ranking of the alternatives, the evaluation table of maps has to be transformed into one final ranking of alternatives. Actually, the function has to aggregate not only the effects but also the spatial component. To define such a function is rather complicated.
Therefore, the function is simplified by dividing it into two operations: (i) aggregation of the spatial component, and (ii) aggregation of the criteria. These two operations can be carried out in different orders, which are visualized in Figure 2.5 as Path 1 and Path 2. The distinguishing feature of these two paths is the order in which aggregation takes place. In the first path, the first step is the aggregation across spatial units (spatial analysis is the principal tool); the second step is the aggregation across criteria (multicriteria analysis playing the main role). In the second path, these steps are taken in reverse order. In the first case, the effect of one alternative for one criterion is a map. This case can be used when evaluating the spatial evaluation problem using the so-called 'Path 1'. In the second case, every location has its own zero-dimensional problem and can best be used when evaluating the spatial problem using the so-called 'Path 2' (Figure 2.5).

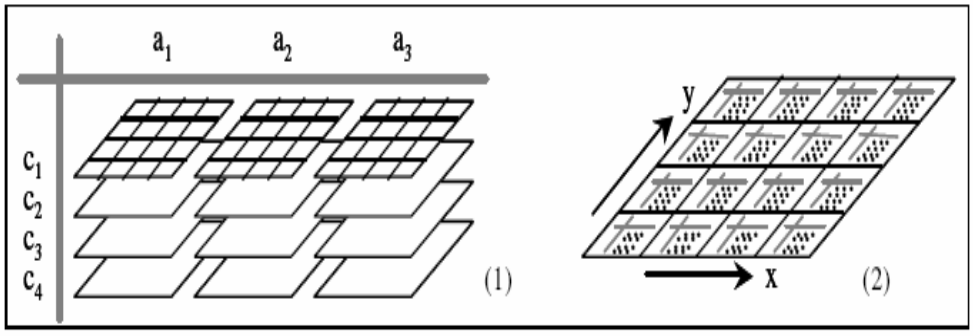

Figure 2.4 Two interpretations of a two-dimensional decision problem (1: table of maps, 2: map of tables)

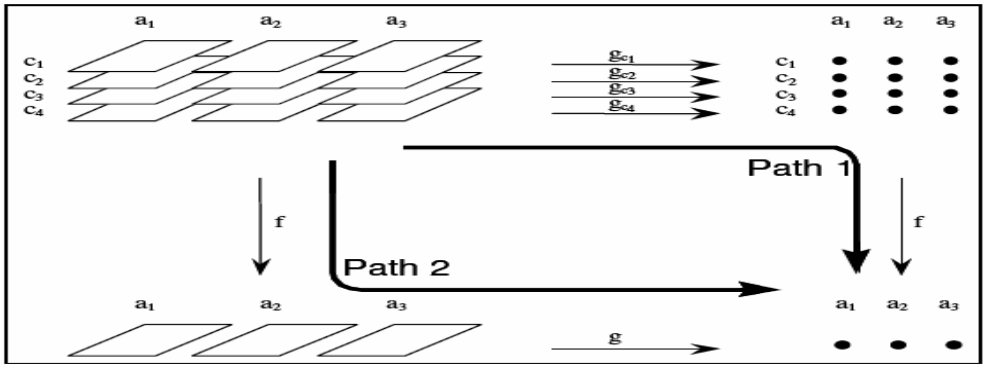

Figure 2.5 Two paths of spatial multicriteria evaluation

2.1.9 Spatial AHP

Spatial AHP is a compensatory approach of the SMCE method, which through utilizing knowledge-based user preferences and interrelated spatial data combines GIS and AHP to identify and rank areas that are suitable for floodwater schemes. By using thematic layers, the spatial AHP method will be designed to analyse and support decisions in which multiple, and even competing, objectives are involved and multiple alternatives are available.

In spatial AHP, a problem is divided into a number of simpler problems in the form of a decision hierarchy. By giving different preference values to main criteria in this study, different scenarios will be produced. According to the AHP decomposition principle, by breaking down reality into homogeneous clusters and subdividing these clusters into smaller ones, large amounts of information will be integrated into the structure of the problem and form a more complete picture of the whole system.

The idea of perceiving relationships among the things observed in nature, of comparing pairs of similar things against certain criteria, and of discriminating between both members of a pair by judging the intensity of their preference for one rather than the others creates a form of priority setting. The judgments are then synthesized with AHP through new logical processes, and better understanding of the whole system is gained during the study. AHP incorporates both the qualitative and quantitative aspects of human thought: the qualitative to express judgments and preferences concisely and the quantitative to define the problem and its hierarchy. Spatial AHP uses selection criteria and area attributes recorded in GIS to identify and rank potential options.

The AHP decision-making method as used in spatial AHP involves the following five steps (Siddiqui et al., 1996): (i) identifying the issues and objectives (i.e. the main criteria) associated with the problem; (ii) structuring them in a decision hierarchy; (iii) judging the relative importance of decision hierarchy elements (the relative importance of decision hierarchy elements for floodwater spreading area selection judged based on expert knowledge, literature, and modelling/simulations); (iv) aggregating these measures in order to calculate a suitability index of the alternatives; and (v) ranking the spatial objects (polygons or raster) according to the suitability index.

In this study, the objective is to identify and rank potential floodwater spreading areas. To do so, study areas will be divided into cells, and AHP is used to rank each cell. The suitability of each cell can be considered to be the function of the utility of the cell indicator values. In spatial AHP, cell indicator values are pairwise compared for each indicator. Cells are grouped into finite elements of categories, based on the pre-existing form of the data/information, modelling and expert judgment.

Relative importance (RI)

Pairwise comparison of all related criteria for the selection of suitable areas for floodwater spreading (see Chapter 6, Figure 6.2) will be used to establish the relative importance of the hierarchy of criteria. Decision makers or experts verbally

judge pairs of grouped criteria in terms of their relative importance concerning the objective to which they contribute (i.e. the factor they are connected with at the next highest level (decision structure or decision tree)).

For the hierarchy (decision structure; see Figure 2.3) of the suitable floodwater spreading area selection (see Chapter 6, Figure 6.2), the relative importance of four main criteria – floodwater, infiltration, water application and flood damage – for area suitability for floodwater spreading will be compared using a pairwise comparison method. Then, within a sub-criterion, the relative importance of each criterion will be compared. For example (see Figure 2.6), the sub-criteria for the main criterion infiltration are topography, aquifer and soil. These sub-criteria will be compared pairwise.

Each sub-criterion has some main indicators. For example, the main indicators for the topography criterion are slope, river type and stability, and surface area features. The relative importance of slope and other main indicators (river type and stability, and surface area features) will be evaluated. Finally, for each main indicator the relative importance of each possible sub-indicator will be compared. The verbal pairwise comparisons of the criteria, using the linguistic measure of preference (LMP) (Saaty, 1980; Table 2.1), will be converted to ratio scale by calculating the geometric mean of each row. For example, the decision matrix/table for slope indicator is shown in Table 2.2. In this table, the suitabilities of different slope classes (0 to 1%, 1 to 2%, 2 to 3%, etc.) are compared using LMP.

Table 2.2 Calculation of the relative importance weights for slope map

(Slope class)	0 to 1	1 to 2	2 to 3	3 to 5	>5	Geometric Mean	Relative Importance
0-1	1	5	7	8	9	4.7894	0.5469
1-2	1/5	1	6	7	8	2.32	0.2649
2-3	1/7	1/6	1	6	7	1	0.1142
3-5	1/8	1/7	1/6	1	6	0.4471	0.0511
>5	1/9	1/8	1/7	1/6	1	0.2013	0.0230

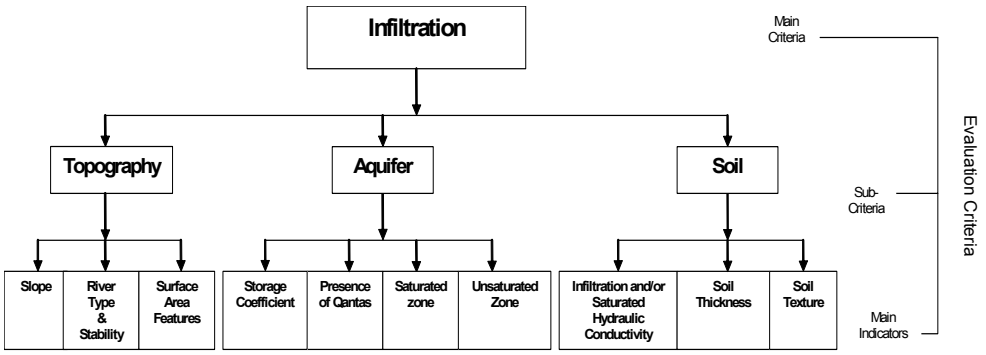

Figure 2.6 Decision structure of suitable floodwater infiltration sub-area evaluation for floodwater spreading

For example, the first row compares the suitability of slope class '0 to 1' with other slope classes, e.g. class '1 to 2'. Here, based on the Saaty scale (LMP), '5' represents strong preference or more suitable, and so on. The cells above and

below the diagonal are reciprocals, indicating opposite preferences. The relative importance assigned to each hierarchy element or criterion is determined by normalizing the geometric mean of the decision matrix.

The decision makers/experts may have various ideas about the importance of different criteria; therefore, by giving dissimilar preference values to different evaluation criteria, different scenarios can be created.

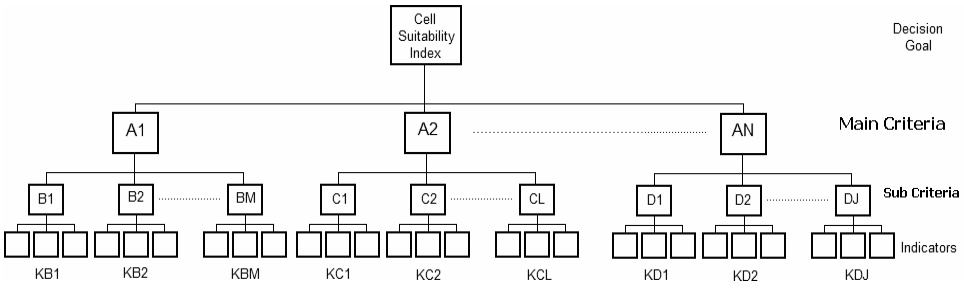

Figure 2.7 Decision criteria structure consisting of four hierarchical levels

Suitability index (SI)

A suitability index for each cell is determined by aggregating the relative importance (RI) at each level of the hierarchy, using Equation 2.1. Suitability indices for all cells are determined simultaneously using GIS operation or map algebra. Equation 2.1 for a four-level hierarchy is expressed as:

$$SI = RIA1 * \sum_{i=1}^{m} RIBi * RIKBi + RIA2 * \sum_{y=1}^{L} RICy * RIKCy + \ldots\ldots\ldots RIAN * \sum_{z=1}^{j} RIDz * RIKDz \qquad [2.1]$$

where SI = the suitability index of each cell; N = the number of main criteria A (see Figure 2.7); RIA1, RIA2 and RIAN = the relative importance of the main criteria A1, A2 and AN respectively; M, L and J = the number of sub-criteria directly connected to the main criteria A1, A2 and AN respectively; RIB, RIC and RID = the relative importance of sub-criteria B, C and D directly connected to the main criteria A1, A2 and AN respectively; RIKB, RIKC and RIKD = the relative importance of indicators category k of sub-criteria B, C and D and main criteria A1, A2 and AN respectively. If a decision hierarchy has more or fewer levels, the equation must be appropriately modified.

2.2 Hierarchical DSS for floodwater spreading site selection

The DSS for floodwater spreading site selection (see Figure 2.8) developed in this research has a scale hierarchy consisting of three levels of scale and data contents:

- small scale (cartographic) for the identification and selection of potential zones
- medium scale for area(s) suitability evaluation
- large scale for evaluating the suitability of site and type of design.

The DSS diagram has been developed based on further elaboration of Figure 2.2. The input data are related to the external and internal database management; the three models for three scales are elements of the model base management. In the small-scale phase, suitable zones for floodwater spreading will be selected, leading to the grouping of potential areas into a few broad categories of relative suitability. In the medium-scale phase, the potential areas in the selected zone will be evaluated and ranked based on their suitability for floodwater spreading, and will be used for selecting an area. The selected area will be studied further in the large-scale phase in order to identify, evaluate and select the suitable site and design types for floodwater spreading schemes. The product consists of options for a decision maker, noting global costs and benefits associated with a suitable design type for the site.

2.2.1 Zone selection (small scale)

At the first scale (small scale), screening is done for potentially suitable zones with the assistance of remotely sensed data, available knowledge and expert knowledge. A zone is a more or less contiguous tract of land where alluvial aquifers are found, with ephemeral or perennial rivers traversing the alluvial areas that are not fully occupied by irrigated lands. Zones generally have much internal variation; hence 'areas' must be identified using additional criteria in order to group areas according to their overall suitability. As mentioned in Chapter 1, the main objective of this phase is to develop and evaluate a method for screening zones containing feasible areas, as a component of the DSS.

The criteria for the small scale are judged qualitatively and the suitable zones containing potential areas for floodwater spreading are selected. Once they have been assessed, the MCE method is used at semi-detailed (medium scale) level to identify one or more highly promising areas for which it is worthwhile to acquire more detailed field data (quantitative and qualitative) and locate the suitable site(s).

Method

A problem is to gather the information on the many aspects that have to be considered in a spatial context and on their mutual relations. To do so is a very lengthy process. Moreover, most of the effort is wasted because data of many areas are discarded after the screening because only a few suitable areas inside a zone will remain. Therefore, the approach followed is similar to the one adopted in soil survey and land evaluation: from reconnaissance scale to semi-detailed scale. This scale explores to what extent interpretation of remotely sensed images supported by local field knowledge and supplemented by information from topographical maps and geological maps and by other data leads to the identification of potential areas in the zones. The image interpretation requires knowledge of (photo) geology, geomorphology and the relationships between physiography and soils, supported by knowledge of local conditions or those having similarity.

As discussed later, the interpretation makes use of interrelationships between such factors as catchment geology and relief, the nature of alluvial deposits, tectonic and geomorphological history, and the nature of the rivers and land cover.

The aquifer presence and properties (depth, transmissivity, permeability) are based mainly on interpretation of the tectonic setting and geomorphological history by applying principles of photo-geology (Miller and Miller, 1961; Drury, 1987) and information from geological and topographical maps. Geophysical and drilling data for some aquifers are used, also for extrapolation to unknown areas on the basis of similarity.

Geomorphological interpretation (Verstappen, 1977; Way 1978) is used to assess the nature of alluvial deposits in relation to the tectonic setting and to estimate relative sediment yields (qualitative). Image interpretation for groundwater is reviewed and discussed by Meijerink (1996).

Transmission loss is judged (qualitatively) by variation in channel dimensions, as discussed in Chapter 1.

The land use patterns yielded information on the presence of aquifers, salinity problems and the availability of rangelands in the infiltration areas. The phreatophyte vegetation and water emergence in channels when coupled to soil salinity patterns are taken as an indication of groundwater outflow, hence shallow groundwater conditions.

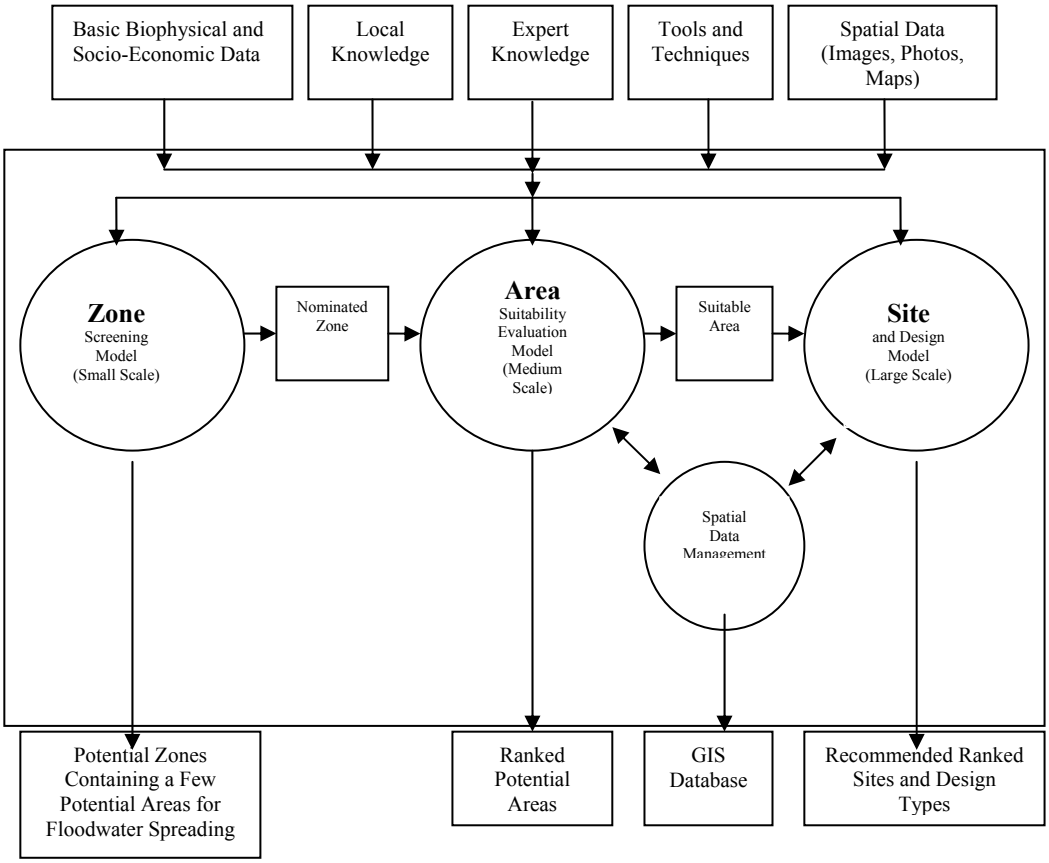

Figure 2.8 Floodwater spreading site selection DSS diagram

Satellite images

The advantage of satellite images is that both catchment areas, infiltration and application areas can be viewed in a single image and that some aspects can be highlighted by using common image processing techniques. Aerial photography has the advantage of high spatial resolution and good stereo display of the terrain.

The colour images used are false-colour Landsat Thematic Mapper (TM) images. Because various combinations are possible, the notation TM 742 stands for a combination whereby band 7 is coded in red, band 4 in green and band 2 in blue, etc. Since irrigated crops have a high reflectance in the near infrared band, band 4, and low reflectance in the other bands, the fields with green crops show up in green tones. If TM band 4 were coded in red (e.g. TM 432), the fields would show up in red tones. Contrasts can be enhanced so as to 'sharpen' features on an image, by using appropriate histogram operations and by using Laplace type of filters. Certain features of interest, such as areas with loose sediments with high infiltration and deposited recently by active floods, can be highlighted by images resulting from orthogonal decomposition of the spectral data, such as the Principal Component method.

Decision criteria

The main criteria (exclusionary) for the qualitative evaluation are given below;

Runoff or floodwater availability

For most of the small and medium-sized catchments in Iran there is no gauged data and therefore the initial selection procedure, or screening, has to rely on estimation methods.

Rainfall data are not considered in the screening *per se* because it is assumed that in all arid and semi-arid regions there is a need for augmenting the groundwater resource. Moreover, in Iran provincial and local authorities decide on the location, and the spatial distribution of rainfall generally does not vary much in the zones of the semi-arid provinces that are in need of and have potential for floodwater spreading schemes. In working out the conceptual designs (medium and large scales), rainfall data are considered in the estimation of the runoff. However, in the arid tracts of Iran with less than 150 mm annual rainfall, settlements and irrigated agricultural lands are so sparse that recharge schemes are only relevant if some increase in qanat discharge is desired.

Because of the absence of runoff regionalization studies in Iran, the relative magnitude of the ephemeral runoff in the screening is judged qualitatively on the basis of catchment size and overall catchment permeability based on the proportion of permeable rocks, as explained in Chapter 1. Catchments with a size of less than some 10 km^2 are not considered, because of the limited runoff volumes. Large catchments of 1000 km^2 or more pose a problem because of the magnitude of the peak flows with longer return periods. Permanent intake structures are expensive and episodic huge amounts of sediment can affect the lifetime of a scheme substantially. However, because of the large amount of water from large catchments, also at lower return periods, they are not excluded in the screening process.

Water quality

As flood runoff is a fast response to rainfall and the catchments have generally only a sparse rangeland cover and no industry or settlements, the quality criteria are met, unless rock salt outcrops and their derivatives are present in the catchment. In the latter case, absence of irrigated fields in alluvial areas can be taken as an indication that the groundwater is saline. Erosion of the salt domes causes deposition of pebbles of rock salt in the glacis or bahada deposits and in the riverbeds, rendering the water quality unsuitable. The presence of a salt dome in the aquifer does not necessarily exclude the area from consideration. A water quality study of the Sarchacan Plain aquifer, Hormozgan (Hossainipoor, 2000), showed groundwater that could not be used for irrigation to occur only downstream of a salt diapir, with minor lateral dispersion. Actually, a floodwater spreading scheme is present upstream of the dome. Groundwater in the lower part of alluvial deposits near the coastal plain or playas can have high salinity levels, as witnessed by saline soils and non-contiguous irrigated fields, and that imposes a restriction.

Sediment, amount and type

The relative volume of sediment in the screening at reconnaissance level is judged from the catchment geology, relief, dissection, bankful width of the channel and strong signs of aggradation or sedimentation. It is of interest to detect excessive sediment yields, which affect the lifetime of a scheme to such a degree that it may not be feasible. Excessive sediment yields in Iran are often related to active tectonic uplift affecting weak rocks such as mudstones and shales, causing acceleration of fast geological erosion by landslides, and gully and ravine formation in certain geological and geomorphological settings.

Excessive width of the riverbed for the size of the catchment and the gradient is usually associated with such fast geological erosion, but it should be remembered that aggradation could have been caused by episodic events when tremors occurred during a period with much rainfall. Such catchments have been excluded from further consideration.

Because of the large temporal and spatial variation and the difficulty of estimation, best use of local data on sedimentation should be made. In some cases, the relative sediment yield can be judged by the maintenance required in existing schemes. That information related to catchment geology and relief is of much help in making estimations in adjoining catchments. The relative magnitude of the coarse bedload (sands and coarser) and that of the suspended/saltation load (sands and finer) can be judged from catchment geology and relief, as well as gradient of the fan, nature of the riverbeds and types of depositional patterns of low sediment yield. The alluvial deposition resulting from a suspended load type of river results in different patterns from those of bedload deposition.

Surface area features (land use)

A trivial, but important criterion is that the potential infiltration area should be sufficiently large and the land cover should preferably consist of rangelands or bare areas, which generally belong to the government. Areas suitable for infiltration from a hydraulic point of view are excluded if occupied by irrigated fields and industrial

lands. The high cost of acquiring privately owned lands will be weighted during the next stage of evaluation.

Presence of aquifer and its properties (transmissivity and permeability)

The presence of reflectance due to dense green crops and the absence of surface water irrigation indicates the presence of groundwater and hence an aquifer, because in hot regions with less than 350 mm annual rainfall no rainfed agriculture is possible. The irrigation water can be derived from qanats, which are shown on the topographical maps, and from wells, usually tubewells fitted with diesel-fuelled pumps. It is a safe assumption to relate the extent of irrigated fields with good crops, as observed on RS images, to aquifer properties, except perhaps in some remote areas, where lack of capital and poor marketing conditions could have led to under-utilization of the groundwater, or in areas where water quality is poor.

Also, in the screening process, attention should be paid to the transmissivity of the aquifer. Most recharge by floodwater spreading takes place in mountain-front alluvial fans, where transmissivities vary much in the downstream direction. The general permeability can be interpreted by considering the catchment lithology and relief and the steepness of the alluvial fan, because of the relationship between gradient and average grain size of deposits (Pettijohn, 1957).

Transmission loss

The importance of transmission loss, as discussed in Chapter 1, can be so high that little floodwater of the smaller systems leaves the area, and that can be interpreted on images. When natural recharge is important, the urgency for artificial recharge may be questioned. Such high loss is witnessed by a sharp reduction in the bankful width of ephemeral rivers on alluvial fans. The width to depth ratio or shape of the bankful channel does not change much in the unconsolidated coarse bed and bank materials in the downstream direction. Hence, if the width is reduced, the depth is reduced and thus the cross-sectional area, which indicates loss of discharge (transmission loss) because the gradient becomes less in the downstream direction.

Strong sedimentation or aggradation can cause water to spread out over a wide surface on the alluvial fan, increasing both infiltration area and time for infiltration. In the interpretation for the screening, attention should be paid to the mountain front because most irregularities can be expected here, such as outcrops at shallow depth and the presence of impervious lime crusts. If the tectonic setting indicates rapid fill of a subsidence area along an active fault, the deposits are likely to be thick, fairly homogeneous and permeable.

Saturated zone

Below the infiltration area, the groundwater table should be at sufficient depth to enable an increase in head by recharge without reaching the upper zone. If so, evaporation losses will occur owing to capillary rises. Theoretically, a very deep groundwater table in the infiltration or recharge area can be accepted because it is assumed that infiltrated water percolates down to the saturated zone without being subject to evaporation loss. However, there will be considerable time delays of recharge fluxes if the groundwater table is deep, and the probability of perched

water tables and semi-confined groundwater water is higher in deep aquifers than in relatively shallow phreatic aquifers, and this complicates the evaluation of the effectiveness of the recharge scheme.

In the lower alluvial fan, outflow of groundwater can occur in riverbeds, signifying the intersection of the piezometric surface and the topographical surface. Assuming a semi-logarithmic shape of the groundwater surface and by having information of a few depths to groundwater in the middle or upper fan, a fair idea of the groundwater surface can be obtained and, in combination with estimated depth and hydrogeological parameters typical of alluvial fans, the aquifer properties can be estimated at a level that is sufficient for the screening.

In some areas, the lower part of the fan has an incised river. If groundwater from the fan flows into the river, increase in the head by artificial recharge increases the outflow, and hence loss of water. In such cases, a proper pumping scheme has to be adhered to. A groundwater or piezometric surface well below the capillary zone in the lower alluvial fan is favourable in terms of absence of salinity hazard.

Soil properties affecting infiltration

The effect of soil texture on infiltration will be discussed in Chapter 3. At the screening level, only the overall soil conditions in the floodwater infiltration sub-area with respect to infiltration are considered for the basin and canal type of schemes. Non-dissected sloping alluvial surfaces are likely to have good infiltration because of the coarse-grained texture of the soil, especially if the soils are relatively young (i.e. signs of sub-recent river deposits are present). The presence of lime crusts causes poor infiltration and for that reason the recharge experiment in Zanjan Valley, near the river Zaker, Iran, was abandoned.

Rangeland conditions on large accumulation glacis that had never been cultivated had lower runoff, and thus higher infiltration, compared with runoff from lands on the same glacis that had been cultivated, as the observations of Liaghati (2000) and Eftekhari (2000) at soil and water conservation works in central Iran show.

Water demand

In this phase, the water demand will be estimated (qualitatively) based on the presence of areas suitable for irrigation, agricultural lands, villages, cities and industrial areas as indicators. The presence of irrigated lands on the lower to middle part of the fan indicates that soils are suitable for irrigation because textures become gradually finer in the downstream direction. The increase of clay contents accounts for increase in water holding capacity and soil fertility. It can be judged on images at the screening stage by how much the irrigation can be expanded. Also the presence of agricultural lands, villages, cities and industrial areas in the lower parts of the fan (water application part) will be a good indicator for water demand.

Soil salinity

The semi-arid climate, the presence of heavier textured soils on the lower part of the fan, and a shallow groundwater table usually lead to a salinity hazard (discussed in Chapter 5) in some of the cases situated near the coastal region or playas.

Emergence of groundwater in the riverbeds, which can be observed on images, is a sign of a shallow groundwater table in the lower part of the fan.

The presence of saline soils owing to capillary rise from shallow groundwater complicates the screening process. A recharge scheme upstream of the affected areas raises the head of the freshwater body in the aquifer and could move the sweet-brackish water interface in the downstream direction. However, an increased groundwater level will move the zone with capillary rises upslope, as has been noted, for example, in the Goorband scheme in Iran, where irrigation from canals caused the rise of the groundwater level in the middle and lower parts of the fan (Pishkar, 2003). In such cases, a recharge scheme should be accompanied by controlled pumping operations to prevent the rise of the groundwater table in the lower part. However, control of pumping is still difficult to achieve in Iran.

Remarks

The screening primarily focuses on exclusionary criteria to reject areas or parts of the alluvial zone bordered by catchments. Those parts that have not been rejected are grouped into a few broad categories of estimated relative suitability for further scrutiny in the next stage. In Chapter 5, a number of examples from Iran are provided that discuss why certain areas that may fulfil all but one criterion are rejected and how the potentially suitable areas within a broad zone are judged and categorized.

2.2.2 Area(s) selection (medium scale)

An evaluation method is proposed for the second scale (medium scale). This method aims at avoiding time-consuming and data-demanding deterministic hydrological simulation models (see Figure 2.8) by using a knowledge-based model. Knowledge could be obtained from experienced farmers, qualified experts and formalized scientific knowledge bases. Examples of information that may be required include history of the flood events, and agricultural management and socio-economic data. As mentioned in Chapter 1, the main objective of this phase is to develop and evaluate a DSS for finding the 'suitable area' within a zone.

Area definition

A floodwater spreading area is a system that consists of a catchment area where floodwater runoff and sediment are generated, an infiltration area and an application area, as sketched in Figure 2.9. The catchment area is usually not isotropic in terms of runoff and sediment delivery and can be separated from the infiltration area by a transitory channel. The infiltration area should consist of permeable alluvial deposits of sufficient depth. It has some natural recharge by transmission loss because the groundwater is below the riverbed, and by diversion of floodwater to a controlled infiltration scheme the recharge is artificially augmented. The application area benefits from the artificial recharge by withdrawal of groundwater for irrigation or drinking water and possibly by reduction of flood damage by diversion of part of the floodwaters. The suitability of all the spatial elements defines the appropriateness of the whole system for a floodwater spreading scheme.

Decision criteria structure

A suitable area for floodwater spreading can be characterized by four main criteria, as structured[3] in Figure 2.10. This means the suitability of an area for floodwater spreading will be judged based on the aggregate suitability of its floodwater, infiltration, water application, and finally the amount of damage caused by the previous floods. In the following, each of the above main criteria are further elaborated.

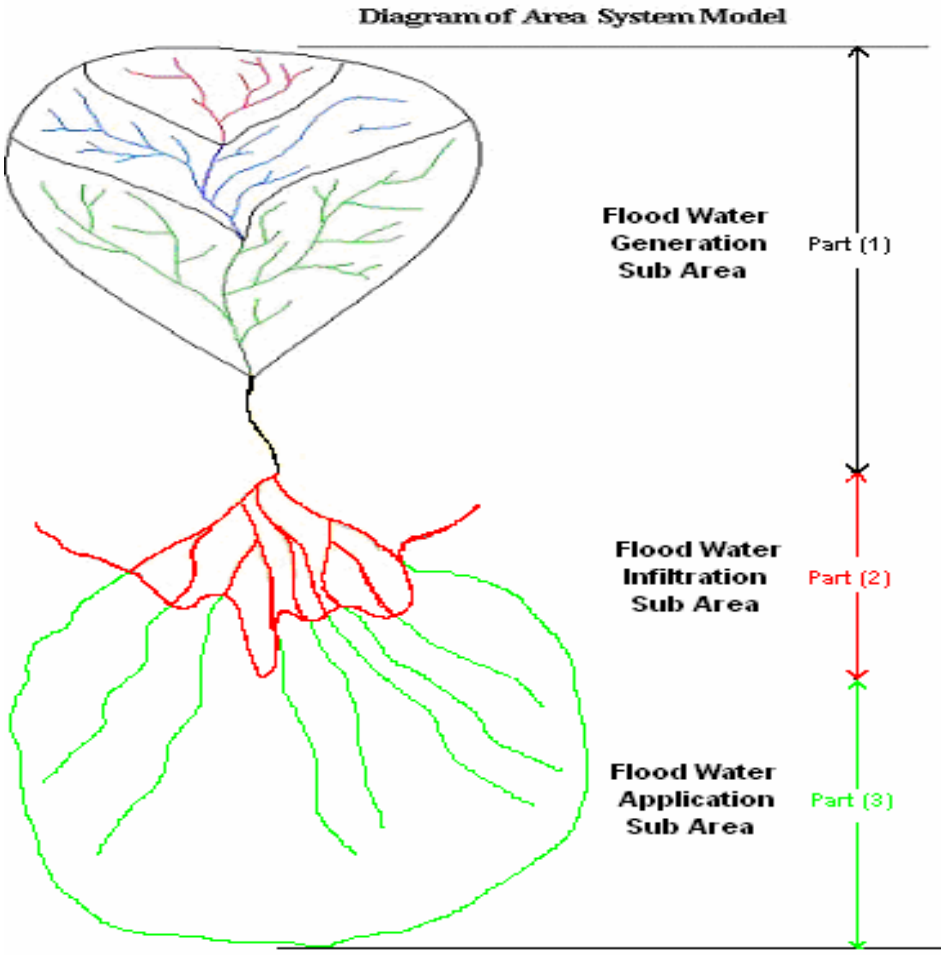

Figure 2.9 Schematic overview of the elements of a floodwater spreading system

[3]Before starting and structuring the decision criteria, it should be considered that many listed criteria and indicators in the following are based on an analysis of the system that governs generation of runoff and sediment and infiltration of diverted floodwater on alluvial fans waters for artificial recharge. The criteria listed under 'social acceptance' are based on interviews with many persons that have been involved in the selection and design of flood spreading schemes in Iran, apart from the personal experience of the author in this domain.

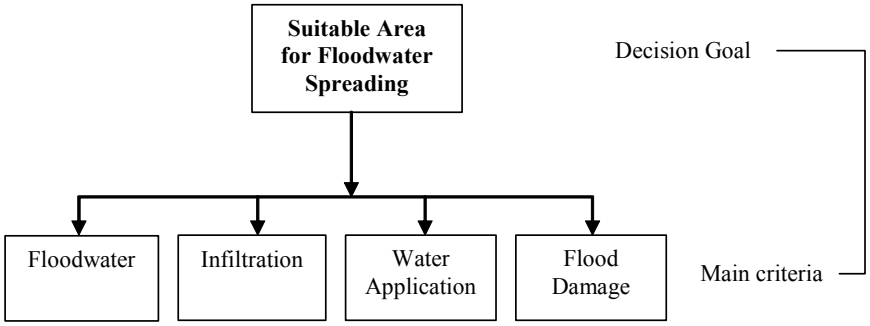

Figure 2.10 The four main criteria for suitable floodwater spreading area selection

Main criterion floodwater

The structure for evaluating the main criterion floodwater is shown in Figure 2.11.

Sub-criterion water

An important factor in floodwater spreading projects is of course the amount of water that is generated by daily floods. This can be characterized by the volume of water generated (runoff), its quality, and the intensity of occurrence.

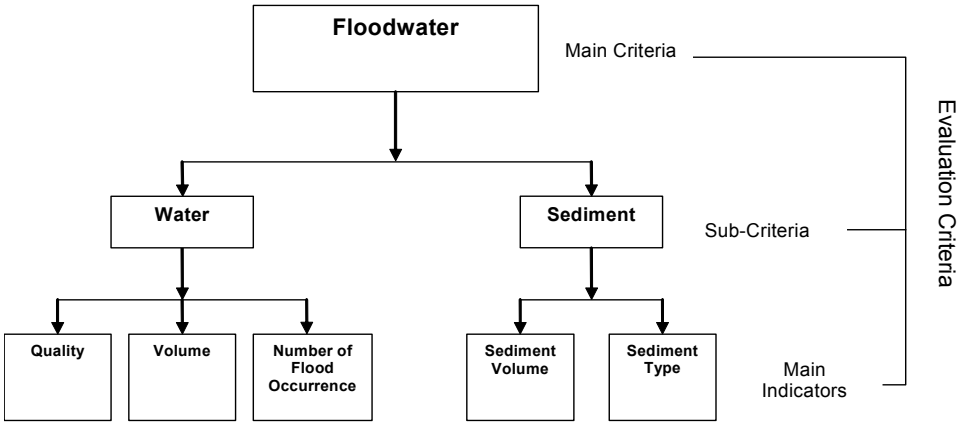

Figure 2.11 The criteria structure for suitable floodwater generation area evaluation

(1) Main indicator water volume
If no discharge records exist, the water volume of the study areas is estimated based on available rainfall information and the well-known curve number method of the Soil Conservation Service (SCS, 1972).

(2) Main indicator number of flood occurrences
In addition to floodwater volume, the number of flood occurrences in the study areas is also important for catchment selection. In Chapter 3, it will be explained that flood events with the same amount of water volume but

occurring at relatively short intervals have more recharge efficiency. The number of flood occurrences (per year) in the study areas are estimated based on available data and/or results of the SCS method and/or interviews with the local people.

(3) Main indicator water quality
The chemical water quality of the floods in the study areas is assessed based on available information and/or using the qualitative method explained by the Ministry of Jahad-e Agriculture (Peyrovan, 1997), based on the geological formation of the study areas. In this method, the quality of the water that passes through the specific formation is qualitatively classified.

Sub-criterion sediment

(1) Main indicator sediment volume
Another important factor is the amount of sediment that a flood can generate. This is characterized by its volume and type. The sediment volume of the study areas is estimated based on available information and/or well-known empirical methods such as MPSIAC.

(2) Main indicator sediment type
The main indicator sediment type is estimated based on two sub-indicators, sediment texture and soil erodibility factor (K), using the well-known USLE (Wischmeier and Smith, 1965) method. The sediment texture of the study areas is estimated using lithological units supported by granulometric sampling. The soil erodibility factors are obtained based on the nomogram of the USLE method.

Main criterion infiltration

The structure for the evaluation of the factors for the main criterion infiltration is shown in the Figure 2.12.

Sub-criterion topography

An important sub-criterion for infiltration evaluation is topography. This can be characterized by the main indicators slope, river type and stability, and surface area features.

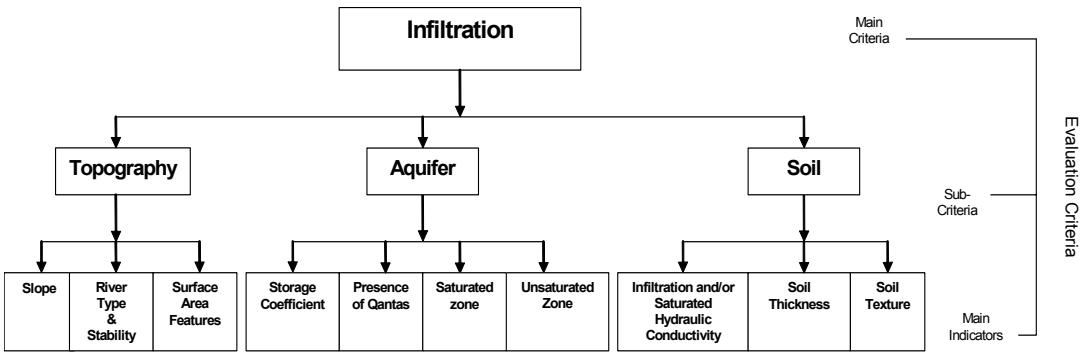

Figure 2.12 The criteria structure for suitable floodwater infiltration area evaluation

(1) Main indicator slope
In this phase, slope steepness is determined using the interpolation of data with standard GIS procedure (ILWIS 3.0 Academic: User's Guide).
(2) Main indicator river type and stability
The suitability of the river type and stability (intake possibility and need for river training) for floodwater spreading is classified/estimated using available literature, expert opinion and field observation.
(3) Main indicator surface area feature
The main indicator surface area feature of the study areas is estimated based on five sub-indicators: land use type, existence of infrastructure (power lines, pipe lines, etc.) passing through the areas, evenness of the surface area, distance of each surface point to the main river, and existence of access road indicators. These indicators are estimated based on available information such as topographical or land use maps. On the other hand, as all the mentioned indicators are spatial objects, different RS-GIS techniques, such as supervised classification, distance operation and image interpretation, are used to measure them. Field checks and local interviews complete the information.

Sub-criterion aquifer
The second sub-criterion is the aquifer. This criterion can be estimated by four main indicators: storage coefficient, presence of qanats, unsaturated zone and saturated zone.
(1) Main indicator storage coefficient
The storage coefficient of the aquifer for the alternative areas is estimated based on maps published by the Iranian Ministry of Power.
(2) Main indicator presence of qanats
The presence of qanats obviously signifies favourable aquifer properties. In this phase, the presence of qanats is determined using topographical maps.
(3) Main indicator unsaturated zone
The main indicator unsaturated zone is measured by two sub-indicators: thickness and hydraulic conductivity. These indicators of the unsaturated zone are estimated based on maps published by the Ministry of Power, or they could be measured in an observation or in irrigation wells in the study areas.
(4) Main indicator saturated zone
The main indicator saturated zone is measured by three sub-indicators: hydraulic gradient, transmissivity and groundwater quality. These indicators are estimated based on maps published by the Ministry of Power or are measured in the available wells in the study areas.

Sub-criterion soil
The last sub-criterion for the main criterion infiltration is soil. The soil criterion of the alternative areas is estimated based on three main indicators: soil infiltration, thickness and texture. These indicators are estimated based on available maps published by the Iranian Soil and Water Research Institute. In the case of lack of data, these indicators are observed in the field.

Main criterion water application

The criteria structure for the main criterion water application that has to be considered for the implications of a scheme is shown in Figure 2.13. The sub-criteria pertain to water demand, social acceptability and environmental aspects.

Sub-criterion water demand

The water demand (for industrial, agricultural and drinking purposes) in the study areas is estimated based on available information about agricultural lands, industrial areas/units and villages/cities published by the Tehran Province Planning and Management Organization of Iran (TPPMO) and on interviews with local responsible government offices.

Sub-criterion social acceptability

The sub-criterion social acceptability is estimated based on five main indicators, which are given below.

(1) Main indicator water rights of people living near the flooding river
    Information about water rights is available from the local government offices.
(2) Main indicator presence of qanats
    In addition to the importance of the presence of qanats in the infiltration area, the presence of qanats in the application area is also of relevance because upstream artificial recharge increases their performance in the application area.
(3) Main indicator unemployment rate
    The third indicator is the unemployment rate for the people of the villages or cities in the study areas. This index is estimated based on information published by the TPPMO and/or on interviews with local responsible government offices.
(4) Main indicator aquifer depletion and/or land subsidence
    The fourth indicator is the aquifer depletion and/or land subsidence problems in the study areas. Information about aquifer depletion is available from the Ministry of Power. Also, by using the groundwater table maps of different years of the study areas, the rate of water depletion can be obtained. Information about land subsidence problems, which are normally caused by aquifer depletion, is available from the local government offices.
(5) Main indicator population growth rate
    The last indicator for the social acceptability criterion evaluation is the population growth rate in the cities/villages of the study areas. This indicator is measured based on information published by the TPPMO and/or on interviews with local responsible government offices.

Main criterion flood damage

The fourth main criterion for suitable floodwater spreading area selection is flood damage. The decision structure for the evaluation of this criterion is shown in Figure 2.14.The flood damage criterion is measured based on available information published by the government and/or on local interviews regarding the three indicators loss of life, agricultural damage, and infrastructure and industrial damage caused by flood events in the study areas.

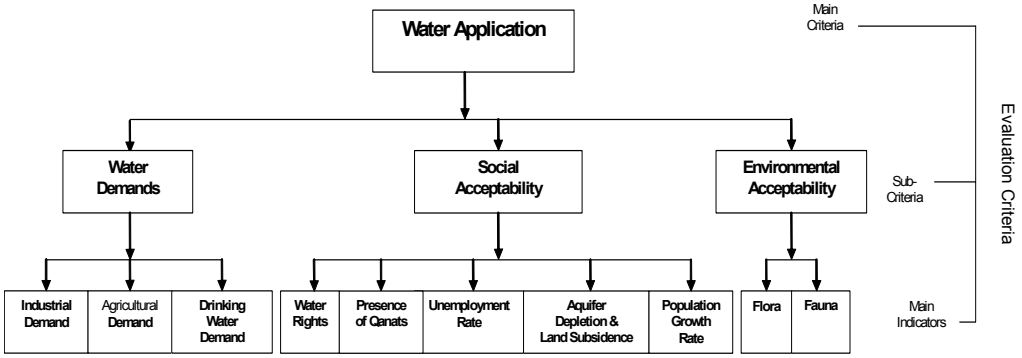

Figure 2.13 The criteria structure for suitable floodwater application evaluation

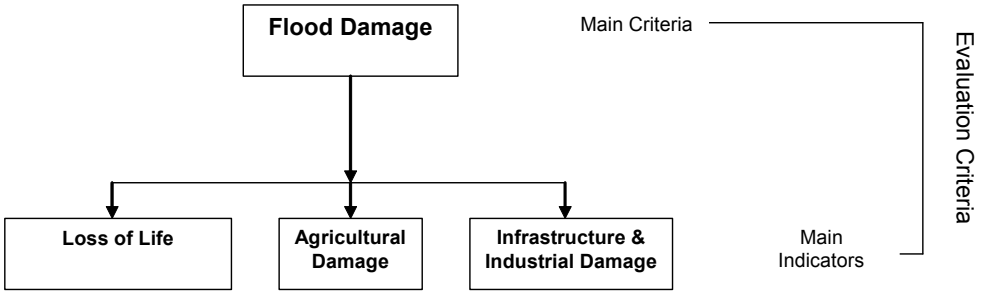

Figure 2.14 The criteria structure for flood damage criterion evaluation

After all the above-mentioned criteria have been estimated for the alternative areas, the SMCE module explained earlier is used for selecting the most suitable area. The procedure is applied to the Varamin Plain zone that was identified in the zone selection scale as a potential/suitable zone.

It should be noted that different decision makers/experts may give different importance to the evaluation criteria. Therefore, different scenarios are generated by assigning different relative importance (RI) to the main four decision criteria.

2.2.3 Site and scheme selection (large scale)

When a suitable area is selected, the floodwater infiltration sub-area part is evaluated as a potential site for developing a floodwater spreading scheme. In this phase, hydraulic, hydrological and technical design type and precise site delineation are determined. Here 'site' is defined as 'a designated area within the floodwater infiltration sub-area for which one or two different types of schemes are feasible'. As mentioned in Chapter 1, the main objective at this scale is to work out a method to arrive at options for decision makers with regard to type and size of scheme that honours the site-specific characteristics of the 'suitable area'.

Before the criteria for suitable site and design type selection are discussed, it is useful to first present the types of scheme differentiated here. Considering the

characteristics of the river and the site, only two common types of scheme are discussed:

(1) the canal and basin type, which consists of one or more intakes at the river to divert floodwater via a supply canal to spreading canals. The dimensions allow overflow into an infiltration basin along the canal, formed by a soil surface of sloping terrain to a downslope earth dam.
(2) the deep basin type, consisting of one or more fully or partly excavated basins in a cascade.

Other types exist, such as the one consisting of long dikes across wide, active alluvial fans without suitable intake sites, as well as hybrid types. However, the method for working out the options for decision makers will be – *mutatis mutandis* – similar to the one discussed here.

Definition and structuring of the decision criteria

The criteria decision structure for the suitable site is shown in Figure 2.15.

The suitable site and design type selection decision structure has two main criteria: costs and benefits. The costs criterion is evaluated based on construction and maintenance costs indicators. These indicators are measured for different scenarios based on the types of scheme and project design diversion discharge.

The benefits criterion is estimated based on the volume of the harvested water and on life saved (human or animal), infrastructure, and agricultural, industrial and residential areas. The volume of harvested water is estimated based on the results of the simulations in Chapters 3 and 4. As already mentioned, the site selection and scheme development take place in the infiltration part of the area selected as suitable during the evaluation in the medium-scale phase. The GIS database is expanded for working out the types of scheme design.

The first step is to use exclusionary criteria to exclude sites from further consideration, based on physical impracticality – for example, areas covered by surface water, residential area, infrastructure, roads, industrial lands, etc. The second step is to use non-exclusionary criteria to evaluate the suitable site and related design types based on data/information recorded on GIS maps.

The hydraulic/hydrological parameters of the study area (such as peak discharges with different return periods, floodwater volumes with different return periods and sediment characteristics) are estimated using proper methods in relation to data availability. Since gauging data for the catchments with ephemeral rivers are scarce, the computed results using hydrological methods or models should be checked with fieldwork, interviews with local people, and any related available data, even though the data may have been recorded for a short period of time.

Based on available information in the GIS database (such as slope, storage coefficient, transmissivity, infiltration rate, etc.), simulation results explained in Chapters 3 and 4, expert knowledge, field observation (such as possible/suitable intake locations), technical/hydraulic design considerations and main design types, a few alternatives are generated and their performance under various scenarios is assessed in terms of amount of harvested water, costs and benefits. The result is presented to the decision makers in a suitable format. The alternatives to be presented should elucidate the quantity of recharge water that could be expected

with the different types of schemes at the particular site, the costs involved, and the estimated collateral benefits, such as mitigation of flood damage.

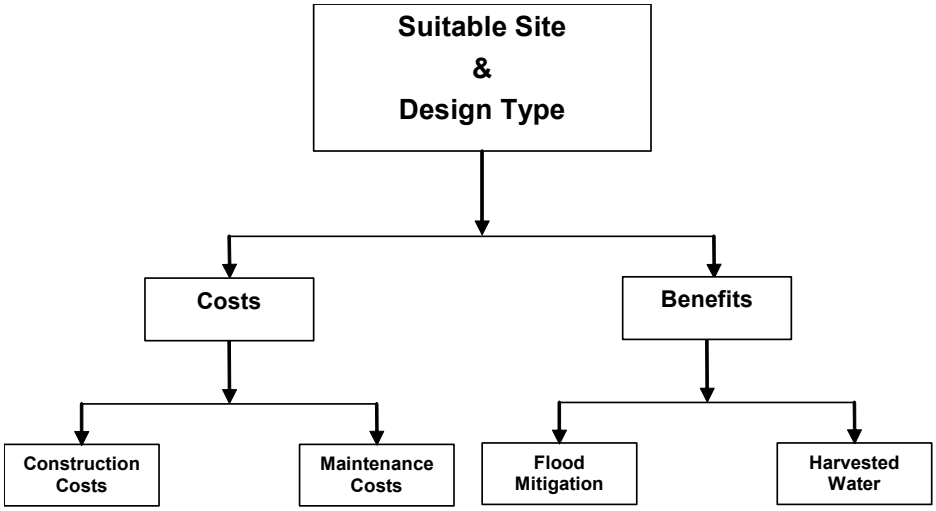

Figure 2.15 The criteria decision structure for suitable site and design type selection

CHAPTER 3
Water Recharge Assessment Using a Numerical Model

3.1 Introduction

Various designs for floodwater spreading have been put in practice (Kowsar, 1982, 1995; UNDP/FAO, 1987; Van Arst, 1987; Prinz, 2002), but little is known about the tradeoff between construction and maintenance costs versus the benefits of the cubic metres of recharged groundwater (discussed in Chapter 7). However, as the selection of proper sites and designs will influence that tradeoff, it is important to know the effects of a number of technical criteria/factors, and these will be investigated here.

Since one of the most important objectives is to maximize recharge, evaporation loss should be minimized. The question then is, what is the influence of soil texture on the proportion of water applied reaching the groundwater table, or in other words, the recharge. Depending on the design of the scheme, the floodwaters can be distributed with different depths over designated infiltration areas. Hence the effect of water depths on the recharge will be investigated. A related question concerns the frequency of the inundations in the scheme. Assuming the same average annual volume of diverted water, what results in more recharge? Several events of low magnitude or a single or a few events of larger magnitude? Finally, the diversion and spreading of floodwaters cause sedimentation and it is necessary to know the effects that sand, silt or clay layers on top of the soil or geological deposits have on the proportion of recharge.

As there is a lack of accessible published data to answer the above questions, it was decided to do simulations using a one-dimensional soil moisture model (SWAP) (Feddes, et al., 1978) that had already been widely used under various field conditions (e.g. Belmans et al., 1983; Tedeschi and Menenti, 2002; Gusev and Nasonova, 2003; Droogers et al., 2000; Singh, 2004; Utset, 2004). The main objectives of this chapter are to study:

(1) the influence of soil texture on the recharge
(2) the influence of sedimentation on top of the soil or geological deposits on the recharge
(3) the effect of water depths on the recharge
(4) the effect of inundation frequency on the recharge
(5) the effect of the Mualem (1976)-Van Genuchten (1980) and Campbell (1985) PTF methods on simulation results, when they are used for calculating soil hydraulic functions[4].

[4] In Chapter 4, the accuracy of the SWAP mathematical modelling results and the pedo-transfer function (PTF) methods of Mualem-Van Genuchten (MG) and Campbell (CA) are checked and evaluated in the Sorkhehesar floodwater spreading scheme, Varamin Plain, Iran.

First, for the sake of simplicity, simulations were done for a soil profile with a uniform texture extending up to 230 cm depth. Water passing that depth in the downward direction is the bottom flux. Because of the absence of vegetation, it was assumed that that bottom flux equals the recharge to the groundwater surface.

Alluvial deposits in semi-arid terrain are of direct interest for floodwater harvesting because of their proximity to ephemeral rivers. Since such deposits seldom have uniform profiles, simulations were also done for layered profiles consisting of two or three layers. Diversion of floodwater for infiltration is associated with the deposition of the suspended load of the floodwaters. The deposits range from sands to clays. Simulations were done for a top layer of sand, sandy clay and clay.

In order to study the effect of water depths, three main factors – evaporation losses, soil water storage changes and the bottom flux – were calculated as a function of soil textures for two different depths of water on the soil, 20 and 50 cm. The simulation was done for one year, following a single inundation.

Using five depths of water on the soil (30, 60, 90, 120 and 150 cm) as single and frequent inundations, the effect of the timing of inundations was studied.

While accepting a reasonably accurate performance of the SWAP model, the parameterization of the soil's hydraulic functions remains a problem. In this contribution, attention is paid also to the effects of the selection of functions (Mualem (1976)-Vna Genuchten (1980); Campbell 1985) for parameter values.

In order to make the simulation results mutually comparable, the same rainfall and evaporation values, based on data from the semi-arid Gareh Baygan area in southern Iran, were used in all simulations.

3.2 Theoretical background

3.2.1 The SWAP numerical model

Numerous numerical models have been developed for simulating water flow and solute transport through the vadose zone to the aquifer. Examples are codes such as SWAP (Feddes et al., 1978), VAM2D (Huyakorn et al., 1984, 1985) and SWMS-2D (Simunek et al., 1994). Numerical models solve the Richards water flow equation for flow through porous media. SWAP was developed from the agrohydrological models SWATRE and SWACROP (Feddes et al., 1978; Belmans et al., 1983). SWAP aims at simulating water, solute and heat transport in the soil-water-atmosphere-plant environment (Figures 3.1 and 3.2).

Water flow in porous soils in the unsaturated zone occurs as a result of gradients in the total hydraulic head H=h+z. According to Darcy's law, water movement through a one-dimensional unsaturated, vertical soil column can be written as:

$$q = -K(h)\frac{dH}{dz} = -K(h)\frac{dh}{dz} - K(h) \qquad [3.1]$$

where q is soil water flux density (positive upward) (cm d^{-1}), K(h) is unsaturated hydraulic conductivity (cm d^{-1}), h is soil water pressure head or matrix head (cm),

and z is the elevation head or vertical coordinate (cm) taken positively upward. Water balance consideration of an infinity-small soil volume results in the continuity equation for soil water:

$$\frac{\partial \Theta}{\partial t} = -\frac{\partial q}{\partial z} - R_w \qquad [3.2]$$

where Θ is volumetric water content ($cm^3\ cm^{-3}$), t is time (d), and R_w is the root water extraction ($cm^3\ cm^{-3}\ d^{-1}$). Combining Equations 3.1 and 3.2 yields the well-known Richards equation:

$$\frac{\partial \Theta}{\partial t} = C(h)\frac{\partial h}{\partial t} = \frac{\partial}{\partial z}k(h)\left[\frac{\partial h}{\partial z} + 1\right] - R_w \qquad [3.3]$$

where $C(h) = d\Theta(h)\ dh^{-1}$ is the soil water capacity (cm^{-1}).

SWAP solves Equation [3.3] numerically, subject to specified initial and boundary conditions and with known relations between Θh and K. These relationships can be measured directly in the soil, or might be obtained from basic soil data (discussed in Section 3.2.2). A schematic overview of the lower boundary conditions that can be used in SWAP is shown in Figure 3.3.

The SWAP model and its earlier version SWATR have been used in numerous studies, and a selection has been made of those studies relevant to estimating recharge in semi-arid regions.

- Bastiaanssen and Menenti (1989) used the SWATRE model and satellite measurements of surface reflectance and surface temperature to evaluate evapotranspiration and simulate water flow through the unsaturated/saturated zone in order to mapping groundwater losses in the Western Desert of Egypt. They classified the soils in the study area into six groups and the MG model parameters were derived for each group.
- Bastiaanssen et al. (1996) used the SWAP model to analyse water and salt balances in Harayana, India. The role of irrigation and drainage on yield (evapotranspiration), water table fluctuation, status of soil salinity and deep percolation was investigated using SWAP for a wide variety of physiographical conditions encountered in Harayana. They classified 113 soils into 12 groups. The MG parameters for each of the 113 soils were analysed using a least-square optimization technique to fit Pf curves optimally.
- Beekma et al. (1997) used the SWAP model to estimate the recharge that occurred during the first half of this century from irrigated fields in Punjab Province, Pakistan. For the recharge simulation, three basic soil profiles were considered representative of the area. Then the soil hydraulic functions for the three basic profiles were characterized by the MG parameters.
- Droogers et al. (2000) used the SWAP model in a distributed manner to reveal all the terms of the water balance for an irrigated area in the western part of Turkey. A combination of point data and distributed aerial data was used as input for the model.

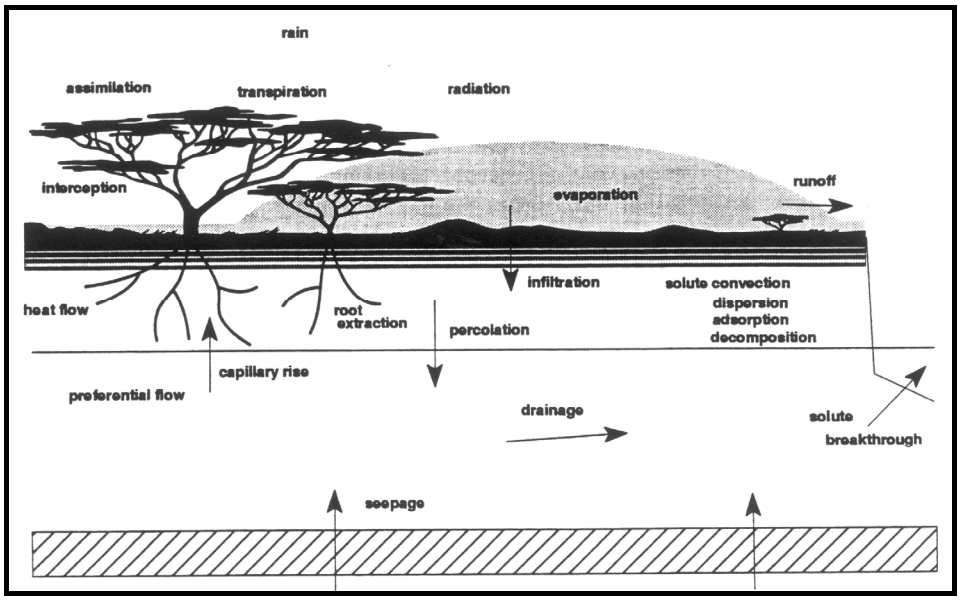

Figure 3.1 Water flow, solute transport and crop growth processes at the field scale, as applied in SWAP

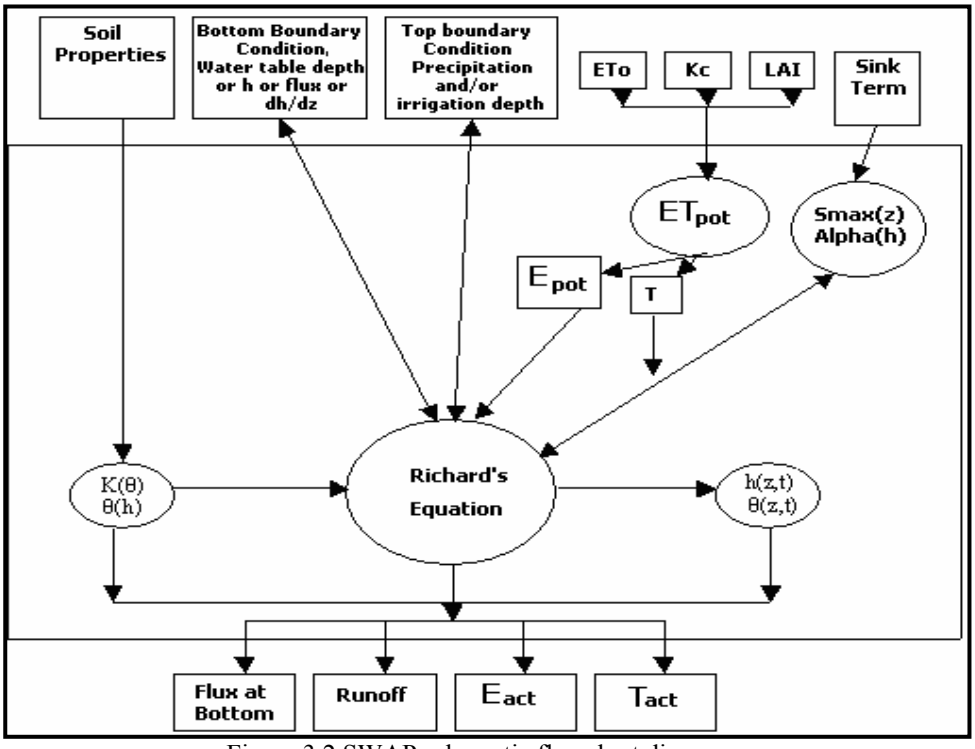

Figure 3.2 SWAP schematic flowchart diagram

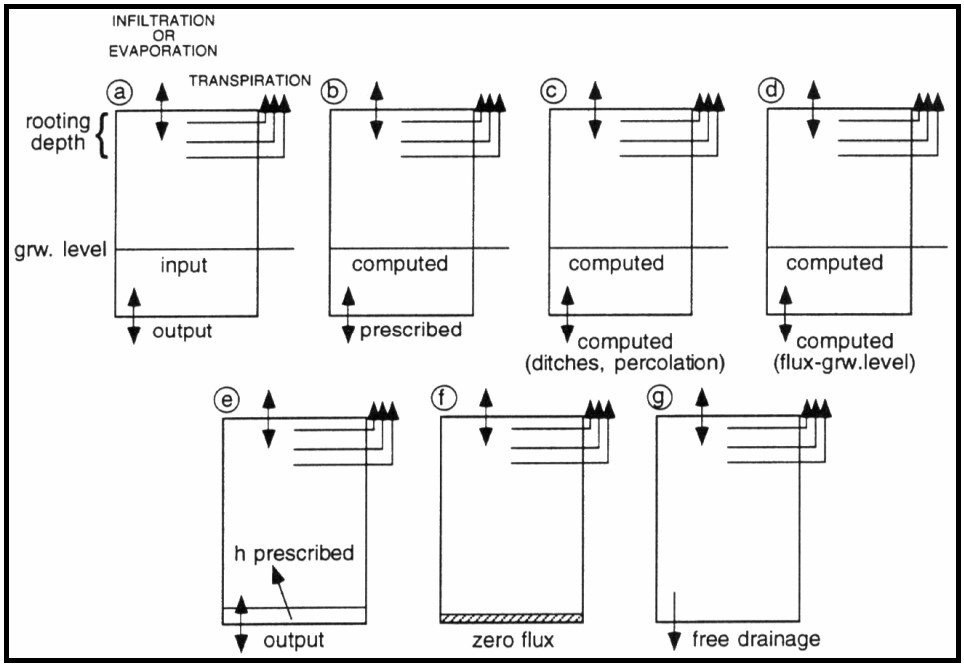

Figure 3.3 Schematic presentation of possible boundary conditions in the numerical model SWAP

Simulations were carried out for the period 1985-1996 and detailed analyses were performed for two successive years, a pre-drought year, 1988, and a dry year, 1989. All the changes in irrigation deliveries, lateral fluxes to drains, bottom fluxes, evapotranspiration and relative yield were obtained for specific sites by combining existing soil data with cropping patterns. They concluded that the use of the SWAP model in a distributed way was a useful tool for analysing all the components of the water balance for a whole irrigation system.

The results of the above studies provide reference values for the present recharge study, which also uses SWAP.

3.2.2 Soil hydraulic functions

The relationship between water content and soil-water potential is very important, because it is needed for many soil-water studies, such as artificial recharge. However, measurement of this relationship is costly, difficult, and often impractical, and general estimates based on more readily available information such as soil texture are sufficient for many purposes. This relationship has been expressed in different ways. Brooks and Corey (1964) presented Equation [3.4] for the soil-water potential curves.

$$\Psi = \Psi_e \left[(\Theta-\Theta_r)/(\Theta_s - \Theta_r)\right]^{B} \qquad [3.4]$$

where Ψ is soil-water potential (kPa), Ψ_e is soil-water potential at air entry (kPa), Θ is soil-water content ($m^3\ m^{-3}$), which is an empirical value to straighten curved data on a log-log scale, Θ_r is residual soil moisture content ($m^3\ m^{-3}$), Θ_s is saturated soil moisture content ($m^3\ m^{-3}$) and B is a fitted value. Substituting $\Theta_r = 0$ and $A = \Psi_e \Theta_s^{-B}$ in Equation 3.4 will result in Equation 3.5.

$$\Psi = A\ \Theta^B \qquad [3.5]$$

Equation 3.5 has been supported by several studies (Campbell, 1974; Clapp and Hornberger, 1978; Gardner et al., 1970a, b; Rogowski, 1971; Williams et al., 1983; McCuen et al., 1981).

Arya and Paris (1981) presented a model to predict the soil-water tension curve from particle size distribution and bulk density data. Their model calculates a pore size distribution from particle size distribution, bulk density and particle density. The pore radii are converted to equivalent soil-water tensions, using the equation of capillarity at the corresponding volumetric water content.

Gupta and Larson (1979) used multiple linear regression equations of the form:

$$\Theta_p = a\ (\%\ \text{sand}) + b\ (\%\ \text{silt}) + c\ (\%\ \text{clay}) + d\ (\%\ \text{organic matter}) + e\ (\text{bulk density, mg m}^{-3}) \qquad [3.6]$$

to predict the soil-water content (Θ_p, $m^3\ m^{-3}$) for 12 given soil-water potentials, where a, b, c, d, and e are regression coefficients. Intermediate values could be linearly interpolated between the calculated points.

Rawls et al. (1982) also reported a multiple linear regression analysis of soil-water content for 12 soil-water potentials with soil attributes, using a very extensive data set (2541 soil horizons with a wide range of each correlated variable). They used three linear regression equations of which the simplest is:

$$\Theta_p = a + b\ (\%\ \text{sand}) + c\ (\%\ \text{silt}) + d\ (\%\ \text{clay}) + e\ (\%\ \text{organic matter}) + f\ (\text{bulk density, mg m}^{-3}) \qquad [3.7]$$

where a, b, c, d, e and f are regression coefficients and textures defined by the USDA system (soil texture defined by the USDA system, where sand = 2.0 to 0.05 mm, silt = 0.05 to 0.002 mm, and clay <0.002 mm).

When they applied regression and discriminate analysis to these and other data, Cosby et al. (1984) demonstrated that soil texture could be related to hydraulic characteristics.

Saxton et al. (1985) examined some previous methods for estimating the relationships of soil-water content to potential and hydraulic conductivity. Using the results of previous broad-based correlations, equations were derived to estimate continuous relationships of soil-water moisture content to potentials and hydraulic conductivity from soil textures. A complete summary of the derived equations and coefficients by Saxton et al. (1985) is shown in Table 3.1. Saxton showed that the soil-water potential relationship with moisture content is continuous and nonlinear

from 10 to 1500 kPa, linear from 10 kPa to air entry potential, and a constant water content below air entry potential.

Table 3.1 Summary of derived soil-water characteristic equations by Saxton et al. (1985)

	Equation	Coefficients		Definitions
> 1500 to 10	$\Psi = A\,\Theta^{B}$	a = -4..396	k = 0.1276	Ψ = water potential, kPa
	$A = \exp[a + b(\%C) + c(\%S)^2 + d(\%S)^2(\%C)]$ 100.0	b = -0.0715	m = -0.108	Ψ_e = water potential at air entry, kPa
	$B = e + f(\%C)^2 + g(\%S)^2(\%C)$	$c = -4.880\times10^{-4}$	n = 0.341	Θ = water content, $m^3\ m^{-3}$
10 to Ψ_e	$\Psi = 10.0 - (\Theta - \Theta_{10})\,(10.0 - \Psi_e)/(\Theta_s - \Theta_{10})$	$d = -4.285\times10^{-5}$	p = 12.012	Θ_s = water content at saturation, $m^3\ m^{-3}$
	$\Theta_{10} = \exp[(2.302 - \ln A)/B]$	e = -3.140	$q = -7.55\times10^{-2}$	Θ_{10} = water content at 10 kPa, $m^3\ m^{-3}$
	$\Psi_e = 100.0\,[m + n\,(\Theta_s)]$	$f = -2.22\times10^{-3}$	r = -3.8950	K = water conductivity, m s^{-1}
	$\Theta_s = h + j\,(\%S) + k\,\log_{10}(\%C)$	$g = -3.484\times10^{-5}$	$t = 3.671\times10^{-2}$	(%S) = percent sand (e.g. 40.0)
Ψ_e to 0.0	$\Theta = \Theta_s$	h = 0.332	u = -0.1103	(%C) = percent clay (e.g. 30.0)
> 1500 to 0.0	$K = 2.778\times10^{-6}\ \{\exp[p + q\,(\%S) + [r + t\,(\%S) + u\,(\%C) + v(\%C)^2](1/\Theta)]\}$	$j = -7.251\times10^{-4}$	$v = 8.7546\times10^{-4}$	

Two main methods are available for measuring soil hydraulic functions: direct measurement and modelling. The direct method consists of laboratory and field methods (Hillel, 1980; Dirksen, 1991; Stolte et al., 1994). In the modelling method, two general expressions are available for Θ(h) and K(Θ), a tabular one and an analytical one. Although tabular forms of Θ(h) and K(Θ) have been used for many years, currently analytical expressions are generally applied for a number of reasons (Van Dam et al. 1997). Analytical expressions are more convenient as model input, and a rapid comparison between horizons is possible by comparing parameter sets. Scaling, which is used to describe the spatial variability of Θ(h) and K(Θ), requires an analytical expression of the reference curve. Extrapolation of the functions beyond the measured data range is possible.

Mualem (1976) derived a predictive model of the K (Θ) relation, based on the retention function. Van Genuchten (1980) proposed a more flexible Θ (h) function than the Brooks and Corey relation and combined it with Mualem's predictive model to derive K (Θ). This model has been used in numerous studies; it forms the basis of several national and international databanks (e.g. Carsel and Parrish, 1988; Wösten et al., 1994; Leij et al., 1996), and is implemented in SWAP.

Van Genuchten's (1980) Θ(h) function is:

$$\Theta = \Theta_{res} + (\Theta_{sat} - \Theta_{res})/(1 + |\alpha h|^{n})^{m} \qquad [3.8]$$

$$m = 1 - 1/n \qquad [3.9]$$

where Θ_{sat} is the saturated water content (cm^3 cm^{-3}), Θ_{res} is the residual water content in the very dry range (cm^3 cm^{-3}), and α (cm^{-1}), n (-) and m(-) are empirical shape factors. He applied Mualem's (1976) theory on unsaturated hydraulic conductivity to the above equations, resulting in the following $K(\Theta)$ function:

$$K=K_{sat}S_e^{\lambda}[1- (1-S_e^{1/m})^{m}]^2 \quad [3.10]$$

where K_{sat} is the saturated hydraulic conductivity (cm d^{-1}), λ is a shape parameter (-) depending on $\partial K/\partial h$, and S_e is the relative saturation defined as:

$$S_e=(\Theta - \Theta_{res})/(\Theta_{sat}-\Theta_{res}) \quad [3.11]$$

Van Genuchten et al. (1991) developed the program RETC to estimate the parameter values of this model from measured Θ (h) and K (Θ) data. Wösten et al. (1994) derived model parameters from a database of more than 600 soil samples in the Netherlands, known as the Staring Series. Carsel and Parish (1988) derived model parameters for the USDA textural classes. They developed a regression model and tested the model using 95 soils with a textural classification ranging from clays to sand. Yates et al. (1992) derived model parameters for 23 different soil types and 36 distributions for the water-retention relationship and unsaturated hydraulic conductivity.

Campbell (1985) proposed a set of equations to calculate the moisture release function, using soil texture. The equations are:

$$\Psi_{es}=-0.5dg^{-0.5} \quad [3.12]$$
$$b=-2\Psi_{es}+0.2\delta_g \quad [3.13]$$
$$dg=\exp(a),a=\Sigma m_i*\ln(d_i) \quad [3.14]$$
$$\delta_g=\exp(b),b=[\Sigma m_i*(\ln(d_i))^2-a^2]^{0.5} \quad [3.15]$$
$$\Psi_e=\Psi_{es}(pb/1.3)^{0.67b} \quad [3.16]$$
$$\Psi_m=\Psi_e(\Theta/\Theta_s)^{-b} \quad [3.17]$$
$$K=K_s(\Theta/\Theta s)^{m}\ m=2*b+3(b \text{ derived from equation [3.15]}) \quad [3.18]$$
$$K_s=4*10^{-3}(1.3/pb)^{1.3b}*\text{Exp}(-6.9*m_c-3.7m_s) \quad [3.19]$$

where Ψ_{es} = air entry potential at bulk density 1.3 g cm^{-3}, dg = geometric standard deviation (dimensionless), δ_g = geometric mean diameter (mm), dg and δ_g can be estimated from texture diagram derived by Shirazi and Boerma (1984) (see Figure 3.4), K_s = saturated hydraulic conductivity (cm day^{-1}), K = unsaturated hydraulic conductivity (cm d^{-1}), pb = bulk density (g cm^{-3}), m_c = clay mass fraction (weight/weight), m_s = silt mass fraction (weight/weight), m_i = mass fraction of texture class i, and d_i = arithmetic mean diameter of class i.

In the present study, in order to determine soil hydraulic functions for the combination of different soils and profiles, both the Campbell (CA) and analytical Mualem-Van Genuchten (MG) model have been used.

3.3 Method and materials

3.3.1 Model parameterisation/initial conditions

The average of 20 years' (Table 3.2) monthly rainfall and monthly potential evapotranspiration (Penman-Monteith method) information on Gareh Baygan Plain, located in Fasa Province, Iran (Fatehi-Marj, 1994), was used as input rainfall and reference evapotranspiration data in the SWAP model. This location is typical of the central and southern parts of Iran. Monthly rainfall was used as a single rainfall event on the first day of each month (from January to December) of the simulated year. Monthly potential evapotranspiration was divided by the number of days in each simulated month and used as daily reference evapotranspiration.

In the case of a dry soil, SWAP calculates actual soil evaporation by using the soil hydraulic functions. In the case of a wet soil, actual evaporation equals potential evaporation.The average of 20 years' (Table 3.2) monthly rainfall and monthly potential evapotranspiration (Penman-Monteith method) information on Gareh Baygan Plain, located in Fasa Province, Iran (Fatehi-Marj, 1994), was used as input rainfall and reference evapotranspiration data in the SWAP model. This location is typical of the central and southern parts of Iran. Monthly rainfall was used as a single rainfall event on the first day of each month (from January to December) of the simulated year. Monthly potential evapotranspiration was divided by the number of days in each simulated month and used as daily reference evapotranspiration.

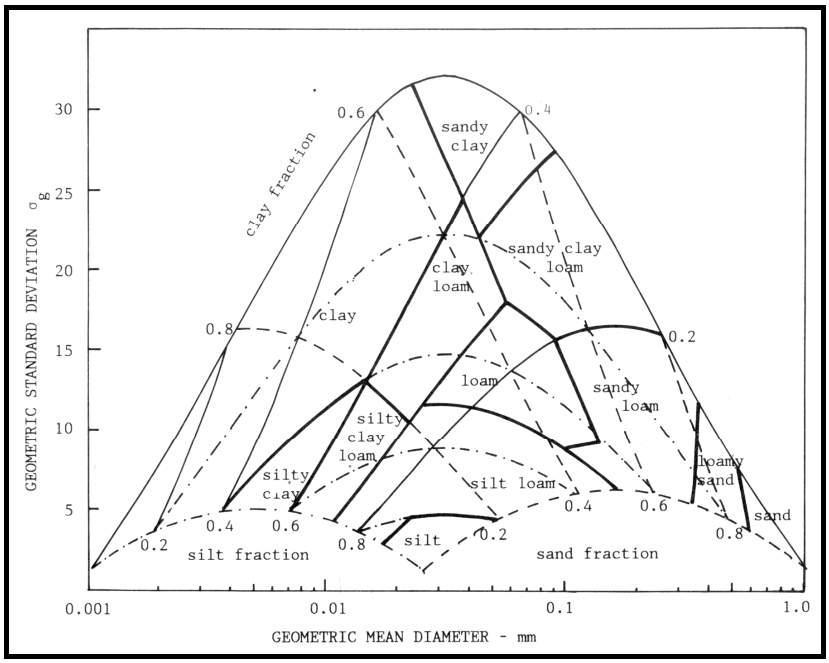

Figure 3.4 Presentation of the soil texture diagram using USDA particle size limits (after Shirazi and Boersma, 1984)

Table 3.2 Potential evapotranspiration (ET_p) and mean monthly rainfall (average 20 years) for Gareh Baygan Plain in Fasa Province, Iran

Month	Jan	Feb	Mar	Apr	May	Jun	Jul	Aug	Sep	Oct	Nov	Dec
Rainfall (mm)	47.2	54.7	38.4	22	6.8	0	0	0	0	0	10.4	36
ET_p (mm mth^{-1})	53	61	99	126	167	183	189	174	153	115	69	53
ET_p (mm d^{-1})	1.71	2.18	3.2	4.2	5.4	6	6	6	5.1	3.7	2.3	1.71

A total of 40 compartments were chosen in soil profiles of 2.30 m, consisting of one, two and three layers, with free drainage at the bottom of the soil profile to a 10 m deep groundwater level for the lower boundary condition (Figure 3.5).

Initial soil moisture conditions were chosen as an equilibrium profile with the groundwater table. In this case, the nodal pressure at the groundwater table equals zero and the nodal pressure decreases linearly with height towards the soil surface.

Soil hydraulic properties Θ(h) and K(Θ) were calculated using MG and CA methods. The results of these methods were imported in the SWAP model, in both tabular and analytical expressions.

All simulations were done for a one-year duration, starting 1 January with a bare soil condition. It should be considered that in Iran January corresponds approximately to the first month of the flood season.

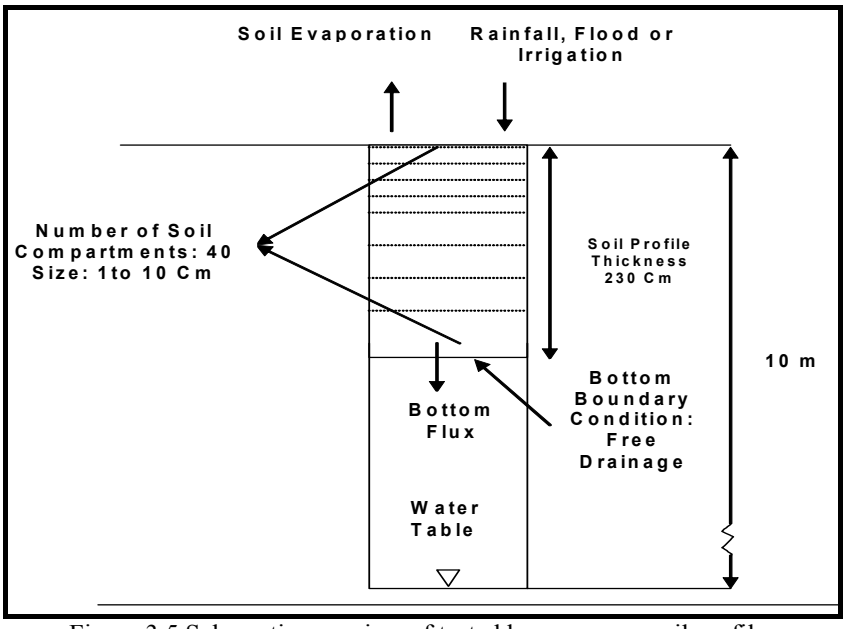

Figure 3.5 Schematic overview of tested homogenous soil profiles

3.3.2 Homogenous soils

Soil texture
The soil data set consisted of 63 homogeneous soil profiles (Figure 3.5), 2.30 m in depth, representing 20 different soil parent materials commonly found in Iran: clay, silty clay, silty clay loam, silt, clay loam, loam, silt loam, sandy clay, sandy clay loam, sandy loam, light loamy sand, loamy sand and sand were used. In addition, soil textures described by Menenti et al. (1991) as hummocky, porous clayey puffy, porous puffy, fine sandy puffy, sandy puffy and coarse sand puffy were used.

Saturated hydraulic conductivity Ks
The Ks range of the simulated soils was between 0.5 and 712.8 cm d^{-1}.

Inundation depth
In the simulation, the effects of inundation depths on recharge were studied using two water depths, 20 and 50 cm.

Soil hydraulic functions
The hydraulic functions of the Gareh Baygan soils were calculated based on the CA method. Both the CA and MG methods were used for the USDA soils. The soil hydraulic functions of the remaining soil data sets were based on the MG method. Since very few Iranian soils have been hydraulically characterized, soil properties (i.e. MG parameters) for this set of soils were selected from:

- the Staring Series (Wösten et al., 1994), nine soils, B1, B2, B3, B4, B7, B10, B11, B12 and B14
- USDA texture classes reported by Carsel and Parrish (1988), 22 soils (10 soil classes based on MG PTF and 12 soil classes based on CA PTF)
- the Western Desert of Egypt, reported soils by Bastiaanssen and Menenti, (1989), six soils
- Harayana, India, reported soils by Bastiaanssen et al. (1996), 10 soils
- Punjab Province, Pakistan, reported soils by Beekma et al. (1997), three soils
- Gareh Baygan Plain, Fasa Province, Iran, reported soils by Fatehi-Marj (1994), 13 soils.

3.3.3 Non-homogenous soil profiles

Simulations for non-homogenous soil profiles (Figure 3.6) consist of two major parts: the study of the effects of, first, sedimentation and, second, flooding frequency on recharge.

Sedimentation effect

Texture of the initial soils and sedimented top soils
Among the above soils (Section 3.3.2), some were selected from the Staring Series soils (B3, O3, B4 and B11) and USDA soils (sandy loam, loamy sand, sand, clay and sandy clay) in order to simulate non-homogenous soil profiles 2.30 m deep,

consisting of two initial soil layers (2 m depth), while B3 overlaying O3 (Staring Series, see Figure 3.7) and sandy loam overlying loamy sand (USDA Soils, see Figure 3.8), sedimented by 30 cm sand and clay (B4 and B11) from Staring Series soils and 30 cm sand, clay and sandy clay from USDA soils.

Inundation depth
Water depths were varied from 10 to 50 cm, as a single inundation event on the first day of simulations.

Soil hydraulic functions
The hydraulic functions of the Staring Series soils were calculated based on the MG method. Both the CA and MG methods were used for the USDA soils.

Flooding frequency effect

Texture of the initial soils
Simulations were based on:

- Staring Series soils, while B3 and B11 overlaying O3 (Figure 3.9b)
- USDA soils, while sandy loam and clay overlaying loamy sand (Figure 3.9a).

Inundation depths and flooding frequencies
Simulations were done over a one-year period, with five different total flooding depths of 30, 60, 90, 120 and 150 cm. For the first simulation runs, the water of each total depth was distributed equally over the first three consecutive days at the start of the year (thus for a total depth of 30 cm, each day received 10 cm, and so on). The second run was done by applying one third of the total depth to the first days of the first three months, starting with the first month of the year.

Soil hydraulic functions
The hydraulic functions of the Staring Series soils were calculated based on the MG method. Both the CA and MG methods were used for the USDA soils.

3.4 Results for homogenous soil profiles

3.4.1 Detailed results

Staring Series (MG)
As Table 3.3 shows, the highest bottom flux was calculated for the sand (B4) soil, which has the highest saturated hydraulic conductivity. The lowest bottom flux was calculated for the loam soil (B7). The highest soil water storage change was calculated for the clay (B11), which has the maximum saturated water content. The lowest soil water storage and the highest actual soil evaporation were calculated for the clay (B10) soil. The bottom flux ratio for 50 and 20 cm flood depths (50/20 ratio) varied from 3.8 (sand B4) to 17.15 (clay B11).

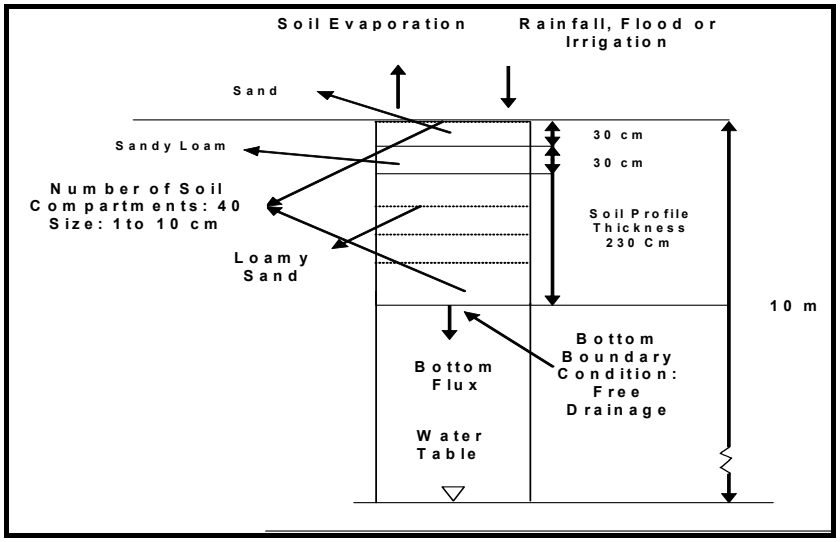

Figure 3.6 Schematic overview of non-homogenous soil profiles consisting of two or three layers

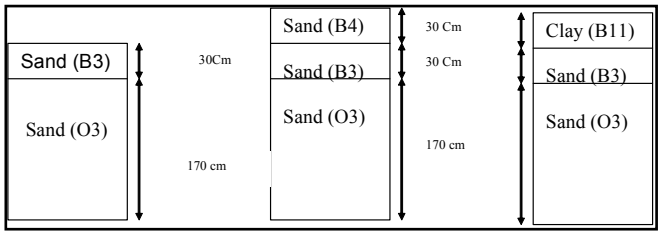

Figure 3.7 Schematic overview of tested Staring Series soil profiles

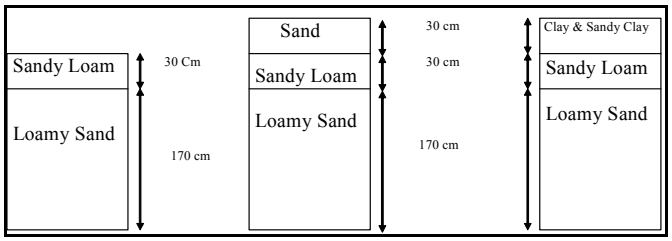

Figure 3.8 Schematic overview of tested soil profiles based on USDA soil texture classes

(a) (b)

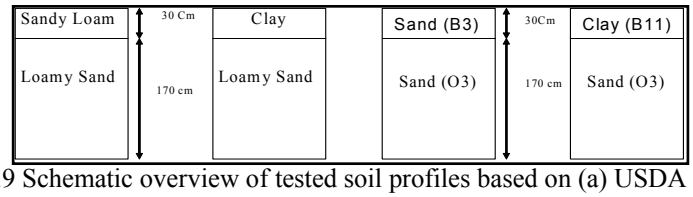

Figure 3.9 Schematic overview of tested soil profiles based on (a) USDA soils (b) Staring Series soils

The scatter plot of Figure 3.10a shows that the saturated hydraulic conductivity and recharge are not highly correlated for the soil parameter used.

Since alluvial deposits in semi-arid areas can have very coarse-grained textures, simulations were also made for higher K_{sat} values.

USDA texture classes (MG)

According to Table 3.4, the simulations resulted in the lowest evaporation and the highest recharge for the sand soil, which had the highest saturated hydraulic conductivity. The lowest recharge and the highest soil evaporation were obtained for the silt soil. The clay soil had the lowest water storage change. The bottom flux ratio (the 50/20 ^{cm} ratio) varied from about 2 (sand) to 43.8 (silt).

The results shown in graph 3.10b indicate much variation in the recharge as a function of K_{sat}. For higher K_{sat} values, the increases in the recharge were according to expectation. The overall correlation is poor. The saturated hydraulic conductivity and recharge are not highly correlated for USDA soil texture classes, as shown in Figure 3.10b.

For the sake of comparison, the CA functions were also used for simulations with the USDA soil texture classes for the range K_{sat} = 2.4 to 236 (cm d^{-1}).

USDA texture classes (CA)

Saturated water content and percentages of sand, silt and clay reported by Carsel and Parish (1988) for the USDA soil texture classes, and bulk density 1.3 gr cm^{-3} were used as input data for the CA model in order to estimate Pf and K curves for all soils, which were used for the SWAP simulations.

The results show that the sand soil had the highest recharge and saturated hydraulic conductivity and the lowest evaporation loss. The lowest recharge was simulated for the silt soil, which had the highest evaporation loss. The recharge ratio (the 50/20 ^{cm} ratio) varied from about 2.2 (sand) to 3.5 (silt). The R^2 regression coefficients of Figure 3.10c show that the recharge and saturated hydraulic conductivity had a high linear correlation when the Campbell PTF model was used.

Gareh Baygan Plain, Iran (CA)

The soil textures were classified based on USDA soil texture classes. For the simulations, percentages of sand, silt and clay were used for the Saxton (1985) model in order to estimate bulk densities and saturated water contents for reported soil textures. Obtained bulk densities and saturated water contents, together with percentages of sand, silt and clay, were used in the CA model for K and Pf curves simulation.

Calculated soil hydraulic functions were used as tabular input data for the SWAP model. The highest recharge and saturated hydraulic conductivity were calculated for the sand soil (bulk density = 1.78), which had the lowest evaporation losses. The lowest saturated hydraulic conductivity, the bottom flux and the highest evaporation loss were obtained for the silty loam (bulk density = 1.4) soil.

Figure 3.10d shows that the bottom flux and saturated hydraulic conductivity of the tested soils have a positive weak linear correlation. The ratio of

50/20 cm varied from about 2 for the sandy loam soil (bulk density = 1.67) to 3.6 for silt loam (bulk density = 1.4).

Harayana, India (MG)
The soil with a sand texture had the highest recharge and saturated hydraulic conductivity and the lowest soil evaporation. Opposite results were obtained for the sandy clay and clay. The scatter plot of Figure 3.10e shows a weak overall correlation between saturated hydraulic conductivity and bottom flux. By splitting the data according to $K_{s,}$, the bottom flux increases approximately linearly for higher K_s values. The 50/20 cm ratio for higher K_s varies from 2.65 (sand) to 10.77 (clay loam).

Western Desert of Egypt (MG)
The highest recharge was obtained for the second soil group (loam**,** clay**,** hummocky) in the table. The lowest recharge was calculated for the third soil group (coarse sand, puffy), which had the lowest saturated hydraulic conductivity. The highest evaporation loss and water storage change were obtained for the fifth soil group (porous clay, puffy).

The scatter plot of Figure 3.10f shows a very weak linear correlation. The 50/20 cm ratio varied from 2.8 (second soil group) to 8.2 (first soil group).

Punjab Province, Pakistan (MG)
The highest saturated hydraulic conductivity and recharge and the lowest soil evaporation loss were calculated for sand soil (Figure 3.10g). Loam and silt loam soils had the lowest recharge and storage respectively. The 50/20 cm ratio varied from 3.08 (sand) to 3.8 (loam).

3.4.2 Aggregated results: K_{sat}

The recharges as a function of the saturated conductivity, as calculated by the mentioned methods and data sets, are shown in Figure 3.11. It should be considered that K_{sat} and soil texture are not independent. The contents of the graph indicate that there is no strong correlation between recharge and Ks. A closer look at the data shows that for Ks >25 cm d^{-1} the recharge is positively related to Ks.

3.4.3 Aggregated results: hydraulic functions (CA vs MG)

In order to investigate the effects of different methods of soil hydraulic function simulations, the recharge as a function of saturated hydraulic conductivity, as calculated by the CA and MG methods and data sets, has been compiled in the scatter plots of Figure 3.12.

The relationship between K_s and recharge shows a positive trend when the CA method was used for calculating the soil hydraulic function relationship, but the correlation is not very strong (R^2 = 0.4913 and 0.4979 for flood depths of 50 and 20 cm respectively).

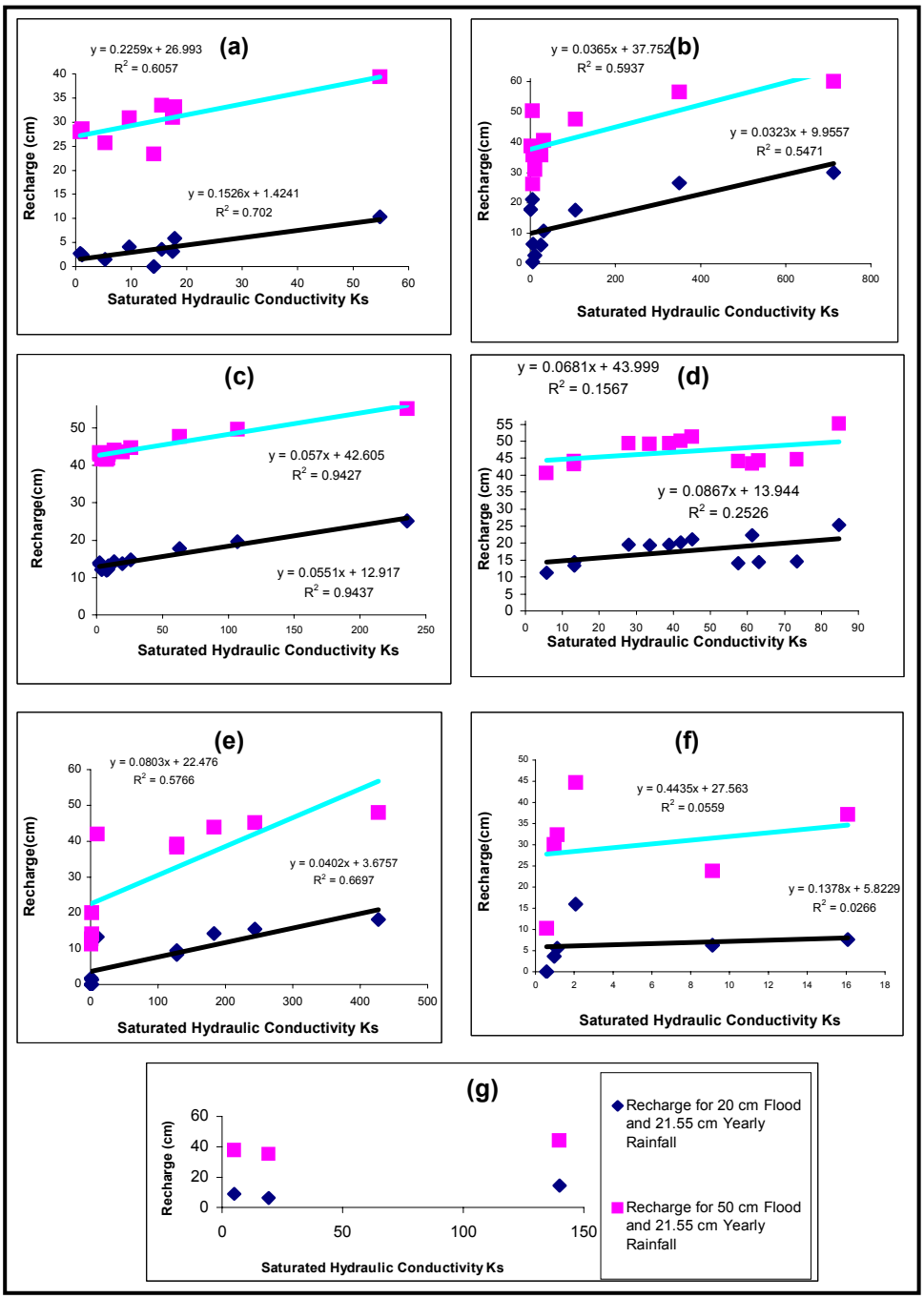

Figure 3.10 Saturated hydraulic conductivity (Ks, cm d^{-1}) and recharge (cm) relationship simulation results for homogenous soil profiles: (a) Staring Series, MG; (b) USDA, MG; (c) USDA CA; (d) Gareh Baygan Plain, Iran, CA; (e) Harayana, India, MG; (f) Western Desert of Egypt, MG; (g) Punjab, Pakistan, MG

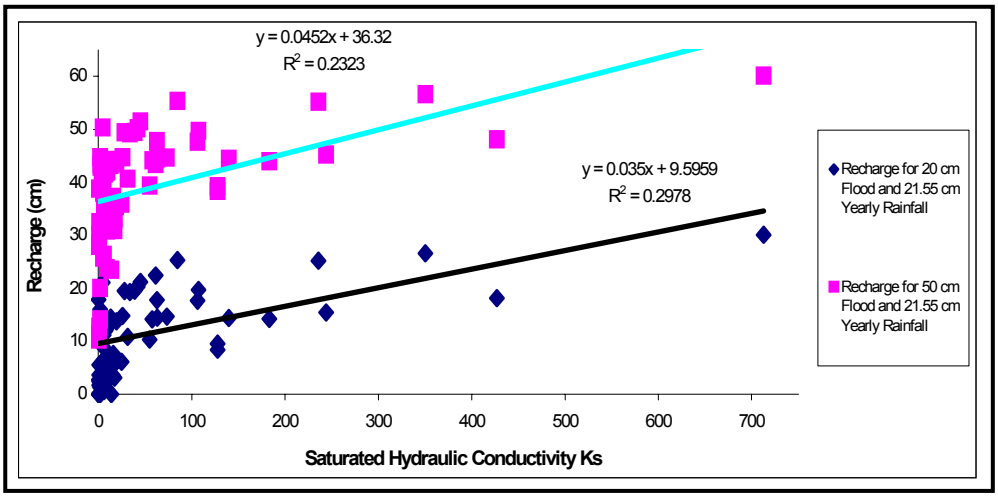

Figure 3.11 Aggregation of saturated hydraulic conductivity (Ks, cm d^{-1}) and recharge (cm) relationship simulation results for all soils, methods and homogenous soil profiles

When the MG model was used for soil hydraulic function computation, the correlation between saturated hydraulic conductivity (K_s) and recharge did not change much (R^2 = 0.4055 and 0.5314 for flood depths of 50 and 20 cm respectively) compared with the CA method, but the slope of the positive trend increased.

The contents of Figure 3.12 MG indicate that for the computed soil hydraulic function based on the MG model, the data set can be split up into a group with Ks >15 cm d^{-1} and a group with Ks <15 cm d^{-1}. More detailed illustrations for the Ks >15 cm d^{-1} and Ks<15 cm d^{-1} data are shown in Figures 3.13a and 3.13b respectively. The contents of Figure 3.13b indicate that for K_s <15 cm d^{-1} no correlation is apparent, as is shown by the low and insignificant R^2s for flood depths of 50 and 20 cm respectively. For Ks >15 cm d^{-1}, the bottom flux is positively related to Ks, and also correlation is reasonably good (R^2 = 0.7795 and 0.7932 for flood depths of 50 and 20 cm respectively).

3.4.4 Aggregated results: texture

It should be considered that K_{sat} and soil texture are not independent. The relationships between Ks and the recharge were investigated per texture class. Although the number of simulations for varying Ks values was limited, the correlations obtained were poor and insignificant for all the heavier textures (Figures 3.14a and 3.14b) and both CA and MG methods, up to and including medium texture classes (Figures 3.14c and 3.14d). For the light texture classes, the relationship between Ks and recharge is somewhat better defined, as shown in Figures 3.14e and 3.14f. The recharge and Ks relationship for all tested light soils indicate that the saturated hydraulic conductivity and bottom flux have a linear correlation (R^2 = 0.8799 and 0.8628 for flood depths of 20 and 50 cm respectively) when the MG method is used for simulating the hydraulic function (Figure 3.14f).

Table 3.3 Simulation results of the recharge and saturated hydraulic conductivity relationship using the SWAP mathematical model for all the soils of the databases (duration one year, flood depth 20 and 50 cm, yearly rainfall 21.55 cm, yearly potential evapotranspiration 174.4 cm)

Soil type	Ks (cm d^{-1})							Recharge (cm)													
								20 cm Flood							50 cm Flood						
	Staring Series	USDA MG	USDA CA	Gareh Baygan	Harayna India	Egypt	Pakistan	Staring Series	USDA MG	USDA CA	Gareh Baygan	Harayna, India	Egypt	Pakistan	Staring Series	USDA MG	USDA CA	Gareh Baygan	Harayna, India	Egypt	Pakistan
Silty Clay	-	0.5	2	-	1	-	-	-	18	14	-	2	-	-	-	39	43	-	13	-	-
Silt	-	6	8	-	-	-	-	-	0.6	12	-	-	-	-	-	26	42	-	-	-	-
Silt B14	0.8	-	-	-	-	-	-	3	-	-	-	-	-	-	28	-	-	-	-	-	-
Clay	-	4.8	3	-	0.5	-	-	-	21	14	-	0	-	-	-	50	43	-	11	-	-
Clay B10	1.2	-	-	-	-	-	-	2.4	-	-	-	-	-	-	29	-	-	-	-	-	-
Clay B11	5.3	-	-	-	-	-	-	1.5	-	-	-	-	-	-	26	-	-	-	-	-	-
Clay B12	15.5	-	-	-	-	-	-	4	-	-	-	-	-	-	33.5	-	-	-	-	-	-
Porous Clayey Puffy	-	-	-	-	-	9	-	-	-	-	-	-	6	-	-	-	-	-	-	24	-
Clay Loam	-	6	9	-	2	-	-	-	7	13	-	1	-	-	-	36	43	-	14	-	-
Silty Loam	-	11	9	6	-	-	5	-	3	12	11	-	-	9	-	31	42	41	-	-	38
Loam	-	25	19	13 42	-	-	19	-	6	14	13 20	-	-	6	-	36	44	43 50	-	-	35
Loam B7	-	-	-	-	-	-	-	0	-		-	-	-		23.5	-		-	-	-	-
Loam, Clay, Hummocky	-	-	-		-	2	-		-		-	-	16			-		-	-	45	-
Sandy Clay Loam	-	-	-	-	-	-	-	-	11	15	-	-	-	-	-	41	45	-	-	-	-
Sandy Loam	-	106	63	13 34 61 28 39	128 128	-	-	-	18	18	14 19 22 20 20	8 10	-	-	-	48	48	44 49 43 49 49	38 39	-	-
Loamy Sand,	-	350	107	47 57 63	244	-	-	-	27	20	21 14 14	15	-	-	-	57	50	52 44 44	45	-	-
L Loamy Sand	-		-		183	-	-	-	-	-		14	-	-	-	-			44	-	-
Sand,	-	713	236	85 73	427	-	140	-	30	-	25 15	18	-	14	-	60		55 45	48	-	44
Sand B2,	10	-	-	-	-	-	-	4.1	-	-	-	-	-	-	31	-	-	-	-	-	-
Sand B1,	17	-	-	-	-	-	-	3.2	-	-	-	-	-	-	31	-	-	-	-	-	-
Sand B3	18	-	-	-	-	-	-	6	-	-	-	-	-	-	33	-	-	-	-	-	-
Sand B4,	55	-	-	-	-	-	-	10	-	-	-	-	-	-	39	-	-	-	-	-	-
Sand, Sandy Puffy,	-	-	-	-	-	1	-	-	-	-	-	-	4	-	-	-	-	-	-	30	-
Coarse Sand, Puffy	-	-	-	-	-	0.6	-	-	-	-	-	-	0	-	-	-	-	-	-	10	-
Fine Sandy Puffy	-	-	-	-	-	16	-	-	-	-	-	-	8	-	-	-	-	-	-	37	-
Silt Clay Loam	-	-	4	-	2	-	-	-	-	12	-	0	-	-	-	-	42	-	20	-	-
Sandy Clay	-	-	13	-	10	-	-	-	-	14	-	13	-	-	-	-	44	-	42	-	-
Porous Puffy	-	-	-	-	-	1	-	-	-	-	-	-	6	-	-	-	-	-	-	32	-

Table 3.4 Simulation results of the actual evaporation and water storage change relationship using the SWAP mathematical model for all the soils of the databases (duration one year, flood depths 20 and 50 cm, yearly rainfall 21.55 cm, yearly potential evapotranspiration 174.4 cm

Soil Type	Actual Evaporation (cm y^{-1})														Water Storage Change (cm y^{-1})													
	Staring Series MG		USDA MG		USDA CA		Gareh Baygan CA		Harayana India MG		Egypt MG		Pakistan MG		Staring Series MG		USDA MG		USDA CA		Gareh Baygan CA		Harayana India MG		Egypt MG		Pakistan MG	
	Flood (cm)		Flood (cm)		Flood (cm)		Flood (cm)		Flood (cm)		Flood (cm)		Flood (cm)		Flood (cm)		Flood (cm)		Flood (cm)		Flood (cm)		Flood (cm)		Flood (cm)		Flood (cm)	
	20	50	20	50	20	50	20	50	20	50	20	50	20	50	20	50	20	50	20	50	20	50	20	50	20	50	20	50
Silty Clay	-	-	17	27	29	28	-	-	43	52	-	-	-	-	-	-	6	6	0	0	-	-	-4	7	-	-	-	-
Silt, Silt B14	29	32	24	26	30	30	-	-	-	-	-	-	-	-	10	11	16	19	0	0	-	-			-	-	-	-
Clay			17	18	28	29	-	-	33	38			-	-	-	-	3	3	0	0	-	-	8	22			-	-
Clay B10	42	44													-3	-0.7												
Clay B11	27	27													13	18												
Clay B12	26	26													12	12												
Porous ,Clayey, Puffy	-	-									56	63													21	-16		
Clay Loam	-	-	21	22	28	29	-	-	38	45	-	-	-	-	-	-	14	14	0	0	-	-	2	12	-	-	-	-
Silty Loam	-	-	23	24	29	30	30	31	-	-	-	-	23	24	-	-	16	17	0	0	0	0	-	-	-	-	9	9
Loam			18	19	28	28	28	28	-	-			20	21			17	17	0	0	0	0	-	-			15	15
							22	21													0	0						
Loam B7	29	32													12	16												
Loam,Clay,Hummocky											20	21													6	6		
Sandy Clay Loam	-	-	15	15	27	27	-	-	-	-	-	-	-	-	-	-	16	16	0	-	-		-	-	-	-	-	-
Sandy Loam	-	-	11	11	24	24	27	27	23	23	-	-	-	-	-	-	13	13	0	0	0	0	11	11	-	-	-	-
							22	22	26	27											0	0	6	6				
							19	19													0	0						
							22	22													0	0						
							22	22													0	0						
Loamy Sand	-	-	7	7	22	22	20	20	28	28	-	-	-	-	-	-	8	8	0	0	0	0	-2	-2	-	-	-	-
							18	18													9	9						
							18	18													9	9						
L Loamy Sand									23	23													5	5				
Sand			5	5	16	16	16	16	17	17				11			7	7	0	0	0	0	6	6			16	16
							17	17													10	10						
Sand B2	28	30													9	11												
Sand B1	25	26													14	15												
Sand B3	30	32													6	7												
Sand B4	28	28													4	4												
Sand Sandy Puffy											25	27													13	15		
Coarse Sand Puffy											30	33													12	28		
Fine Sandy Puffy											24	24	11												10	11		
Silt Clay Loam	-	-	-	-	29	30	-	-	27	27	-	-	-	-	-	-	-	-	0	0	-	-	15	24	-	-	-	-
Sandy Clay	-	-	-	-	27	27	-	-	31	32	-	-	-	-	-	-	-	-	0	0	-	-	-2	-2	-	-	-	-
Porous Puffy	-	-	-	-	-	-	-	-	-	-	25	27	27	-	-	-	-	-	-	-	-	-	-	-	11	12	-	-

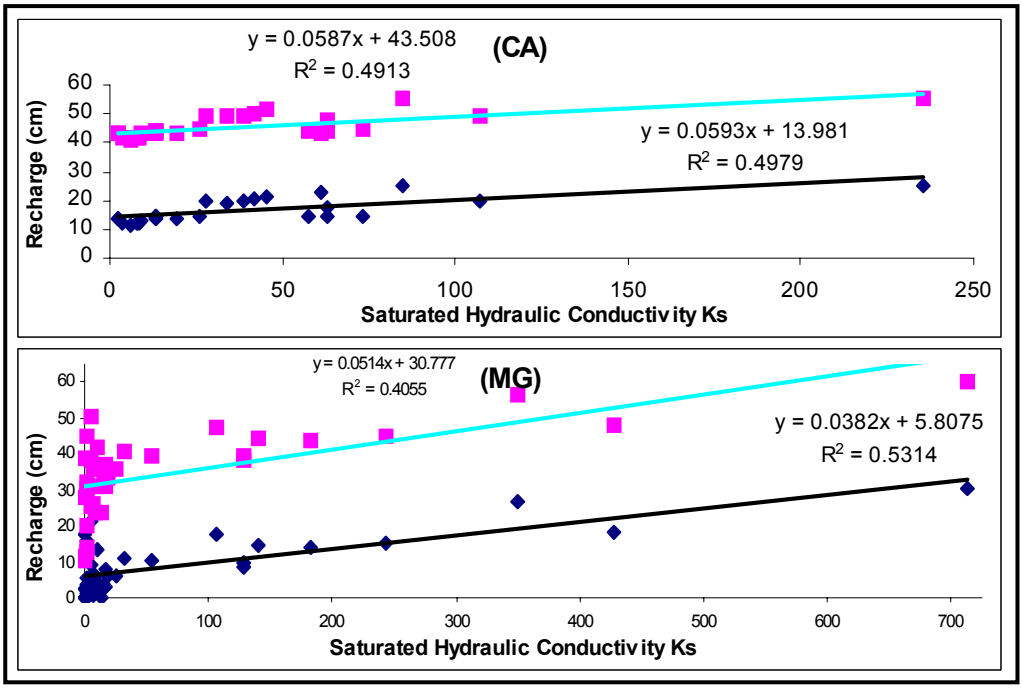

Figure 3.12 Aggregation of saturated hydraulic conductivity (Ks, cm d^{-1}) and recharge (cm) relationship simulation results for all homogenous soil profiles: (CA) when soil hydraulic function calculated using the Campbell method; (MG) when soil hydraulic function calculated using the Mualem-Van Genuchten method

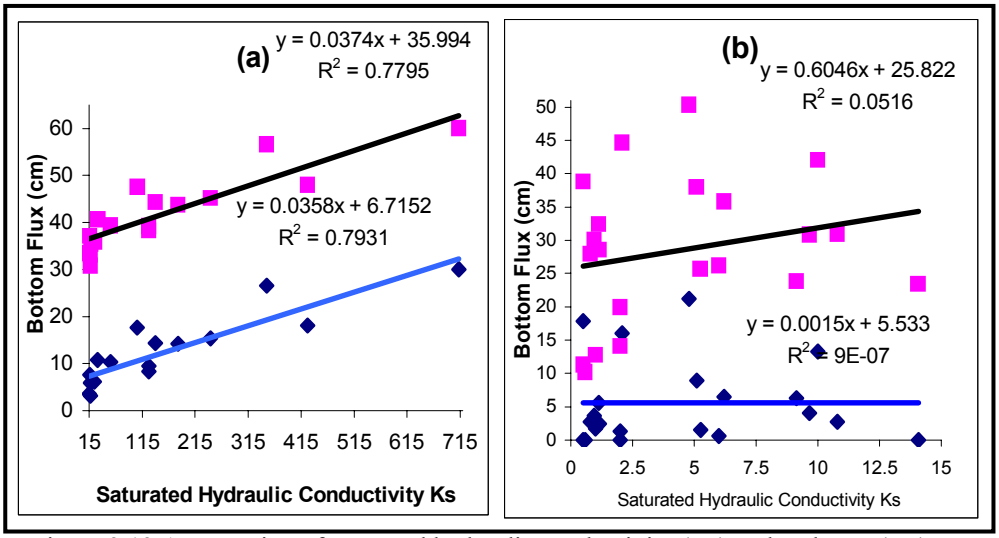

Figure 3.13 Aggregation of saturated hydraulic conductivity (Ks) and recharge (cm) relationship simulation results for all soils using MG method and homogenous soil profiles: (a) when Ks > 15 and (b) when Ks < 15 cm d^{-1}

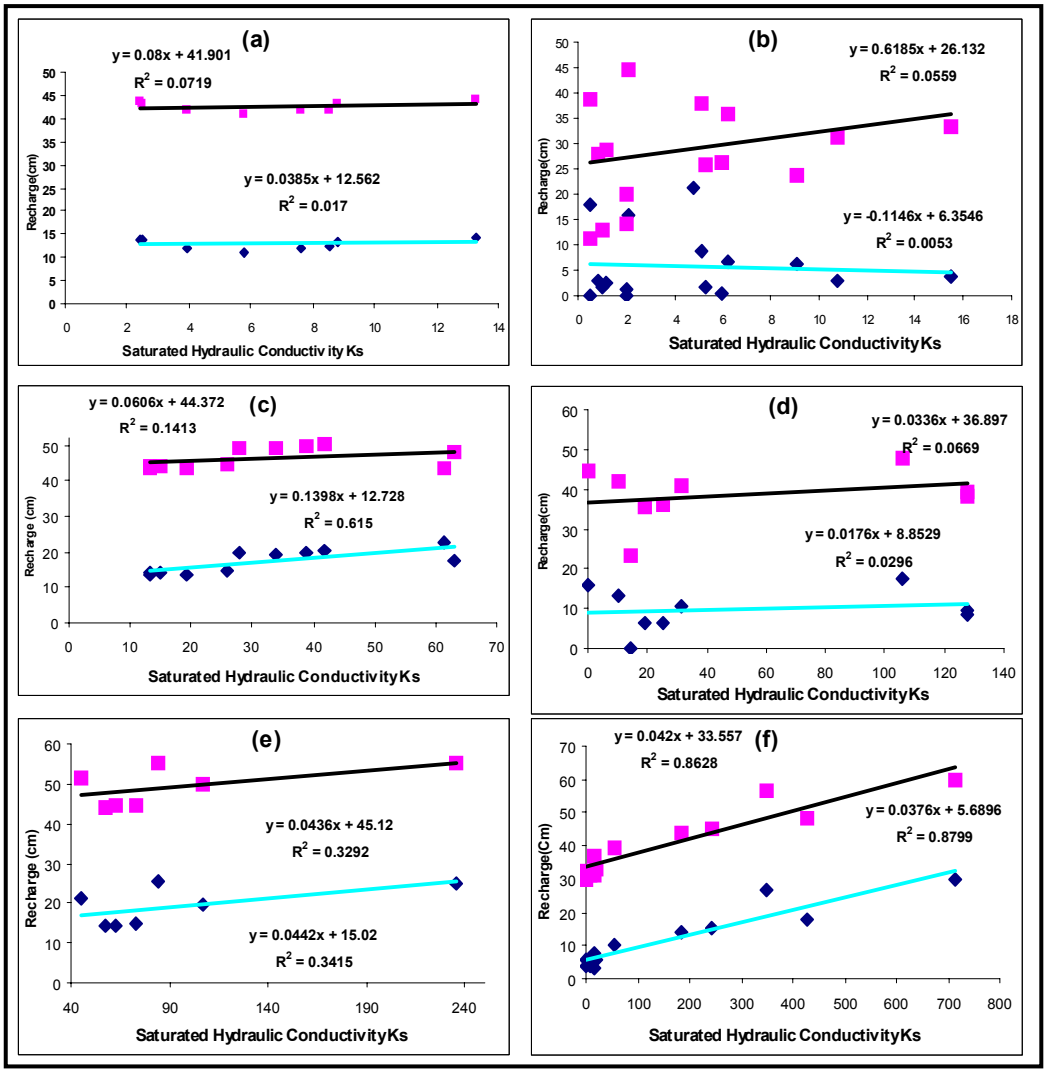

Figure 3.14 Simulation results for Ks (cm d^{-1}) and recharge relationship for (a) heavy soil textures, CA method; (b) heavy soil textures, MG method; (c) medium soil textures, CA; (d) medium soil textures, MG; (e) light soil textures, CA; (f) light soil textures, MG

3.5 Discussion and conclusion: homogenous soils

The effects of different factors on recharge will be discussed below.

3.5.1 Soil texture and saturated hydraulic conductivity (Ks)

As the Ks and soil texture are not independent, the effects of these factors on recharge will be discussed together. The saturated hydraulic conductivity (Ks) and recharge are not correlated when the soil hydraulic properties have been calculated based on both the MG and CA PTFs in the following situations:

- the aggregation of all the tested soils (Figure 3.12 CA, $R^2 = 0.49$; Figure 3.15b, $R^2 = 0.53$)
- the heavy soil textures (Figure 3.14a, $R^2 = 0.07$; Figure 3.14b, $R^2 = 0.05$)
- the medium soil textures (Figure 3.14c, $R^2 = 0.61$ for 20 cm flood and $R^2 = 0.14$ for 50 cm flood; Figure 3.14d, $R^2 = 0.06$)
- the light soil texture classes (Figure 3.14e, $R^2 = 0.34$, CA PTF).

The average recharge efficiencies for heavy soil textures under 20 and 50 cm flooding depths (and 21.55 cm yearly rainfall) respectively ranged from 14 to 40% (MG) and from 30 to 59% (CA), and for medium soil textures from 24 to 54% (MG) and from 41 to 65% (CA). The ranges for light soil textures were from 34 to 61% (MG) and from 46 to 70% (CA).

The average recharge efficiency for the aggregated results (for both CA and MG methods) for clay and clay loam soils was found to be 14% (20 cm inundation depth) to 39% (50 cm inundation depth); for silty clay and silty clay loam soils 18 to 44%; for sandy clay and sandy clay loam soils 22 to 40%; for silt and silt loam soils 14 to 49%; for loamy and sandy loam soils 24 to 65% and for sandy soils 45 to 70%.

Based on Ks, the above ranges are between 13 and 40% for Ks <15 cm d^{-1} and between 29 and 63% for Ks >15 cm d^{-1} (MG), and between 31 and 60% for Ks <15 cm d^{-1} and between 40 and 64% for Ks >15 cm d^{-1} (CA).

It is generally accepted that heavy to medium textured soils, or deposits occurring in the upper 2 m or so, and sedimentation by clay and silt in the infiltration basins will reduce the efficiency substantially. However, the SWAP simulation results for about 2.30 m homogenous soil profiles indicated that some of the heavier textured (clay and sandy clay) soils still had reasonable recharge efficiency.

3.5.2 Inundation depth

The results of the SWAP mathematical modelling also show that the efficiency of the floodwater recharge has a direct relationship with the floodwater inundation depth. For example, for all the above tested soils, an increase of 30 cm inundation depth caused about a 2 to 23 times rise in water recharge efficiency (Table 3.5). Also the results show no recharge for heavy (clay) and medium (loam) soil textures, or very low recharge efficiency (10%) for light (sand) soil textures, when flooding depth is 20 cm and yearly rainfall is 21 cm. However, when the flooding depth for the mentioned soils increases to 50 cm, the recharge efficiency rises to 15, 33 and 42% respectively. This finding indicates that scheme design should aim at deep inundation.

Table 3.5 Summary of simulation results, using SWAP model for homogenous soil profile, when soil hydraulic functions calculated based on CA and MG models (Ks, cm d^{-1})

Soil Texture Class	PTF Model	Minimum Recharge Ratio (R) (flooding depth 50/20 cm)			Maximum Recharge Ratio (R) (flooding depth 50/20 cm			Minimum Recharge Efficiency (%)				Maximum Recharge Efficiency (%)				Average Recharge Efficiency (%)		Aggregation of all the tested soils based on saturated hydraulic conductivity (Ks) and recharge efficiency (%)							
		Ks	R	Soil Type	Ks	R	Soil Type	Ks	Soil Type	21.55 cm Rain		Ks	Soil Type	21.55 cm Rain		21.55 cm Rain		MG PTF Model				CA PTF Model			
										20 cm Flood	50 cm Flood			20 cm Flood	50 cm Flood	20 cm Flood	50 cm Flood	21.55 cm Rain							
Heavy	MG	0.5	2.17	Silty Clay	2	20	Silty Clay Loam	0.5	Clay	0	15	4.8	Clay	50	70	14	40	20 cm Flood		50 cm Flood		20 cm Flood		50 cm Flood	
Heavy	CA	13.3	3.0	Sandy Clay	5.77	3.64	Silty Loam	5.8	Silty Loam	27	57	13.3	Sandy Clay	34	61	30	59	Ks		Ks		Ks		Ks	
																		< 15	> 15	< 15	> 15	< 15	> 15	< 15	> 15
Medium	MG	106.1	2.7	Sand Loam	14.07	23	Loam	14.7	Loam	0	33	106.1	Sandy Loam	42	67	24	54	13	29	40	63	31	40	60	64
Medium	CA	61.3	1.9	Sandy Loam	13.3	3.22	Loam	19.4	Loam	33	61	41.90	Loam	49	70	41	65	Average recharge efficiency for different soil texture classes (MG&CA)							
																		Soil Texture				20 cm Flood		50 cm Flood	
Light	MG	712.8	2	Sand	0.96	8	Sand	0.96	Sand	10	42	712.8	Sand	75	90	35	61	clay and clay loam soils				14		39	
																		silt clay and silt clay loam				18		44	
																		sandy clay and sandy clay loam				22		40	
Light	CA	84.7	2	Sand	57.47	3	Loamy Sand	57.4	Loamy Sand	34	61	235.7	Sand	61	77	46	70	silt and silt loam				14		49	
																		loamy sand and sandy loam				24		65	
																		Sandy soils				45		68	

3.5.3 Hydraulic function methods (PTFs)

When MG and CA methods were both used for simulating hydraulic functions, the recharge and Ks were not correlated, except in one case. This case pertains to all the light soil texture classes ($R^2 = 0.87$, Figure 3.14f). The soil hydraulic functions were calculated using MG PTFs.

As mentioned above, some of the heavier textured (clay and sandy clay) soils still had reasonable recharge efficiency, especially when the soil hydraulic functions were calculated based on CA PTFs. From the above results, it can be concluded that the estimation of the efficiency of water recharge for floodwater spreading schemes is sensitive to the methods of soil hydraulic functions assessment.

3.5.4 Comparing the recharge efficiency results with other studies

Results of other studies also show that some heavy soil textures could have reasonable recharge to the groundwater. Tomoseen (1991) draws attention to the point that recharge could be substantial in the case of heavy textured soils if ponding by runon occurs.

Burke et al. (1999) used a coupled hydrology and vegetation growth model ± PATTERN of Mulligan (1996) to explore the relationship between irrigation and productivity for different soils typical of the upper Guadiana catchment in central Spain. Analysis of the model results showed that irrigation efficiency is highly sensitive to both soil texture and irrigation volume. They concluded that efficient irrigation in terms of water losses (recharge) occurs at the lowest volumes of applications. They studied typical K/ θ (soil moisture content) curves for the most typical classes of soil texture in that area. Clearly, coarsely textured soils had the highest K (by several orders of magnitude) over most of the range of soil moisture, whereas more finely textured soils showed very low conductivities at low soil moisture but a strong response of hydraulic conductivity to increasing soil moisture, so that above 0.5 (m^3 m^{-3}) soil moisture content silts and loam soils had higher hydraulic conductivities than the coarser textured soils. Therefore, under ponding, recharge can be high with heavy textured soils.

They also modelled the annual recharge for 35 years in the study areas under six soil textures (clay, silt, sandy loam, clay loam, loam and sand) and irrigation (18 cm per year). The annual recharge varied from a minimum of 30 to a maximum of 130 cm y^{-1}. The recharge losses under sandy soils were 15 to 20 cm per year higher than under finer-grained soils. It means that the heavier soil textures decrease recharge efficiency between 15% (for 120 cm y^{-1} rainfall and 18 cm y^{-1} irrigation) and 53% (for 20 cm y^{-1} rainfall and 18 cm y^{-1} irrigation) compared with the light soil texture. Our SWAP model simulation results for almost the same soil textures (see Table 3.5) show the above range between 42% (50 cm flood) and 69% (20 cm flood). It seems that the ranges are different because of the difference in rainfall and flooding depths. They also concluded that ponding enhances recharge efficiency, which is in line with our simulation results with regard to inundation depths.

Munevar and Marino (1999) developed a modelling approach to evaluate the potential for artificial recharge on alluvial fans in Salinas Valley, California. They calculated soil hydraulic functions using the MG analytical model for five different soil textures: two sands, silty sand, silt and clay. After several runs of the model for seven alternative scenarios (sites), the results showed that the recharge varied from 51% (high for heavy soils) to 79%. The minimum and maximum amounts for the saturated hydraulic conductivity used in the model were about 0.024 cm d^{-1} (clay) and 480 cm d^{-1} (sand) respectively.

In order to verify the possibility of significant quantities of diffuse recharge caused by 100 years of precipitation in the American Southwest (Las Cruces), Kearns and Hendrickx (1998) used SWAP for the study area. Four soil textures (two sandy loams, loamy fine sand, and clay) were simulated in soil profiles, some 2 m, some 6 m deep, both barren and vegetated. They mentioned that sandy loam and even clay soils showed localized recharge under ponded conditions.

Hendrickx et al. (1991) mention that, if the depth of ponding at the start of infiltration is more than 1 m, at least 90% of the applied recharge water will reach the water table, providing that the ponding area is bare of vegetation. They developed a numerical analysis of groundwater recharge through stony soils, using limited data for Quetta Valley (Baluchistan, Pakistan).

Kennett-Smith et al. (1994) used data from 18 field studies in the southwestern Murray Basin, Australia. A simple water balance model was used to study the importance of factors that affect diffuse recharge in that area. Generally, as the texture of the soil became heavier, the recharge decreased. Under cropped land with mean annual rainfall of 31 to 38 cm, as the clay content in the top 2 m of the soil profile increased from 0 to 20%, recharge decreased by one order of magnitude (from about 30 to about 3 mm $year^{-1}$). Sites with an average clay content of about 10% in the top 2 m and a mean annual rainfall of 27 cm had an estimated recharge of about half that of sites with a mean annual rainfall of 31 to 38 cm (ponding effect). Also the results show that there is no linear relation between clay content percentage (in the 2 m upper part of the soil profile) and potential recharge. The soils with the same amount of clay content showed significant difference in recharge potential. When the rainfall increased, some soils with a high clay percentage still had a reasonable potential recharge magnitude.

Recharge in the Pisoes catchment in Portugal was researched by Cortez (2004) by studying daily fluctuations of the groundwater table of 13 observation wells. The catchment is underlain by basic rocks, and the top soils consist of clay loam and silty clay loam of 10 to 40 cm thickness, underlain by a compact sticky clay with a thickness of 5 to 400 cm. Ponding in flat areas during high rainfall was attributed to the presence of the sticky clay layer. The average annual recharge was 38% of the mean annual rainfall of 606 mm. The spatial variation in the recharge was 18 to 59% of the mean annual rainfall.

The evidence of the above studies support what was found in the simulations done by using SWAP and a variety of soil textures. The consequence for the selection of areas and sites for artificial recharge schemes is that light textured soils are preferred but locations with heavier textures should not be excluded *per se*, because when other factors are favourable, an acceptable

proportion of water applied can be expected, provided large ponding depths are aimed at in the design of such schemes.

3.6 Results for non-homogenous soil profiles

3.6.1 Simulation results for non-homogenous soil profiles before and after sedimentation

Figures 3.15, 3.16 and 3.17 showing the SWAP simulation results are arranged as follows. On the left side the graphs pertain to a hypothetical soil column with two layers, the upper one is 30 cm thick and the lower one is 170 cm, referred to as the 'original column'. The upper graphs refer to a simulation period of one month and the lower ones to a period of one year. The central graphs show the results with a 30 cm thick sand layer and the right-hand graphs the results with a 30 cm clay layer on top of the same soil column. In each graph, the recharge (or bottom flux), the soil evaporation and the water storage in the total column are given as a function of flooding depths. The initial moisture content and evaporation were the same as used in the previous section.

Figure 3.15 and Table 3.6 show the results using the Staring Series soil textural classes and corresponding hydraulic parameters. The original column consisted of sand B3 on sand O3, while the sediment was sand B4 and clay B11. It can be noted that the evaporation loss tended to even out for larger flooding depths, but, as the soil moisture store has to be filled sufficiently for water to pass, the recharge during the first month was limited to the largest flooding depths only. For the one-year period a larger part of the water applied flowed to depths below the soil column, more or less linearly with the amount of water applied exceeding 20 cm depth, and the flooding depth of 10 cm had no effect on the recharge. The evaporation did not increase with larger flooding depths because of the lowering of the zero flux plane and the dryness of the upper soil for most of the simulation period. As can be noted from the water storage changes, the full column dried out to reach the initial value or less (the small negative value). The layer of sand had little influence, but the clay layer caused some increase in the water storage and a small reduction in the evaporation for the period of one month; however, the latter was not the case for the period of one year.

Figure 3.16 and Table 3.7 pertain to the simulation results of an original soil column, with sandy loam on top of loamy sand of the USDA texture classes and the hydraulic functions given by the CA model. With these parameters, the evaporation loss was stabilized at lower flooding depths, while for the one-year period the recharge was more than was the case with a sandy original soil column and the Staring Series, despite the fact that in this simulation the texture was heavier. It is interesting to note that there was not much difference in the effect of the layer of sand or clay on the recharge, but the clay layer caused more evaporation loss. The results shown in graph b1 indicate that the sand layer hindered evaporation and some moisture was still left at the end of the year.

Figure 3.17 represents the same original soil column just described, but now the analytical functions of the MG model have been used. The differences in the recharge with various flooding depths for the simulation periods of one month and one year were much less than in the two cases discussed above. For the period of one year, a 10 cm flooding depth resulted in some recharge, but not with sand or clay sedimentation. Evaporation losses were not much influenced by the amount water applied. In comparison with the column with clay sediment, the sand layer did not cause any reduction in the evaporation, but, when compared with the column without sediment, both types of sediment increased the evaporation. Recharge is almost fully linearly related with flooding depth in the simulation for one year.

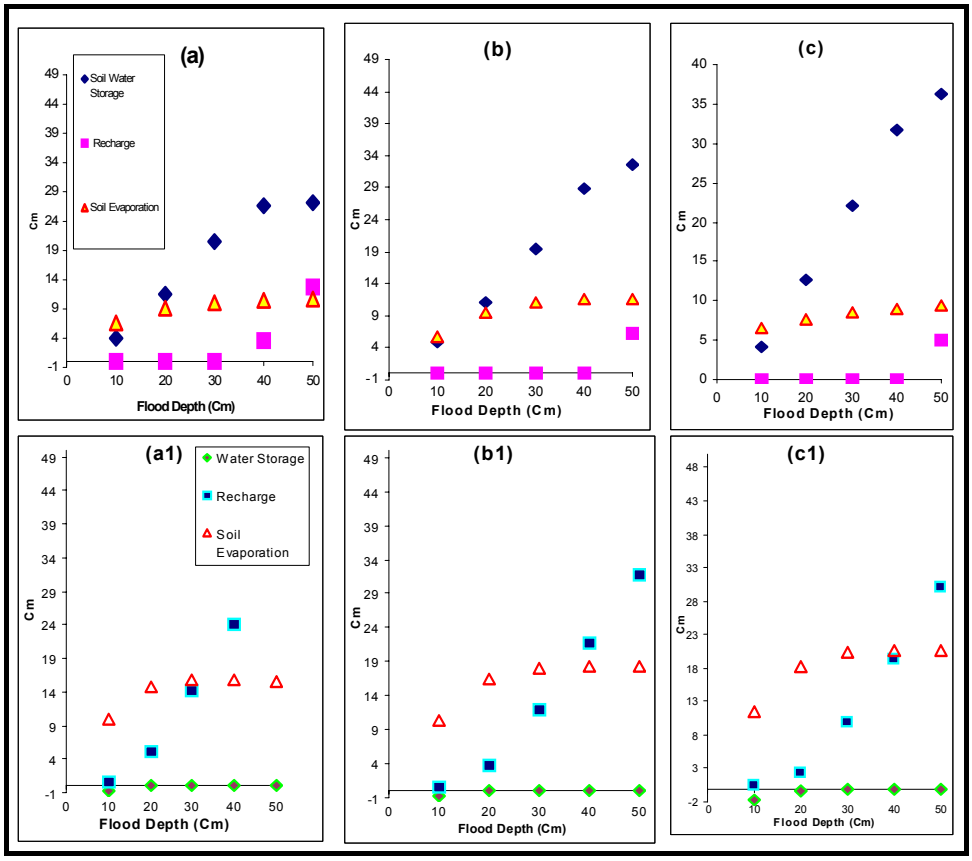

Figure 3.15 Simulation results for the relationship of flooding depth, recharge, soil evaporation and soil water storage change for Staring Series soil texture classes, using MG model, consisting of two layers, sand B3 (30 cm) overlying sand O3 (170 cm), before sedimentation for one-month and one-year simulation periods respectively. Figure (b) and (b1): after sedimentation of 30 cm sand B4 on top of the same profile for one-month and one-year simulation periods respectively. Figure (c) and (c1): after sedimentation of 30 cm clay B11 on the same profile for one-month and one-year simulation period respectively.

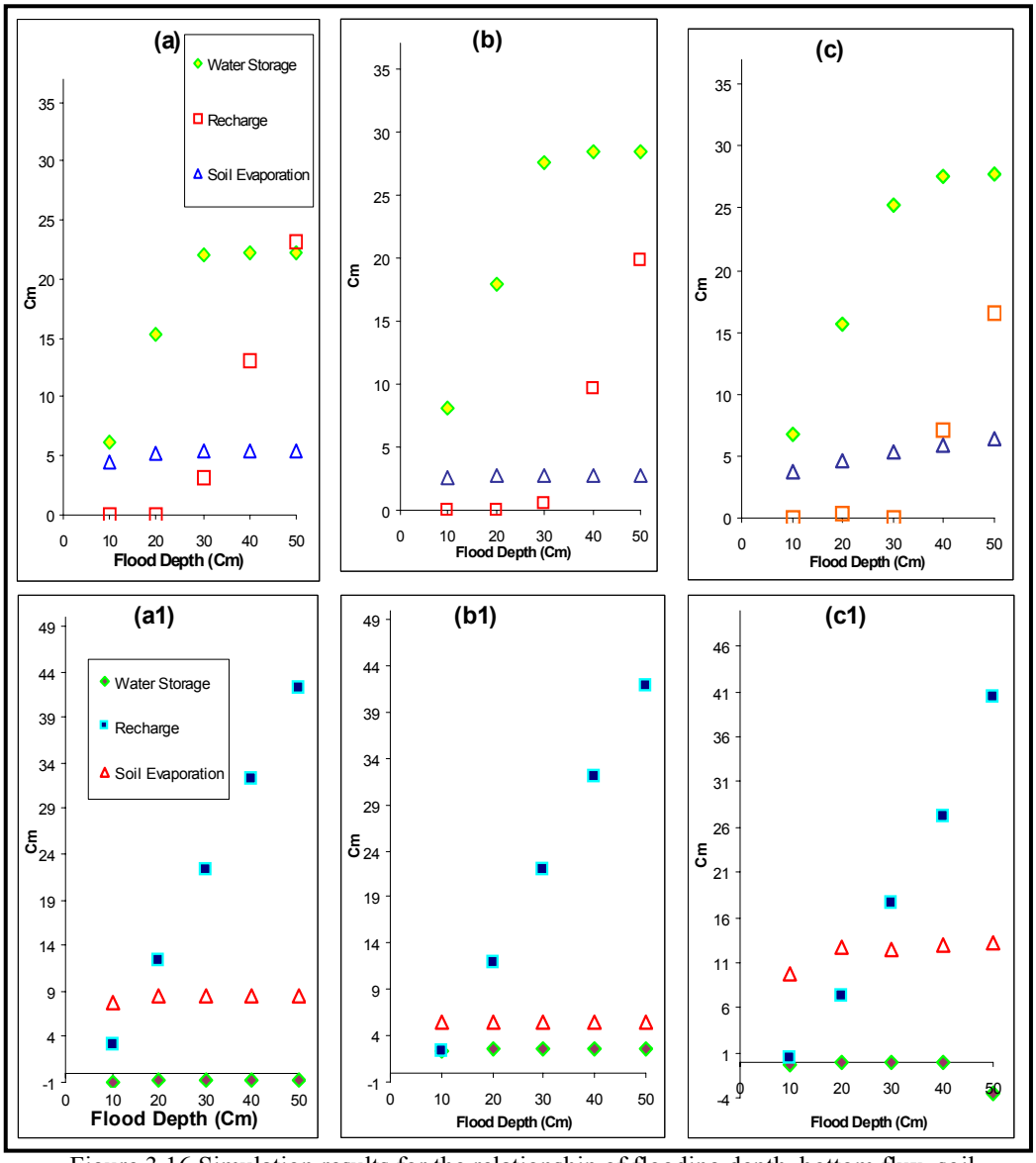

Figure 3.16 Simulation results for the relationship of flooding depth, bottom flux, soil evaporation and soil water storage change for USDA soil texture classes, using CA model, consisting of two layers, sandy loam (30 cm) overlying loamy sand (170 cm), before sedimentation for one-month and one-year simulation periods respectively. Figure (b) and (b1): after sedimentation of 30 cm sand on top of the same profile for one-month and one-year simulation periods respectively. Figure (c) and (c1): after sedimentation of 30 cm clay on the same profile for one-month and one-year simulation periods respectively.

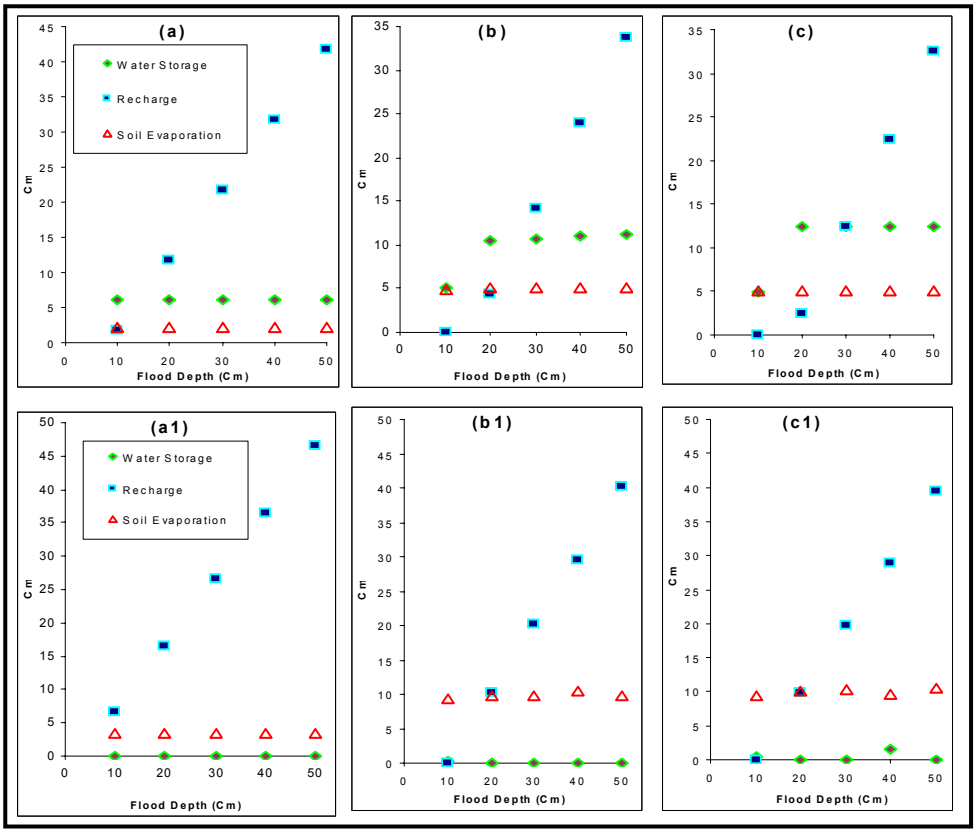

Figure 3.17 Simulation results for the relationship of flooding depth, bottom flux, soil evaporation and soil water storage change for USDA soil texture classes, using MG model, consisting of two layers, sandy loam (30 cm) overlying loamy sand (170 cm), before sedimentation for one-month and one-year simulation periods respectively. Figure (b) and (b1): after sedimentation of 30 cm sand on top of the same profile for one-month and one-year simulation periods respectively. Figure (c) and (c1): after sedimentation of 30 cm sandy clay on the same profile for one-month and one-year simulation periods respectively.

3.6.2 Simulation results for non-homogenous soil profiles under different flooding depths and frequencies

First the sandy soil column with 30 cm sand B3 overlaying 170 cm sand O3 (Staring Series) and the column of 30 cm clay B11 on top of 170 cm sand O3 were investigated with hydraulic functions based on the analytical MG model. The results are shown in Table 3.9. The recharge decreased and the evaporation increased when the frequency was changed from three consecutive days (3*d) to first three months (1d/3 months), but the soil water storage remained the same, with the exception of a flooding depth of 90 cm. Interestingly, replacing the top layer of sand by clay (Table 3.10) increased the recharge a little for the 3*d frequency, except for the 150 cm flooding depth with the 1d/3 months frequency.

The next set of simulations were done using the USDA textures and the MG model with the above flooding frequencies. The soil column was changed to 170 cm loamy sand overlain by 30 cm of sand (Table 3.9) or 30 cm of clay (Table 3.10). As in the previous case, the recharge was a little higher and evaporation lower for the 3*d than for the 1d/3 months frequencies for both top soils. The presence of the clay layer reduced the recharge, particularly for the 1d/3 months frequency. Obviously, the longer period between inundations lowered the soil moisture content prior to the next inundation, with due consequences for the distribution of the hydraulic conductivity and the pF values in the soil column, as discussed below.

The third set of simulations used the same soil column and top layers, but the hydraulic functions were computed with the CA model. The comparative results are similar to the two previous sets of simulations: recharge is a little higher for the 3*d frequency and replacement of the top layer of sand by clay did not reduce the recharge much.

3.7 Discussion and conclusion: non-homogenous soils

3.7.1 Effect of sediment layers

In the floodwater spreading schemes, generally on alluvial fans in Iran, deposition will occur because sediment-laden floodwater is diverted. Sand will be deposited in the conveyance canals and the upper parts of the infiltration basins, while clay deposition takes place in the parts where the water accumulates and stagnates. Although the set-ups for the simulations were limited, they were chosen to represent common conditions encountered in the field.

The results of the simulations for the effects show that sedimentation will reduce the recharge efficiency, as shown in Table 3.11, which presents in a condensed form the data of Tables 3.6 to 3.8. For a one-month simulation period and 10 cm of water applied, only in one of the three columns was there a recharge of 16%, but no recharge after the addition of a sediment layer. For 50 cm of water and a one-year simulation period, the recharge varied from 69 to 93% for the original column, from 64 to 84% with the additional sand layer, and from 60 to 79% with the additional clay layer.

The results can also be given by way of 'recharge reduction (RR)': RR = (REo-REs)/REo, where REo is the recharge efficiency in % of the original soil column and REs is the recharge efficiency (%) of the same soil with a sediment layer. The 50 cm flooding depth and a simulation period of one year may be considered as typical events that cause substantial recharge by floodwater diversion in the semi-arid regions of Iran and elsewhere. The recharge reduction obtained for 50 cm of water and a one-year simulation period ranged from 7 to 15% in the case of clay sedimentation and from 1 to 13% in the case of sand sedimentation, the difference being slight. However, for lesser flooding depths and shorter simulation periods the reduction in recharge, and its variation, is much more, particularly when clay sediment is present.

Table.3.6 Simulation results for effects of the sedimentation and flooding depth on recharge, using Staring Series soil texture classes for the non-homogenous soil column

Flooding Depth (cm)	Soil Water Storage (cm)						Recharge (cm)						Soil Evaporation (cm)						Saturated Hydraulic Conductivity of the Soil Profile Layers (cm d^{-1})								
	2 layers		3 layers Sand B4 top		3 layers Clay B11 top		2 layers		3 layers Sand B4 top		3 layers Clay B11 top		2 layers		3 layers Sand B4 top		3 layers Clay B11 top		2 layers		3 layers Sand B4 top			3 layers Clay B11 top		
	Simulation Period (Month)																		Top	Sub	Top	Middle	Sub	Top	Middle	Sub
	1	12	1	12	1	12	1	12	1	12	1	12	1	12	1	12	1	12								
10	4.0	-0.7	4.9	-0.8	4.1	-1.8	0.0	0.6	0.0	0.6	0.0	0.4	6.6	10.0	5.7	10.2	6.5	11.4	17.8	18.3	54.8	17.8	18.3	5.3	17.8	18.3
20	11.5	0.0	11.0	-0.1	12.8	-0.3	0.0	5.3	0.0	3.7	0.0	2.2	9.1	14.7	9.6	16.3	7.7	18.1	17.8	18.3	54.8	17.8	18.3	5.3	17.8	18.3
30	20.5	0.0	19.4	0.0	22.1	0.0	0.0	14.2	0.0	12.0	0.0	9.8	10.1	15.8	11.2	18.0	8.5	20.2	17.8	18.3	54.8	17.8	18.3	5.3	17.8	18.3
40	26.6	0.0	28.9	0.0	31.7	0.0	3.6	24.1	0.1	21.8	0.0	19.4	10.5	15.9	11.6	18.2	8.9	20.6	17.8	18.3	54.8	17.8	18.3	5.3	17.8	18.3
50	27.1	0.0	32.6	0.0	36.4	0.0	12.8	34.5	6.2	31.8	5.0	30.0	10.7	15.5	11.7	18.2	9.3	20.8	17.8	18.3	54.8	17.8	18.3	5.3	17.8	18.3

Table 3.7 Simulation results for effects of the sedimentation and flooding depth on recharge using USDA soil texture classes, for the non-homogenous soil and CA PTF

Flooding Depth (cm)	Soil Water Storage (cm)						Recharge (cm)						Soil Evaporation (cm)						Saturated Hydraulic Conductivity of the Soil Profile Layers (cm d^{-1})								
	2 layers		3 layers Sand B4 top		3 layers Clay B11 top		2 layers		3 layers Sand B4 top		3 layers Clay B11 top		2 layers		3 layers Sand B4 top		3 layers Clay B11 top		2 layers		3 layers Sand B4 top			3 layers Clay B11 top		
	Simulation Period (Month)																		Top	Sub	Top	Middle	Sub	Top	Middle	Sub
	1	12	1	12	1	12	1	12	1	12	1	12	1	12	1	12	1	12								
10	6.2	-1.0	8.1	2.4	6.8	-0.4	0.0	3.1	0.0	2.3	0.0	0.5	4.4	7.8	2.6	5.4	3.8	9.8	90.8	114.5	235.7	90.8	114.5	4.4	90.8	114.5
20	15.3	-0.7	17.9	2.6	15.6	0.0	0.0	12.3	0.0	12.0	0.4	7.4	5.3	8.4	2.8	5.4	4.6	12.6	90.8	114.5	235.7	90.8	114.5	4.4	90.8	114.5
30	22.1	-0.7	27.5	2.6	25.2	0.0	3.2	22.3	0.5	21.9	0.1	17.5	5.4	8.4	2.8	5.5	5.4	12.5	90.8	114.5	235.7	90.8	114.5	4.4	90.8	114.5
40	22.2	-0.7	28.4	2.6	27.6	0.0	13.1	32.3	9.7	32.0	7.1	27.1	5.4	8.4	2.7	5.5	5.9	12.9	90.8	114.5	235.7	90.8	114.5	4.4	90.8	114.5
50	22.2	-0.7	28.3	2.6	27.7	-3.6	23.2	42.3	19.7	42.0	16.5	40.4	5.4	8.4	2.7	5.5	6.4	13.2	90.8	114.5	235.7	90.8	114.5	4.4	90.8	114.5

Table.3.8 Simulation results for effects of the sedimentation and flooding depth on recharge using USDA soil texture classes, for the non-homogenous soil and MG PTF

Flooding Depth (cm)	Soil Water Storage (cm)						Recharge (cm)						Soil Evaporation (cm)						Saturated Hydraulic Conductivity of the Soil Profile Layers (cm d^{-1})								
	2 layers		3 layers Sand B4 top		3 layers Clay B11 top		2 layers		3 layers Sand B4 top		3 layers Clay B11 top		2 layers		3 layers Sand B4 top		3 layers Clay B11 top		2 layers		3 layers Sand B4 top			3 layers Clay B11 top		
	Simulation Period (Month)																		Top	Sub	Top	Middle	Sub	Top	Middle	Sub
	1	12	1	12	4.87	12	1	12	1	12	1	12	1	12	1	12	1	12								
10	6.2	0.0	5.1	0.2	12.4	0.5	1.7	6.6	0.0	0.0	0.0	0.0	2.1	3.4	4.9	9.3	5.1	9.5	106.1	350.2	712.8	106.1	350.2	4.4	106.1	350.2
20	6.2	0.0	10.5	0.0	12.4	0.0	11.7	16.6	4.4	10.3	2.5	9.9	2.1	3.4	5.1	9.7	5.1	10.1	106.1	350.2	712.8	106.1	350.2	4.4	106.1	350.2
30	6.2	0.0	10.7	0.0	12.4	0.0	21.7	26.6	14.2	20.3	12.5	19.8	2.1	3.4	5.1	9.7	5.1	10.2	106.1	350.2	712.8	106.1	350.2	4.4	106.1	350.2
40	6.2	0.0	10.9	0.0	12.4	1.5	31.7	36.6	23.9	29.7	22.5	28.9	2.1	3.4	5.1	10.3	5.1	9.7	106.1	350.2	712.8	106.1	350.2	4.4	106.1	350.2
50	6.2	0.0	11.1	0.0	4.9	0.0	41.7	46.6	33.7	40.3	32.5	39.6	2.1	3.4	5.1	9.7	5.1	10.5	106.1	350.2	712.8	106.1	350.2	4.4	106.1	350.2

Table 3.9 Relationship between flooding depth, soil evaporation, soil water storage change and recharge for a soil column with 30 cm high permeable soil (sand, sandy loam) overlying 170 cm high permeable (sand, loamy sand) soils

Total Flood Depth (cm)	Ks Top (cm d^{-1})			Ks Sub (cm d^{-1})			Water Storage Change (cm)						Recharge (cm)						Soil Evaporation (cm)					
							Staring Series		USDA MG		USDA CA		Staring Series		USDA MG		USDA CA		Staring Series		USDA MG		USDA CA	
	Staring Series	USDA MG	USDA CA	Staring Series	USDA MG	USDA CA	Fr. 3*d	Fr. 1d 3 Months	Fr. 3*d	Fr. 1d 3 Months	Fr. 3*d	Fr. 1d 3 Months	Fr. 3*d	Fr. 1d 3 Months	Fr. 3*d	Fr. 1d 3 Months	Fr. 3*d	Fr. 1d 3 Months	Fr. 3*d	Fr. 1d 3 Months	Fr. 3*d	Fr. 1d 3 Months	Fr. 3*d	Fr. 1d 3 Months
30	17.81	106.1	90.76	18.30	350.2	114.46	0	-0.03	0	0	0	0	13.96	4.2	26.23	21.95	21.36	13.72	16.04	25.83	3.77	8.05	8.68	16.59
60	17.81	106.1	90.76	18.30	350.2	114.46	0	0	0	0	0	0	43.36	32.02	56.23	53.47	51.44	43.55	16.14	27.98	3.77	6.54	8.68	16.59
90	17.81	106.1	90.76	18.30	350.2	114.46	11.21	0	0	0	0	0	62.46	61.89	86.23	83.46	81.4	73.85	16.34	28.11	3.77	6.54	8.68	16.59
120	17.81	106.1	90.76	18.30	350.2	114.46	0	0	0	0	0	0	103.4	91.75	116.23	113.47	111.41	103.96	16.6	28.25	3.77	6.54	8.68	16.59
150	17.81	106.1	90.76	18.30	350.2	114.46	0	0	0	0	0	0	133.28	121.6	146.23	143.47	141.42	133.86	16.86	28.4	3.77	6.53	8.68	16.59

Table 3.10 Relationship between flooding depth, soil evaporation, soil water storage change and bottom flux when 30 cm low permeable soils (clay) overlying 170 cm high permeable (sand, loamy sand) soils

Total Flood Depth (cm)	Ks Top ($cm\,d^{-1}$)			Ks Sub ($cm\,d^{-1}$)			Water Storage Change (cm)						Recharge (cm)						Soil Evaporation (cm)					
							Staring Series		USDA MG		USDA CA		Staring Series		USDA MG		USDA CA		Staring Series		USDA MG		USDA CA	
	Staring Series	USDA MG	USDA CA	Staring Series	USDA MG	USDA CA	Fr. 3*d	Fr. 1d 3 Months	Fr. 3*d	Fr. 1d 3 Months	Fr. 3*d	Fr. 1d 3 Months	Fr. 3*d	Fr. 1d 3 Months	Fr. 3*d	Fr. 1d 3 Months	Fr. 3*d	Fr. 1d 3 Months	Fr. 3*d	Fr. 1d 3 Months	Fr. 3*d	Fr. 1d 3 Months	Fr. 3*d	Fr. 1d 3 Months
30.0	5.3	2.9	8.7	18.3	350.2	114.5	0.0	0.1	0.0	0.1	0.0	0.0	16.9	9.8	24.9	15.8	17.4	6.5	13.1	20.1	5.1	14.1	12.6	23.5
60.0	5.3	2.9	8.7	18.3	350.2	114.5	0.0	0.0	0.0	0.0	0.0	0.0	46.5	38.7	54.1	43.3	47.2	35.7	13.5	21.3	5.9	16.7	12.9	24.3
90.0	5.3	2.9	8.7	18.3	350.2	114.5	0.0	0.0	0.0	0.0	0.0	0.0	76.2	68.1	82.6	71.1	77.0	65.5	13.8	21.9	7.4	18.9	13.0	24.5
120.0	5.3	2.9	8.7	18.3	350.2	114.5	0.0	0.0	0.0	0.0	0.0	0.0	105.5	97.6	111.2	99.1	106.4	95.3	14.5	22.4	8.8	20.9	13.6	24.7
150.0	5.3	2.9	8.7	18.3	350.2	114.5	0.0	11.9	0.0	0.0	0.0	0.0	134.9	115.3	139.8	126.0	136.7	125.2	15.1	34.7	10.2	24.0	13.3	24.9

Table 3.11 Summary of SWAP model simulation results when soil hydraulic functions calculated based on CA and MG models for non-homogenous soil profile under sedimentation

Soil Profile Layers	Recharge (%) Staring Series Soil Classes				Recharge (%) USDA Soil Classes (CA)				Recharge (%) USDA Soil Classes (MG)				Water Storage Change (%) Staring Series Soil Classes				Water Storage Change (%) USDA Soil Classes (CA)				Water Storage Change (%) USDA Soil Classes (MG)				Evaporation (%) Staring Series Soil Classes				Evaporation (%) USDA Soil Classes (CA)				Evaporation (%) USDA Soil Classes (MG)			
Simulation Period (month)	1		12		1		12		1		12		1		12		1		12		1		12		1		12		1		12		1		12	
Flood Depth (cm)	10	50	10	50	10	50	10	50	10	50	10	50	10	50	10	50	10	50	10	50	10	50	10	50	10	50	10	50	10	50	10	50	10	50
Initial Soil Profile before Sedimentation (two layers 200 cm)	0	25	6	69	0	46	31	85	16	82	66	93	37	54	-7	0	58	44	-10	-1	58	12	0	0	63	21	100	31	42	11	78	17	20	4	34	7
After 30 cm Sand Sediment	0	12	5	64	0	39	23	84	0	67	5	81	47	64	-8	0	76	56	24	5	48	27	2	0	53	23	103	36	25	5	54	11	46	10	93	19
After 30 cm Clay Sediment	0	10	4	60	0	33	5	81	0	64	0	79	39	72	-18	0	64	55	-4	-7	46	24	5	0	61	18	114	42	36	13	98	26	48	10	95	21

The practical implication is that by simulation an estimate can be obtained of the reduced efficiency of a scheme after commissioning, and an estimate of the effect of removal of sediment. As discussed in a later part of this chapter, the estimate so obtained is subject to modification by considering the types of clay.

3.7.2 Effect of inundation depth

The simulation results all indicate that recharge efficiency increased with larger depths of inundation of flooding. However, much variation was found. For example, with a five-times increase in inundation depths, from 10 to 50 cm, and a simulation period of one year for layered soil columns with and without a sediment layer on top (Tables 3.6 to 3.8), the recharge efficiency increased 13 to 77 times for the soils described by the Staring Series and by the USDA classes/CA, and even higher values when the USDA/MG was used – except when no sediment was on top (seven times higher recharge). It is interesting to note that the largest increase occurred in the simulations with a clay layer on top. It should be remembered that the sediment layer reduces the total recharge.

The effect of the rapid downward propagation of the water flux after deeper inundation of a soil column with a 30 cm clay layer on top is illustrated in Figure 3.18, which shows the water flux, the moisture content and the soil suction (pF) one day and five days after applying 10 and 50 cm of water on the two-layered sandy soil column (Staring Soil Series and MG method) with 30 cm clay sediment on top.

As can be noted from the graphs, the wetting front proceeded to a depth of about 200 cm after five days when 50 cm of water was applied and saturated the upper two soil layers and the lowermost layer to a depth of 170 cm. The wetting front stayed after five days at a depth of about 40 to 50 cm with only 10 cm inundation depth, which saturated only the upper layer. The graph with the moisture content indicates that the zero flux plane developed at about 15 cm depth after five days for the 10 cm inundation depth. This plane will be lowered in the subsequent days, with the result that a large part of the soil moisture will return to the surface and evaporate (illustrated in Figure 3.19).

When the frequency of inundations was changed in the simulations (Tables 3.9 and 3.10), namely one third of the total amount on the first three consecutive days in the first month (1d) and one third on the first day of the first three months (1d/3 months), the ratio between the 150 and 50 cm total inundation depth had a range of 5.6 to 9.7, with the exception of the simulation with the 1d/3 months frequency, using the Staring Series and the sand top layer (ratio 28), and the simulation using the USDA/CA method with the clay top layer (ratio 19). The lower ratios resulting from more frequent application than just one signify the role of higher soil moisture levels, which influence the pF and hydraulic conductivity, making the recharge process more efficient. This is also shown in Table 3.11. By considering 50 cm flooding depths and a simulation period of one year, representative of important flood events, the recharge efficiencies of the simulations done worked out to be in the range of 60 to 93%, but the efficiency greatly decreases for lesser inundation depths.

The significance for designs is that when the floodwaters have much fine-grained sediment, the design of the scheme should aim at large inundation depths. The large amount of water and the large head provided can raise soil moisture contents so that the downward flux of water accelerates to contribute to the recharge, minimizing evaporation losses. Smaller amounts of water are held up in the upper zone and the infiltrated water is held fully or partly by the soil, causing a relative increase in the evaporation, particularly when sedimentation takes place in the scheme.

3.7.3 Effect of flooding frequency

The compiled results for the effects of flooding frequencies on the relationships between flooding depths, recharge, soil storage and evaporation are shown in Tables 3.12 and 3.13.

Table 3.12 shows the results when the soil profile consists of 30 cm high permeable soil layering 170 cm light texture. Table 3.13 shows the results for the soil profile consisting of 30 cm low permeable soil layering 170 cm light texture. For both profiles, soil layers were selected from the Staring Series and the USDA soil texture classes, and the soil hydraulic functions were computed using MG and CA PTFs. The simulated flooding frequencies were one day (first three days of the first month of the one-year simulation period) and one month (first day of the first three months of the one-year simulation period). Flooding depths were 10, 20, 30, 40 and 50 cm, inundated three times based on flooding frequencies for each single simulation. For example, when flooding depth is 10 cm and frequency is one day, 10 cm flood inundated on the first, second and third days of the first month of the simulation period means in total 30 cm flood for the simulation.

For the high permeable soil column (Table 3.12), when the flooding frequency increased from 3*d to 1d/3 months, the recharge reduced considerably. The reduction rates vary between 9% (50 cm) to 70% (10 cm) for the Staring Series, 5% (50 cm flood) to 35% (10 cm flood) for USDA (MG method), and 1% (50 cm flood) to 16% (10 cm flood) for USDA (CA method) soil texture classes. Also when the flooding frequency changed to 1d/3 months, soil evaporation greatly increased. The percentages of increase range from 62% (10 cm flood) to 72% (50 cm flood), 84% (50 cm flood) to 90% (10 cm flood), and 33% (50 cm flood) to 108% (10 cm flood).

For the soil profile with the low permeable top soil layer, the above reduction ranges (Table 3.13) for recharge with the same soil texture classes database vary from 14% (50 cm flood) to 41% (10 cm flood), 9% (50 cm flood) to 62% (10 cm flood), and 10% (50 cm flood) to 36% (10 cm flood). The increasing evaporation rates range from 52% (10 cm flood) to 130% (50 cm flood), 86% (50 cm flood) to 89% (10 cm flood), and 129% (50 cm flood) to 176% (10 cm flood). Soil water storage did not change for any of the simulations.

The above results indicate that when flooding frequency increased, the soil column with a low permeable top layer, compared with a high permeable one, shows much more reduction in recharge and increase in soil evaporation rates.

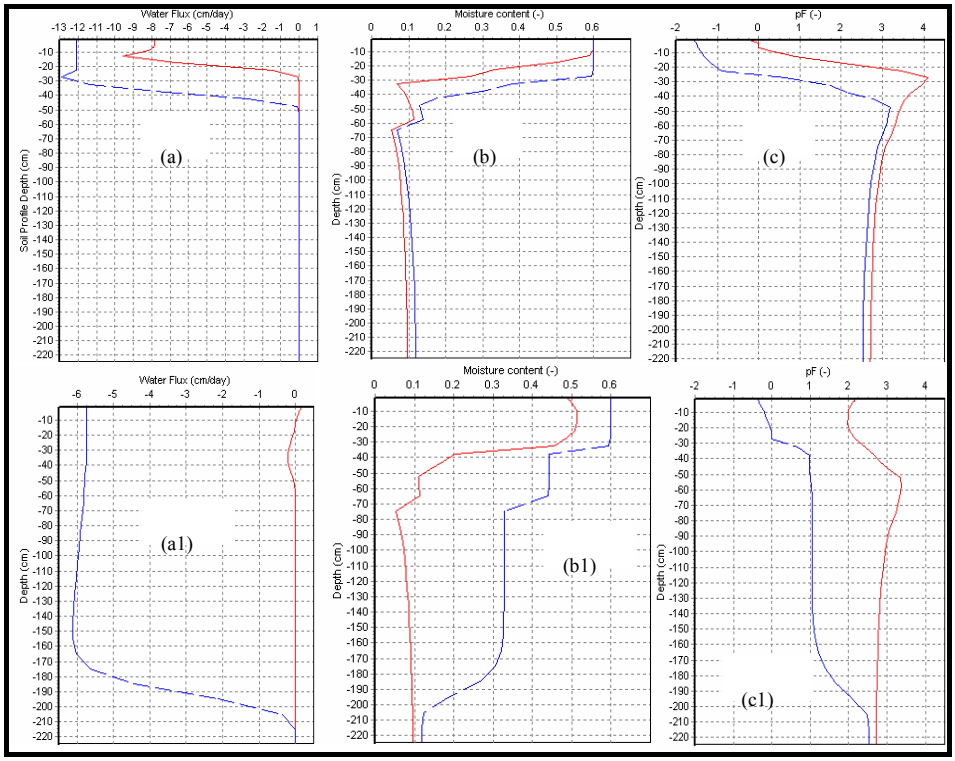

Figure 3.18 SWAP simulation of flooding depth (10 cm red line and 50 cm blue line), soil profile depth, (a and a1) water flux, (b and b1) soil moisture content and (c and c1) pF at the end of the first day and fifth day of the simulation period respectively, after 30 cm clay sediment (MG method)

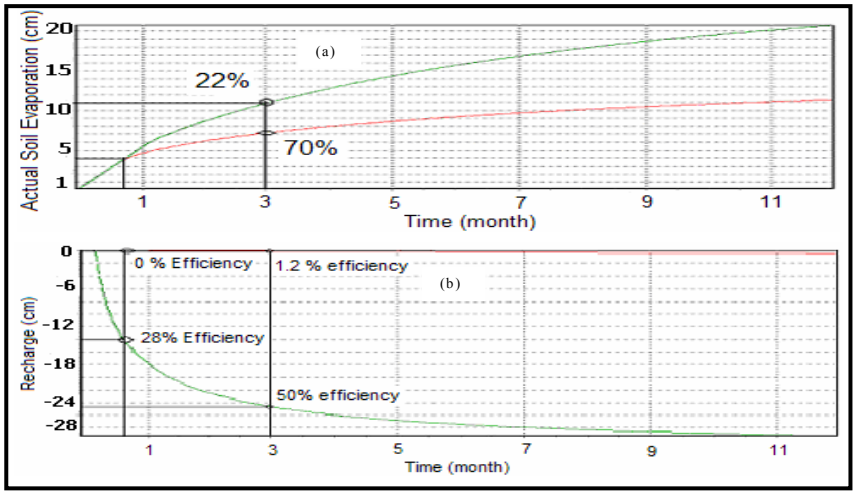

Figure 3.19 Comparison (a) between cumulative soil evaporation and (b) cumulative recharge for the 10 cm (red line) and 50 cm (green line) flooding depths for the soil profile with 30 cm clay sediment on top

Table 3.12 Effects of flooding frequencies and depths on relationship between recharge, evaporation and soil water storage changes when soil profile consists of 30 cm high permeable soil layering 170 cm light texture soil

Flooding Frequency	Recharge (%) Staring Series		Recharge (%) USDA Soil Texture Class CA PTF		Recharge (%) USDA Soil Texture Class MG PTF		Water Storage Change (%) Staring Series		Water Storage Change (%) USDA Soil Texture Class CA PTF		Water Storage Change (%) USDA Soil Texture Class MG PTF		Evaporation (%) Staring Series		Evaporation (%) USDA Soil Texture Class CA PTF		Evaporation (%) USDA Soil Texture Class MG PTF	
	3*10 cm Flood	3*50 cm Flood	3*10 cm Flood	3*50 cm Flood	3*10 cm Flood	3*50 cm Flood	3*10 cm Flood	3*50 cm Flood	3*10 cm Flood	3*50 cm Flood	3*10 cm Flood	3*50 cm Flood	3*10 cm Flood	3*50 cm Flood	3*10 cm Flood	3*50 cm Flood	3*10 cm Flood	3*50 cm Flood
3*d	47	89	71	94	87	97	0	0	0	0	0	0	53	11	29	6	13	3
1d/3 months	14	81	46	89	73	96	0	0	0	0	0	0	86	19	55	11	27	4
Reduction Rate (%)	70	9	35	5	16	1	0	0	0	0	0	0	0	0	0	0	0	0
Increasing Rate (%)	0	0	0	0	0	0	0	0	0	0	0	0	62	72	90	84	108	33

Table 3.13 Effects of flooding frequencies and depths on relationship between bottom flux, evaporation and soil water storage changes when soil profile consists of 30 cm low permeable soil layering 170 cm light texture soil

Flooding Frequency	Recharge (%) Staring Series		Recharge (%) USDA Soil Texture Class CA PTF		Recharge (%) USDA Soil Texture Class MG PTF		Water Storage Change (%) Staring Series		Water Storage Change (%) USDA Soil Texture Class CA PTF		Water Storage Change (%) USDA Soil Texture Class MG PTF		Evaporation (%) Staring Series		Evaporation (%) USDA Soil Texture Class CA PTF		Evaporation (%) USDA Soil Texture Class MG PTF	
	3*10 cm Flood	3*50 cm Flood	3*10 cm Flood	3*50 cm Flood	3*10 cm Flood	3*50 cm Flood	3*10 cm Flood	3*50 cm Flood	3*10 cm Flood	3*50 cm Flood	3*10 cm Flood	3*50 cm Flood	3*10 cm Flood	3*50 cm Flood	3*10 cm Flood	3*50 cm Flood	3*10 cm Flood	3*50 cm Flood
3*d	56	90	58	91	83	93	0	0	0	0	0	0	44	10	42	9	17	7
1d/3 months	33	77	22	83	53	84	0	8	0	0	0	0	67	23	78	17	47	16
Reduction Rate (%)	41	14	62	9	36	10	0	0	0	0	0	0	0	0	0	0	0	0
Increasing Rate (%)	0	0	0	0	0	0	0	0	0	0	0	0	52	130	86	89	176	129

The differences in the flux of water as a function of soil moisture and pF changes in the permeable soil column with two layers (Staring Series) for the two inundation frequencies are illustrated in Figures 3.20 and 3.21. The left-hand graphs of Figure 3.20 show the situation on the third day of simulation (graphs a) The curve for the 3*d frequency when 10 cm of water was given on each of the three consecutive days (a total of 30 cm) shows that the wetting front had penetrated to a depth of about 110 to 130 cm, and the curve for the flux shows two maxima (10 and 12 cm d-1) in the higher part of the profile, at about 100 cm and 30 cm depths. The flux arriving at 190 cm depth (Figure 3.22b) takes place with a maximum of 11.5 cm d-1 a few days after the start of the simulation. The cumulative bottom flux (at 200 cm depth) after one year is about 14 cm, or 47% of the amount of water applied. The remaining 16 cm is entirely lost through evaporation, as shown in Figure 2.21a.

The curves for the 1d/3 months showed partial saturation of the upper sand layer of 30 cm thickness, and moisture increase reached a depth of 70 cm, but only a very small flux occurred, with a maximum at about 40 cm depth. On the second day of the third month (graphs b), the moisture content for the 3*d simulation was so low that the flux practically ceased; most of the recharge or bottom flux had passed earlier. The curve for the 1d/3 months simulation showed a small flux with a maximum of 1.1 cm d-1 at 60 cm depth, due to the 10 cm of water applied the previous day. However, little of that water, namely about 4 cm, passed the bottom of the column (Figure 3.21b), with a maximum flux of about 1 cm/d reaching the bottom about 10 weeks after the start of the simulation. Earlier simulations (Table 3.6) showed that a single application of 10 cm resulted in no bottom flux at all. The 1d/3 months frequency of water application showed strong evaporation when the soil was wet or moist, as shown in Figure 3.21a.

In brief, the application of 10 cm of water during each of the first three days of simulation caused rapid downward percolation and resulted in appreciable recharge, whereas the same amount of water applied on the first day of each of the first three months caused little recharge and high evaporation loss because most of the water stayed in the upper part of the soil.

From the above, it can be concluded that shorter flooding frequency increased soil moisture contents and water flux of the deeper parts of the soil profile faster, and as a result bottom flux increment was much more. Longer frequency affected the upper part of the soil profile and consequently soil evaporation greatly increased, and as a result the increments in the water flux in the deeper part of the soil profile and bottom flux were very low.

3.8 Limitations of the simulations

The simulations were based on soil textures and PTFs only. Soil texture is generally the most important criterion for estimating potential recharge (Kearns and Hendrickx, 1998; Haimerl, 2001) but, as discussed earlier, the choice of PTFs affects the results. However, there are more factors that play a role in the recharge efficiency of a floodwater spreading scheme, and these will be briefly reviewed below.

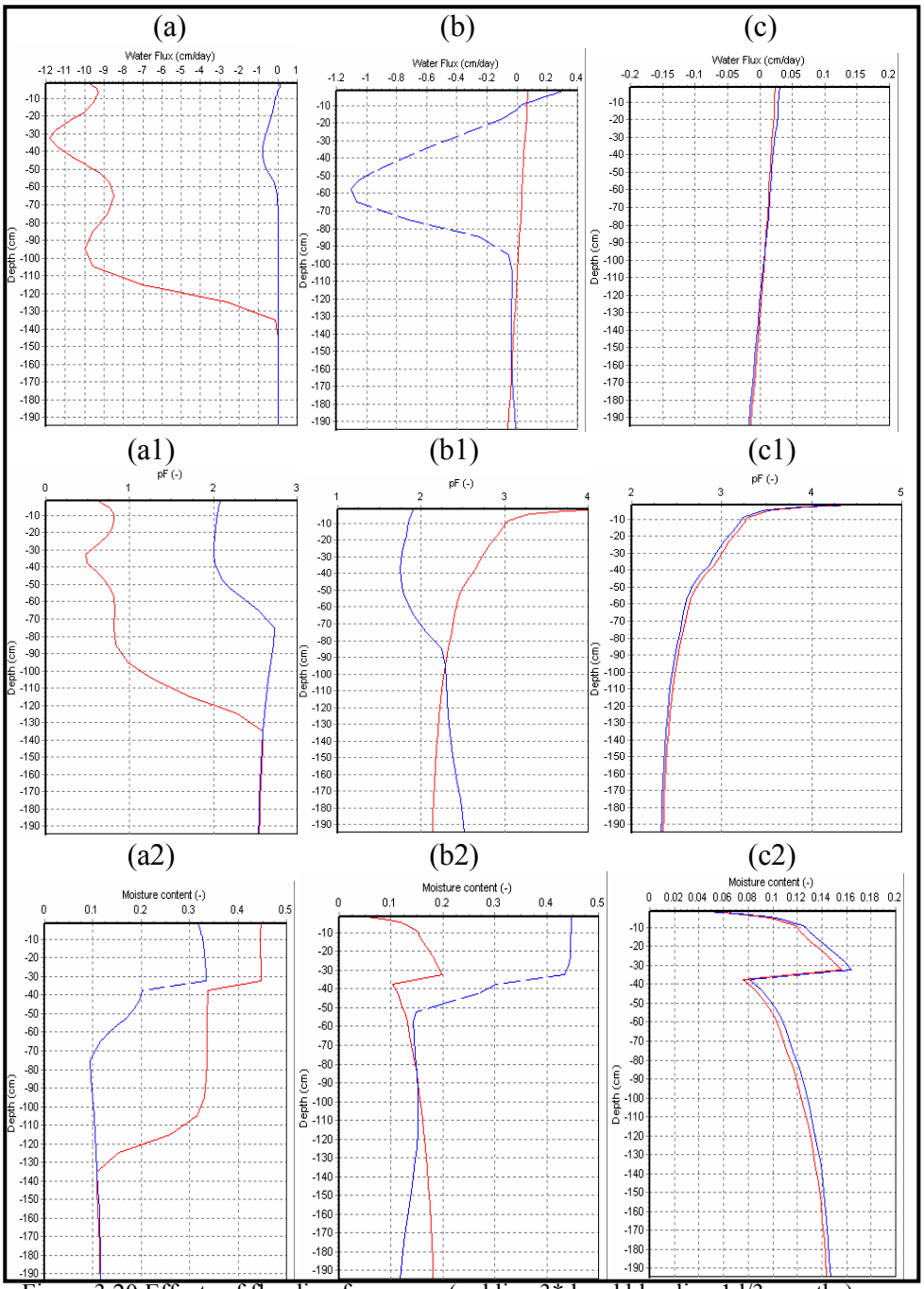

Figure 3.20 Effects of flooding frequency (red line 3*d and blue line 1d/3 months) on the relationship between soil profile depth, water flux, pF and soil moisture content on (a,a1,a2) third day of the first month, (b,b1,b2) second day of the third month and (c,c1,c2) first day of the sixth month of the simulation period, for 10 cm flooding depth and high permeable layering (two layers) soil profile (Staring Series)

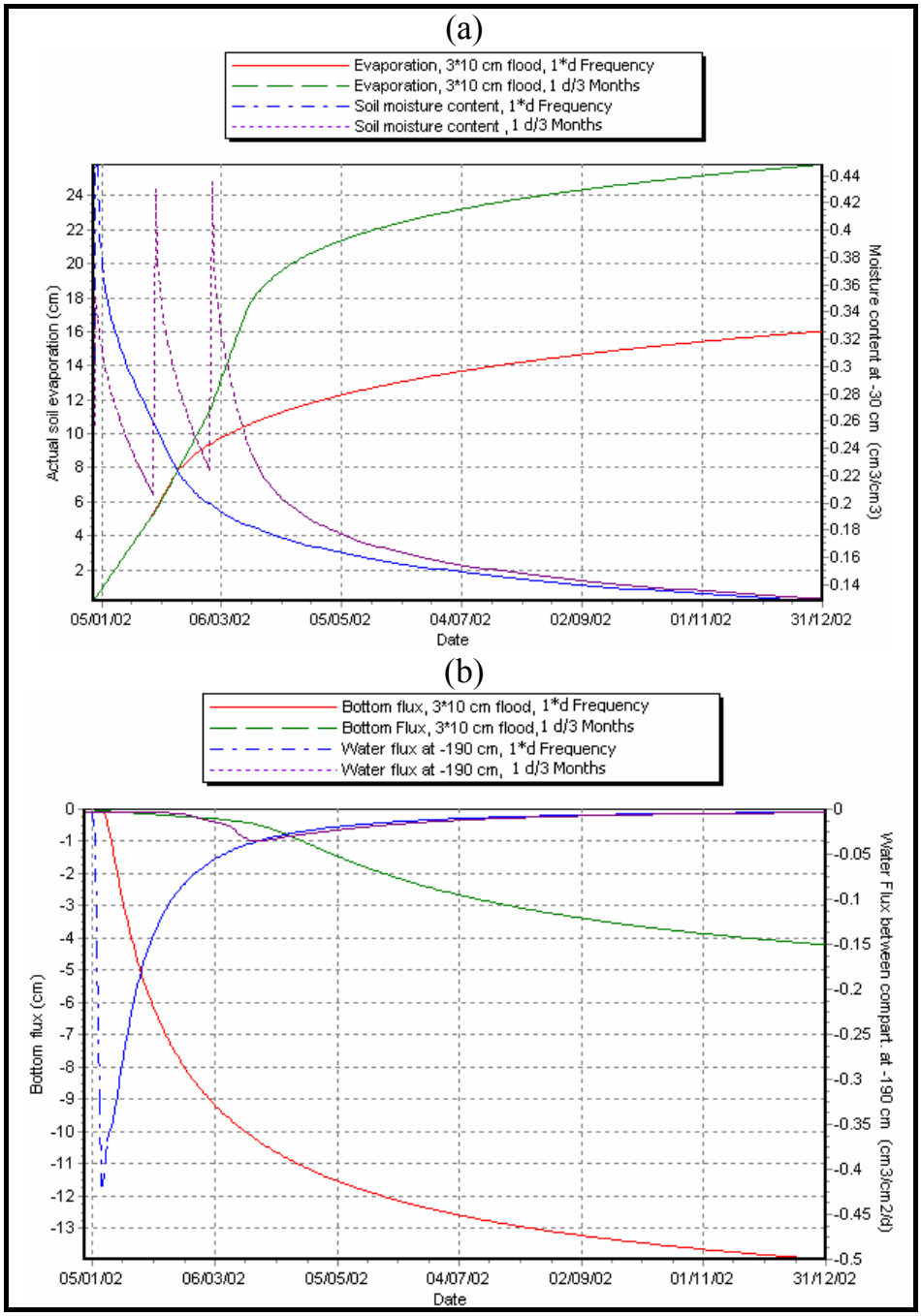

Figure 3.21 Relationship between (a) cumulative soil evaporation and soil moisture content at 30 cm deep, and (b) cumulative bottom flux and water flux at 190 cm deep, for the soil profile consisting of two light and high permeable soil layers, for one-year simulation period, 3*10 cm flood, 3*d and 1d/3 months flooding frequencies

One of the initial assumptions of this study was that soil-saturated hydraulic conductivity and bottom flux (recharge) are strongly correlated (directly). But the simulation results have shown that this is not the case; correlation can be weak for the heavy textures. Only for sandy soils was a good correlation ($R^2 = 0.84$) found. Large differences in results were noted, depending on the method (PTF) used. Different studies (e.g. Christiaens and Feyen, 2001; Marcel et al. 2002; Guber et al., 2003) comparing laboratory-measured hydraulic parameters with those derived by PTFs showed appreciable variation.

The wide variation in the expected recharge when heavy textured soils are present can be attributed to the complex role of the clays. The movement of clay particles down the profile, or eluviation, can block pore space and reduce hydraulic conductivity. The eluviation process is enhanced if dispersion takes place influenced by the salinity and sodicity of the soil. Clay soils hold more water than sand soils, and the evaporation loss is higher, as also shown by the simulations, with due consequences for the salt content and thus the dispersivity of the soil.

Repeated wetting and drying of a clay soil, as occurs in a floodwater spreading scheme, causes clay dispersion. The soil will re-form and solidify with little or no structure (Warrence et al., 2002). For that reason, deep ripping of the infiltration basins is often done to maintain permeability. This aspect is of relevance in selecting catchments in Iran, where river water may have high salinity if salt-bearing outcrops occur. Apart from the fact that the recharge efficiency will be low, also the water quality of the recharge to be used for irrigation or drinking water may be below accepted standards.

Another factor of importance is the swelling of the soil, which can take place up to some 10 m from the ground surface. Factors that affect the swelling properties of clays are discussed by Olive et al. (1989), but the most significant factor is the proportion of montmorillonite. Clays of this type are the most prone to swelling and dispersion, whereas koalinites are the least likely to swell and disperse (Warrence et al., 2002). The nearly impermeable nature of the vertisols (such as the black cotton soils) when wet is well known. Montmorillonite has a lattice structure that is favourable for the binding of sodium, and the more sodium clay can hold, the more infiltration and hydraulic conductivity is reduced.

Some other clays composed of fine-grained, randomly oriented, non-expandable clay minerals have swelling potentials as great as those of clays composed of expandable clay minerals. In the Gareh Baygan floodwater spreading scheme, such clays are present and limit the infiltration (Kowsar, 1995). In some other schemes in Iran, such as the Yazd scheme located on the downstream end of a large alluvial fan, no infiltration and percolation had taken place within a thick, inundated clay layer, because the evaporation measured in a container floating in the water matched precisely the lowering of the water surface in a field experiment lasting five days. The general recommendations for floodwater spreading schemes (Kowsar, 1995) mention that infiltration areas with clay-rich soils should be avoided.

As mentioned earlier, in some studies substantial recharge, as found in soils rich in clay and also in our simulations in some heavy textured soils with a low hydraulic conductivity, a reasonable recharge efficiency was found, provided

inundation depths were large. Such simulations assume diffuse flow only and not by-pass flows. A special form of by-pass flow is the flow through cracks that can be wide and deep in clay soils with the swelling type of clays. The high initial infiltration will depend on how fast the cracks close. Closure times vary widely, and so will the initial infiltration, adding to the recharge not captured by simulation of diffuse flow. The same can be said for by-pass flow through root tunnels and cracks in the original soil of a floodwater spreading scheme.

The presence of impeding soil horizons or layers also reduces recharge, even rendering the process insignificant. Cementation of clays but also of coarser-grained soils, usually by lime, can render the layer impermeable, as, for example, the recharge experiment in the eastern Zanjan Valley has demonstrated. Such cementation at the surface or at various depths below the surface is usually found on the older alluvial fan deposits. The existence of impeding layers at limited depths may require the selection of a scheme type consisting of deep basins, where the layers are removed by excavation.

The simulation results indicate that a given amount of water is best diverted in as short a time span as possible. Long dry intervals reduce the recharge efficiency. This finding is useful in estimating the recharge efficiency of an intended scheme, by considering the interval times of the runoff events in the river and the design of the intake structure. This aspect also has an implication for the selection of areas and catchments for floodwater spreading schemes. Within a given region in Iran, there are catchments at higher altitudes with permeable lithology, such as limestone and sandstone, and orographic rainfall effects, next to catchments at lower altitudes and lesser catchment permeability. Therefore, important differences in the magnitude of the runoff events and the intervals between important events can be expected. Catchments with runoff events clustered in time are preferred, all other factors being equal.

Sedimentation within a floodwater spreading scheme cannot be avoided, because the flash flows that are diverted generally have large sediment loads, particularly the important flows. As the simulations show, in line with what is generally observed, sedimentation reduces the recharge efficiency and increases the evaporation, especially sedimentation of clay. Layers of clay thicker than the 30 cm used in the simulation will reduce the recharge efficiency substantially because much more water will be used for increasing the soil moisture after long dry periods and consequently the evaporation loss will increase. In order to maintain recharge efficiency, thick layers of clay should be removed periodically, raising the maintenance cost of a scheme.

Because of all such complications, it is advisable to carry out long-duration infiltration tests in the potential infiltration area of an envisaged floodwater spreading scheme when soils contain clay. The best type would be ponding tests with variable depths, because all simulations and reports in the literature highlight that recharge depends much on ponding depth. The spatial variations in infiltration and hydraulic conductivity, which have been demonstrated by many authors (e.g. Shafique and Skogerboe, 1983; Vogel et al., 2000; Entin et al. 2000), and the large amounts of water required for ponding

tests limit the practical application and make simulation studies attractive. However, simulation results need to be verified by field studies, particularly by using existing schemes where important sedimentation of clay has taken place. In this context, an evaluation of a large scheme is discussed in the next chapter.

CHAPTER 4
Modelling Recharge on Varamin Plain, Iran

4.1 Introduction

The recharge efficiency of the soil columns with different hydrophysical and flooding characteristics has been studied using one-dimensional soil moisture flux modelling (SWAP), and two different PTFs, as discussed in Chapter 3.

The main objective in this chapter is to explore whether upscaling the results of the above-mentioned modelling would have any practical significance when used to simulate the recharge of a complete scheme.

Of the many schemes in operation in Iran, only the Sorkehesar scheme had an accurate record of an important inflow event which allowed assessment of the recharge efficiency. This scheme has been in operation since 1975 and has developed over the years into a fairly complex hydraulic situation. The upper infiltration basins have developed sinuous channels between spillways, and the middle basins have clay and silt blankets, which are absent in the lower basins. Hence, the situation is what can be expected in floodwater spreading basins of this type without removal of the fine-grained sediment.

The recharge event from March to July 2002 (four months) was used because a record of the inflow existed and the extension of the inundated parts could be surveyed, as well as the end stage of the recharge event. The complexity necessitated the development of a model to simulate depth and duration of inundation. A floodwater spreading scheme with simpler geometry would have been preferable, but no accurate inflow data could be found for the Iranian schemes in which sediment was allowed to accumulate.

4.2 The study area

Varamin Plain (see Figure 4.1) is a southerly trending alluvial fan, which has been deposited primarily by the Jaj Rud (*rud* is river in Parsee). The plain lies about 40 km southeast of Teheran, while the Jaj Rud drainage is located to the northeast of Teheran, on the southern slope of the Alburz Mountains. The Latian dam is located on the Jaj Rud about 20 km east of Teheran, and water from the river is being diverted to the city of Teheran, thus reducing surface supplies to Varamin Plain. After being used for irrigation purposes on Varamin Plain, the wastewater and occasional floodwater drain southeasterly to a vast salt flat called Dasht-I-Kavir, which extends about 300 km to the east. Rainfall on Varamin Plain is very low and therefore agriculture depends entirely on irrigation, partly by present sources of the Jaj Rud, which are diverted through many canals to the fields, and partly by groundwater. Groundwater was first developed by the construction of qanats, and then by drilled and cased water wells.

The approximate latitudes of the plain are 51º 28' 42″ and 51º 49' 40″ E and the longitudes are 35º 2' and 35º 29' 52″ N. The approximate area of Varamin Plain is 1870 km^2. Topographical elevation varies between 800 and 1100 m and the

average elevation is 950 m asl. An Aster image (false-colour composite, July 2001) of Varamin Plain is shown in Figure 4.2.

Climate

Varamin Plain has an arid to semi-arid climate. The summers are very hot and dry and the winters are very cold and dry. Maximum temperatures are 40 to 45°C and minimum temperatures are below zero. The difference between day and night temperatures in this area is considerable, and precipitation appears in the form of rainfall and snow. The average yearly rainfall (40 years) is 160 mm. The monthly reference evaporation, ETo (average 40 years) calculated by the US class A pan evaporation and Penman-Monteith (Monteith, 1965) methods, is as shown in Table 4.1.

Varamin aquifer

The aquifer has a surface area of 1310 km^2 and consists of alluvial fan deposits with the typical facies changes from coarse-grained textures (mixtures of sands and gravels with pebble and boulder beds) in the upper part to clayey and silty textures in the lower part. Maximum thickness of the alluvial deposits is about 300 m, but average thickness is 100 m. The deposits overlay formations of low permeability.

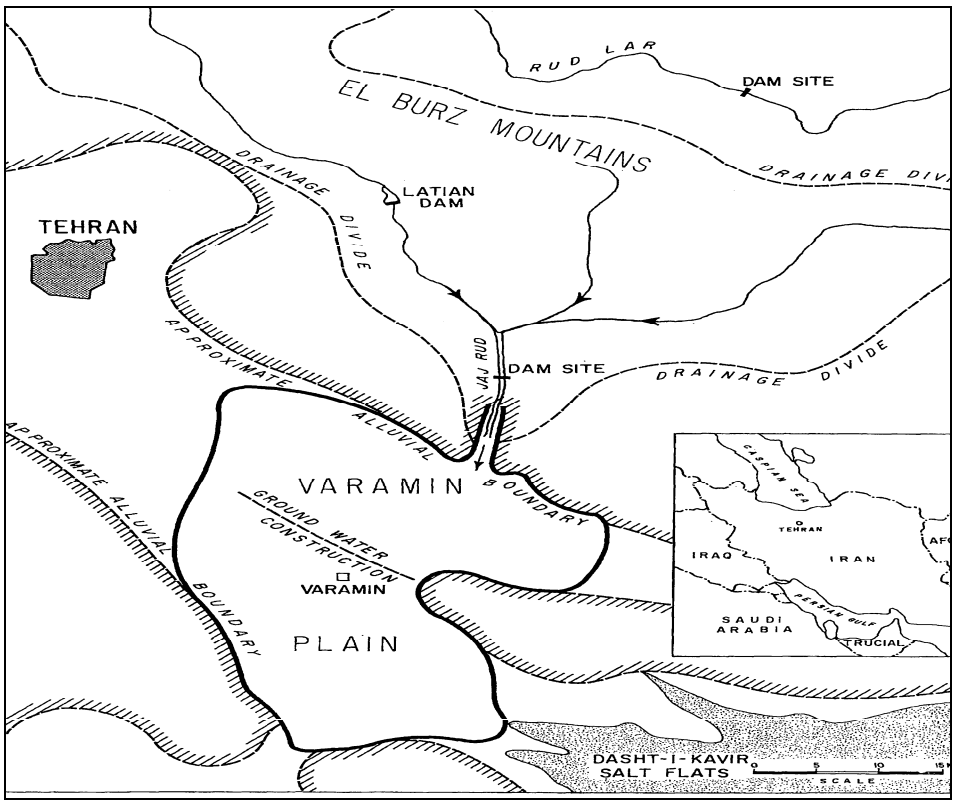

Figure 4.1 Location map of Varamin Plain, Iran

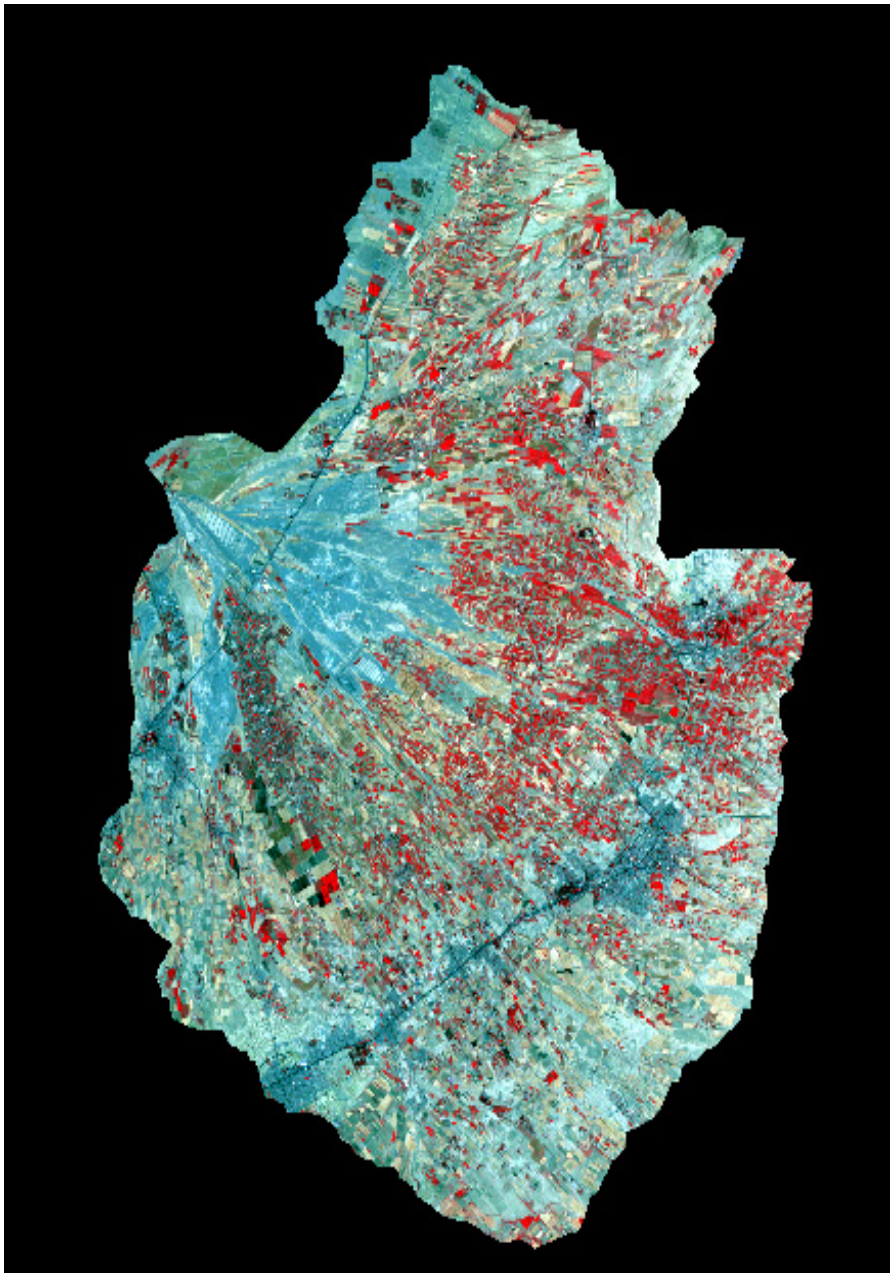

Figure 4.2 Aster image (false-colour composite 321) of Varamin Plain

Table 4.1 Varamin Plain average (40 years) monthly evapotranspiration and rainfall

Month	Max Temp (ºC)	Min Temp (ºC)	Humid (%)	Wind (km d^{-1})	Sunshine (hrs)	Solar Radiation (mj m^{-2} d^{-1})	Rain (mm /month)	ETo Penman-Monteith (mm d^{-1})	Pan Eva. (mm d^{-1})	Eva. after Pan Coeff (0.7) (mm d^{-1})
January	9.2	-2.9	70	190	5.7	9.6	25.8	1.4	0.87	0.61
February	12.4	-0.9	62	242	6.4	12.5	21.6	2.2	1.3	0.93
March	17.8	3.4	55	285	6.6	15.7	22.4	3.5	3.03	2.12
April	24.4	8.9	49	285	7.2	19.0	20.9	5.0	5.6	3.92
May	30.3	13.4	45	242	9.3	23.4	13.5	6.3	9.1	6.37
June	36.0	17.6	38	242	11.4	26.9	3.9	7.9	11.3	7.93
July	38.4	20.0	38	242	11.2	26.3	1.9	8.3	13.6	9.52
August	37.2	18.6	40	190	10.8	24.4	0.9	7.1	13.3	9.29
September	33.5	14.2	44	190	10.0	20.8	1.0	5.8	8.77	6.14
October	26.4	8.6	51	242	8.3	15.5	9.7	4.5	5.4	3.78
November	18.3	2.9	60	242	6.9	11.2	15.4	2.7	2.87	2.01
December	11.6	-1.3	68	216	6.0	9.2	21.9	1.6	1.3	0.93
YEAR	24.6	8.5	52	234	8.3	17.9	158.9	1713	2295	1606

A groundwater flow system typical of an alluvial fan exists: the intake or recharge area in the upper part with a groundwater level 150 m bgl, and an exfiltration area in the lower part with shallow groundwater tables. A complicating factor is the presence of a subsurface ridge in the bedrock topography, which causes an upwelling of groundwater in the middle part, where the groundwater level varies from 60 to 30 m. Further down, the groundwater level decreases gradually and is close to the surface, causing salinity.

The groundwater water quality, as indicated by the electrical conductivity, varies from values up to 400 µm cm^{-1} in the north to values up to about 10,000 µm cm^{1} in the south. The chloride contents of the groundwater vary from about 60 mg l^{-1} to 1000 mg l^{-1}.

Water resources

The situation before the construction of the Latian dam (completed in 1962) to provide Tehran with drinking water was the occurrence of flash floods from the 1775 km^2 long Jaj Rud at the apex of the fan. As can be noted on the satellite image (Figure 4.2), the wide zone consisting of pebbles, gravels and sands acted as a natural floodwater spreading area associated with infiltration. The larger flash floods reached the middle and lower parts of the fan through many channels, which diminished in size because of transmission losses. The low flows of much longer duration were diverted into a system of unlined irrigation canals.

Because of the construction of the Latian dam with its large reservoir, the discharge at the apex of the Varamin alluvial fan decreased, but it is still about 220 million m^3 per year. As a compensation measure for the reduction in discharge, a programme to line the irrigation channels was completed in 1975. It was estimated (Ministry of Energy, 2002) that about 65 million m^3 was recharged to the groundwater by canal losses in the old situation.

In the period after 1962, it was observed that discharges from the 14 qanats in the middle to lower part of the fan were much reduced (by 61%) and that spring discharges had dwindled. The number of tubewells has increased by 50% since 1994, to a total of 3310 wells, although the total well discharge increased by only

15% to 485 million m^3 in 2001 (Ministry of Energy, 2002). As the abstraction exceeds river inflow potentially available for recharge, the groundwater levels are declining.

The reduction in river recharge with the associated decline in groundwater level, the foreseen growth of the population of Tehran, and the need to produce more food (Ministry of Energy, 2002) led to the construction of an artificial recharge scheme at the apex of the Varamin fan so that use could be made of the occasional floodwater. That water consists of spills from the Latian dam and runoff from the catchment downstream of the dam. The Sorkhesar scheme was completed in 1977.

4.3 The recharge scheme

The scheme consists of regulatory weirs at the Jaj Rud main channel to distribute water into the main irrigation canals and to divert floodwaters or excess water into a series of basins, as shown on the image in Figure 4.3 and the field survey map in Figure 4.4.

Since 1977, a number of runoff diversions have caused substantial sedimentation in the upper infiltration basins. In the first four basins, the sediment has accumulated to at least the level of the concrete spillways or basin overflows, and sinuous channels have formed. The level of the suspended load deposits (clays and silts) exceeds the level of the channel bottom, where a mixture of textures is found. In basins 5 to 11 heavy textured deposits are found, but basins 11 to 17 have no signs of deposition. Either no water or only clear water has reached those basins.

Records of inflow at the intake existed for the recharge event of 21 March to 21 July 2002. A field survey was done in July 2002 to measure the topography of the infiltration basins and the extension of the water surface, and to take soil samples in basins 1 to 10, because, according to the scheme operator, the water reached infiltration basin 9. The grain size and saturated hydraulic conductivity of the basin soil and sediment samples were analysed in the SCWMRI laboratory. The results are summarized in Table 4.2.

4.4 The spreadsheet model

To estimate the inundation duration and depth in the Sorkhehesar artificial recharge basins, a daily simulation model was developed in a spreadsheet program. Total infiltration was worked out in the model, which describes duration of inundation (infiltration) and a simplified situation in terms of water depth. To do so, data from a topographical survey of maximum inundation limits in each basin and cross section were used in conjunction with inflow and outflow estimation, under seepage loss and evaporation. It is a water budget model; hence recharge, evaporation and changes in storage equal inflow.

The model is based on the slope-area method, hydraulic aspects of the spillways, information collected by surveying (such as water marks and elevations), and oral information from the scheme operators.

Table 4.2 Summarized characteristics of the infiltration basins.

Basin no.	Area (m^2)	Soil and Sediments Characteristics								Observed water surface area (m^2)	Average depth of the available water (m)	Maximum depth of the observed water Mark (m)	Average volume of the observed water (m^3)
		% Clay	% Silt	% Sand	Texture	Soil hydraulic conductivity (Ks m d^{-1})	Bulk density(g cm^{-3})	Saturated moisture content (m^3 m^{-3})	Sediment depth (cm)				
1	34644	33	53	14	Si.C.L	0.02	1.5	0.52	>200	2215	0.25	1.39	554
		15	19	66	S.L	0.84	1.45	0.43					
2	18727	13	15	72	S.L	0.86	1.45	0.42	>200	1001	0.24	1.36	240
		24	74	2	Si.L	0.075	1.54	0.51					
3	33492	29	57	14	Si.C.L	0.03	1.5	0.51	>100	1627	0.26	1.36	423
		15	47	38	L	0.19	1.42	0.45					
4	56694	41	55	4	Si.C	0.013	1.55	0.53	>100	3494	0.26	1.33	908
		23	75	2	Si.	0.048	1.55	0.51					
5	75371	38	60	2	Si.C	0.016	1.55	0.54	30-50	31549	0.2	3.5	6310
		51	39	10	C	0.01	1.55	0.54					
6	72778	51	45	40	Si.C	0.018	1.55	0.55	20-40	18646	0.18	2.00	3356
		46	46	8	Si.C	0.019	1.55	0.54					
7	70330	42	40	18	C	0.012	1.55	0.53	10-25	24922	0.18	5.00	4486
8	82790	57	33	10	C	0.005	1.55	0.55	10-15	0	0	3.20	0
9	113250	30	16	54	S.C.L	0.29	1.45	0.53	10-15	0	0	2.80	0
10	76039	24	48	28	L	0.35	1.43	0.49	5-10	0	0	----	0
11	89901	---	---	---	Gravel	86.4			----	0	0	----	0
12	123821	---	---	---	Gravel	86.4			----	0	0	----	0
13	102246	---	---	---	Gravel	86.4			----	0	0	----	0
14	198244	---	---	---	Gravel	86.4			----	0	0	----	0
15	122948	---	---	---	Gravel	86.4			----	0	0	----	0
16	137336	---	---	---	Gravel	86.4			----	0	0	----	0
17	129075				Gravel	86.4			----	0	0	----	0

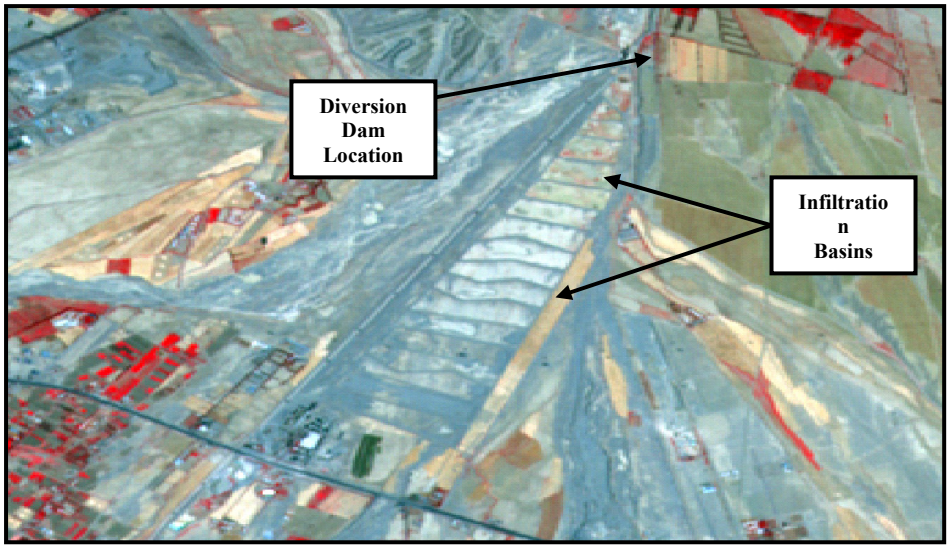

Figure 4.3 Aster image (false-colour composite 321) of the Sorkhehesar artificial recharge site

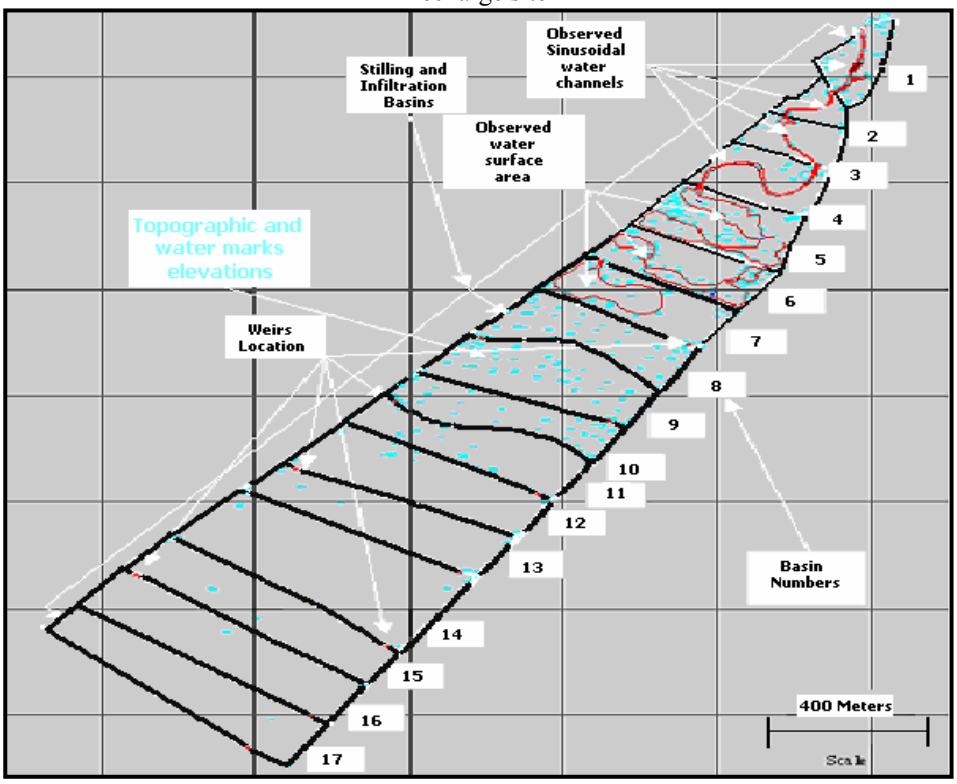

Figure 4.4 The map plan of the Sorkhehesar artificial recharge basins (surveyed during the fieldwork period)

4.4.1 The slope-area method for the first four basins

In the first four infiltration basins, the present inundation areas and depths are controlled by the sinus channels, through which the water flows to the lower basins where inundation spreads out over larger areas. In this study, as the discharges, watermarks and other necessary information were accessible for the simulation period, the slope-area method has been used in such a way as to compute the flooded area for each day during the flooding event until the date of the field survey. The slope-area method is based on the well-known Manning's equation for determining discharge:

$$Q = (AR^{2/3}S^{1/2})/n \qquad [4.1]$$

where A is the cross-sectional area (L2), R (L) is the hydraulic radius (cross-sectional area/wetted perimeter), S is the slope (L/L dimensionless) and n is the Manning roughness coefficient (dimensionless). The field data include the determination of the elevation and location of high-water marks along the channel, the measurement of the channel cross section and wetted perimeter by surveying, tape and compass, or GPS, and the selection of a roughness coefficient for the section of the stream in question. The procedure (see Figure 4.5) starts with the selection of two cross sections along a reach. High-water marks must be clearly evident on both sides of the river, at both cross sections. The reach of the channel between the cross sections must have similar roughness characteristics. The next step is the calculation of the water surface slope ((hu-hd)/L; Figure 4.5), which is simply the slope of the high-water marks between the upstream (hu) and downstream (hd) sections, and is the slope of the water surface during maximum discharge. The water surface slope is used as a first approximation for the energy slope, which is ultimately the slope that the slope-area method relies on. The energy slope ((Hu-Hd)/L) is the slope between the upstream and downstream cross sections of the high-water marks plus the velocity head (energy, or v2/(2g)), such that

$$S_e = ((h_u + \alpha_u v_u^2/(2g)) - (h_d + \alpha_d v_d^2/(2g)))/L \qquad [4.2]$$

where Se is the energy slope, h_u and h_d are the high-water marks, α is a correction factor that accounts for expanding or contracting reaches (and is typically ignored by giving it a value of 1 for both upstream and downstream sections), L is the distance between the two sections, and g is acceleration gravity.

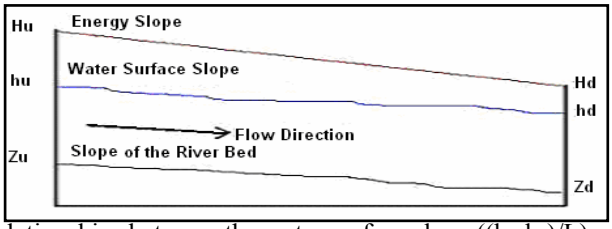

Figure 4.5 The relationships between the water surface slope ($(h_u-h_d)/L$) and the energy slope ($(H_u-H_d)/L$)

The steps in the calculations are:

(1) Computation of the values of cross-sectional area (A), hydraulic radius (R), and roughness (n) for each cross section, and water surface slope (S) between the cross sections.

(2) Calculation of the upstream and downstream conveyance values (Ku and Kd), such that:

$$K_u = A_u R_u^{2/3}/n_u \text{ and } K_d = A_d R_d^{2/3}/n_d \quad [4.3]$$

(3) Calculation of the average conveyance of the reach of river between the cross sections:

$$K = (KuKd)0.5 \quad [4.4]$$

(4) Calculation of the first estimation of peak discharge by multiplying the average conveyance (K) by the square root of the water surface slope. This answer is in L^3T^1, and gives a rough approximation of the maximum discharge.

$$Qp = KS0.5 \quad [4.5]$$

(5) Calculation of the difference in the velocity heads (dh_v) of the upstream and downstream sections according to:

$$dhv=(Qp2/2g)\,((\,\alpha u/Au)-(\,\alpha d/Ad)) \quad [4.6]$$

where g is acceleration gravity (L T-2), and A_u and A_d are the upstream and downstream cross-sectional areas. Also $\alpha = 1$.

(6) Computation of a new energy slope:

$$Se = ((hu - hd) + dhv)/L \quad [4.7]$$

(7) Computation of a new maximum discharge using the energy slope:

$$Qp = KSe0.5 \quad [4.8]$$

(8) Repeating steps 6 and 7 above, using this new maximum discharge until Q_p does not vary.

In the spreadsheet model, as the daily discharge data for the simulation period time were available, the above procedure was used in the manner where the model computes the proper cross-sectional areas and finally the flooded surface for each of the first four infiltration basins. When inflow exceeds the capacity of the

spillway, overbank inundation is calculated using an area-capacity relation based on field survey. In the first four basins with sinusoidal stream channels, the water ponding depth means the computed flooded depth of the water flow in the channels after each flood event. Then the model calculates recharge based on the computed flooded surface, depth, and soil hydraulic conductivity characteristics of the infiltration basin. The evapotranspiration of the basin was computed using the calculated flooded area and potential daily evapotranspiration (pan evapotranspiration) for each day during the flooding event and after, until the time when there was no stored water in the infiltration basins. Finally, dead water volume (Q_{remain}) and the overflow discharge to the next basin through the spillways was computed. For the calculation of the recharge by infiltration, various saturated hydraulic conductivity (Ks) values for each basin were considered.

The outflow runoff from upper part basins to the lower ones through concrete broad-crested spillways is given by:

$$Q = C.L.H^{3/2} \qquad [4.9]$$

where Q is discharge, C is coefficient (C = 1.7 in the SI system), L is length (8 m) of the crest, and H is effective head of water (m).

4.4.2 Water budget computation in basins 5 to 17

It takes time for water depth to reach to the elevation of the spillway crests. In other words, in each basin we have a specific amount of dead volume of water and, if inflow exceeds that specific amount, there will be overflow through the spillway to the next lower infiltration basin. The dead water volume was calculated from the surveyed depth and surface area. High-water marks and many spot heights in the infiltration basins allowed the reconstruction of the detailed topography by interpolation. The spreadsheet model thus calculated the volume of the available dead water and its surface area. Then the model compared them with the daily amount of water through the spillway of the upper part of each basin, up to the maximum possible volume and surface area in the specific basin.

An area-storage relationship for each basin was determined for calculating the timing and amount of water transferred to the next lower basin and the amount remaining in storage. When full capacity was reached, overflow to the next basin was calculated. Evaporation and infiltration losses depending on flooded area were included in the daily time step.

4.5 Model parameterization

4.5.1 Saturated hydraulic conductivity (Ks)

In addition to the granulometric analysis, ring samples were taken in the field for determining saturated hydraulic conductivities in the laboratory (Table 4.2). The data sets allowed evaluation of the CA and MG PTF models. The bulk density, organic content and saturated moisture content were also determined (Table 4.2).

The result for laboratory-measured and computed saturated hydraulic conductivity is shown in Figure 4.6.

The statistical T test results (see Table 4.3) show a significant difference between the averages (total 100 samples) of saturated hydraulic conductivities for each texture category measured in the laboratory and the Ks value calculated using both the CA and MG PTFs at 95% confidence level. Also, the saturated hydraulic conductivity calculated using the CA model is significantly different from the MG method with the same confidence level.

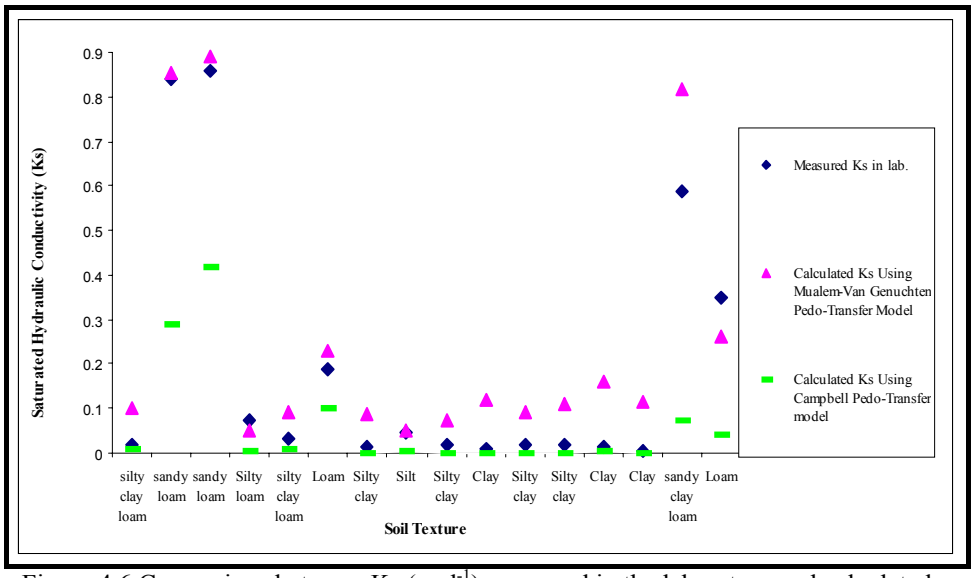

Figure 4.6 Comparison between Ks (m d^{-1}) measured in the laboratory and calculated using CA and MG PTFs

Table 4.3 The results of the paired-samples T test between measured and calculated saturated hydraulic conductivities for the sampled soils of the Sorkhehesar artificial recharge basins, based on CA and MG models

		Paired Differences					t	df	Sig. (2-tailed)
		Mean	Std. Deviation	Std.Error Mean	95% Confidence interval of the Difference Lower	Upper			
Pair 1	Lab-MG	-6.3E-02	7.174E-02	1.7E-02	-.101118	-2.5E-02	-3.51	15	.003
Pair 2	Lab-CA	.13344375	.19818325	4.95E-02	2.78E-02	.23904815	2.693	15	.017
Pair 3	MG-CA	319633562	.20687836	5.17E-02	8.61E-02	.30657332	3.796	15	.002

The SWAP modelling is valid for the overburden consisting of sediment layers. In the infiltration basins of the scheme, the fine-grained sedimentation layers overlay coarse-grained fanglomerates that do not have impeding horizons, and thus the SWAP simulation results (Chapter 3) are valid and used in the spreadsheet model for evaluating the recharge. As some of the basins have different soil types, their soil hydraulic properties are different too. The computed recharge for each basin consists of accumulated recharge from different soil type units, according to the inundation calculated by the model.

4.5.2 Evapotranspiration and rainfall

In this study, the average of 40 years' (Table 4.4) monthly evapotranspiration (US class A, pan coefficient of 0.7) information for Varamin Plain in Tehran Province, Iran, was used as input evapotranspiration data in the spreadsheet model. Monthly pan evapotranspiration was divided by the number of days of each simulated month and used as daily evapotranspiration (see Table 3.17). The spreadsheet model calculates evapotranspiration by using the computed flooded area for each specific month. During the simulation period the rainfall was insignificant.

Table 4.4 Daily potential evapotranspiration for spreadsheet model simulations

Month	Evapotranspiration (mm d^{-1})
March	2
April	4
May	7
June	8
July	10

4.5.3 Simulation

The simulation time period was four months, from 21 March to 21 July 2002 (spring 2002). The amount of water remaining in the basins pertains to the last date for both simulation and field observation. Based on reliable daily discharge information, a total of 18,266,688 m^3 of water was diverted to the recharge basins. For all simulations, it was supposed that the daily diverted discharge flow from dam to the scheme was uniform (steady state flow).

4.6 Simulation results

First, a simulation based on recharge as computed with the laboratory-measured soil hydraulic conductivities (Ks) was done without considering the effect of water depth. After that, the model was run with simulations based on computed soil hydraulic conductivities (Ks) using MG-PTF, CA-PTF, the aggregation of both PTF methods, and SWAP mathematical modelling results. The only way to validate model results was by comparing the simulated with the observed amount of water remaining in the scheme of the recharge by flood event. The groundwater observation well closest to the scheme was about 1000 m away from basin 9, but the data could not be used because several production wells were in close proximity to the observation well.

The simulation results for the water budget in the Sorkhehesar artificial recharge basins during spring 2002 are given below.

4.6.1 Simulation results based on measured soil hydraulic conductivities (Ks)

For this simulation, the maximum recharge depth per day was limited to the measured soil hydraulic conductivity (Ks) for each soil type in the basin. The simulation results for the Sorkhehesar artificial recharge basin after using the above method are shown in Figure 4.7 and Table 4.5.

Figure 4.7 shows that observed and calculated Q_{remain} (dead water body) are much different after basin 4. For the first four basins, the simulated and observed results do not differ greatly, because channels are shallow and overbank areas are limited. Thus, the effect of ponding depth (not taken into account in this simulation) is not pronounced as is the case in basin 5 onwards. Any large daily inflow smaller than the maximum channel water flow capacity is rapidly transferred to the next basin once the channels are full. Furthermore, changing the Ks value for the soil type of the first four basins had little effect on the Q_{remain}.

The simulation shows that overflow reached basin 14 (see recharge column in Table 4.5) and there was some dead water in basin 8, which was not possible because basins 8, 9 and 10 were already dry. Therefore, the computed elements of the water balance after basin 7 cannot be correct. Evidently, infiltration is too low for the first 10 basins due to the fact that the effect of water depth on infiltration was ignored.

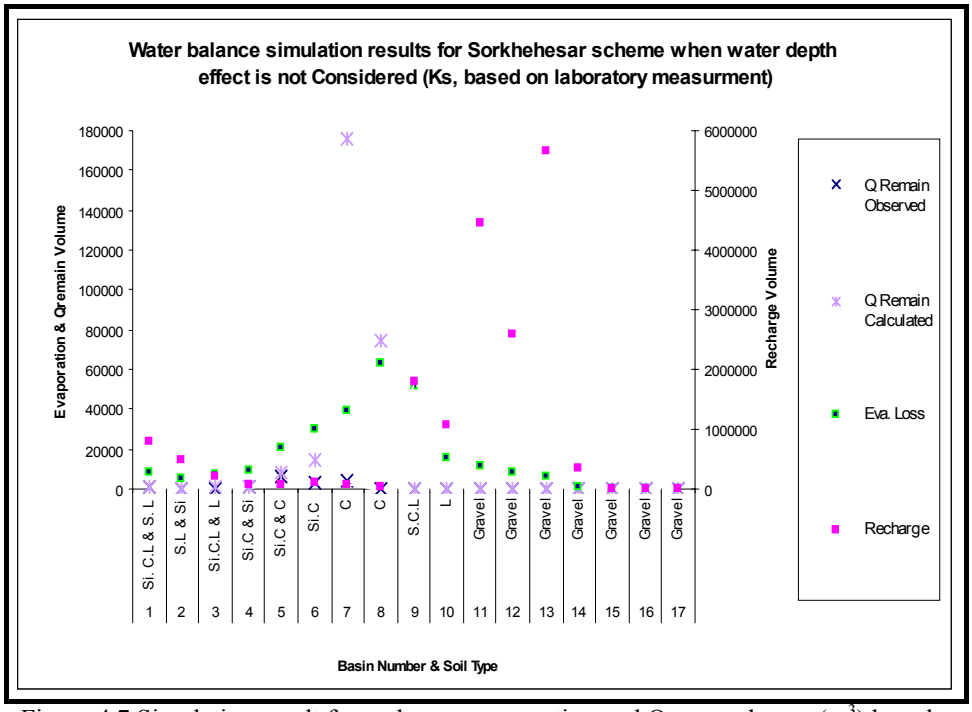

Figure 4.7 Simulation result for recharge, evaporation and Q_{remain} volumes (m^3) based on measured Ks (cm d^{-1}) and no water depth effect

Table 4.5 The water balance simulation results for the Sorkhehesar artificial recharge basins based on computed K_s in the laboratory without considering ponding depth effect

Basin No.	Q_{In} (m^3)	Eva. Loss (m^3)	Recharge (m^3)	Q_{Out} (m^3)	Q_{Remain} (m^3)	$Q_{Remain\ Observed}$ (m^3)
1	18266688	8000	804095	17453837	756	554
2	17453837	4691	474977	16973823	346	240
3	16973823	6776	198481	16767940	626	423
4	16767940	9446	68560	16688584	1350	908
5	16688584	20438	56126	16603460	8560	6310
6	16603460	29689	89071	16470700	14000	3356
7	16470700	39490	85578	16169985	175647	4486
8	16169985	62998	44478	15987844	74665	0
9	15987844	51726	1778867	14157251	0	0
10	14157251	15327	1061497	13080427	0	0
11	13080427	11361	4458404	8610662	0	0
12	8610662	8473	2597300	6004889	0	0
13	6004889	5749	5655719	343421	0	0
14	343421	706	342715	0	0	0
15	0	0	0	0	0	0
16	0	0	0	0	0	0
17	0	0	0	0	0	0

4.6.2 Simulation results based on computed soil hydraulic conductivities

The hydraulic spreadsheet model was used to simulate the effect of water ponding depth based on the SWAP modelling results for two PTFs and the soil texture classes. Results for the Sorkhehesar artificial recharge basin are shown in Figure 4.8 and Table 4.6.

For the Ks values of each texture, the estimate was based on the line of best fit (shown in the graphs presented in Chapter 3) for both the MG and the CA PTFs. In addition, simulation was also done using the average of the computed saturated hydraulic conductivities and the MG and CA PTF methods for the soils in the basins.

Figure 4.8 shows that the observed and calculated Q_{remain} are different for all the methods used. But the differences are much greater after basin 4. The results calculated using the MG method show dead water (Q_{remain}) in basin 7 but not in the consecutive basins. Also the computed evaporation in the basins differs little between the three above methods for calculating water budget elements. None of the three methods indicates overflow after basin 9.

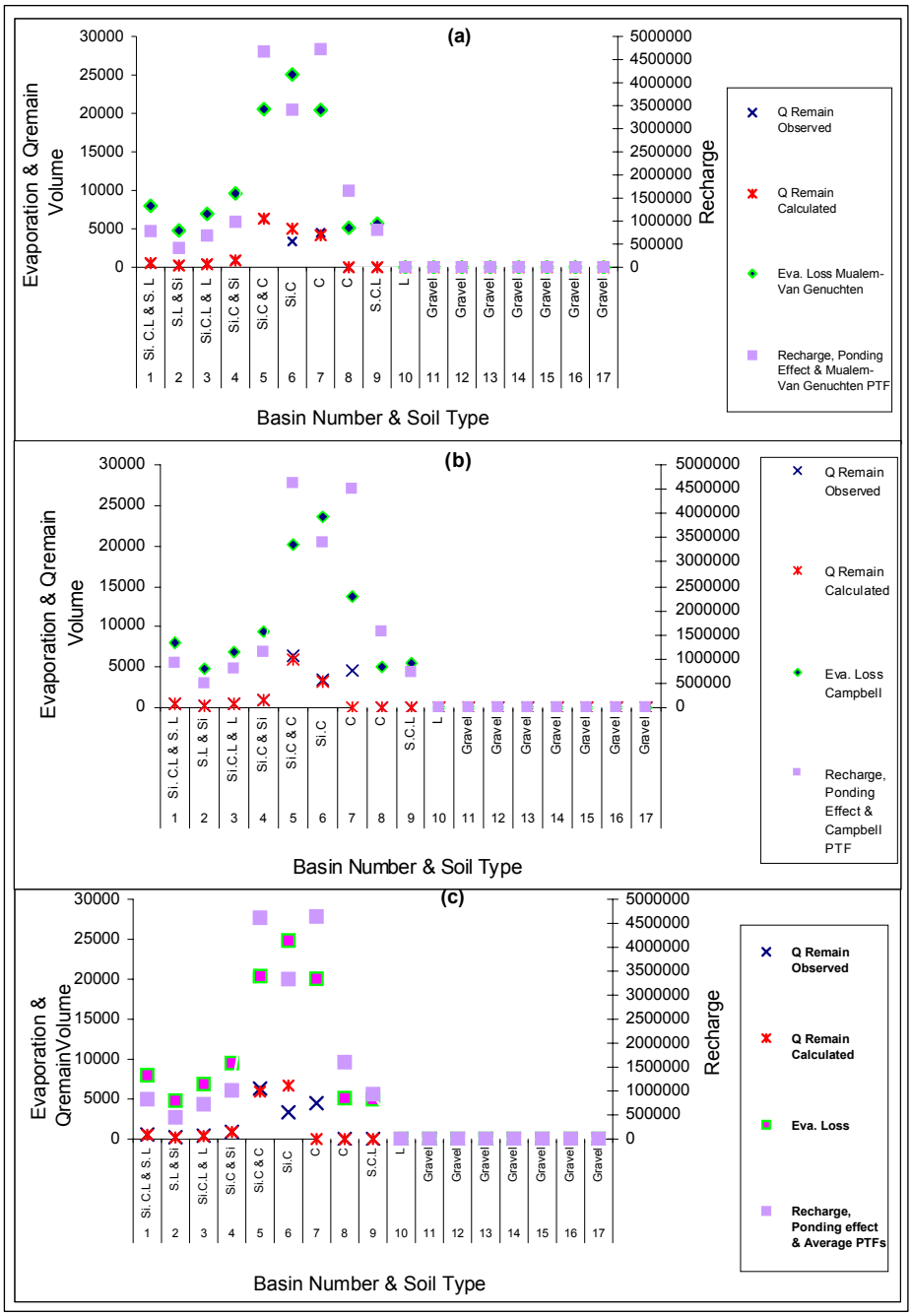

Figure 4.8 Simulation results for recharge (m^3), evaporation (m^3), and Q_{remain} (m^3) based on computed soil hydraulic conductivities (K_s, cm d^{-1}), recharge efficiency knowledge, and data resulting from the SWAP modelling using: (a) MG PTF, (b) CA PTF, and (c) average of both PTF methods

Table 4.6 Water budget simulation results for the Sorkhehesar artificial recharge scheme, based on computed K_s using PTF methods of SWAP simulations

Basin No.	Q_{In} (m^3)			Eva. Loss (m^3)			Recharge (m^3)			Q_{Out} (m^3)			Q_{Remain} (m^3)			Q Remain Observed (m^3)
	Average of MG & CA	MG	CA	Average of MG & CA	MG	CA	Average of MG & CA	MG	CA	Average of MG & CA	MG	CA	Average of MG & CA	MG	CA	
1	18266688	18266688	18266688	8000	8000	8000	831402	786158	900466	17426778	17471981	17357727	508	549	495	554
2	17426778	17471981	17357727	4773	4777	4773	454289	418185	486997	16967513	17048782	16865765	203	237	193	240
3	16967513	17048782	16865765	6874	6926	6858	721593	686382	797937	16238661	16355072	16060586	386	403	384	423
4	16238661	16355072	16060586	9487	9590	9464	1014888	983945	1142701	15213385	15360631	14907615	900	906	806	908
5	15213385	15360631	14907615	20369	20551	20121	4614068	4672084	4627633	10573008	10661687	10253960	5940	6309	5901	6310
6	10573008	10661687	10253960	24834	25053	23599	3333327	3411257	3402401	7208166	7220375	6824747	6681	5001	3213	3356
7	7208166	7220375	6824747	20036	20418	13749	4643881	4721314	4504276	2544250	2474475	2306723	0	4168	0	4486
8	2544250	2474475	2306723	5113	5115	5109	1600794	1657015	1581567	938343	812345	720047	0	0	0	0
9	938343	812345	720047	4978	5653	5404	933364	806693	714643	0	0	0	0	0	0	0
10	0			0			0			0			0			0
11	0			0			0			0			0			0
12	0			0			0			0			0			0
13	0			0			0			0			0			0
14	0			0			0			0			0			0
15	0			0			0			0			0			0
16	0			0			0			0			0			0
17	0			0			0			0			0			0

4.6.3 Discussion of the simulation results

Summaries of the above water balance simulation results (accumulation of the four months' simulation period) for the Sorkhehesar artificial recharge scheme are shown in Figures 4.9 and 4.10.

Figure 4.9 describes the differences between calculated evaporation and Q_{remain} (dead water, compared with the observed) using all the simulation methods. The calculated Q_{remain} using measured Ks without considering the effect of water ponding depth differs greatly from the observed situation, namely water in basin 8, which was actually dry. It means that the infiltration should be much higher because of the water ponding depth.

There was water at the end of the period in basin 7. Inspection of the graphs shows that the CA method and the method using the aggregated CA and MG PTFs failed to predict that, but the MG method came close to what was observed. In order to judge the results, a non-parametric test, namely the Wilcoxon Signed Rank test, using pairs of samples was applied for all methods used. The Q_{remain} observed and simulated, as well as the evaporation calculated by the spreadsheet model from the acreage of inundation, were used in the test, and the results are shown in Table 4.7. The only non-significant difference between the observed and the simulated Q_{remain} was found for the MG method and the aggregation of the MG and CA methods, but the rank score indicates that the MG performs best. The simulation results using the measured Ks values, but also those using the CA method, differed significantly from the observed Q_{remain}.

Evaporation loss simulated with the MG method differed significantly from the evaporation loss resulting when using the other methods mentioned. The loss based on CA differed significantly from the loss based on the measured Ks but not from the loss based on the aggregated method (CA&MG).

Figure 4.10 shows the differences between calculated recharge using all the above-mentioned methods and their relationships with flooding depth, sediment depth, basin depth, dead water storage volume, flooded surface area, saturated hydraulic conductivity (Ks), inflow discharge and basin area size. Figure 4.10 shows that calculated recharge using measured Ks without considering the ponding effect is much different with other methods. In addition to soil type and Ks, flooding depth, flooded area size, inflow discharge and sediment layer depth (or top soil layer depth) are other factors that control recharge efficiency. When the flooding depth in the infiltration basin increased considerably (such as in basins 5 and 7, with 2 and 4 m maximum observed flooding depths respectively), the recharge efficiency increased by about 25% of the total inflow volume (Figure 4.10). The first four basins with the thick sediment depths had lower recharge efficiency than the rest of the basins. Although basin 9 has good characteristics, such as light soil texture, thin sediment layer and high Ks, its recharge efficiency was low because of less inflow.

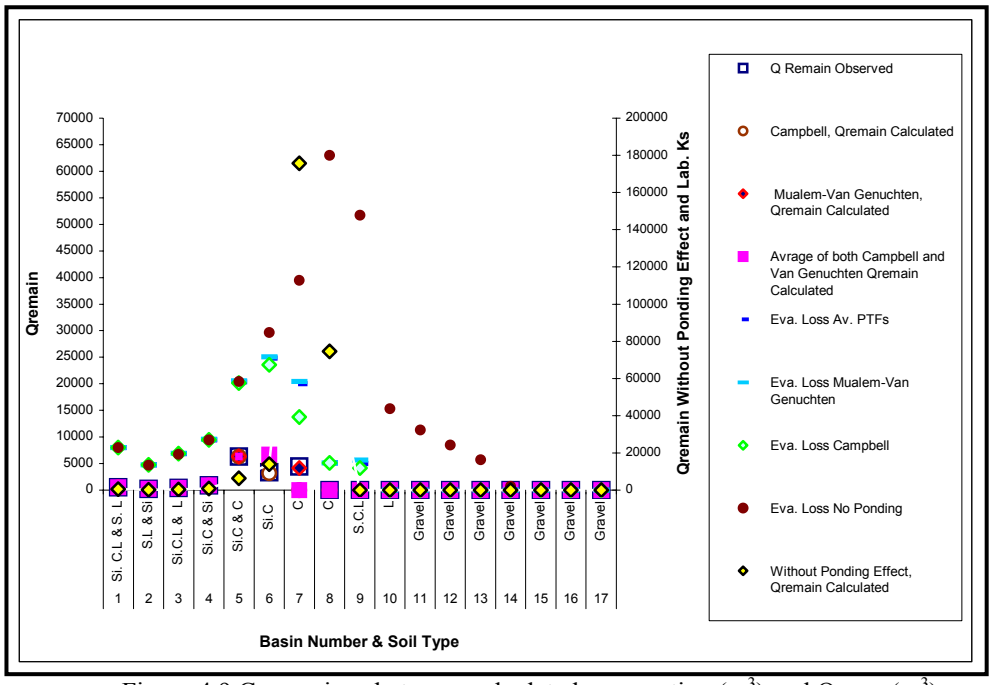

Figure 4.9 Comparison between calculated evaporation (m^3) and Q_{remain} (m^3) for all methods used

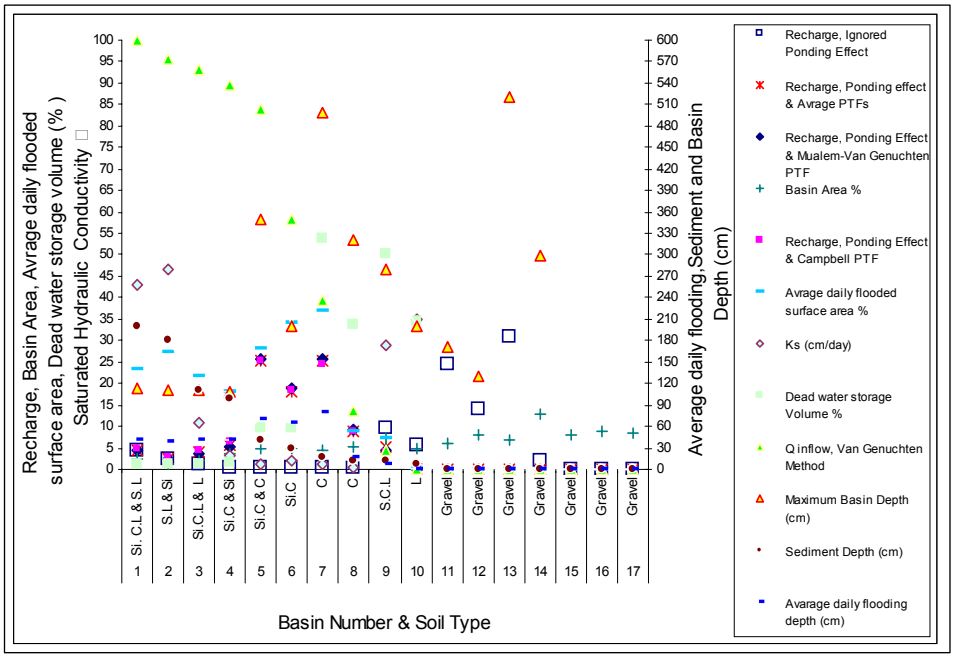

Figure 4.10 Effects of flooding depth, sediment depth, basin depth, dead water storage volume, flooded surface area, saturated hydraulic conductivity (Ks, cm d^{-1}), inflow discharge and basin area size on recharge calculation using all the methods

Table 4.7b Test statistics of the Wilcoxon Signed Ranks Test results for all methods used to calculate the Q_{remain} and evaporation in the Sorkhehesar artificial recharge scheme

Methods	Calculated Evaporation MG & Measured K_s	Calculated Evaporation CA & Measured K_s	Calculated Evaporation Aggregation Of the both PTF Methods & Measured K_s	Calculated Evaporation CA & MG	Calculated Evaporation Aggregation Of the both PTF Methods & MG	Calculated Evaporation Aggregation Of the both PTF Methods & CA	Observed Q_{remain} & Calculated Using Measured K_s and No Ponding Effect	Observed Q_{remain} & Calculated Using MG PTF	Observed Q_{remain} & Calculated Using CA PTF	Observed Q_{remain} & Calculated Using Aggregation Of the both PTF Methods
Z	-2.481[a]	-2.761[a]	-1.400[a]	-2.521[a]	-2.521[a]	-1.521[b]	-2.521[a]	-1.183[a]	-2.366[a]	-1.355[a]
Asymp. Sig (2-tailed)	0.013	0.006	0.161	0.012	0.012	0.128	0.012	0.237	0.018	0.176

[a] Based on positive ranks

[b] Based on negative ranks

[c] Wilcoxon Signed Ranks Test

4.7 Uncertainty analysis

In order to explore the effects of the above studied variables on recharge efficiency in the Sorkhehesar floodwater spreading scheme, a linear multiple regression model was developed. The linear regression model was based on the daily simulation results with the MG method, since that gave the best results. The dependent variable used was computed daily recharge volume (m^3) and the independent variables were flooding height (FH), sediment depth (SD), saturated hydraulic conductivity (Ks), inflow discharge (Qin), flooded area size (FAS), dead water storage capacity (DSC), basin depth (BD) and basin area size (BAS).

The scatter plots of the dependent variable and independent variables and their statistical characteristics are shown in Figure 4.11 and Table 4.8 respectively. Based on the stepwise method for linear multiple variables regression analysis, different models for recharge prediction in the Sorkhehesar artificial recharge scheme were developed using SPSS statistical software. The entered and removed variables, model summary results, ANOVA test results and model coefficients are shown in Tables 4.9, 4.10, 4.11 and 4.12 respectively.

Tables 4.9 and 4.11 show that the DSC (dead water body storage capacity) variable was removed by the model as its effect on the dependent variable was not significant. Tables 4.10 and 4.12 show that all the models have relatively high R square values (0.89 and 0.94 minimum and maximum respectively). Model 7 has the highest number of the independent predictor variables, and the P value results (Table 4.12 column Sig.) show that the effects of all the variables, including constant value, on the dependent variable (recharge) are significant. According to the Beta coefficients (Table 4.12), the flooding height (FH) and basin area size (BAS) independent variables have the highest and lowest effects on the dependent variable (recharge). As the R square coefficient of model 7 is 0.94 (Table 4.10), about 94% of the variation in the computed recharge is explained by the mentioned variables. The tolerance and VIF (variance inflation factor) coefficients (Table

4.12) do not indicate a collinearity problem for model 7. However, Beta coefficients for the three variables of models 7 and 6, inflow discharge (Qin), basin depth (BD) and flooded area size (FAS), two variables of model 5, inflow discharge (Qin) and basin depth (BD), and one variable of model 4, basin depth (BD), have a negative sign, while the single correlation between these variables and the dependent variable is in the form of a direct relationship.

Tables 4.10 and 4.12 show that, after the removal of the three independent variables, model 3 with three variables has more or less the same explanatory value (Table 4.10, R) as the model with seven variables (model 7), and all the variables show significant effects on recharge estimation. From Table 4.12 the regression equation based on the MG method is:

$$Y(\text{recharge}) = -6496.522+71192.235*(FH)-17973.1*(SD)+35846.197(Ks) \quad [4.10]$$

The R square coefficient (Table 4.11) of multiple determinations is 0.964; therefore, about 96% of the variation in the computed recharge is explained by flooding height (FH), sediment depth (SD) and saturated hydraulic conductivity (Ks). The regression equation appears to be very useful for making predictions since the value of R2 is very close to 1. For example, (Table 4.12) the flooding height variable of model 7 has the highest value of the Beta coefficient, and therefore most effect on the dependent variable (recharge). The saturated hydraulic conductivity (Ks) has the lowest effect (Beta = 0.141) on the recharge compared with the other independent variables.

Table 4.8 Statistic and unit characteristics of the dependent and independent variables

	Mean	Std. Deviation	N
Recharge (Dependent variable, m^3)	14875.4900	44990.75425	1220
Inflow Discharge (m^3)	92142.1704	225561.82618	1220
Flooding Height (m)	.4017	.60255	1220
Flooded Area Size (m^2)	15044.4740	21911.97051	1220
Sediment Depth (m)	70.4000	69.38289	1220
Basin Area Size (m^2)	55807.6000	32177.50150	1220
Basin Depth (m)	209.4000	142.92930	1220
Dead Water Storage Volume (m^3)	47977.1200	68705.58087	1220
Saturated Hydraulic Conductivity, Ks (m/day)	13.7660	17.66415	1220

Table 4.9 Entered/removed variables

Model	Variables Entered	Variables Removed	Method
1	FH	.	Stepwise (Criteria: Probability-of-F-to-enter <=.050. Probability-of-F-to-remove >=.100).
2	SD	.	Stepwise (Criteria: Probability-of-F-to-enter <=.050. Probability-of-F-to-remove >=.100).
3	Ks	.	Stepwise (Criteria: Probability-of-F-to-enter <=.050. Probability-of-F-to-remove >=.100).
4	BD	.	Stepwise (Criteria: Probability-of-F-to-enter <=.050. Probability-of-F-to-remove >=.100).
5	Qin	.	Stepwise (Criteria: Probability-of-F-to-enter <=.050. Probability-of-F-to-remove >=.100).
6	FAS	.	Stepwise (Criteria: Probability-of-F-to-enter <=.050. Probability-of-F-to-remove >=.100).
7	BAS	.	Stepwise (Criteria: Probability-of-F-to-enter <=.050. Probability-of-F-to-remove >=.100).

Table 4.10 Model summary results

Model	R	R square	Adjusted R Square	Std. Error of the Estimate
1	.945[a]	.893	.893	14701.30907
2	.960[b]	.922	.922	12594.33501
3	.964[c]	.930	.930	11939.33625
4	.966[d]	.933	.933	11635.74464
5	.968[e]	.937	.937	11293.24905
6	.968[f]	.938	.937	11263.78797
7	.969[g]	.938	.938	11225.68246

Table 4.11 The ANOVA test results

Model		Sum of Squares	df	Mean Square	F	Sig.
1	Regression	2.20E+12	1	2.204E+12	10198.638	.000[a]
	Residual	2.63E+11	1218	216128488.4		
	Total	2.47E+12	1219			
2	Regression	2.27E+12	2	1.137E+12	7169.533	.000[b]
	Residual	1.93E+11	1217	158617274.4		
	Total	2.47E+12	1219			
3	Regression	2.29E+12	3	7.647E+11	5364.571	.000[c]
	Residual	1.73E+11	1216	142547750.1		
	Total	2.47E+12	1219			
4	Regression	2.30E+12	4	5.757E+11	4252.441	.000[d]
	Residual	1.64E+11	1215	135390553.2		
	Total	2.47E+12	1219			
5	Regression	2.31E+12	5	4.625E+11	3626.589	.000[e]
	Residual	1.55E+11	1214	127537474.1		
	Total	2.47E+12	1219			
6	Regression	2.31E+12	6	3.856E+11	3039.214	.000[f]
	Residual	1.54E+11	1213	126872919.4		
	Total	2.47E+12	1219			
7	Regression	2.31E+12	7	3.307E+11	2624.078	.000[g]
	Residual	1.53E+11	1212	126015946.7		
	Total	2.47E+12	1219			

a. Predictors: (Constant), FH

b. Predictors: (Constant), FH,SD

c. Predictors: (Constant), FH,SD, KS

d. Predictors: (Constant), FH,SD, KS,BD

e. Predictors: (Constant), FH,SD, KS,BD, Qin

f. Predictors: (Constant), FH,SD, KS,BD, Qin, FAS

g. Predictors:(Constant), FH,SD, KS,BD, Qin, FAS, BSA

h. Dependent Variable: RECHARGE

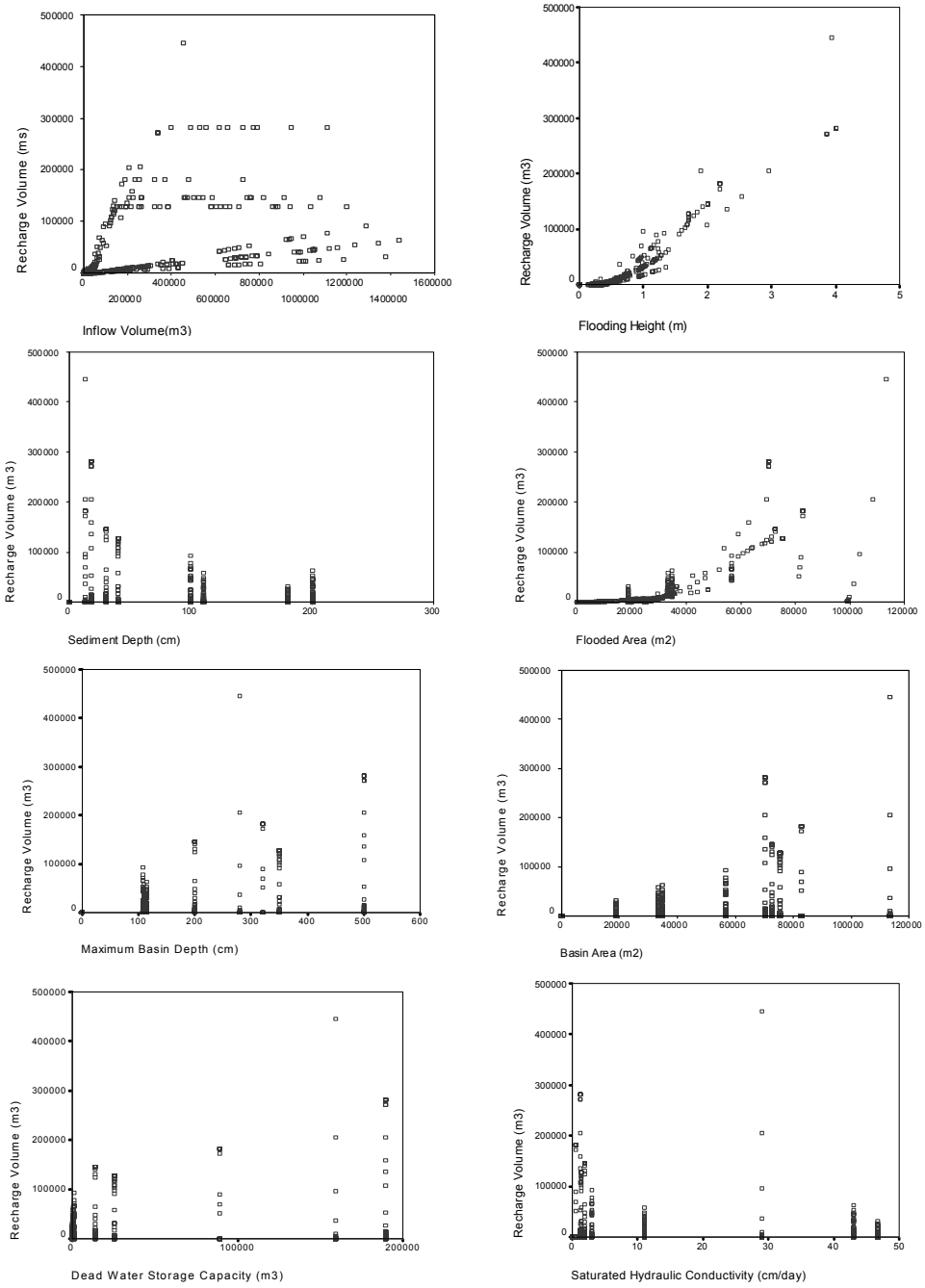

Figure 4.11 The relationship between recharge (dependent variable) and different computed/measured/observed independent variables using MG method and SWAP mathematical modelling results for spring 2002 in the study area

Table 4.12 Model coefficients using eight independent variables

Model		Unstandardized Coefficients		Standardized Coefficients			Collinearity Statistics	
		B	Std. Error	Beta	t	Sig.	Tolerance	VIF
1	(Constant)	-13470.5	505.904		-26.627	.000		
	FH	70572.398	698.818	.945	100.988	.000	1.000	1.000
2	(Constant)	-6009.809	559.991		-10.732	.000		
	FH	71192.235	599.388	.953	118.775	.000	.998	1.002
	SD	-10951.2	520.531	-.169	-21.039	.000	.998	1.002
3	(Constant)	-6496.552	532.479		-12.201	.000		
	FH	72426.105	577.829	.970	125.342	.000	.965	1.037
	SD	-17973.1	774.792	-.277	-23.197	.000	.405	2.471
	KS	35846.197	3049.295	.141	11.756	.000	.403	2.481
4	(Constant)	-922.805	863.240		-1.069	.285		
	FH	73840.768	589.727	.989	125.212	.000	.880	1.137
	SD	-20781.7	831.257	-.320	-25.000	.000	.334	2.995
	KS	39357.478	3003.366	.155	13.104	.000	.395	2.534
	BD	-22.197	2.747	-.071	-8.080	.000	.720	1.388
5	(Constant)	-713.232	838.177		-.851	.395		
	FH	78428.428	777.957	1.050	100.813	.000	.476	2.100
	SD	-20461.7	807.626	-.316	-25.336	.000	.333	3.001
	KS	40442.424	2917.624	.159	13.861	.000	.394	2.539
	BD	-26.107	2.704	-.083	-9.655	.000	.700	1.428
	Qin	-1.75E-02	.002	-.088	-8.707	.000	.512	1.954
6	(Constant)	-546.909	838.235		-.652	.514		
	FH	80290.190	1035.896	1.075	77.508	.000	.267	3.743
	SD	-20662.7	808.920	-.319	-25.544	.000	.330	3.027
	KS	40082.609	2913.034	.157	13.760	.000	.393	2.544
	BD	-24.709	2.746	-.078	-8.999	.000	.676	1.480
	Qin	-1.65E-02	.002	-.083	-8.143	.000	.497	2.012
	FAS	-7.32E-02	.027	-.036	-2.713	.007	.297	3.362
7	(Constant)	-2107.965	980.494		-2.150	.032		
	FH	80689.297	1040.699	1.081	77.534	.000	.263	3.804
	SD	-19724.6	863.174	-.304	-22.851	.000	.288	3.470
	KS	37321.248	3041.854	.147	12.269	.000	.358	2.793
	BD	-31.416	3.514	-.100	-8.939	.000	.410	2.441
	Qin	-1.67E-02	.002	-.084	-8.267	.000	.496	2.014
	FAS	-8.29E-02	.027	-.040	-3.061	.002	.293	3.410
	BAS	4.820E-02	.016	.034	3.041	.002	.398	2.515

a. Dependent Variable: RECHARGE

4.8 Conclusions

The water budget study in the floodwater spreading/artificial recharge scheme shows that the simulations gave realistic results when applied to the Sorkhehesar case provided ponding depths were included. Therefore, such simulations may be used for *a priori* studies.

The saturated hydraulic conductivities (Ks) calculated using MG analytical soil hydraulic functions gave the most accurate results. The results calculated using the aggregation of the MG and CA methods did not show any significant difference from the observed field data but were not as accurate as the results obtained with the MG method. Using laboratory-measured saturated hydraulic conductivity (Ks) values and ignoring ponding depths in a scheme with sedimentation resulted in recharge efficiencies that were too low. Simulation results using the CA method were significantly different from the observed field data

Statistical analysis suggests that water ponding depth has an important effect on recharge, as well as sediment depth and saturated hydraulic conductivity (according to the computed Beta value; Table 4.12.).

In the first four basins, where inundation depths of less than 40 cm were limited mainly to the sinuous channels and much sedimentation took place, the maximum recharge efficiency for the simulation period was found to be in the order

of 5% only, despite the fact that in basins 2 and 3 much of the >2 m thick sediment had a moderately light texture. The earlier SWAP simulations indicated a reduction in recharge and an increase in evaporation when sediment layers were present. The model for Sorkhehesar suggests that for the large sediment thickness the recharge is strongly reduced. However, it should be noted that the inundated area was less than in the lower basins.

Basins 5, 6 and 7 had a layer of clayey sediment with a thickness varying from 18 to 30 cm, but average daily ponding depths were 0.71, 0.64 and 0.80 m respectively. The combination of ponding depth and limited thickness of the sediment, although heavy textured, had recharge efficiencies of 25%, 18% and 27% of the total flood volume respectively. This is in accordance with the SWAP simulation results, which showed appreciable recharge when deep ponding depths were considered, even when clay sediment of 30 cm was present.

Recharge efficiency in basins 8 and 9 was about 9% and 4% of the total flood volume. Although the average flooding depth in basin 8 was less than in basins 1 to 4, the recharge efficiency was greater, mainly due to the absence of a thick sediment layer and the large size and capacity of the basin for water storage (dead water body). The recharge efficiency in basin 9 was low because inundation lasted for only a part of the period.

It should be noted that the SWAP modelling results assume that water passing the lower boundary of 2 m drains freely to the groundwater. Such conditions are found in the Sorkhehesar scheme where the fanglomerates near the apex of the alluvial fan have high permeability. The results confirm that permeability is a prime factor in the selection of suitable areas and sites. In the case where the subsoil is less permeable and the sediment has bad hydraulic properties (e.g. predominantly consisting of montmorillonite), the recharge efficiency is likely to be much less than the efficiency of the Sorkhehesar scheme.

The full capacity of the Sorkhehesar scheme seems to be over-designed, because basins 10 to 17 did not receive any, or only little, water during the lifetime of the scheme. However, the complete filling of the first four basins and the partial filling of the next three shows that the design endows the scheme with a long lifetime. The design has given due consideration to the large sediment loads typical of runoff in semi-arid regions, and to the fact that a few major events may carry a large proportion of the total long-term sediment load, making it hazardous to rely on suspended load measurements made during relatively short periods of time.

Although simplifying assumptions were made in the spreadsheet model developed, such as averaging Ks values and thickness of sediment in each basin without mapping the soil textures and depths, such an approach is recommended for evaluating more floodwater spreading schemes. The results can be checked by simple measurement of depths and inundation limits in the basins. Data becoming available in this manner would be welcome in order to validate simulation modelling results and determine the most effective factors in the recharge process.

CHAPTER 5
Zone Selection for Floodwater Spreading Schemes

5.1 Introduction

As mentioned in Chapter 2, a potential zone is a more or less contiguous tract of land where alluvial aquifers are found with ephemeral or perennial rivers traversing the alluvial areas, and which is not fully occupied by irrigated lands. Zone selection is a screening process and the first step in a hierarchical procedure that should lead to the identification of the most promising areas, sites and type of design for constructing a floodwater spreading scheme in order to augment the groundwater resource.

At the zone selection scale, it is very difficult to quantify all the characteristics of the different areas within a zone. Therefore, a prior selection has to be made in qualitative terms in order to find the most promising areas in a zone. To do so, exclusionary criteria (estimated qualitatively) are used, as discussed in Chapter 2. Areas that are not feasible within potential zones will be excluded from further consideration. The final product of this screening phase will be a few potential areas within a zone for floodwater spreading. These potential areas will be evaluated and ranked by a formal procedure, as explained in Chapters 2 and 6.

The application of the exclusionary and suitability criteria by interpretation of satellite images, supplemented by other data, will be illustrated by a number of cases. In order to cover at least a variety of situations, cases in three different regions are discussed. The locations of the cases in Iran are shown in Figure 5.1.

As mentioned earlier, most potential areas for floodwater spreading schemes in Iran are the alluvial fans or bahadas (i.e. coalescing fans forming a contiguous permeable area), usually located in the intramontane depressions or as footslopes on the hills and mountains bordering plains along the coast or large tectonic depressions, often with playas. Other fluvial plains, not in the form of alluvial fans, could also be suitable for schemes if the deposits are coarse-grained and of sufficient thickness. Such conditions are associated with large rivers. The high flood discharges and large size of the mobile channels of large rivers when flowing in alluvium cause major obstacles for the construction of intakes for floodwater spreading schemes. Therefore, attention in this study is focused on the alluvial fans.

A floodwater spreading scheme is typically located in the upper part of a fan, where the permeability of the aquifer is high owing to the presence of predominantly coarse-grained fluvial deposits. Because of the gradual interfingering clay and silt deposits towards the lower part of a fan, the unconfined conditions of the upper part change into semi-confined conditions in the lower part, while in certain cases the deeper groundwater may be in a confined state.

The first case is the eastern Zanjan Valley zone and is presented to illustrate the exclusionary criteria principle. Based on this principle, it can be concluded that the zone is not suitable. Transmission loss leads to the exclusionary argument.

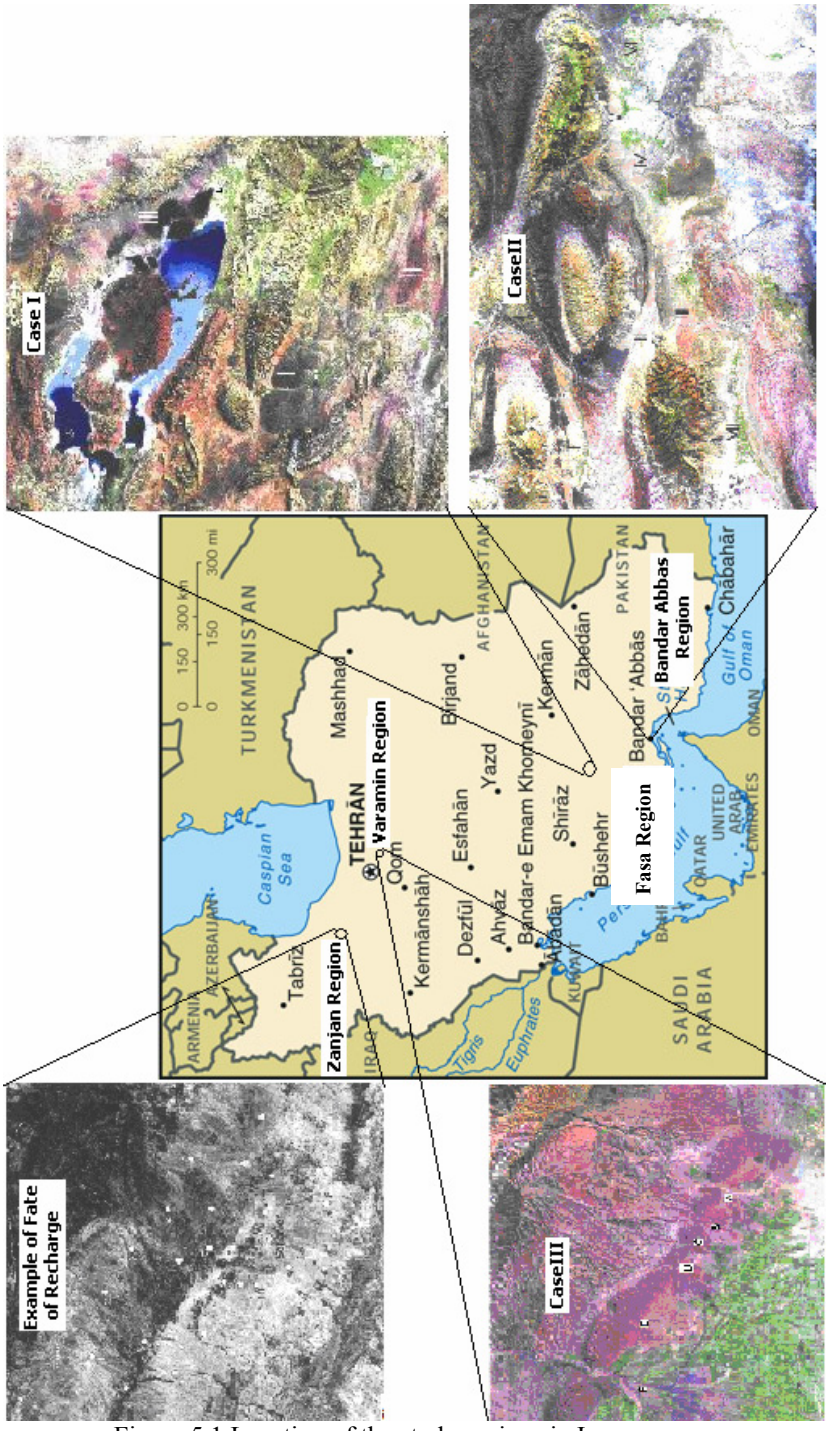

Figure 5.1 Location of the study regions in Iran

This example is included because the importance of transmission loss on recharge can be demonstrated, rendering recharge schemes doubtful in a large part of the zone.

In three other cases (Fasa, Bandar Abbas and Varamin), screening focuses on the major arguments in favor of areas for possible schemes, as well as on their limitations. In all these cases, agriculture depends almost entirely on irrigation water, because the mean annual rainfall is generally less than 300 mm and the mean annual evaporation exceeds 2000 mm, except possibly in the highest parts of the mountains.

Common to all cases is the occurrence of flash floods of erratic nature and the desirability to augment groundwater resources.

5.2 Fate of recharge

Natural recharge in a semi-arid climate occurs chiefly in the form of river recharge, since most of infiltrated rainfall is held by the upper soil and is lost by evapotranspiration. River recharge is important on the upper to middle fans because of the depths of water; duration of flow, which exceeds rainfall duration; and the low proportion of clay and silt in the riverbed materials because their settling is limited to the very last stage of a runoff event. Transmission losses are discussed in this case study and some evidence of the effect of river recharge on groundwater levels is given.

The groundwater surface is determined by the recharge, the permeability, the configuration of the impermeable base of the aquifer, and possibly by the presence of incised rivers draining the lower part of a fan. Generally, the depth to groundwater decreases from a depth of several tens of meters to a few meters or less in the downstream direction. The configuration of the impermeable base below an alluvial fan aquifer and deposits with low permeability along the lower margin may force the outflow of groundwater to the surface, since its movement is governed by a groundwater flow system driven by the recharge in the upper part of the aquifer. The slow flow of the groundwater increases the salt content of the groundwater body itself in the downstream direction because of the uptake of salts.

Water budget

If steady state conditions are assumed and no-flow conditions for the upper boundary, the water balance, can be written as:

$$\mathbf{Qrain + Qtrans + Qar = Qout\text{-}s + Qout\text{-}ss + Et + Ec}$$

where Qrain is the net recharge due to rainfall falling on the fan, usually a negligible quantity in very dry regions; Qtrans is the river recharge or transmission loss; Qar is the artifical recharge; Qout-s is the surface outflow; Qout-ss is the subsurface outflow; Et is the evapotranspiration loss, mainly from the lower part of the fan in the case of a shallow groundwater table in the lower part of the fan; and Ec is the evapotranspiration loss of crop irrigated by groundwater plus water pumped and transported for drinking water.

The addition of an artificial recharge term on the left-hand side of the equation results in increases in the quantities of terms on the right-hand side

because the heads of the water surface or the pressure-driven flow system will be increased by a scheme. Ec can be considered as the term that benefits from a recharge scheme. It is obvious that the three other terms will reduce the effect of a scheme and therefore they should be minimized by implementing a controlled pumping scheme. If Ec equals the artificial recharge, the steady state conditions are maintained.

Since in many of Iran's aquifers the water tables are declining, artificial recharge could also be used to restore the steady state, or restore the sustained use of an aquifer. The amount needed to achieve this could be estimated by multiplying the groundwater lowering by the specific yield or the storativity of the aquifer. The estimated recharge efficiency of a scheme could thus be used to predict its beneficial effect on the depletion of the aquifer. Only if the artificial recharge amount exceeds the amount of overdraft could the surplus be used for additional pumping for irrigation or drinking water supply. In such applications, no groundwater modelling would be required *per se*; determination or proper estimation of the terms of the water budget would suffice.

Role of qanats

As is well known, qanats are an age-old system of sustained groundwater use where the aquifer is drained by near-horizontal subsurface tunnels that carry groundwater from the upper to middle part of an alluvial fan or aquifer onto the surface by gravity flow. Lowering of the groundwater surface is limited to the elevation of the upper part of the source part of the tunnel. Pumping endangers the discharge of qanats, as has happened in many cases. Recharge by floodwater spreading could revive the water supply by qanats, depending on the amount of recharge, and the location and size of scheme in relation to vertical dispersion of the recharged water and the location of the mother wells of a qanat.

Although rehabilitation of qanats is generally considered desirable, two aspects need to be mentioned. First, a traditional qanat also keeps draining the groundwater during the winter period, although there is no need for water for irrigation in that period. The second aspect is of a practical nature, namely the shortage of willing personnel capable of maintaining qanats.

These aspects have been taken into consideration when determining the weights in the multicriteria approach based on pairwise comparison of preferences which is used in this case study. For example, stronger preference could be given to the continuation or rehabilitation of qanats if the winter discharge could be made to infiltrate if pumping takes place at the middle to lower part of the aquifer.

Operational aspects

In more complex situations, the groundwater situation and management options can be best evaluated by groundwater modelling, particularly when in the lower part of the fan shallow groundwater conditions exist or when an incised river is present. In the latter case, the velocities of the flow system are relatively high, and therefore the introduction of Qar may increase both outflow terms within a short period of time. In the case of a shallow groundwater table, artificial recharge may lead not only to more outflow, but also to an increase in the area suffering from salinization,

which may encroach on cultivated lands – as was observed in the Goorband fan, Iran, where the groundwater table in the middle and lower parts of the fan was increased because of leakages from irrigation canals and return flow from irrigated fields (Pishkar, 2003). Both these sources can be considered as a form of artificial recharge.

With the aid of a properly calibrated groundwater model, the location and pumping rates could be worked out to make optimal use of the amount of water recharged artificially and to avoid adverse effects. However, the modelling of the groundwater flow of an aquifer is no simple matter, because of the data requirements pertaining to the spatial distribution of the transmissivity, the spatial patterns of recharge, evaporation loss, surface outflow, and the need to know other specific parameter values such as the horizontal and vertical permeabilities, which are quite different in the case of fanglomerates, with the differences varying in the downstream direction. Furthermore, head data are required. Steady state solutions of a groundwater model are the easiest to achieve, but the non-uniqueness of the solution (recharge interacts directly with transmissivity) requires transient modelling to increase the reliability of the results (Lubczynski, 2005). However, transient modelling is even more data-intensive.

It is regrettable that in Iran installation of some hydrometric devices for the proper evaluation of the effects of artificial recharge on the groundwater started only very recently, although many schemes are in operation. It is therefore difficult to obtain proper weightings for the preferences in the multicriteria evaluation method used.

In this study, the zone and area selected for applying the methods for selecting area, site and design type did not require specific groundwater data, because of the large overdraft from the aquifer that will benefit from a recharge scheme and because any surplus would be readily used by increased water use for irrigation and drinking water supply.

Transmission loss leading to exclusive argument, Zanjan example

This case study is included because the importance of transmission loss on recharge can be demonstrated, rendering recharge schemes doubtful in a large part of the zone. Figure 5.2 (Landsat TM band 4) shows a large tectonic depression, consisting of alluvial fan deposits (fanglomerates) of the east Zanjan Valley (see zone location in Figure 5.1) and bordered by mountains and hills in the north and the south. Sizeable catchments drain into the depression. The aquifer limits can be interpreted by noting outcrops. In the southwestern part, the geological map shows alluvial deposits. In fact, the deposits in that part consist of glacis deposits of limited thickness overlaying impervious rocks. The strike lines of these rocks can be seen on the satellite image and are easily missed as outcrops in the field. The aquifer limit is thus much further east than would be supposed on the basis of the geological map, and well 10 (Figure 5.2) is not penetrating the aquifer, unlike well 9.

The alluvial fans fed by catchments in the northern part have different tones (due to differences in reflection; also on colour composites (not shown)) because of variation in the composition of the sediment attributable to differences in

catchment lithology. The westernmost river (the Zaker) drains a catchment with a large quantity of granites and the riverbed deposits are lighter in colour than those of the catchments with volcanic rocks of the central and eastern parts.

The older alluvial fan surfaces closer to the mountain front have lighter tones owing to the presence of lime crusts. These have low permeability, as was evident from a recharge experiment by the Zanjan office of the Water and Power Ministry (pers. comm.). The experiment was abandoned because no measurable loss of water in the elongated recharge basins could be noted other than evaporation loss. Hence rainfall recharge on the older fans can be ignored.

Rivers are stable in the upper zone of the fans because they are incised. In the downstream direction, the recent and sub-recent riverbed deposits widen and consist of coarse materials, but further downstream most of the riverbeds disappear. Recharge by transmission loss is important, as can be demonstrated by comparing hydrographs (Figure 5.3 a and b) of observation wells annotated on the image. Hydrographs 1, 5 and 3 are from wells located in the northern zone close to the riverbeds, but well hydrographs 2 and 4 are situated between major riverbeds. The effect of drawdown caused by pumping in the wells in the southern and middle parts of the aquifer during the growing season from April-May to September can be noticed in Figure 5.3b (concave curve), as well as the recovery (convex curve).

The prominent peaks on the recovery curves (Figure 5.3a) are due to recharge by flash flows, and particularly to snowmelt runoff that infiltrates in the upper parts of the river. The graph shows the substantial recharge peaks of the wells close to the rivers and much less recharge by sheetwash in the lower part of the fan (Figure 5.3 b) and in wells away from the major rivers (Figure 5.3a). In addition, the long-term lowering of the groundwater level, due to the fact that pumping rates exceed the recharge, is depicted.

In the central part of the aquifer is a small perennial river bordered by wet grasslands (whitish tones). Field enquiries revealed that the water is never turbid and flow does not fluctuate much. Therefore, all the floodwaters infiltrate on the fans. The grasslands and outflow are maintained by the exfiltration area of the groundwater flow system, driven by the natural recharge provided chiefly by the transmission loss in the channels. This case describes the classical hydrogeology of an alluvial fan, an upstream recharge zone with phreatic conditions gradually changing into a (semi-) confined condition in the lower part with upward pressure. The case also illustrates that increased drafts will result in the drying up of the base flow river.

Evaluation

Despite the fact that catchments of sufficient size exist in the mountains, as well as an aquifer consisting of permeable fanglomerates of sufficient thickness (about 200 m in the central part (Bani Hashemi, 1994)), the entire area should not be considered as suitable for floodwater spreading schemes. The reason is that all the runoff infiltrates and no surface runoff leaves the area (transmission loss exclusionary criterion). Therefore, the new reservoir feeding recharging wells south of Soltanieh (Figure 5.3; reservoir built after image was recorded) affects mainly the location of the recharge and not so much the quantity.

The exception is the Zaker river in the west, because its river course extends beyond the alluvial fan area and the only suitable area for a scheme is that of the Zaker river deposits in between the areas with the lime crust. The question of the total amount of water leaving the Zaker area remains to be considered.

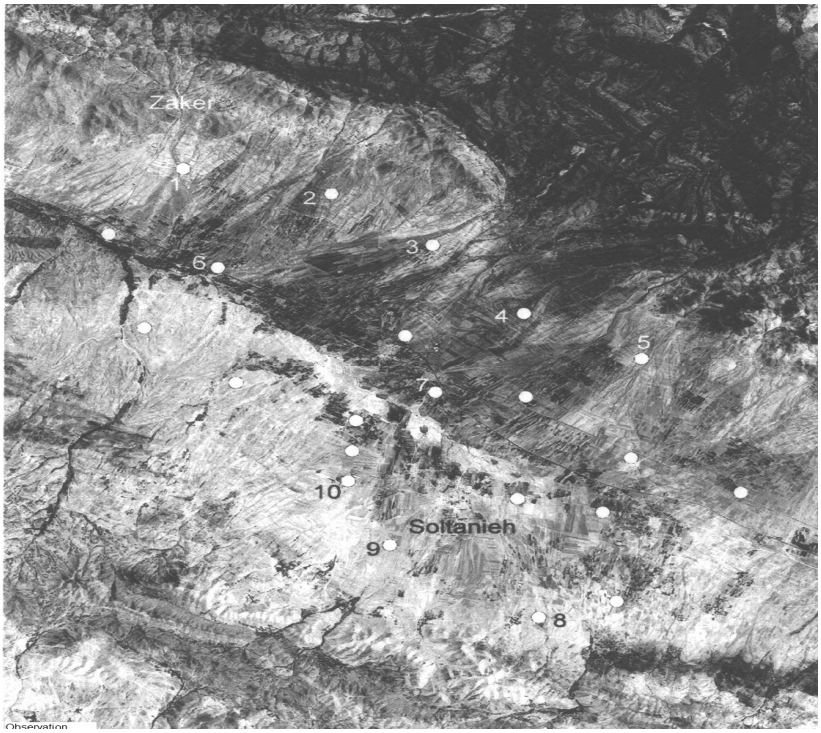

Figure 5.2 Aquifer eastern Zanjan Rud: location of observation wells (Landsat TM, band 4)

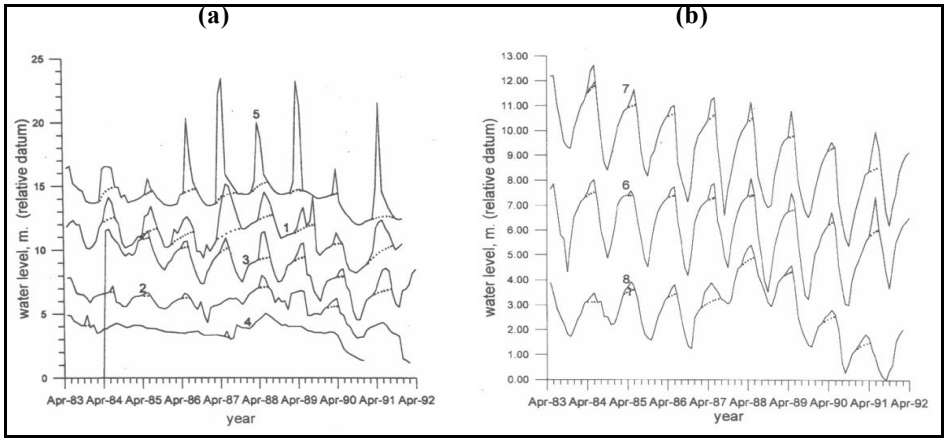

Figure 5.3 Observed groundwater table in the observation wells, (a) 1 to 5, and (b) 6 to 8, in the Zanjan region

5.3 Fasa

The Fasa zone is located in the Zagros chain, where folded structures form the hills and mountains and where the synclines and other tectonic depressions contain the alluvial deposits that are of direct interest for floodwater spreading schemes. In most of the Kohr zone, neotectonics have influenced erosion and deposition. The zone is shown on a false-colour image (TM, 742) in Figure 5.4, with the locations of sub-zones I to III, which will be discussed below.

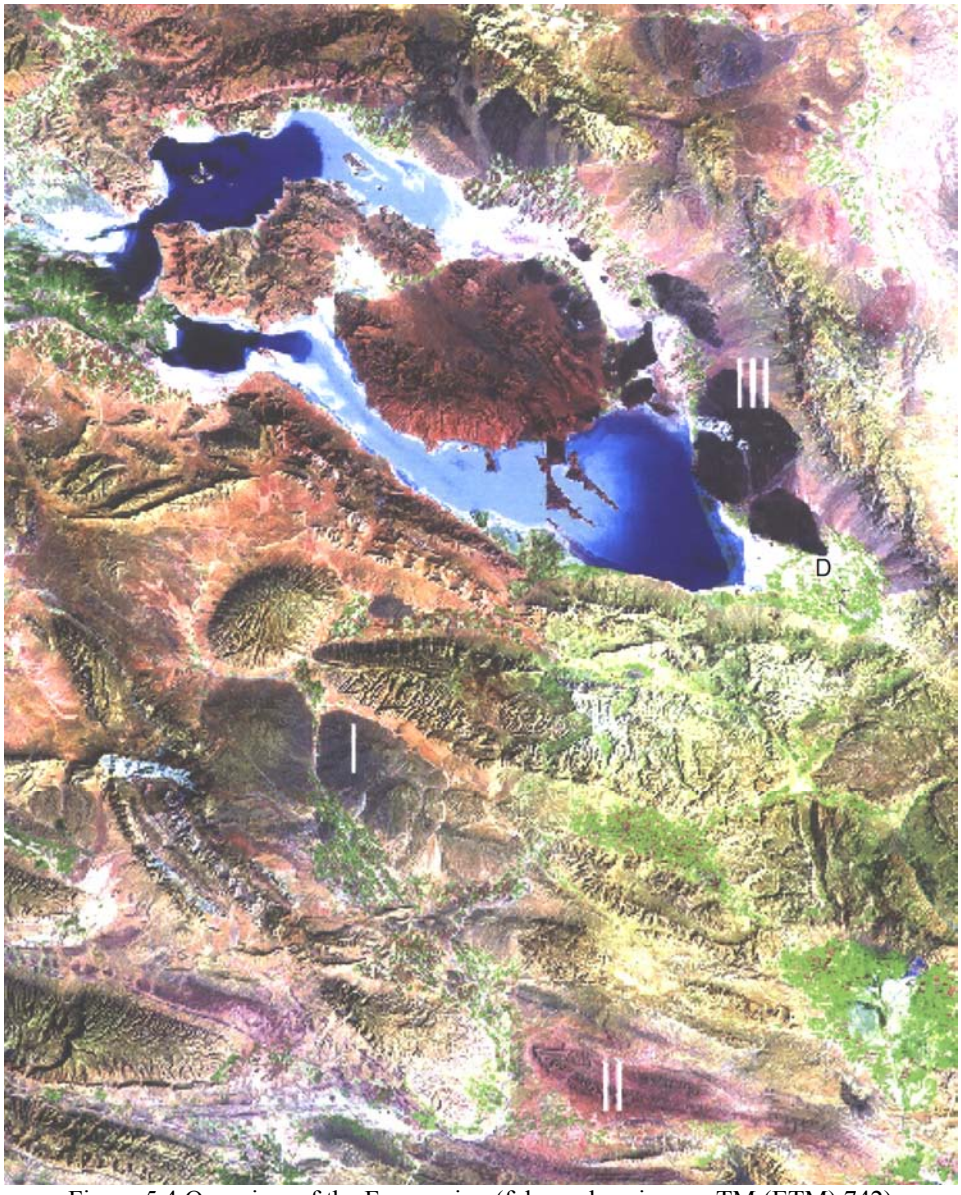

Figure 5.4 Overview of the Fasa region (false-colour image, TM (ETM) 742)

The general hydrological situation is that the rivers are ephemeral, except in the area southeast of the large playa (in between annotations II and III) and west of annotation II. The base flow in the rivers in the former area is due to the presence of extensive limestone plateaux, where much of the rainfall infiltrates. The green areas correspond to irrigated croplands, deriving their water from diverted base flow and from groundwater.

The combination of exclusionary criteria – (1) sufficient size of catchment for runoff generation, and (2) presence of alluvial fans in connection with an aquifer with rangelands – yields only three zones of limited extension in this zone, denoted I to III on the image.

Sub-zone I: Variation of runoff and sediment yield within catchment and transmission loss (exclusionary criteria) in infiltration area

Most of the upper catchments (A) (see Figure 5.5) are underlain by hard marl and limestone. South of the upper catchments is a zone (B) with coalescing alluvial fans (bahada), where transmission losses occur. South of the bahada, hills are found that consist of continental deposits of Tertiary age (C), composed of semi-consolidated shale, marl, sandy clay, sandstone and pebble beds, overlain partly by a cap of Quaternary pebble beds cemented locally by lime. The intramontane depression (D) is closed off by folded rocks (E), which contain impermeable units (E1). The northern flank of the depression is affected by uplift, which is witnessed by the raised and dissected older alluvial fan deposits that dip below the young floodplain deposits of the depression, indicating subsidence within the depression and thus sufficient thickness of the aquifer. As can be seen on the image, irrigated fields (by groundwater) occupy most of the depression.

Some of the valleys in the upper part (A) of the catchment of fan G3 consist of glacis, whose deposits have good infiltration. The runoff coefficient in the upper catchments is relatively low because of the presence of limestone and glacis deposits, and so is the sediment yield. The runoff and sediment load increase in the hill area (C) and flood flows reach alluvial fan G3. As can be seen, floodwater spreads out on the active fan and the question is how much of the flows infiltrate on the coarse-grained channel/fan deposits, or in other words what is the transmission loss.

The importance of transmission losses recharging the groundwater can be judged by the near-disappearance of the river (F) in the downstream direction and the disappearance of the active channels of fan G1. In this context, it should be noted that only a small channel exists in the gap just north of E1, indicating that there are also important transmission losses of the runoff on the alluvial fans G2 and G3. Only rarely does some floodwater flow through the gap, and then not sufficient to maintain the channel in the downstream direction. This evidence suggests that the large width of the riverbed of the river (G3) is caused by deposition of the bedload rather than by strong flash flows, and that most of the floodwaters infiltrate, so little water leaves the fan. A matter of concern is therefore that investments in a floodwater spreading scheme will not induce much additional recharge in the fans G1, G2 and G3. Furthermore, the wide depositional pattern on the fan suggests that the long dike type of scheme could be appropriate.

The larger catchment upstream of H1 could be considered because of the runoff potential. However, a suitable area near H1 has the problem that not much space is available for a scheme or for the development of irrigated areas (exclusionary criteria). In addition, because of catchment geology and geomorphology, much of the sediment is fine-grained. The area around H2 also suffers from lack of space and so does the area around H3, because most of the lands there are under irrigated agriculture.
In conclusion, although potentially promising areas seemed to be available, a closer view reveals that there are arguments against their adoption for more detailed field investigations.

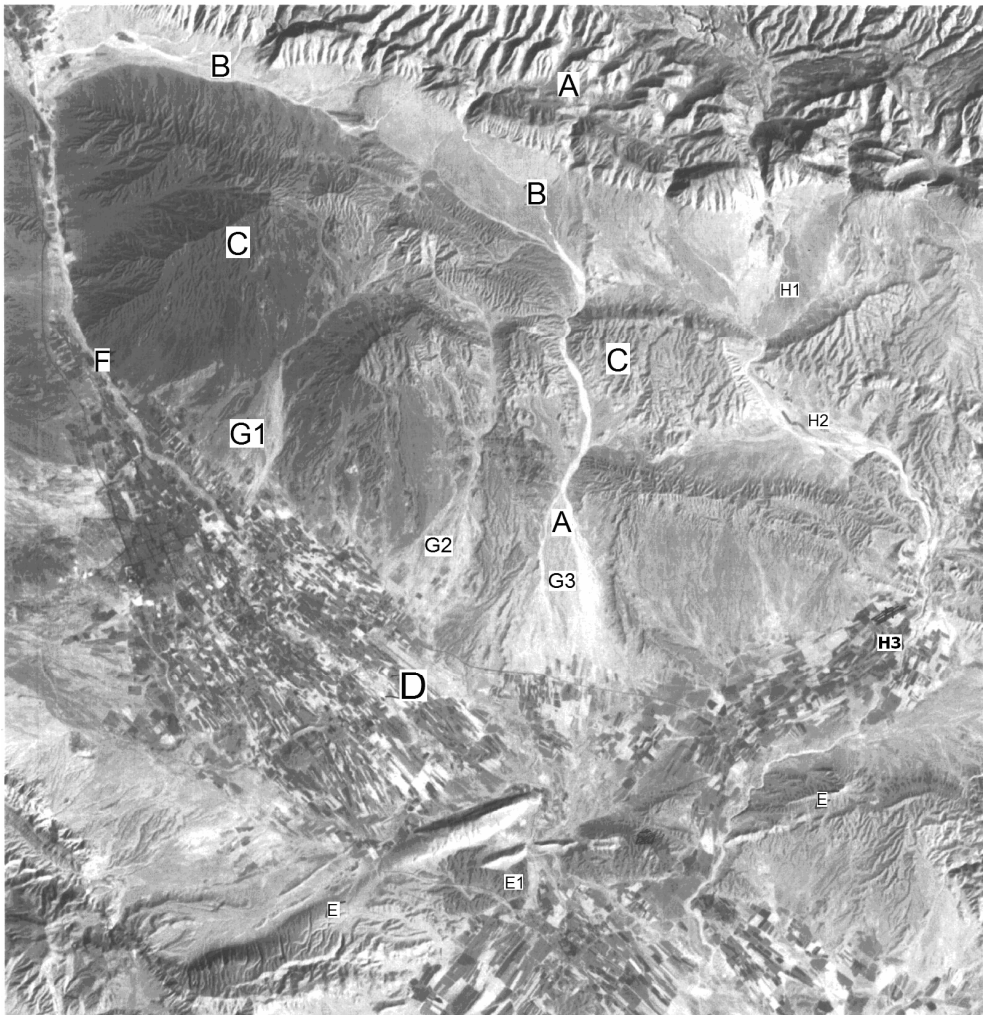

Figure 5.5 Fasa region, sub-zone I

Sub-zone II: Large alluvial fan, groundwater loss by incised river and existing scheme

This sub-zone (Figure 5.6) consists of a wide alluvial fan of a sizeable catchment (193 km^2) of the Bisheh Zard river. The catchment is underlain predominantly by folded rocks of low permeability (shales and marls). However, sandstones, conglomerates and limestone beds occur in the catchment and they give expression to the fold structures (e.g. a synclinal axis runs through A). Figure 5.6 shows the alluvial fan and its surroundings. The river breaks through the sandstone escarpment near B and has formed an alluvial fan with a relatively gentle slope. Only in the northern fringe of the alluvial fan are some outcrops found just south of the scarp slope. The southern part of the fan is bordered by a fault approximately along the east-west flowing river (D1-D2). Just south of the fault, low outcrops of soft (impermeable) rocks are found, forming a barrier for the groundwater. It could be reasoned that the fan was formed in a subsidence depression and the fanglomerates have sufficient thickness to form an aquifer. The presence of large fields irrigated by groundwater demonstrates the aquifer transmissivity and the suitability of the soils for irrigated agriculture.

The good water holding properties of the soils on the lower fan are not surprising because much of the catchment lithology consists of fine-grained rocks (shales, marls). The resistant rocks of the catchment account for the wide nature of the riverbed in the middle part of the fan, which consists of coarse-grained materials (sands and pebbles), as well as for the good permeability of the aquifer in the upper and middle parts of the fan. All observations taken together suggest that the zone consists of a tectonic depression with permeable fanglomerates in the upper and central parts (phreatic conditions) and more fine-grained deposits in the downstream part (semi-confined or confined conditions), as was confirmed by the hydrogeological study of Fatehi-Marj (1994).

The fan surface is not dissected and the upper to middle part consists of light textured soils, overlaying very coarse-grained alluvial fan deposits. The river is incised in the northernmost part of the alluvial fan; thus the river course is stable in that part. The river channel extends to beyond the fan; hence floodwater is 'lost' (low transmission loss). So far, the aspects that favour selecting this area for a floodwater spreading scheme are in the upper-middle part of the fan. However, there are aspects of concern. Comparison of old (1950s) aerial photos and the 1988 TM image shows shifts in the river in the central part of the fan, downstream of the incised course in the upper part of the fan. Such shifts are likely to continue because the river deposits bedload in that part of the fan. Therefore, either river training is included or repair activities are anticipated in any possible scheme, raising the costs.

The east-west flowing river is incised near the confluence with the large north-south flowing river, and a phreatophyte vegetation can be observed in the channel. This indicates outflow of groundwater. The stereo aerial photos show that the incision is deep and the walls are steep, indicating materials of high cohesion and hence the presence of clay and silt. Therefore, the amount of artificial recharge should match the amount withdrawn for irrigation, otherwise recharged groundwater is lost. Towards the east, the thickness of the alluvial deposits is

probably not great, because the depression is pinching out and low outcrops of impermeable rocks appear. Hence it is wise to ascertain the aquifer thickness in the eastern part and the permeability in the southern zone.

The above leads to the conclusion that the area has many factors in favour of a scheme and no exclusionary criteria have been met by the area. In fact, a floodwater spreading scheme of the channel and shallow basin type was started in 1984 (Kowsar, 1992). The planted trees along the channels make the conveyance channels visible (near E) on the 1988 Landsat TM image. Since then, the scheme has been expanded and is considered a success in terms of recharge and ecology, although quantitative figures are not available.

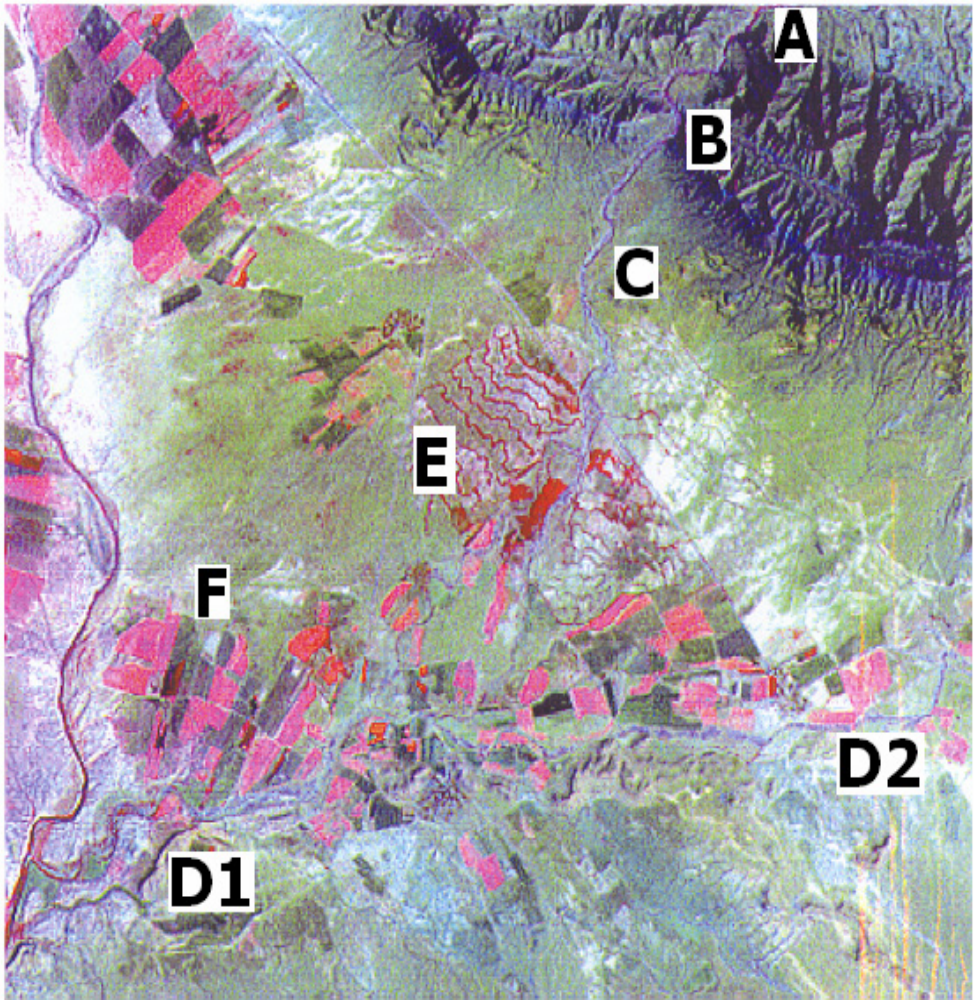

Figure 5.6 Fasa region, sub-zone II, Gareh Baygan area (false-colour composite, TM 742)

Sub-zone III: Constraint of catchment size in relation to transmission loss bahada zone

The image in Figure 5.4 shows a playa with a bahada, with a fringe of cultivated fields in the lowermost part and low hills with shales, which have low reflectance in the TM bands. The irrigation water for cultivation is derived mainly from qanats tapping the water in the bahada. The adjacency of the irrigated fields to the salt lake excludes the use of tubewells in the irrigated area because lowering the pressure by pumping causes upwelling of the brackish water interface. Figure 5.4 shows the moisture and salinity variations within the playa, caused by episodic inflow of flash floods and followed by drying up due to evaporation.

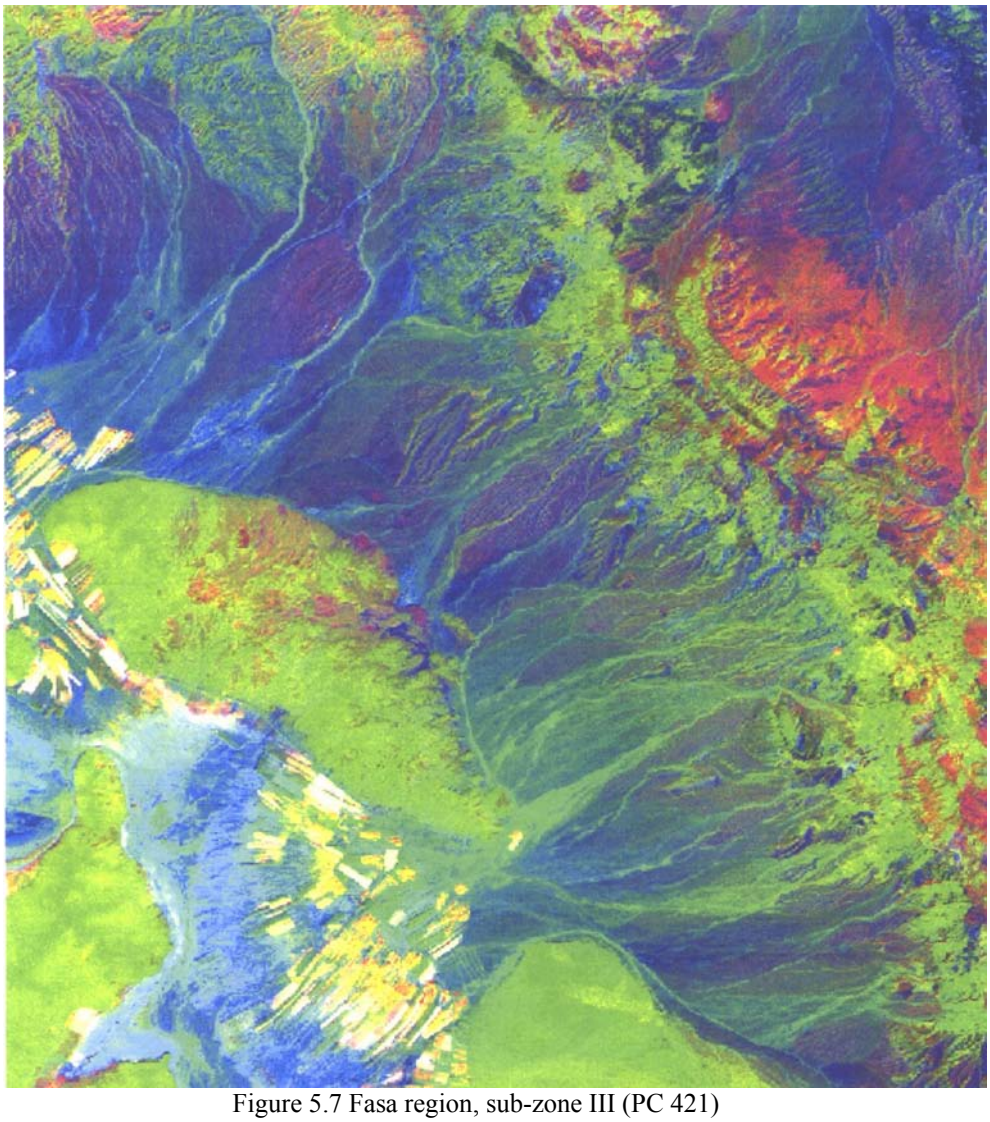

Figure 5.7 Fasa region, sub-zone III (PC 421)

The question in sub-zone III is whether transmission loss (exclusionary criterion) in the bahada is so high in view of the small catchments feeding the bahada, where nearly all water infiltrates, that a scheme is superfluous. To obtain a better view of the active riverbeds, Principle Component (PCA) Analysis was conducted and yielded the desired results, as shown in Figure 5.7, which is a false-colour image of PC's 4, 2 and 1, coded in red, green and blue respectively. The runoff on the bahada is partly concentrated in ephemeral rivers and partly in the form of sheetwash. The PC IV image was included, although it contains about 1% of the spectral information, because it discriminated the parts with active channels or flow paths and parts not affected. The latter parts have soil formation and a (sparse) rangeland vegetation adjusted to the soil conditions. The spreading out of the sheetwash in the lower part is associated with deposition of finer-grained materials (silty clays to sandy clays).

As the image in Figure 5.7 shows, there are no channels reaching the lake. Most of the remaining sheetwash is captured in the fields to augment soil moisture. Obviously more field information on this aspect is needed because, if most of the water infiltrates in the bahada, there is little point in artificial recharge.

Sub-zone III-D: Low sediment yield, constraint of size of infiltration area, alternative for flood control

A township (1; see Figure 5.8) is located on the apex of a gentle sloping alluvial fan cum inland delta of a river with a substantial catchment east of the town and with bahadas in the north and south. West of the town outcrops (2) occur, indicating that the alluvial deposits have probably no great thickness. Water from qanats and shallow wells in the upper part of the delta fan and the bahadas is used for irrigation. East of the city, orchards are watered by wells, and west of the city irrigated agriculture is possible up to the areas where soils are saline.

Flash flows spread out just upstream of the town, causing a flood hazard, and are therefore an additional reason for considering a floodwater spreading scheme that captures at least part of the floodwaters. A man-made diversion channel exists (3) that leads most of the water via location 4 into the lake (5). Such a scheme can mitigate the flood hazard that would otherwise be an argument for a floodwater spreading scheme.

Relatively little sediment is deposited in the alluvial area because of the presence of resistant rocks (limestone) in the catchment and of alluvial fans and colluvial valleys that capture sediment within the catchment. The overall permeability of the catchment is high, as is also evidenced by the small dimensions of the river channel and those of the diversion channel. The limited sediment splay along the playa shores also indicates relatively low sediment yield. The space for a possible floodwater spreading scheme to induce recharge in the upper part of the aquifer is limited to the small triangular area east of the city, thus limiting choice of scheme type.

Evaluation

Of the areas reviewed in this zone, there is only one that has predominantly favourable conditions, namely the Gareh Baygan area, zone II. Area IG3, area III

bahadas, and area III-D have limited possibilities, and data collection for further evaluation will depend much on the depletion of the aquifer and the amount of water that leaves the area. The general results of the evaluation for all the areas discussed in case I and the exclusionary criterion/criteria for each excluded area are shown in Table 5.1.

5.4 Bandar Abbas

An overview of the zone is shown on the TM false-colour image in Figure 5.9, annotated with the sub-zones and areas that are depicted at a different scale in this section. Separated by mountains or hills, there are several alluvial areas that will be discussed.

Sub-zone I: Evaluation of location of small infiltration schemes

The catchments (Figure 5.10) are located in a large anticline, with two massive limestone units (A) separated by marls and an eroded core of the anticline (B) where marls and shales dominate. A soft and impermeable formation (shales, mudstones) is found on the southern flank of the anticline (C1-C2) and a large, eroded anticline (D) occurs in the south, consisting of impermeable rocks of Tertiary age. A depression coinciding with an a-symmetric syncline is found in between the structures. The southern flank is formed by the northwards dipping conglomerates (D1). Quaternary deposits in the form of alluvial fan deposits have filled up the depression. The older alluvial fans E1 and E2, dissected and eroded after uplift of the northern anticlinal structure, dip below the younger deposits in the depression, indicating subsidence of the latter during late Pleistocene times. The massive limestones are karstic; hence a substantial part of the rainwater infiltrating into the limestones will be conveyed through karst conduits to springs located outside the area shown.

Irrigated fields in the depression bear witness to the presence of an aquifer that is fed mainly by transmission loss. The channels near G and H indicate that flood runoff leaves the depression, whereas the irrigation near H points to some groundwater runoff (base flow). The runoff from the western catchment, which is the largest in size and has soft marls and shales in part of the catchment, is much more than that from the eastern catchments. Transmission loss feeding the aquifer will be highest in the western parts, where wide recent river deposits occur (K), explaining some outflow of groundwater on the western side. The strong sedimentation will present a maintenance problem for a floodwater spreading scheme.

A scheme diverting flood runoff with relative low sediment in the channel near J onto the easternmost alluvial fan could be contemplated in order to augment groundwater in the southeastern part of the depression for irrigation. However, the scheme would be of small dimension for reasons of topography and discharge, and the same could be said for the rivers reaching the central part of the alluvial depression.

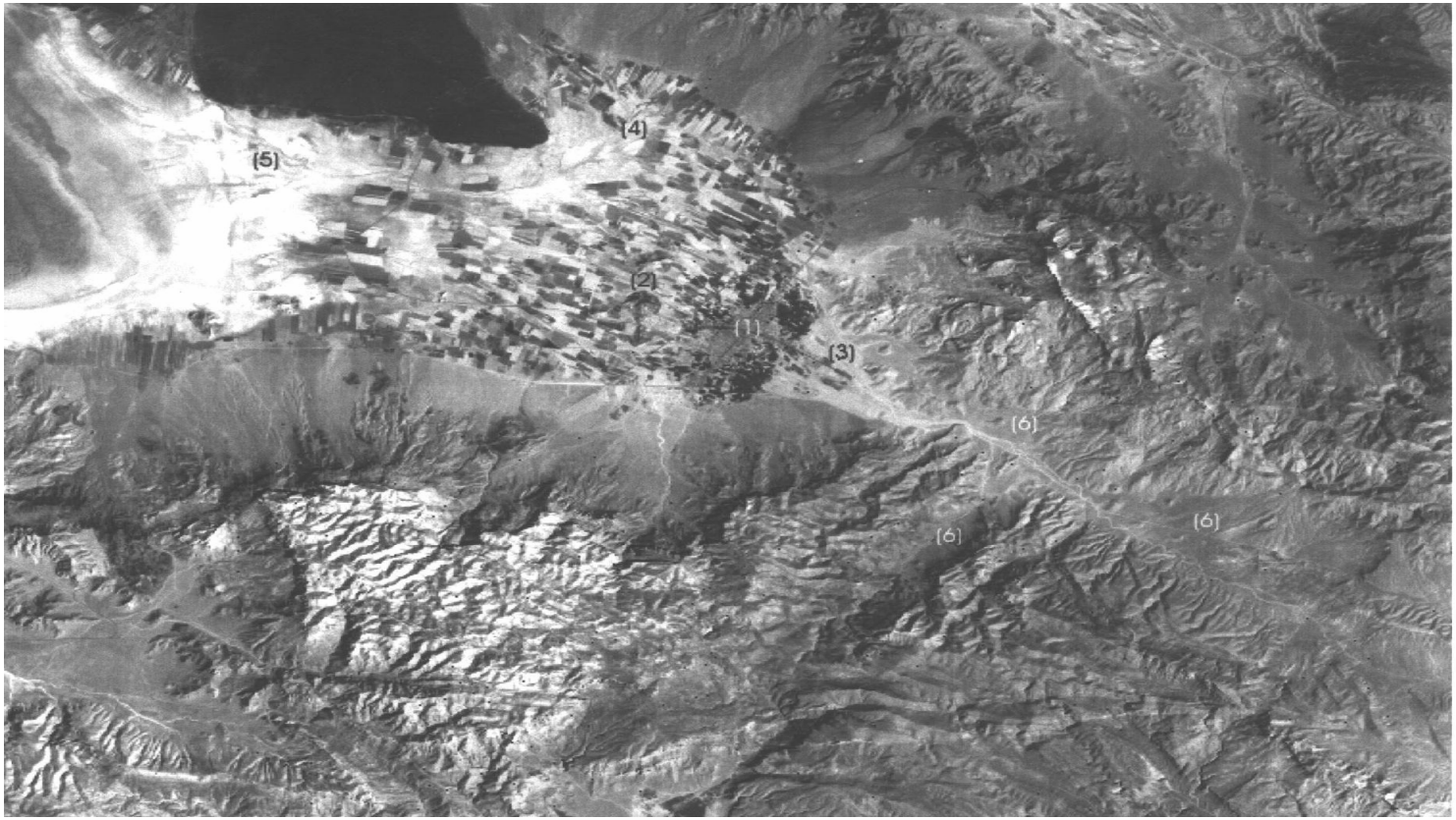

Figure 5.8 Fasa region, sub-zone III, area D (printed in black-and-white FC 453)

Table 5.1 Evaluation results for the studied areas, Fasa region

Zone Or Sub Zone	Areas													
I	F		G1		G2		G3		H1		H2		H3	
	Excluded Area	Potential Area	Excluded Area	Potential Area	Excluded Area	Potential Area	Excluded Area	Potential Area	Excluded Area	Potential Area	Excluded Area	Potential Area	Excluded Area	Potential Area
	Exclusionary Criteria High transmission Loss No Enough space **for Scheme development Fully covered by agricultural lands**	-	Exclusionary Criteria High transmission loss no water escape from the area	-	Exclusionary Criteria High transmission loss no water escape from the area	-	Exclusionary Criteria	+ Depletion of the aquifer and the amount of water that leaves the area should be checked in the field	Exclusionary Criteria **No enough Space For scheme development**	-	Exclusionary Criteria **No enough space for scheme development**	-	Exclusionary Criteria **No enough Space For scheme Development Fully Covered by agricultural lands**	-
II	**All the area of the alluvial fan around the main river (GarehBaygan area)**													
	Excluded Area		Potential Area											
	Exclusionary Criteria		+											
III	Bahada Areas		D											
	Excluded Area	Potential Area	Excluded Area	Potential Area										
	Exclusionary Criteria	+ The amount of water that leaves the area should be checked in the field	Exclusionary Criteria	+ Depletion of the aquifer and the amount of water that leaves the area should be checked in the field										

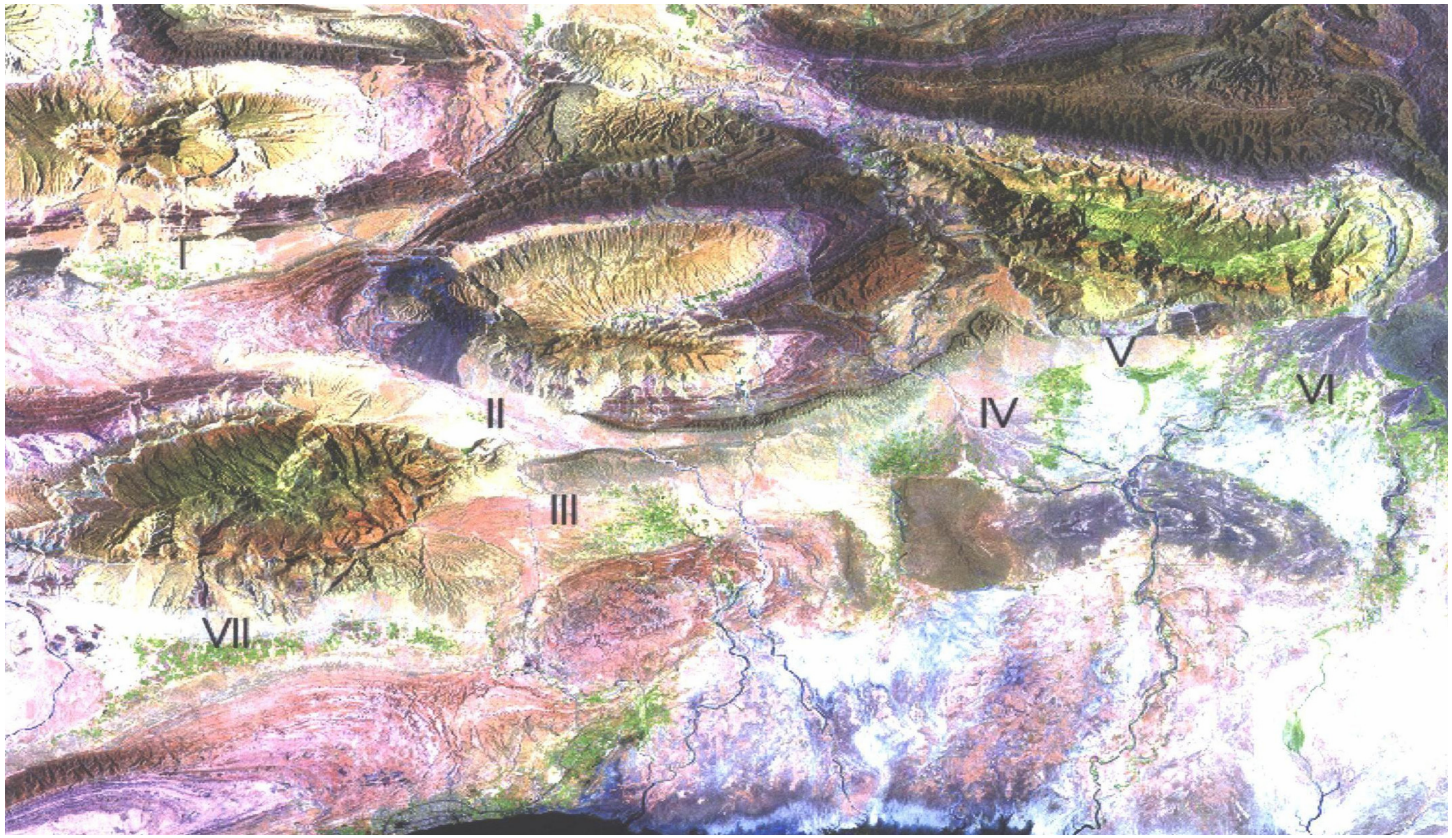

Figure 5.9 Overview of Bandar Abbas region: location of sub-zones (false-colour TM 742)

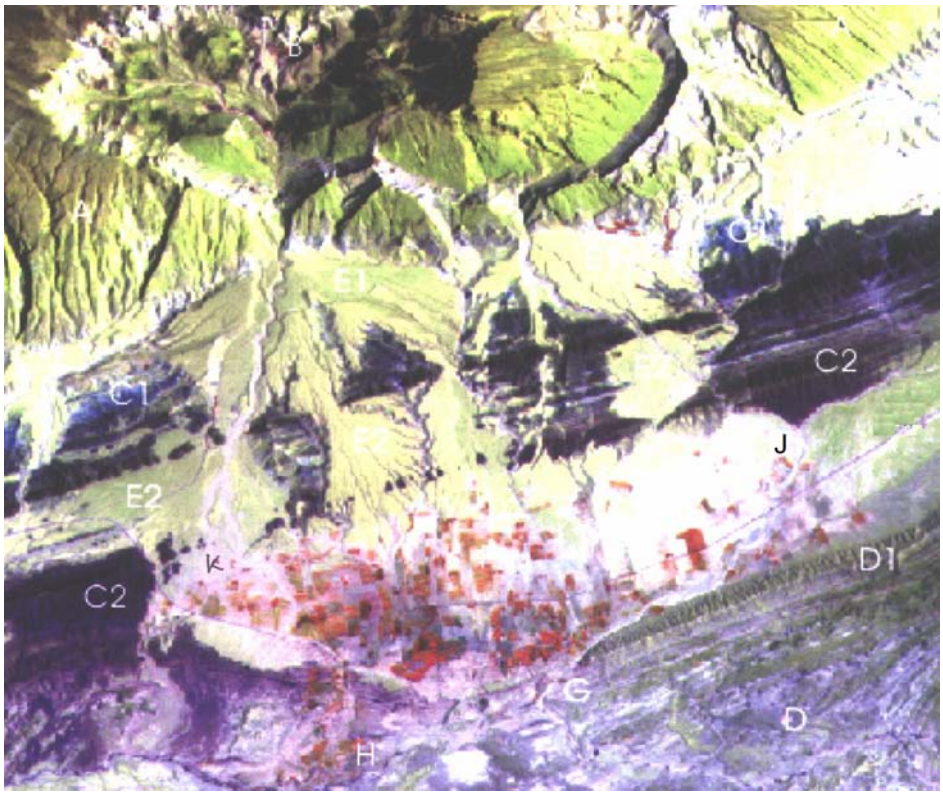

Figure 5.10 Bandar Abbas region, sub-zone I (false-colour 473)

Sub-zone II: Water quality problem

Near locality A1 in the northwest of the image in Figure 5.11, a dissected salt dome is present, intruded in the folded limestones and marls. As the image shows, an accumulation glacis or small bahada is found in between the salt dome and the main river (the Shuh). The deposits consist of gravel and pebbles or rock salt that extend to the main river, where they are carried further downstream. The area near A1 is therefore excluded because of high salinity (water quality exclusionary criterion), and similarly the areas where the main river feeds the groundwater in aquifer zones adjoining the river.

East of A2, bahada A3 could be regarded as a potential zone, because there are no rock salt outcrops in the catchment area and the aquifer materials are permeable. However, the catchments are small, and the rivers are unstable and lose nearly all of the water by natural recharge (exclusionary criteria). No agricultural lands are present, which indicate that there is no qanat which skims off the layer of sweet groundwater on top of brackish or saline groundwater with greater density. Since constructing a qanat is no longer feasible and tubewells are likely to draw up water of bad quality, area A3 has severe limitations.

Substantial infiltration takes place in the large and active fan of a river (B) with a catchment in the mountains in the southwest, maintaining the small croplands near the river in area B1, which make use of the thin layer of sweet water

at shallow depths near the river. Any artificial recharge scheme should be based on increasing the layer of sweet water, for the reasons given above. As can be seen, the river is unstable and occupies a wide bed, suggesting the type of scheme to be considered in the next screening level (the middle or semi-detailed level), namely a series of low dams (gabions) across the active riverbed and fan. Incidentally, the thickness of the alluvial deposits in the main river valley can be judged because of the presence of outcrops traversing the river near B3. In fact, these outcrops mark the upthrown side of a fault that continues along the border of the mountains in the southwest.

Neotectonic movements occur in the area because older alluvial fans have been uplifted, followed by dissection. Hence the thickness of the alluvial deposits depends on the subsidence along the downthrown side of the fault. That subsidence is probably not much, a few tens of metres at maximum, because a few kilometres upstream the main river flows on bedrock.

Sub-zone II:I Flood protection cum artificial recharge example

The area around C in Figure 5.11 shows an alluvial area that is bordered in the west by a series of uplifted and dissected fans with catchments in the adjoining mountains, where resistant rocks prevail. In the south, the alluvial aquifer is bordered by a large anticline consisting of impermeable and soft rocks (Neogene), accounting for the dissection and low relief. The northern boundary is formed by the dip slope of an a-symmetric anticline with low amplitude (cemented Bakhtiary conglomerates, Late Pliocene) and in the east by the saline Shur river. As can be noted on the image, across the Shur river to the east the thickness of the alluvial deposits is strongly reduced because outcrop patterns can be seen. The neotectonic history of the alluvial area can be interpreted from the series of uplifted fans. After each phase of uplift in the western part, the river shifted its alluvial fan to the central part of the depression, which indicates a subsidence basin and substantial aquifer thickness (over 100 m, as proven by geophysics and drilling).

In the eastern part of the alluvial areas, irrigated fields (by groundwater wells, not by qanats) can be observed, as well as a drainage pattern with dense vegetation in the valley bottom. The observations (assisted by information from the geological map) therefore indicate a promising zone for a floodwater spreading scheme (no exclusionary criteria have been met by the area). Water and sediments from the main river spread out over a wide zone and the recent/sub-recent river deposits form good infiltration areas because of their coarse nature, due to a mountain catchment, high flow velocities, and a relatively steep gradient in the alluvial area. Although the more recent alluvial deposits can be identified and mapped on aerial photographs and various combinations of colour-coded spectral bands of the TM image, they show up on the fourth principal component (PC) images, as shown in Figure 5.12. It should be remembered that within a full scene, the contents of the PC images depend on the sub-window selected.

Occasional floodwaters reach the irrigated lands and settlements, causing damage; hence a floodwater spreading scheme serves a dual purpose: recharge and flood damage mitigation. In addition, some 40 km south of the area shown is Bandar Abbas.

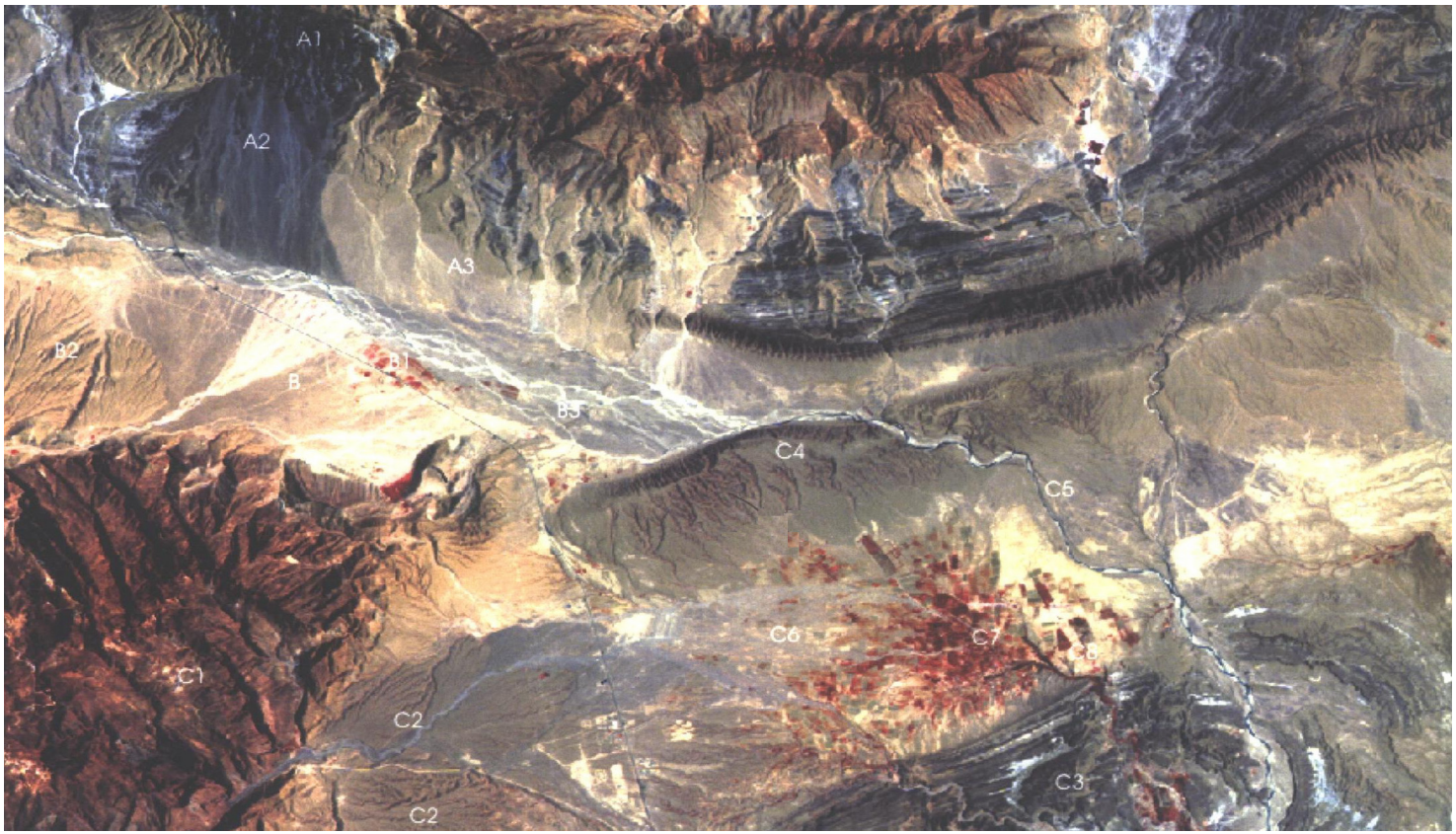

Figure 5.11 Bandar Abbas region, sub-zones II and III (false-colour TM 473)

The drinking water supply for this city is a problem, and this forms an additional argument for increasing the groundwater supply. Part of the flash flows are carried through the incised drainage in the eastern part out of the aquifer area, with an (very minor) outflow of groundwater, as can be noted by the presence of phreatophyte vegetation.

The above gives the interpretation aspects. In fact, a flood mitigation scheme was constructed that proved to be an important artificial recharge scheme as well. The scheme is located just upstream of observation well 5 in Figure 5.13a. It consists of a cascading series of basins that receive part of the flash flows of the river. The importance of the scheme and the recent gravel and sand deposits in the area where the floods have been spreading by natural causes is evident from the well hydrographs shown in Figure 5.13b. The hydrographs of all the wells near the recent alluvium (wells 1, 4, 5, 6, and 8) show substantial rises in the groundwater level after infiltration of flash flow water. In contrast, recharge outside the active alluvial area is small or absent, as shown by the hydrographs of the observation wells. The hydrograph of well 2 takes a special position because of the effect of the Shur river stages.

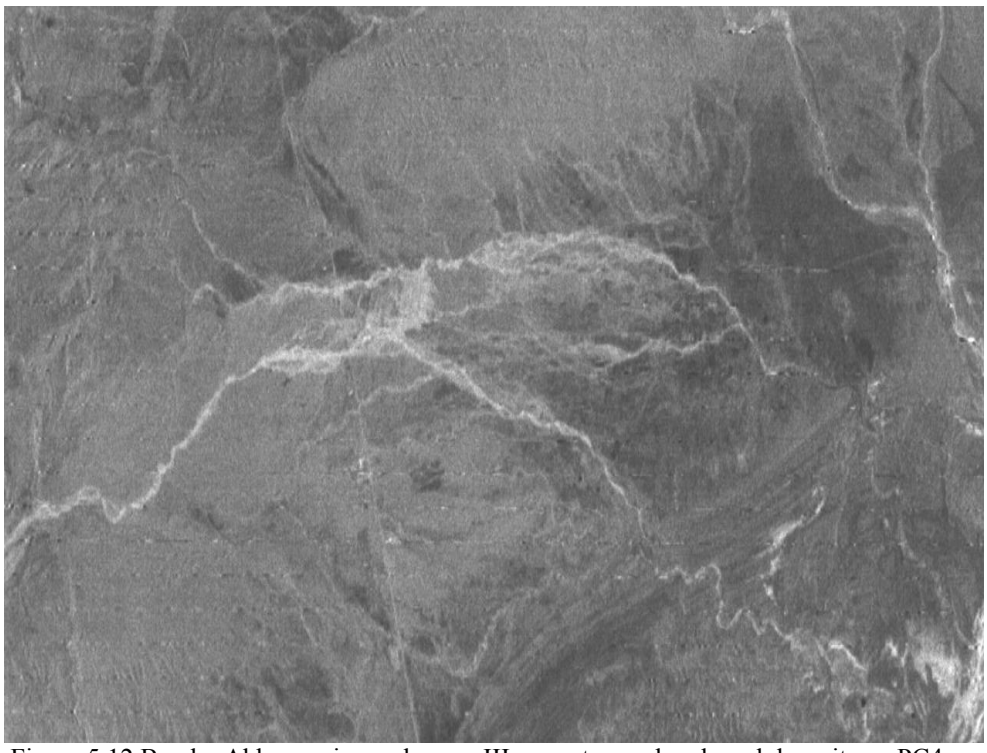

Figure 5.12 Bandar Abbas region, sub-zone III: recent gravel and sand deposits on PC4 image

(a)

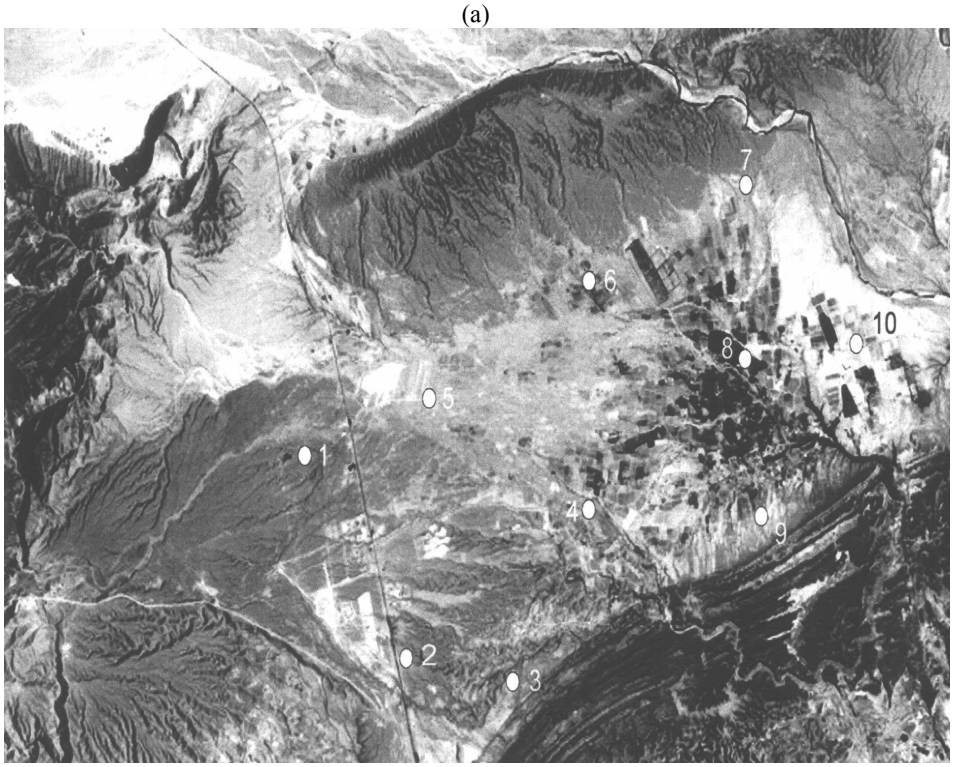

(b)

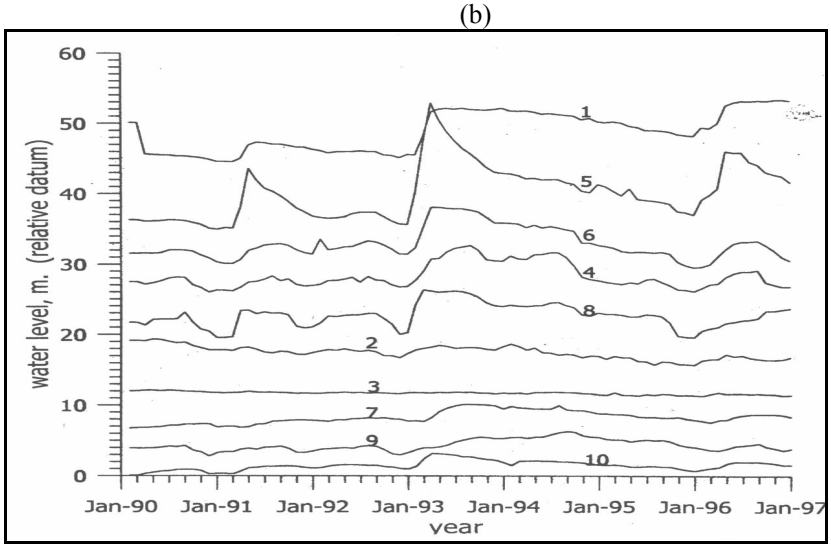

Figure 5.13 Sarkhon aquifer, Bandar Abbas region, zone III: (a) location of observation wells, (b) groundwater levels in observation wells

Sub-zone IV: Large fan, soil salinity hazard

Further eastwards in the alluvial zone, the image in Figure 5.14 shows folded rocks, with permeable and impermeable units, forming hills and mountains drained by larger and smaller rivers. It is important to note that the southern border is formed by a tectonic line (flexure and fault C1-C2). South of that line, impermeable rocks crop out. The presence of such rocks prohibits the flow of deeper groundwater from the higher area in the north to the lower area in the south across the flexure.

In the south are the low hills consisting of impermeable rocks of Tertiary age, the same as in sub-zone III. In between the northern and southern hills is a depression area with alluvial fans, bordered in the south by the line along E-C1-C2. North of E, the alluvial fill of the depression is likely to be of limited thickness because of uplift. The depression opens up to the east and probably the aquifer (fanglomerates) thickness increases.

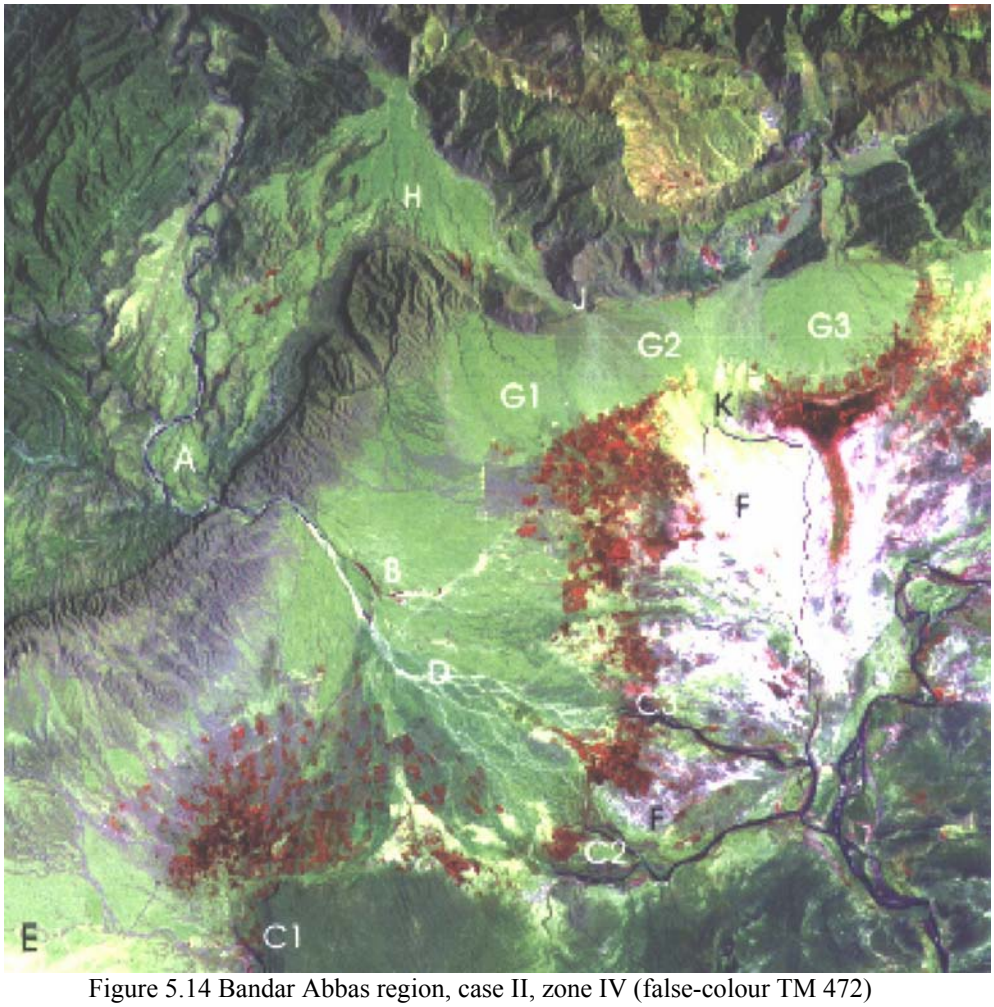

Figure 5.14 Bandar Abbas region, case II, zone IV (false-colour TM 472)

The image shows that the river has base flow until a little distance below the gap (A), where it enters a large alluvial fan in a channel that is incised a little. Near B, phreatophyte vegetation indicates the presence of shallow groundwater, possibly of a perched nature. The groundwater table is close to the surface on the lower part of the fan, and groundwater drains out in the rivers near C1, C2 and C3. The irrigated fields (red tones) derive their water from wells and qanats and are found in a fringe along the lower part of the fans, where the soils are suitable for agriculture because of their water holding capacity due to fine textures. The textures on the upper-middle part of the fan are coarser.

If a scheme is considered, the intake(s) should be upstream of D to avoid the unstable section of the river. No irrigated fields are found in the area with the many (shifting) river channels. Because of the size of the catchment, the flood discharges are substantial and only a small part of the floodwaters are retained on the fan by transmission loss, considering the total widths of the active channels in the lower part of the fan.

The typical sequence of textures associated with an alluvial fan of a large river with a coarse bedload, large discharge, and the presence of irrigable lands is in favour of a floodwater spreading scheme. However, starting south of C3 in the direction of F and beyond, saline soils are found belonging to the large saline coastal plain (see overview image, Figure 5.9). Since the groundwater table in large parts of the fan is shallow, increasing the groundwater level by artificial recharge could lead to salinization of the fields in the lower part of the fan because of capillary rises. Therefore, a recharge scheme should be accompanied by well fields withdrawing water at the same average rate as the recharge.

Sub-zone V: Aggradations and transmission loss by sheetwash

The areas of interest are the alluvial fans G1, G2 and G3 in Figure 5.14. Fan G1 has developed in a synclinal depression whose axis is perpendicular to the main tectonic line that separates the hills and mountains in the north and the alluvial fans and coastal plain deposits in the south. The fan deposits of G3 are older than those of G2. They were laid down at the time when the river formed a fan around H, which after uplift was dissected, and the present, active river shifted to the eastern margin. Since runoff from the dissected fan deposits around H is very low, little water will reach fan G1, and that water will infiltrate fully on the fan itself (low amount of floodwater and transmission loss exclusionary criteria). The small quantity of recharge water is reflected in the disappearance of irrigated fields in the southwestern part of fan G3. Hence there is no scope for a scheme.

The active alluvial fan G2 has a sizeable catchment, while the overview in Figure 5.9 shows relatively dense vegetation on the mountains forming the northeastern part of the catchment, indicating higher rainfall. However, the fast surface runoff is subdued because a large part of the catchment consists of karstic limestones. The high infiltration causes dry season flow at the place where the river leaves the mountain, but that flow infiltrates the fanglomerates around H. The subsurface gradient of the older fan deposits is likely to be steeper to the southwest than to the southeast because of the deep incision of the river near A and the narrow gap in the rocks near J. Little groundwater will flow through the gap (J) and the

recharge supporting the irrigated areas northwest of F must take place by infiltration of flash flows over the fan itself. It is interesting to note that the water spreads out over a wide area downstream of J, as illustrated in Figure 5.15. This figure shows TM band 1, with appropriate 'stretching' of grey tones to highlight the difference between the older, non-active fan parts (O) and the active parts (R) where floodwaters spread out, accompanied by the deposition of sediment consisting of sands, pebbles and boulders near the apex and sand mixtures in the remaining part of the fan.

The sharp transition between the fan and the coastal plain deposits is also a topographical break in slope. The area near K has few or no irrigated fields because of the concavity in between two fans, forming a low topography with saline coastal sediments close to the surface, and the occurrence of episodic flood runoff from the catchment of fan G3. The strong aggradations of the valley upstream of the fan can be noted. The base flow from the mountains infiltrates the coarse alluvial fill deposits but flows below the surface over the contact with the impermeable shales of the dark toned rocks (L). Part of that water emerges as perennial flow at the surface near K (Figure 5.15). Along the southern fringe of alluvial fan G3, there is a waterlogged area that is of ecological value.

The arguments for giving a lower priority to fans G2 and G3 for a scheme are the strong transmission losses and the fact that qanat systems are in operation that do not pose a threat of salinity hazard, as would be the case if well irrigation were introduced.

Sub-zone VI: Area with large fine-grained sediment load, salinity hazard, unstable rivers

The image in Figure 5.16 shows a narrow tectonic depression that is bordered by faults in the north and northeast and by a large anticlinal structure in the south. The image is a false-colour composite of TM 473, and green vegetation is depicted in red tones. Much of the catchment geology is dominated by argillaceous suites of rocks, partly shown in the overview image in Figure 5.9. For this reason, the sediment load of the river has a much higher proportion of clay and silt than those of the rivers discussed earlier. The bedload consists of a mixture of sands and coarser fractions, but has a high proportion of shale fragments. The general fine-grained nature of the fanglomerates is reflected in the gentle gradient of the fan. Aggradation still takes place, starting at the floodplain upstream of the fan and continuing till the downstream part (R), causing instability in plan.

The depth of the alluvial deposits is considerable, but the overall permeability of the aquifer is much less than in the previous cases on account of the richness in clay. Transmission losses on the alluvial fan are relatively low, which explains why the rivers on the fan do not decrease much in width. Sandy lenses do occur throughout the fan deposit, and the groundwater table is not deep in the middle and lower parts of the fan. For this reason, a considerable amount of groundwater emerges in the lower part of the aquifer in the southwest (E) and in the southeast (shown in the overview image, Figure 5.9), caused by the gradual decrease in permeability towards the lower fan. The shallow groundwater table in the lower part has caused waterlogging and salinization in various stages (D).

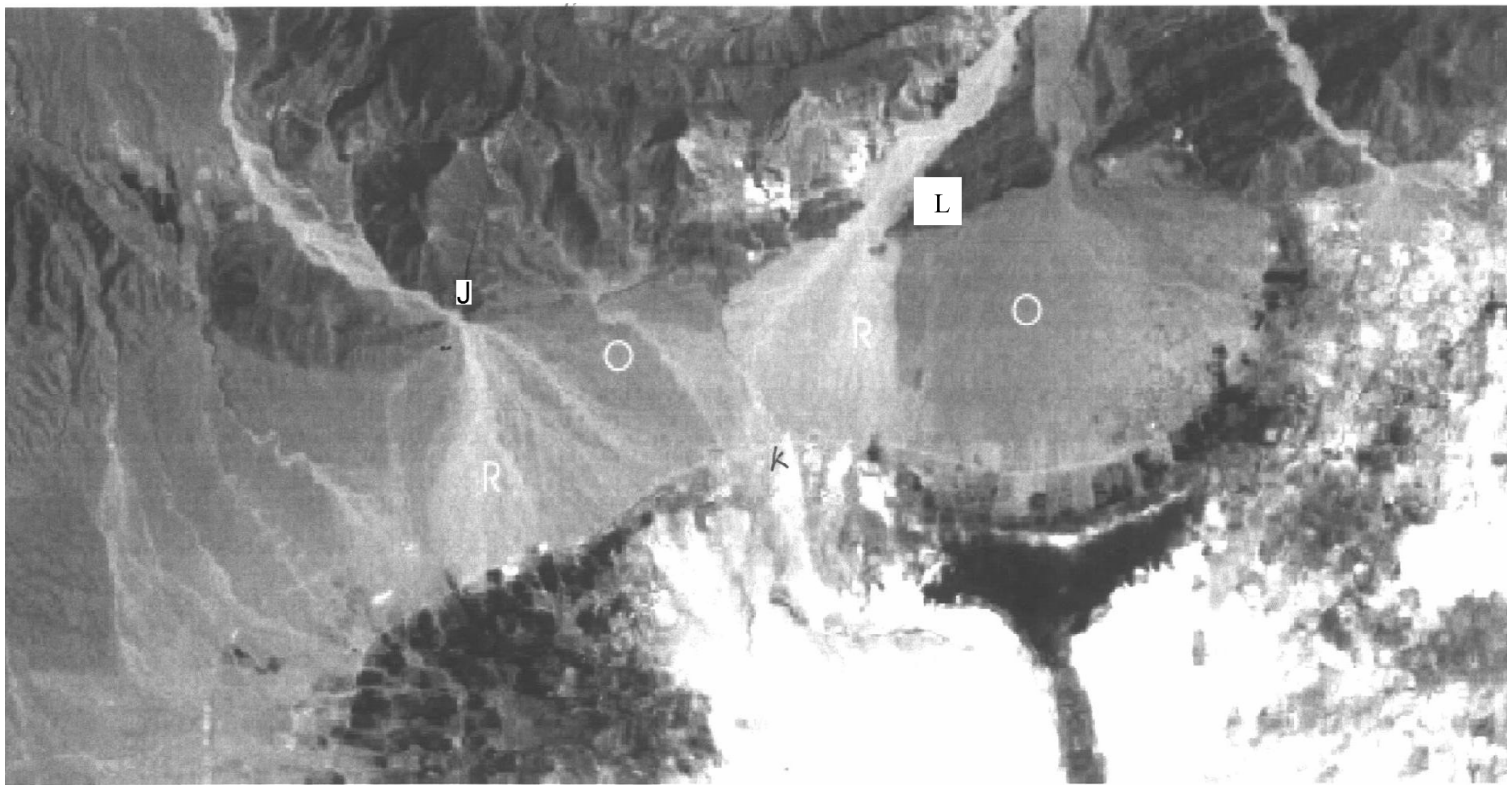

Figure 5.15 Bandar Abbas region, zone V: TM band 1 (stretched) to show active sheetwash traces (transmission loss) in fans G1, G2 and G3 of Figure 5.14

The upper part of the fan is under rangeland vegetation. Along the contact with folded rocks in the north is a narrow fringe with irrigated fields (H) that derive their water from springs and base flow of the rivers in the mountains, where limestone is present. In the middle part of the fan, fields are irrigated by groundwater (C). The fields with a good crop response are not contiguous, as they are separated by fields with poor crop responses and bare patches that point to either salinity or poor groundwater conditions, or both.

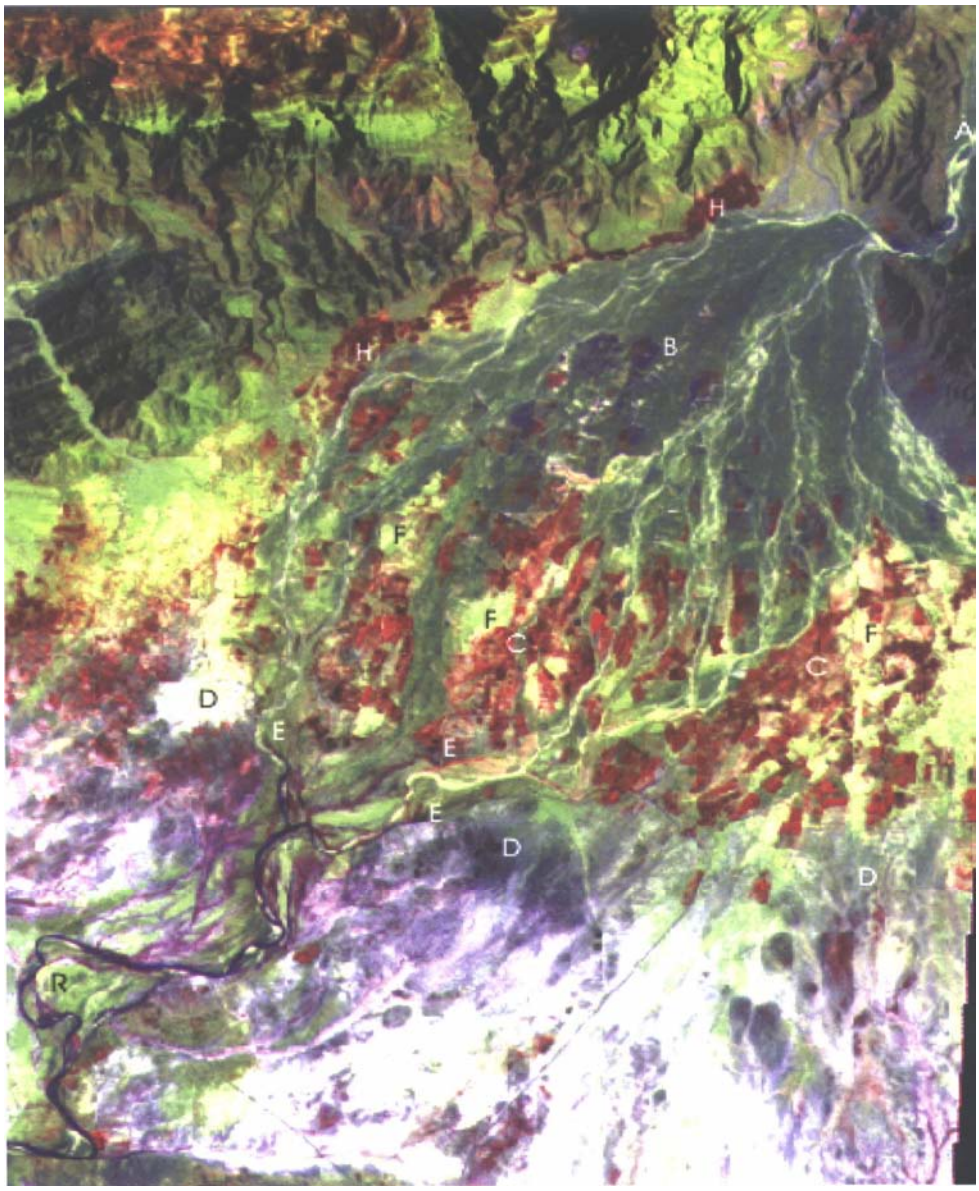

Figure 5.16 Bandar Abbas region, zone VI (false-colour TM 472)

Some of the criteria in favour of a scheme are met: the presence of a large river, much water leaving the area, rangelands in the upper part of the alluvial fan, the presence of groundwater-irrigated agriculture. However, the instability of the rivers; the high sediment load, both bedload and suspended load; poor aquifer properties because of deposits rich in clay in the upper part of the fan; and a salinity hazard in the lower part of the fan; these are matters of concern. Because of the large catchment of the river, hydraulic works to control flows at the apex of the fan are a major investment because of the very large floods.

Sub-zone VII: Variation in sediment load

This sub-zone (Figure 5.17) has great similarity as regards geological and geomorphological setting to sub-zone I. The mountains in the north (A), with hard sandstones, conglomerates, limestone and interbedded rocks or less resistance and permeability, are in steep contact with the steeply dipping impermeable rocks of formation B. In the south is a large anticline of the impermeable Tertiary rocks (C1) that dip gently (C2) below the younger alluvial deposits. Alluvial fans overlying B have been uplifted along the east-west fault D1-D2, and continue in the direction of D4 after an offset by fault D2-D5.

The alluvial depression and aquifer is bordered in the west by outcrops (E) and the deposits of a river (F) with brackish water, and in the east by outcrops of formation C. The aquifer of the depression is recharged by transmission losses of the active fans of the northern catchments and to a lesser extent by the runoff from the low hills in the south. In the east, the phreatophyte vegetation in the small river (G) bears witness to the outflow of groundwater from the eastern part of the depression and indicates shallow groundwater in the lowest part of the depression. The aquifer drains out to the west to the saline fluvial deposits (F), and a broad groundwater divide is located near H. Fields irrigated by groundwater (red tones) occupy a large part of the lower alluvial depression, but there is some scope for expansion of irrigation in some fields that are fallow.

The westernmost part of the alluvial area suffers from much deposition of sands (I1 and I2) from the northern catchments, owing to the occurrence of mass wasting and gulling. The large bedload and the large transmission loss (exclusionary criteria) make that area less attractive for a scheme. Fan J could be considered for a scheme because of the size of the catchment, permeable conditions in the rangelands of the fan, flooding by sheetwash, and sediment deposition in the irrigated area. The same is valid for the area around K, where the sedimentation problem is less, but also the amount of water, because catchments are smaller. However, field data on soils, hydrochemistry and irrigation potential are needed for a proper evaluation of the western part of the zone.

Evaluation

For large schemes sub-zone III is the best. Apart from a relatively large volume of runoff and good infiltration properties for an exploited aquifer (irrigation and drinking water supply), an additional argument is the mitigation of the flood hazard. Sub-zone IV has much inflow and is well watered considering the base flow leaving

the area. Expansion of irrigation by wells in the future may require artificial recharge by floodwater spreading, considering the salinity hazard.

For small schemes the areas I-J and II-B are the most suitable, with area I-K as a second-best option. The general results of the evaluation for all the discussed areas in case II and the exclusionary criterion/criteria for each excluded area are shown in Table 5.2.

5.5 Varamin

This zone southeast of Tehran city contains a large fan of the Jaj Rud river, which has a very large catchment extending into the Alborz Mountains (labelled F in Figure 5.18) and a series of coalescing local fans (labelled A to E). The coarse-grained nature of the deposits in the upper fan is reflected in the absence of cultivation. The remainder of the fan is occupied by fields that are irrigated by groundwater and partly by diverted base flow and sewage water from Tehran at the apex of the fan. There are two major reservoirs in the Jajrood catchment that capture the runoff from the upper parts only. Flood runoff from the lower part of the catchment can be used for artificial recharge. In fact, such a scheme is in operation – the Sorkhesar scheme – and has been described in Chapter 4.

Area E has a very small catchment and most of the runoff disappears in the fan by transmission loss (exclusionary criterion). Areas A to D have catchments of a size to generate sufficient runoff, and the mixed nature of the fanglomerates reflect the catchment lithology, which consists mainly of semi-consolidated Quaternary conglomerates interbedded with sands and clays, while catchments A and B have Tertiary mixtures of sandstones, siltstones, marl and gypsum in their head waters and in B the uppermost part is composed of hard tuffs. The upper parts of the fans have gradients up to 4%, reflecting the presence of considerable coarse deposits and permeable conditions.

The infrastructure of the lower parts of the fans, in the form of settlements, roads and irrigated fields, suffers from flood damage, particularly in areas A and D, as can also be judged from the extension of the active channels. Hence, groundwater recharge and flood damage mitigation are arguments in favour of floodwater spreading schemes, while rangeland is found on most of the infiltration area. Considering the catchment lithology and relief, the sediment supply, including the suspended load, will be high but not excessive.

These considerations make areas A to D worthy of further investigation at semi-detailed level in order to arrive at the most attractive area and site. This investigation is carried out in the next chapter.

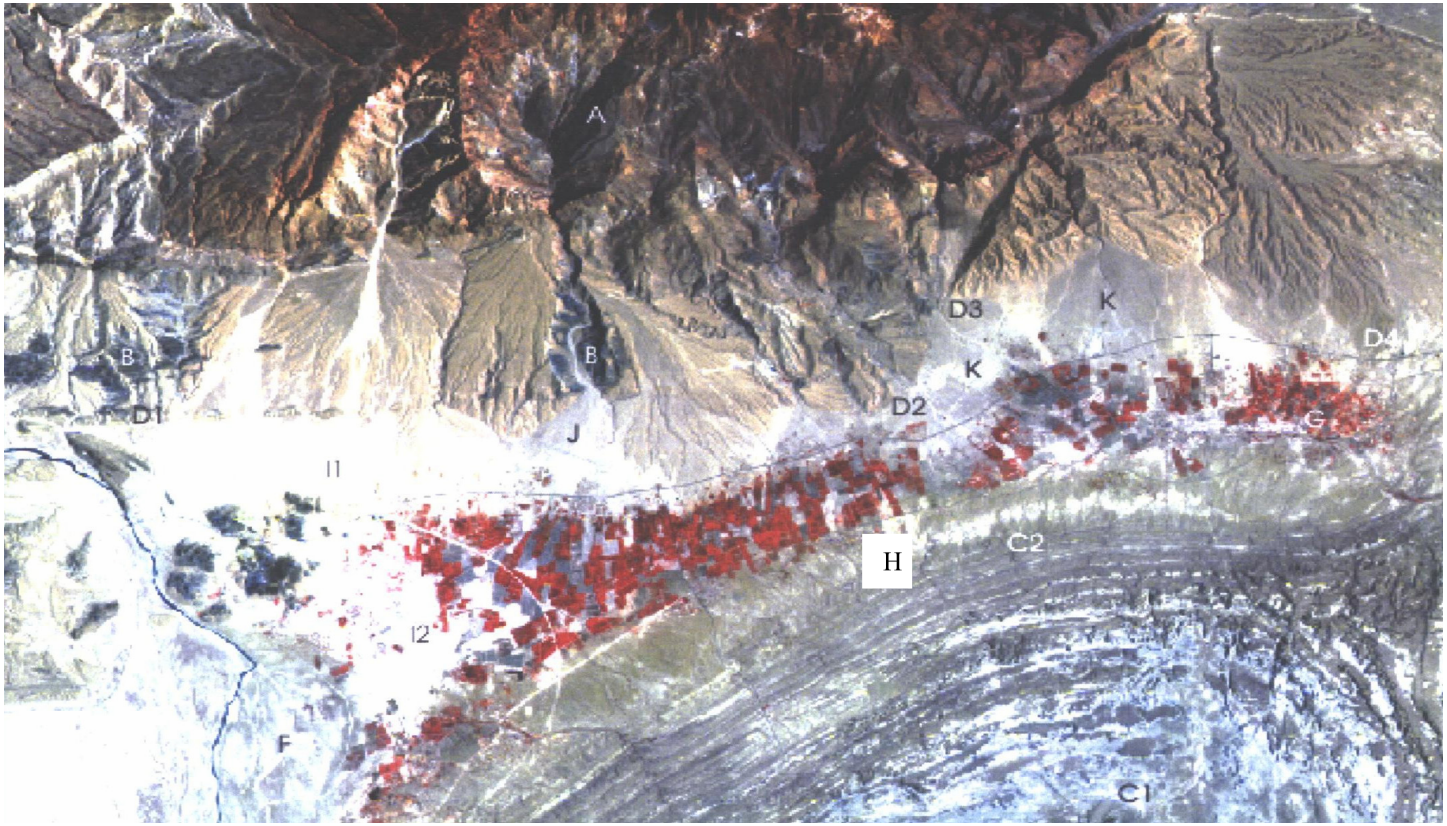

Figure 5.17 Bandar Abbas region, zone VII (false-colour TM 472)

Table 5.2 Evaluation results for the studied areas, Bandar Abbas region

Zone Or Sub Zone	Areas					
I	**J**		**K**			
	Excluded Area	Potential Area	Excluded Area	Potential Area		
	Exclusionary Criteria	+	Exclusionary Criteria	+		
II	**A1**		A3 (Bahada)		B	
	Excluded Area	Potential Area	Excluded Area	Potential Area	Excluded Area	Potential Area
	Exclusionary Criteria	-	Exclusionary Criteria	-	Exclusionary Criteria	+
	Water Quality		**Runoff or flood water availability & Transmission loss & Water demand**			
III	Area around C					
	Excluded Area	Potential Area				
	Exclusionary Criteria	+				
IV	D					
	Excluded Area	Potential Area				
	Exclusionary Criteria	+ The recharge scheme should be accompanied by well fields withdrawing water at the same average rate as the recharge.				
V	G1		G2		G3	
	Excluded Area	Potential Area	Excluded Area	Potential Area	Excluded Area	Potential Area
	Exclusionary Criteria	-	Exclusionary Criteria		Exclusionary Criteria	
	Transmission loss & Runoff or flood water availability		**Transmission loss & Soil salinity**		**Transmission loss & Soil salinity**	
VI	Alluvial fan area					
	Excluded Area	Potential Area				
	Exclusionary Criteria	-				
	Sediment, amount and type & Presence of aquifer and its properties (Transmissivity and Permeability) & Soil salinity					
VII	I1,I2		J		K	
	Excluded Area	Potential Area	Excluded Area	Potential Area	Excluded Area	Potential Area
	Exclusionary Criteria		Exclusionary Criteria	+ Field data on soils, hydrochemistry and irrigation potential is needed	Exclusionary Criteria	+
	Sediment, amount and type & Transmission loss					

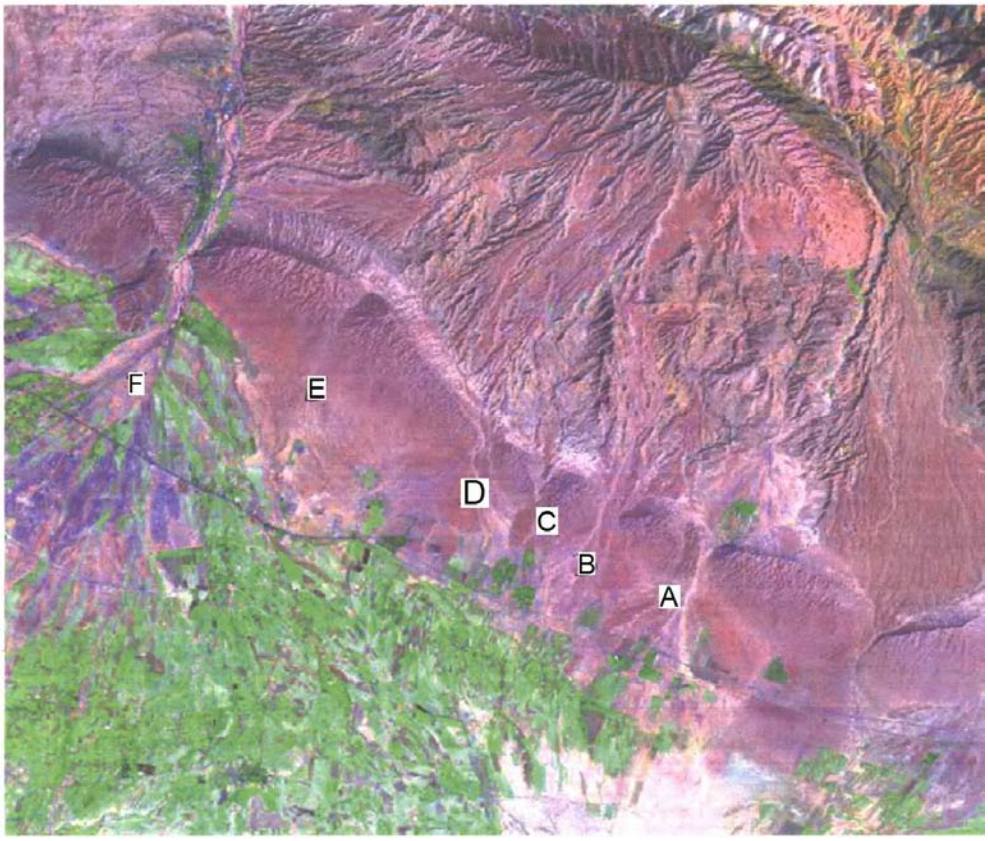

Figure 5.18 Varamin Plain zone (false-colour TM 742)

5.6 Conclusions

The image interpretation was greatly facilitated by field visits to most of the areas and by the presence of hydrogeological data in a few cases. This allowed the accumulation of empirical knowledge for establishing the interrelationships of features on the images and for extrapolation purposes. The features should not be considered in isolation during the interpretation. By placing them in an overall context of geology and geomorphology, most of the relevant aspects could be related to one another, such as catchment permeability and relative runoff, main aquifer properties, transmission loss and salinity hazard.

Exclusionary factors in the examples shown are the presence of saline river water, excessive sediment deposition, the small size of catchment – as a proxy for runoff – and large transmission loss. In addition, land use and infrastructure can be rapidly assessed using the images. The interpretation also leads to formulating some required field observations before a final evaluation can be made at the screening level.

The above examples highlight that zoning based on the interpretation of remote sensing images may lead to the identification of potentially suitable areas

and the exclusion of areas with little or no promise. In each of the three suitable zones, a relative assessment has been made of the suitable areas, but no comparison between zones, because the decision on schemes is a regional affair. In Chapter 6, which deals with the method for selecting the suitable area within a zone at semi-detailed level using MCE, one of the three cases or zones discussed is selected, namely the Varamin zone.

CHAPTER 6
Area(s) Selection for Floodwater Spreading

6.1 Introduction

The suitable area selection methodology (Chapter 2) is implemented and evaluated for Varamin Plain. At the zone selection (middle) scale, several potentially suitable areas are identified. The question now is how to find the most suitable area. The Aster[5] image of Varamin Plain is given in Figure 6.1. Polygon maps of the four potential floodwater spreading areas – Chandab, Koliac, Latshor and Siah Cheshmeh – are shown in Figure 6.2. The geographical location and different characteristics of Varamin Plain have already been explained in Chapter 4.

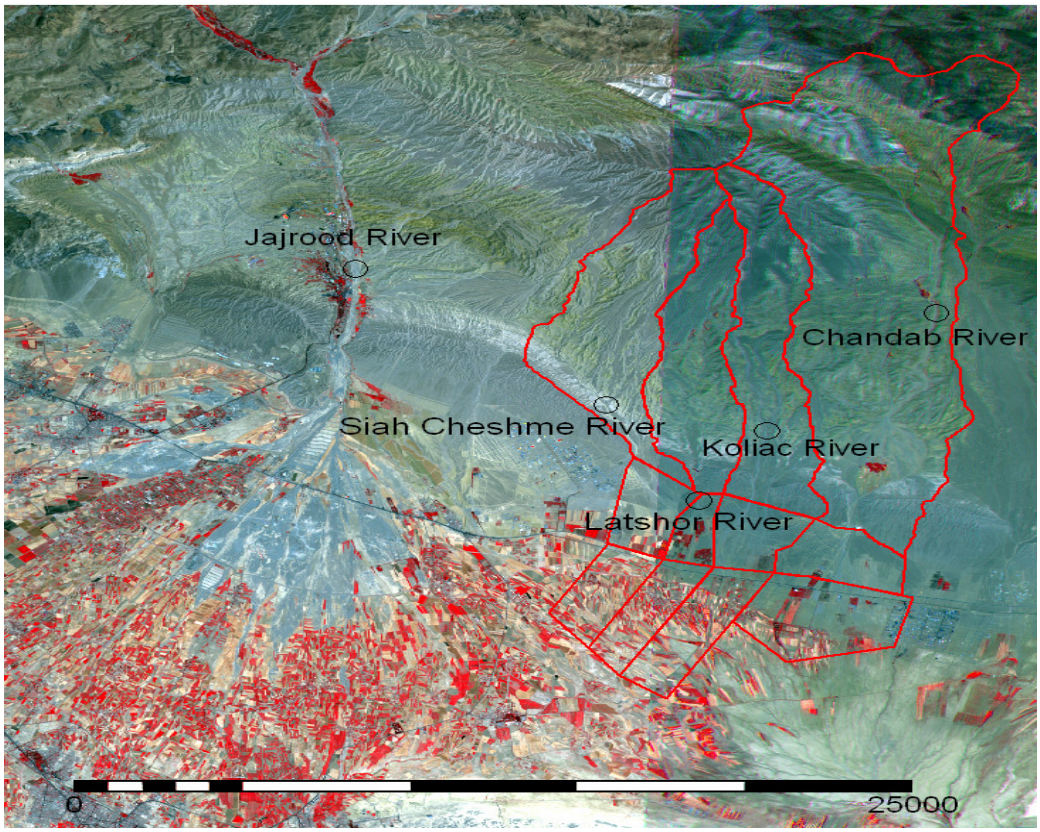

Figure 6.1 Aster image (colour composite, bands 321) of the study zone Varamin Plain, central Iran

[5]Advanced Spaceborne Thermal Emission and Reflection Radiometer is an imaging instrument flying on Terra, a satellite launched in December 1999 as part of NASA's Earth Observing System (EOS).

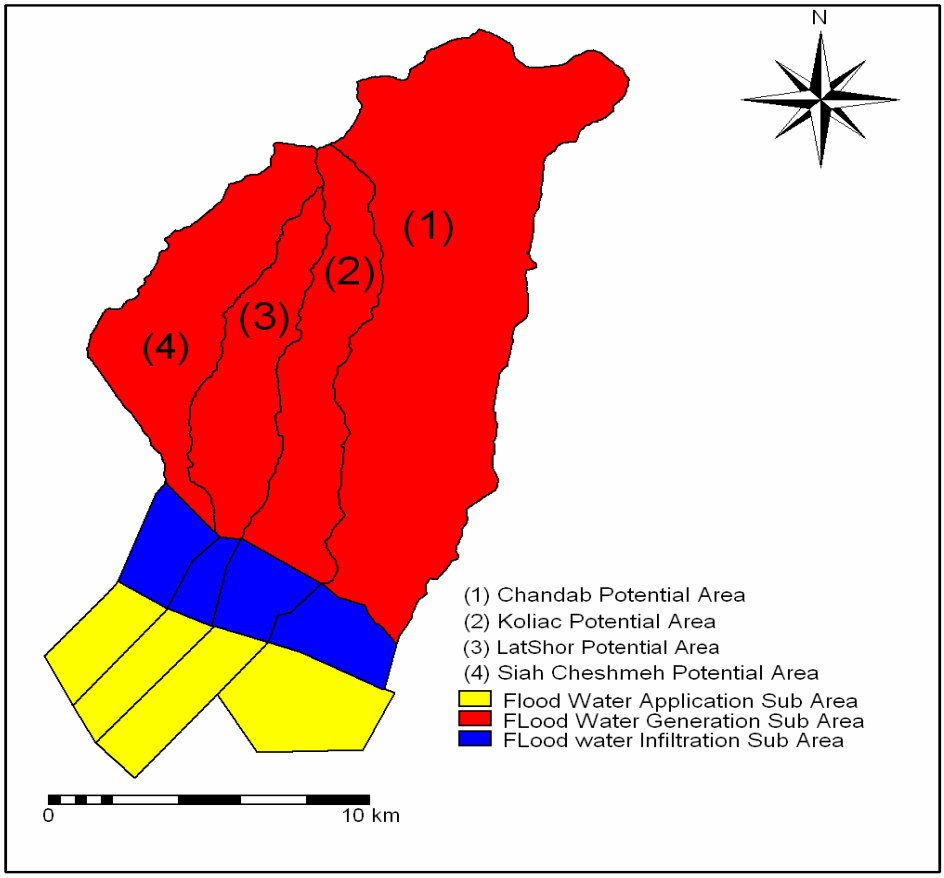

Figure 6.2 Polygon maps of the four potential floodwater spreading areas Chandab, Koliac, Latshor and Siah Cheshmeh in the Varamin Plain

A suitable area for floodwater spreading is selected on the basis of four main criteria, as indicated in Figure 6.3.

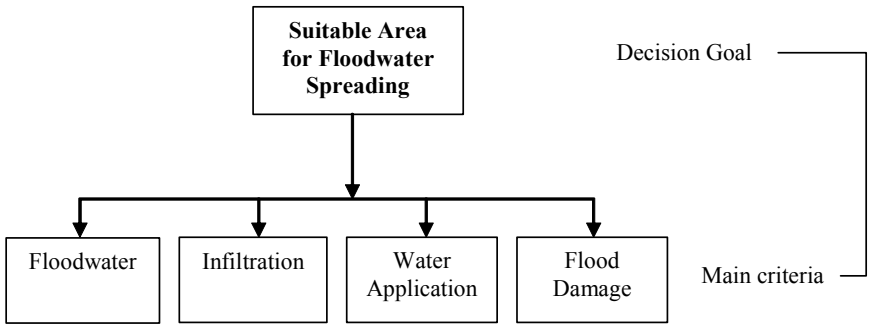

Figure 6.3 Tree of main criteria for selecting a suitable floodwater spreading area

Selecting the area with the best overall suitability is done by a chain of bottom-up steps:

- **Step 1**
  For each of the distinguished main indicators and sub-indicators, value classes are specified and their corresponding relative importance values determined.
- **Step 2**
  Using base maps (obtained through RS) for each potential area, a suitability map for each of the main indicators is made using a GIS.
- **Step 3**
  Suitability maps for each sub-criterion are generated (e.g. Figure 6.4 for the sub-criterion water). These maps are assembled (weighted combination) with the help of the maps derived in step 2 of the main indicators.The importance of the various main indicators is determined using the AHP (analytical hierarchical processes) pairwise comparison (see Chapter 2).
- **Step 4**
  The different maps for the sub-criteria are put together (weighted combination) in a suitability map of the main criterion (e.g. Figure 6.6 is for the main criterion floodwater). The importance of the various sub-criteria is determined using the AHP pairwise comparison (see Chapter 2). Map weighting and combination are performed using the SMCE-GIS module of ILWIS GIS software.
- **Step 5**
  Finally, the overall suitability of each area is estimated using weighted combinations (also called scenarios) of partial suitabilities (e.g. Figures 6.12 to 6.16). Based on the opinion of the decision makers/experts/stakeholders, different relative importance (RI) values will be assigned to the main four decision criteria. As a result five scenarios (one scenario based on equal preference of all the main criteria and four scenarios based on absolute preference of one of the main criteria) will be developed and evaluated.

The classification and preference weights for some of the indicators and sub-criteria (Saaty's linguistic measures of preference, 1980) have been adapted from literature, such as the MPSIAC (Pacific Southwestern Inter-Agency Committee, 1968). For the remaining indicators and sub-criteria, preference weights are based on interviews with staff of the Soil Conservation and Watershed Management Research Institute (SCWMRI), who have been involved in about 40 floodwater spreading projects all around Iran. The results reflect expert opinion, although some modifications to expert opinion have been made based on interviews with local staff, modelling, personal field observations and experience.

6.2 Main criterion floodwater

The suitability assessment of floodwater generation is determined by suitability assessment of the sub-criteria water and sediment (see Figure 6.4).

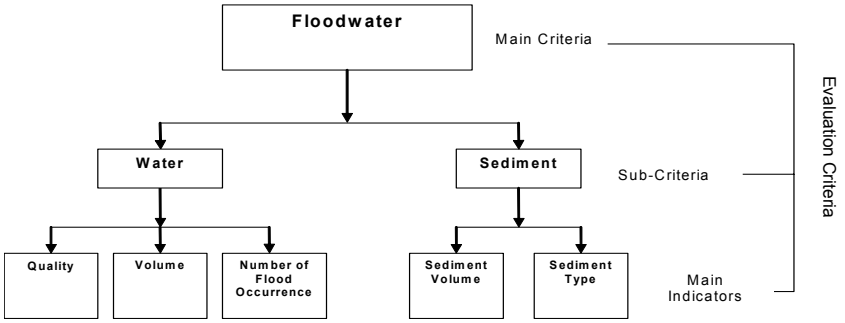

Figure 6.4 Decision tree for the main criterion floodwater, showing sub-criteria and main indicators

6.2.1 Sub-criterion water

For each of the main indicators distinguished, value classes are specified and corresponding relative importance values determined.

Main indicator: water volume

Classes of flood volume were distributed in a linear fashion, since larger volumes of inflow will result in larger amounts of recharge water in a more or less linear manner (Chapter 3). The minimum class of <50,000 m3 y-1 (Table 6.1) corresponds to the guidelines for water harvesting in Iran, which state that such small amounts should be used for drinking water for small settlements only. The maximum value in the table is based on the runoff estimate of the largest of the four catchments under consideration, using the SCS method (Soil Conservation Service, 1972). Using the daily rainfall record for 25 years available for Mamloo station, runoff curve numbers were assigned to the various geological units, each of which has particular relief characteristics. No area-depth correction for the catchment rainfall was made because the reduction factor depends on the duration of the rainfall, which was unknown. It is therefore likely that the runoff volume estimate for the larger catchment (No.1 of Figure 6.2) is on the high side compared with those for the three other catchments, which are smaller in size. The runoff values thus obtained were compared with existing runoff records for short periods, so as to adjust the curve number value initially adopted.

The linguistic measures of preference (LMP) of Saaty (1980) shown in the table reflect the opinion of the Iranian experts consulted. Here, it may be useful to remember that the LMPs indicate how much preference is given to a class in the pairwise comparison. For example, in Table 6.1 the score of 9 for the class 'Very Low' indicates that water volume in the quality class 'Very High' is nine times preferred to water in the class 'Very Low', and so on. The calculated 'Relative Importance' gives the suitability of each class with respect to others.

Main indicator: number of floods

It was found in Chapter 3 that the number of flood occurrences influences infiltration efficiency. Classes shown in Table 6.2 are based on the estimated number of flood occurrences, making use of the SCS method, the incomplete available short-term records (six to seven years; Khalilpour et al., 2003), and local interviews.

Table 6.1 Main indicator water volume: classes and their relative importance

Classes	Very High	High	Moderate	Low	Very Low	Geometric Mean	Relative Importance
Very High (>5,000,000 m^3 y^{-1})	1	3	5	7	9	3.9363	0.5101
High (3,000,000 to 5,000,000 m^3 y^{-1})	1/3	1	3	5	7	2.036	0.2638
Moderate (500,000 to 3,000,000 m^3 y^{-1})	1/5	1/3	1	3	5	1	0.1296
Low (50,000 to 500,000 m^3 y^{-1})	1/7	1/5	1/3	1	3	0.4911	0.0636
Very Low (<50,000 m^3 y^{-1})	1/9	1/7	1/5	1/3	1	0.2540	0.0329

Table 6.2 Main indicator number of floods: classes and their relative importance

Classes	>5 times	3 to 5 times	1 to 2 times	Geometric Mean	Relative Importance
>5 times	1	5	7	3.2711	0.7147
3 to 5 times	1/5	1	5	1	0.2185
1 to 2 times	1/7	1/5	1	0.3057	0.0668

Main indicator: water quality

Because of scarcity of information on the chemical water quality and its effects in floodwater spreading schemes, only three relative classes were considered: 'Good', 'Moderate' and 'Just Acceptable' (Table 6.3). Very saline water was not considered because it is an exclusionary factor in area selection at reconnaissance scale. The chemical quality of floodwater was assessed qualitatively from the geological formations in the catchments and the published information on the effects of geological formations on surface water quality (Peyrovan, 1995).

Table 6.3 Main indicator water quality: classes and their relative importance

Classes	Good	Moderate	Just Acceptable	Geometric Mean	Relative Importance
Good	1	5	9	3.5569	0.7352
Moderate	1/5	1	5	1	0.2067
Just Acceptable	1/9	1/5	1	0.2811	0.0581

Sub-criterion water: suitability map

The suitability maps of the three main indicators of the sub-criterion water are shown in Figure 6.5. Comparison of the relative importance of these main indicators is given in Table 6.4 and is based on expert opinion. The weighted combination of the three indicators (using the SMCE module of ILWIS) generates suitability maps of the sub-criterion water for Chandab, Koliac, Latshor and Siah Cheshmeh, as shown in Figure 6.5.

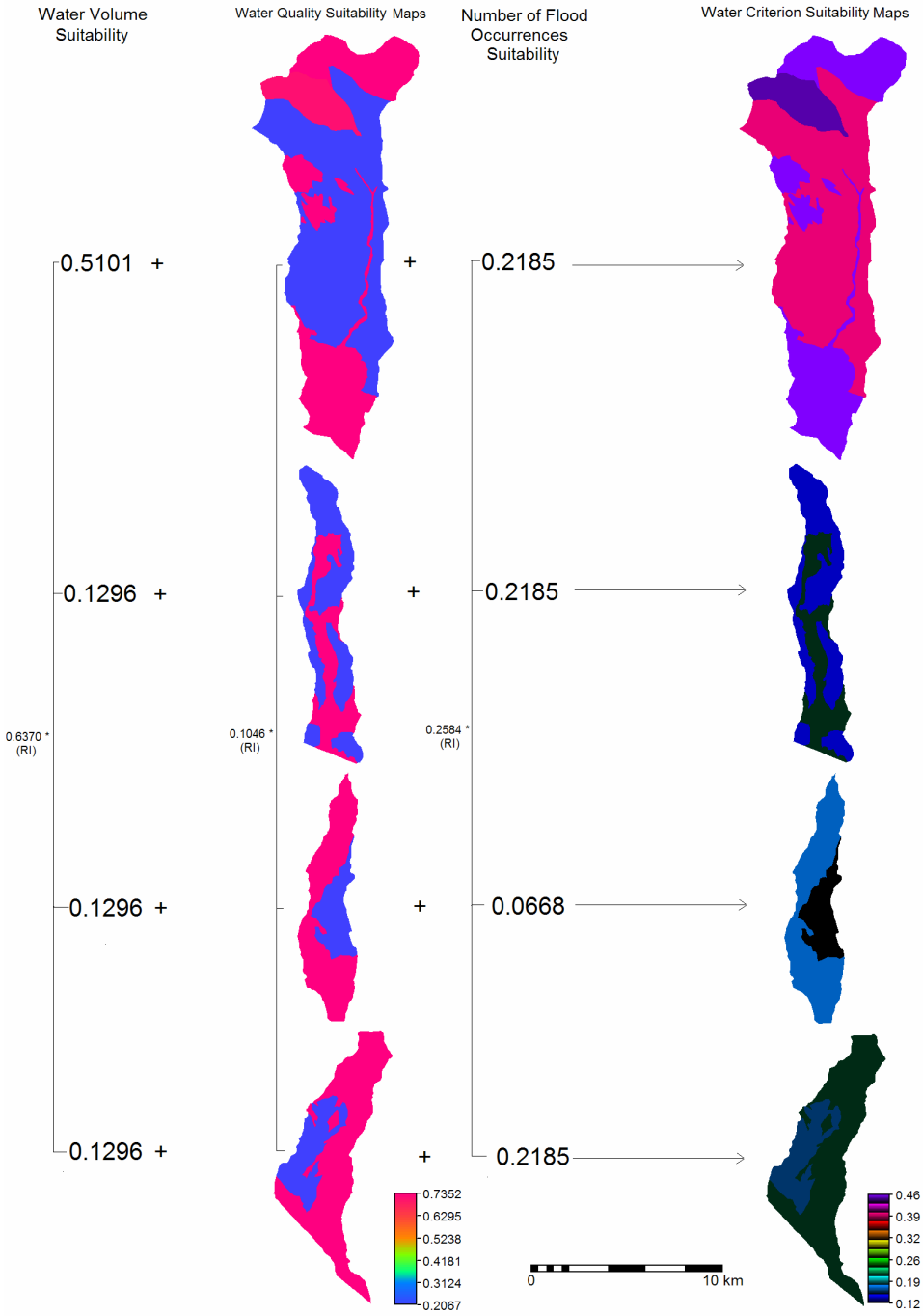

Figure 6.5 Suitability maps for the four potential floodwater spreading areas for the sub-criterion water. The map at the right side is the weighted combination of the three main indicators water volume, number of floods, and water quality.

Table 6.4 Sub-criterion water: main indicators and their relative importance

Main indicators	Water Volume	Number of Flood Occurrences	Water Quality	Geometric Mean	Relative Importance
Water Volume	1	3	5	2.4662	0.6370
Number of Flood Occurrences	1/3	1	3	1	0.2584
Water Quality	1/5	1/3	1	0.4055	0.1046

6.2.2 Sub-criterion sediment

For each of the distinguished main indicators, value classes are specified and corresponding relative importance values determined.

Main indicator: sediment volume

To obtain the relative importance of the sediment volume, sediment yield scores of the modified PSIAC method (Pacific Southwestern Interagency Committee; USDA, 1968) were used, grouped in five relative classes, from very low to very high, and the LMPs were assigned as shown in Table 6.5. The LMP values for the classes 'High' and 'Very High' do not differ much, showing that, according to expert opinion, water with little sediment was much preferred to any large amount of sediment, and the same is expressed in the column 'Relative Importance'.

The sediment yield scores of the four potential areas under consideration were determined by first differentiating terrain mapping units (TMU; Meijerink et al., 1988) on the basis of relief and lithology in the catchments considered. For each terrain unit, the nine scores of the MPSIAC method were determined and aggregated. The results were adjusted somewhat by considering results from other methods, such as sediment mineralogy and the universal soil loss equation (USLE; Wischmeier and Smith, 1978).

Table 6.5 Main indicator sediment volume: classes and their relative importance

Sediment Yield Score Classes	Very Low (0 to 25)	Low (25 to 50)	Moderate (50 to 75)	High (75 to 100)	Very High (>100)	Geometric Mean	Relative Importance
Very Low (0 to 25)	1	3	5	8	9	4.0428	0.5172
Low (25 to 50)	1/3	1	3	6	7	2.1118	0.2702
Moderate (50 to 75)	1/5	1/3	1	3	4	0.9564	0.1224
High (75 to 100)	1/8	1/6	1/3	1	2	0.4251	0.0544
Very High (>100)	1/9	1/8	1/4	1/2	1	0.2805	0.0359

Main indicator: sediment type

The two sub-indicators for this main indicator are the texture of the sediment and the sensibility of the area for erosion. For the latter, the K-factor of the USLE is adopted. The simulation results described in Chapter 3, the experiences in various schemes in Iran with sediment of different textures, and observations in the floodwater spreading scheme in the Varamin zone led to the assignment of LMP values as shown in Table 6.6. The relative importance shown in the table reflects that sands and gravels that do not limit the infiltration efficiency are much more suitable than clays and silts.

The texture classes in the catchments were determined using the geological units and data from Khosheghbal (1999). For the K-factor, the nomograph was used for the soils associated with the geological formations, and five linear classes were used and LMP values assigned (Table 6.7).

Suitability maps of the main indicator sediment type were made for the four areas by combining the two sub-indicators according to LMP values shown in Table 6.8. Here, texture carried more weight than the erodibility factor as regards relative importance.

Table 6.6 Sub-indicator texture: classes and their relative importance

Classes	Very Light	Light	Moderate	Heavy	Very Heavy	Geometric Mean	Relative Importance
Very Light	1	3	5	7	9	3.9363	0.4914
Light	1/3	1	4	6	8	2.2974	0.2868
Moderate	1/5	1/4	1	5	7	1.1184	0.1396
Heavy	1/7	1/6	1/5	1	3	0.4275	0.0534
Very Heavy	1/9	1/8	1/7	1/3	1	0.2313	0.0289

Table 6.7 Sub-indicator soil erodibility: classes and their relative importance

Classes	0 to 0.1 Very Low	0.1 to 0.2 Low	0.2 to 0.3 Moderate	0.3 to 0.4 High	>0.4 Very High	Geometric Mean	Relative Importance
0 to 0.1 Very Low	1	3	5	8	9	4.0428	0.4935
0.1 to 0.2 Low	1/3	1	4	7	8	2.3693	0.2892
0.2 to 0.3 Moderate	1/5	1/4	1	6	7	1.16	0.1416
0.3-0.4 High	1/8	1/7	1/6	1	3	0.3892	0.0475
>0.4 Very High	1/9	1/8	1/7	1/3	1	0.2312	0.0282

Table 6.8 Main indicator sediment type: sub-indicators and their relative importance

Classes	Sediment Texture	Sediment Erodibility Factor	Geometric Mean	Relative Importance
Sediment Texture	1	2	1.4142	0.6667
Soil Erodibility Factor	1/2	1	0.7071	0.3333

Sub-criterion sediment: suitability map

Suitability maps for the sub-criterion sediment are based on the weighted combination of the suitability maps for the main indicators sediment volume and sediment type (Table 6.9). The relative importance of the indicators were compared with the modelling results and the opinion of the experts. As the table indicates, sediment texture is believed to be more important than volume because of the impeding effects of clay sedimentation in the schemes and the simulation results of Chapter 3. Suitability maps generated by SMCE with the above relative importance values are shown in Figure 6.6.

Table 6.9 Sub-criterion sediment: main indicators and their relative importance

Classes	Sediment Type	Sediment Volume	Geometric Mean	Relative Importance
Sediment Type	1	2	1.4142	0.6667
Sediment Volume	1/2	1	0.7071	0.3333

6.2.3 Main criterion floodwater: suitability map

In order to select an area on Varamin Plain for its most suitable properties in terms of water and sediment, the greater importance of water (as found during the simulation modelling in Chapter 4) was expressed as shown in Table 6.10. The resulting suitability value maps are shown in Figure 6.7.

Table 6.10 Main criterion floodwater: sub-criteria and their relative importance

Sub-criteria	Water	Sediment	Geometric Mean	Relative Importance
Water	1	2	1.4142	0.6667
Sediment	1/2	1	0.7071	0.3333

6.3 Main criterion infiltration

The suitability assessment of floodwater infiltration is determined by suitability assessment of the sub-criteria topography, aquifer and soil (see Figure 6.8).

6.3.1 Sub-criterion topography

For each of the distinguished main indicators, value classes are specified, and corresponding relative importance values determined.

Main indicator: slope

Based on the available literature and consultation with experts, the LMP values were assigned to six classes of slope steepness of potential infiltration areas, and for the assignment of LMPs weight was given to the adverse affects of steeper gradients attributable to erosion hazard (see Table 6.11).

Table 6.11 Main indicator slope: classes and their relative importance

Classes	0-1	1-2	2-3	3-5	>5	Geometric Mean	Relative Importance
0-1	1	5	7	8	9	4.7894	0.5469
1-2	1/5	1	6	7	8	2.32	0.2649
2-3	1/7	1/6	1	6	7	1	0.1142
3-5	1/8	1/7	1/6	1	6	0.4471	0.0511
>5	1/9	1/8	1/7	1/6	1	0.2013	0.0230

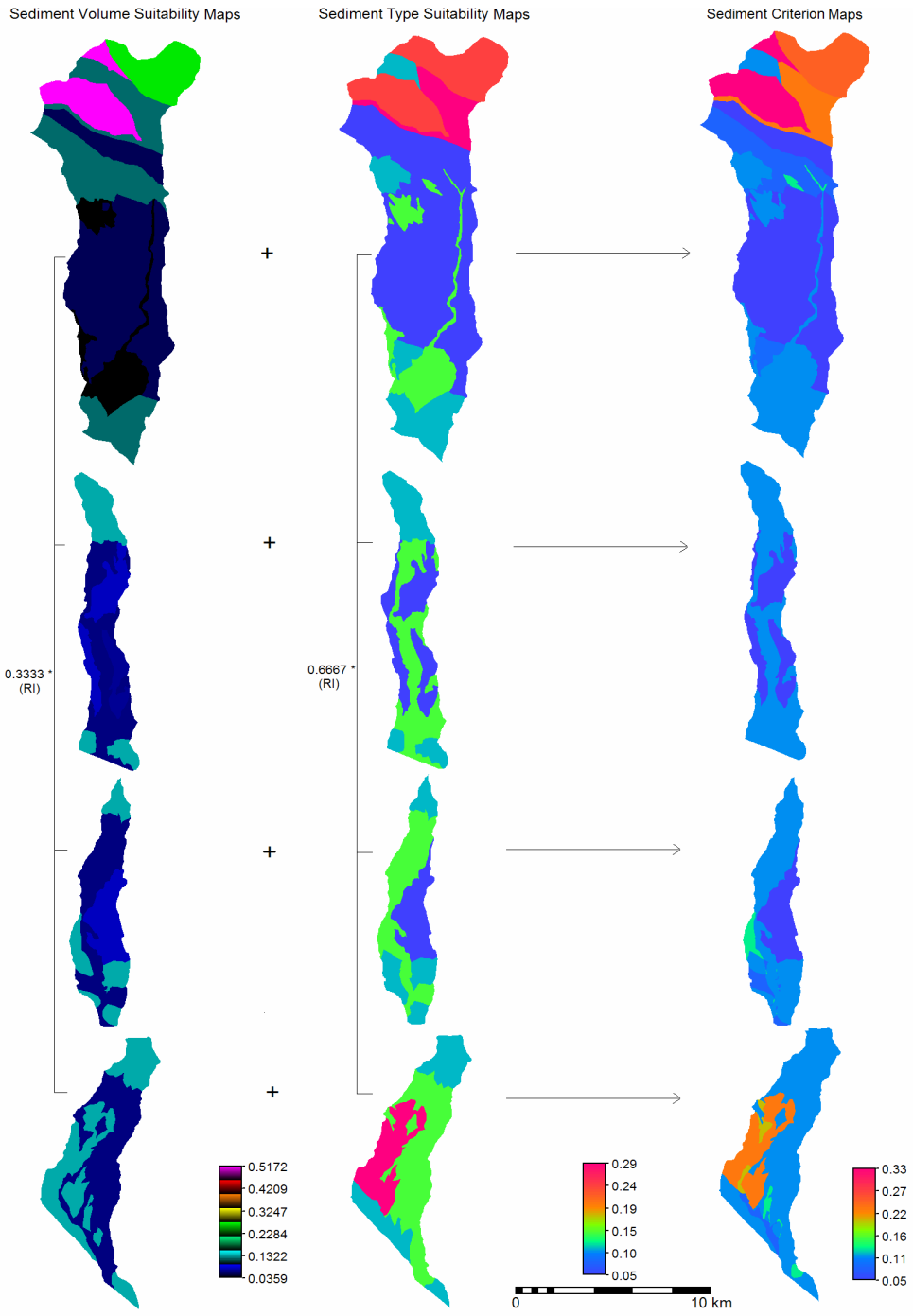

Figure 6.6 Suitability maps for the sub-criterion sediment for the four potential floodwater spreading areas. The map on the right is the weighted combination of the two main indicators sediment volume and sediment type

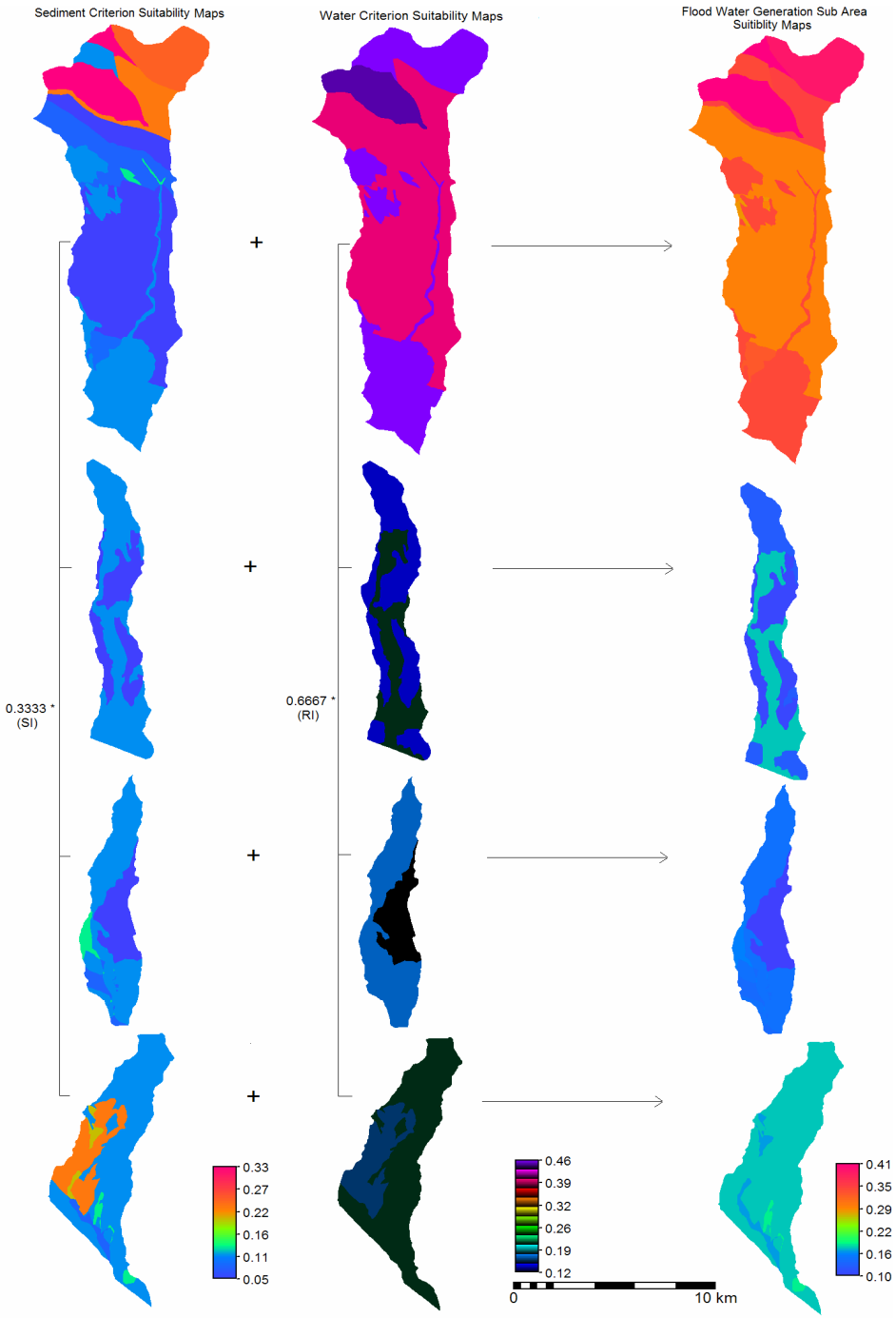

Figure 6.7 Suitability maps for the main criterion floodwater for the four potential floodwater spreading areas. The map on the right is the weighted combination of the two sub-criteria water and sediment

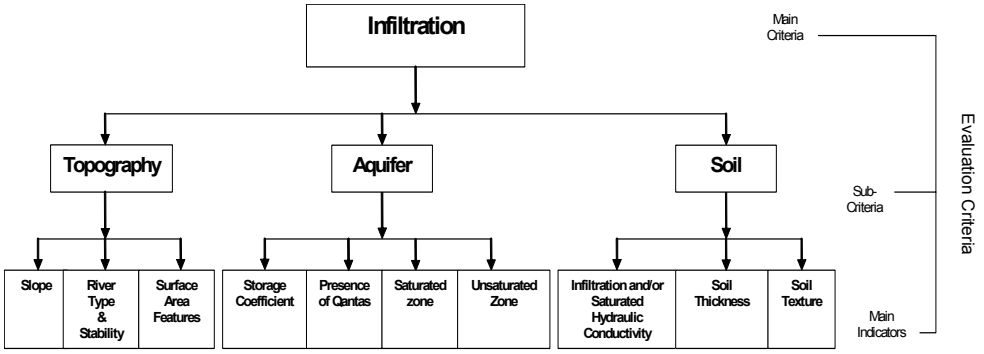

Figure 6.8 Decision tree for the main criterion infiltration, showing sub-criteria and main indicators

Main indicator: river type and stability

The river type and stability indicators are classified based on available literature (Schumm, 1972). The relative importance of each class is derived based on expert opinion and field observation, using pairwise comparison (Table 6.12).

Main indicator: surface area features

The five sub-indicators for this main indicator are land use type, existence of infrastructures (power lines, pipe lines, etc.) passing through the areas, evenness of surface area, distance of each surface point to the main river, and existence of access road indicators. As all mentioned indicators are spatial objects, they have been estimated using different RS-GIS techniques (such as supervised classification for land use using spectral data, distance operations in GIS, etc.). Each indicator was classified and weighted based on expert opinion. The assignment of LMP values for each sub-indicator is shown in Appendix 1.

Suitability maps of the main indicator surface area feature for the four areas were made by combining the five sub-indicators according to LMP values shown in Table 6.13. Here land use carried the highest weight and the shortest distance to the main river carried the lowest weight in the relative importance.

Table 6.12 Main indicator river type and stability: classes and their relative importance

Classes	BL & St	ML & St	BL & Dp	BL & Er	ML & Dp	ML & Er	SL & St	SL & Dp	SL & Er	Geometric Mean	Relative Importance
Bedload & Stable	1	2	3	4	5	6	7	8	9	4.1472	0.3043
Mixed Load & Stable	1/2	1	2	3	4	5	6	7	8	3.00	0.2201
Bedload & Deposition	1/3	1/2	1	2	3	4	5	6	7	2.1131	0.1550
Bedload & Eroding	1/4	1/3	1/2	1	2	3	4	5	6	1.4592	0.1071
Mixed Load & Deposition	1/5	1/4	1/3	1/2	1	2	3	4	5	1	0.0734
Mixed Load & Eroding	1/6	1/5	1/4	1/3	1/2	1	2	3	4	0.8195	0.0601
Suspended Load & Stable	1/7	1/6	1/5	1/4	1/3	1/2	1	2	3	0.4732	0.0347
Suspended Load & Deposition	1/8	1/7	1/6	1/5	1/4	1/3	1/2	1	2	0.3756	0.0276
Suspended Load & Eroding	1/9	1/8	1/7	1/6	1/5	1/4	1/3	1/2	1	0.2411	0.0177

Table 6.13 Main indicator surface area feature: sub-indicators and their relative importance

Sub-indicators	Lu	In	Ev	AR	SDMR	Geometric Mean	Relative Importance
Landuse	1	3	8	8	9	4.4413	0.5262
Infrastructures	1/3	1	7	7	8	2.6499	0.3140
Evenness	1/8	1/7	1	1	2	0.5135	0.0608
Access Road	1/8	1/7	1	1	2	0.5135	0.0608
Shortest Distance to Main River	1/9	1/8	1/2	1/2	1	0.3222	0.0382

Sub-criterion topography: suitability map

The suitability maps (Figure 6.9) of the overall topographical sub-criterion for each of the alternative areas were generated using the weighted combination of the three main indicators as presented in Table 6.14. The relative importance of the three main indicators was assigned based on pairwise comparison carried out by experts.

Table 6.14 Sub-criterion topography: main indicators and their relative importance

Main indicators	SAF	Slope	RT S	Geometric Mean	Relative Importance
Surface Area Features	1	2	3	1.8171	0.54
Slope	1/2	1	2	1	0.2970
River Type and Stability	1/3	1/2	1	0.5503	0.1634

6.3.2 Sub-criterion aquifer

The value classes of the four main distinguished indicators of the sub-criterion aquifer are specified, and corresponding relative importance values determined.

Main indicator: presence of qanat

This main indicator is included because of its meaning for further characterizing the properties of the saturated zone, since most hydrogeological data pertain to the aquifer where pumping takes place (i.e. the application area) and not the upper margin of the aquifer, the infiltration area where wells are non-existent or few in number. The presence of one or more qanats obviously signifies favourable aquifer properties and is therefore strongly preferred (LMP value of 5; Table 6.15). The presence of qanats was determined from the topographical maps for each alternative area, and the relative importance entered in the table operations.

Main indicator: storage coefficient

The storage coefficient of an aquifer is the volume of water it releases from, or takes into storage, per unit surface area of the aquifer per unit change in the component of head normal to that surface. This indicator determines how much water could be stored under phreatic conditions in the nominated aquifers. Using available maps (published by the Ministry of Power), storage coefficient information for the study areas was entered in GIS format, sliced/classified, and compared based on expert opinion. The LMP values assigned to each class are shown in Table 6.16.

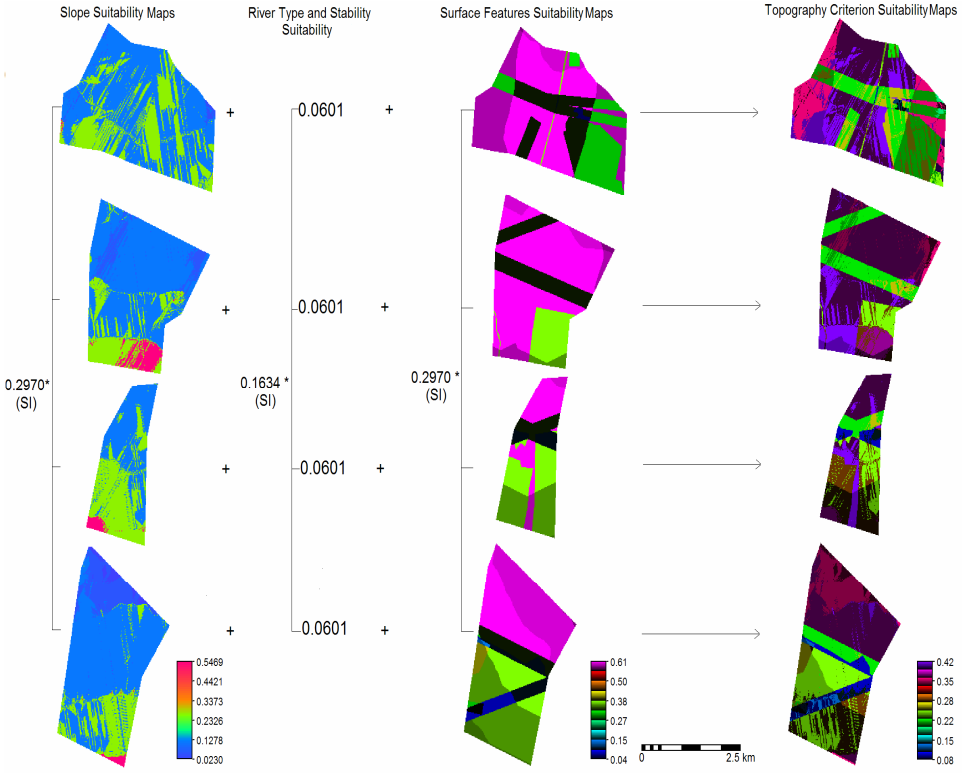

Figure 6.9 Suitability maps for the sub-criterion topography for the four potential floodwater spreading areas. The map on the right is the weighted combination of the three main indicators slope, river type and stability, and surface area feature

Table 6.15 Main indicator presence of qanat: classes and their relative importance

Classes	Presence of Qanat	No Qanats	Geometric Mean	Relative Importance
Presence of Qanat	1	5	2.2361	0.8333
No of Qanats	1/5	1	0.4472	0.1667

Table 6.16 Main indicator storage coefficient: classes and their relative importance

Classes	High	Moderate	Low	Geometric Mean	Relative Importance
High (>10 cm/m)	1	3	9	3.000	0.6484
Moderate (5 to 10 cm/m)	1/3	1	8	1.3867	0.2997
Low (<5 cm/m)	1/9	1/8	1	0.2404	0.0520

Main indicator: unsaturated zone

The two sub-indicators for this main indicator are the hydraulic conductivity and vadose zone thickness. Table 6.17 was completed after hydrogeologists with experience of artificially recharged aquifers in Iran had been consulted. This table shows a slight preference for (vertical) hydraulic conductivity as against thickness of the vadose zone. It should be noted that impeding layers and low conductivity values are generally absent in the upper fanglomerates.

Four thickness classes were considered on the strength that shallow thickness (<20 m) could cause salinization and evaporation losses, and that great thickness (>150 m) would cause substantial delay in the effect of artificial recharge, raising (political) questions as to the short-term effectiveness of the investment in a scheme. The vadose zone thickness of the four areas was obtained from the groundwater contour map and the topographical map. The related LMP values of the sub-indicators are shown in Appendix 2.

Table 6.17 Main indicator unsaturated zone: sub-indicators and their relative importance

Parameters	HC	Thickness	Geometric Mean	Relative Importance
Hydraulic Conductivity	1	2	1.4142	0.6667
Thickness	1/2	1	0.7071	0.3334

Main indicator: saturated zone

The three sub-indicators for this main indicator are the hydraulic gradient, transmissivity and groundwater quality. Equal LMP values (Table 6.18) were assigned to the first two sub-indicators, following Darcy's law, while groundwater quality was given less weight preference because there are generally no major problems with the water quality in the upper fans. The related LMP values of the sub-indicators are shown in Appendix 3.

Table 6.18 Main indicator saturated zone: sub-indicators and their relative importance

Sub-indicators	WTD	Transmissivity	GQ	Geometric Mean	Relative Importance
Hydraulic Gradient	1	1	2	1.2599	0.3853
Transmissivity	1	1	2	1.2599	0.3853
Groundwater Quality	1/2	1/2	1	0.75	0.2294

Sub-criterion aquifer: suitability map

Through the weighted combination of the four above-mentioned main indicators, the suitability value maps of the aquifer criterion for the study areas were generated, as shown in Figure 6.10. The relative importance of the main indicators is shown in Table 6.19.

Table 6.19 Sub-criterion aquifer: main indicators and their relative importance

Main Indicators	UZ	SZ	SC	PQ	Geometric Mean	Relative Importance
Unsaturated Zone	1	1	3	5	1.968	0.3908
Saturated Zone	1	1	3	5	1.968	0.3908
Storage Coefficient	1/3	1/3	1	3	0.7598	0.1509
Presence of Qanat	1/5	1/5	1/3	1	0.3398	0.0675

6.3.3 Sub-criterion soil

For each of the distinguished main indicators, soil infiltration/Ks, soil thickness and soil texture, value classes are specified and corresponding relative importance values determined. Maps were prepared showing classes of measured infiltration rates of the soils in the study area, suitability of textures, and soil depths based on field observations (Soil Map of Varamin Plain, Ministry of Agriculture; Hakimi, 2003; Khosheghbal, 1999).

Main indicator: soil infiltration/saturated hydraulic conductivity

The LMP values of Table 6.20 with the soil infiltration/saturated conductivity (Ks) classes were assigned in such a manner that the resulting relative importance is in line with the simulation modelling results (Chapter 3).

Table 6.20 Main indicator soil infiltration/saturated hydraulic conductivity: classes and their relative importance

Classes (cm d^{-1})	>250	200 to 250	145 to 190150 to 200	100 to 150	50 to 100	25 to 50	0 to 25	Geometric Mean	Relative Importance
>250	1	4	5	6	7	8	9	4.8204	0.4172
200 to 250	1/4	1	4	5	6	7	8	2.8891	0.2500
150 to 200	1/5	1/4	1	4	5	6	7	1.7057	0.1476
100 to 150	1/6	1/5	1/4	1	4	5	6	1	0.0865
50 to 100	1/7	1/6	1/5	1/4	1	4	5	0.5863	0.0507
25 to 50	1/8	1/7	1/6	1/5	1/4	1	4	0.3461	0.0300
0 to 25	1/9	1/8	1/7	1/6	1/5	1/4	1	0.2074	0.0179

Main indicator: soil thickness

During the modelling, it was found that soil thickness was a significant factor in infiltration efficiency and therefore the relative importance of three soil thickness classes was assessed (Table 6.21). Shallow soils overlaying the pebble and sand deposits of the upper fanglomerates are much preferred to a cover with thick soil, which enhances evaporation loss.

Table 6.21 Main indicator soil thickness: classes and their relative importance

Classes cm	0 to 50	50 to 100	>100	Geometric Mean	Relative Importance
0 to 50	1	7	9	3.9791	0.7608
50 to 100	1/7	1	7	1	0.1912
>100	1/9	1/7	1	0.2513	0.0480

Main indicator: soil texture

The simulation modelling also showed that it was difficult to judge infiltration on the basis of the Ks value, which is obtained by PTFs only. To complement the evaluation, the relative importance of soil texture was included, and LMP values were chosen on the basis of literature concerning floodwater spreading schemes, published guidelines on the selection of sites, and the opinion of the experts consulted. As shown in Table 6.22, light textured soils are strongly preferred to soils that contain substantial amounts of clay and silt.

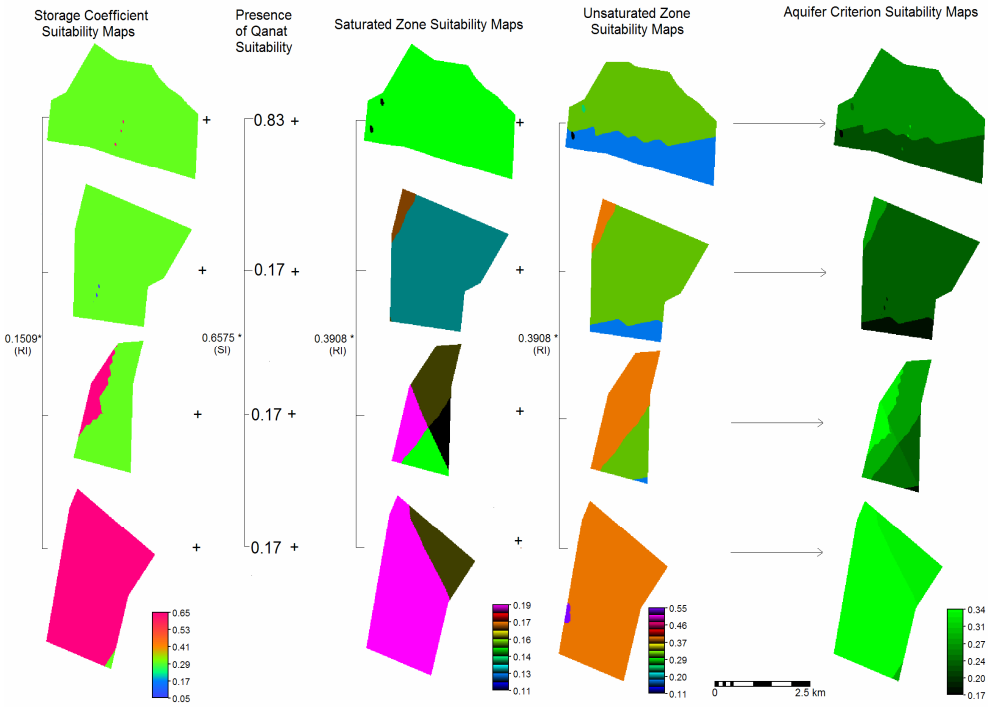

Figure 6.10 Suitability maps for the sub-criterion aquifer for the four potential floodwater spreading areas. The map on the right is the weighted combination of the four main indicators storage coefficient, presence of qanat, saturated zone, and unsaturated zone

Table 6.22 Main indicator soil texture: classes and their relative importance

Classes	VL to L	M to L	H to M	VH to H	Geometric Mean	Relative Importance
Very Light to Light	1	5	8	9	4.3559	0.6231
Moderate to Light	1/5	1	7	8	1.8294	0.2617
Heavy to Moderate	1/8	1/7	1	7	0.5946	0.0851
Very Heavy to Heavy	1/9	1/8	1/7	1	0.2111	0.0302

Sub-criterion soil: suitability map

A weighted combination of the three mentioned main indicators was made for the four alternative areas by giving preference to the texture indicator over the Ks indicator and to the latter over the indicator soil thickness, with equal steps, as is shown by the LMP values in Table 6.23. The resulting relative importance shows a dominance of texture, which reflects the large variability and somewhat contrasting simulation results based on Ks values, particularly for the non-light textured soils, and the relative importance of soil depth is in line with the average reduction in infiltration efficiency of various types of soils. The resulting suitability map for the soil sub-criterion is shown in Figure 6.11.

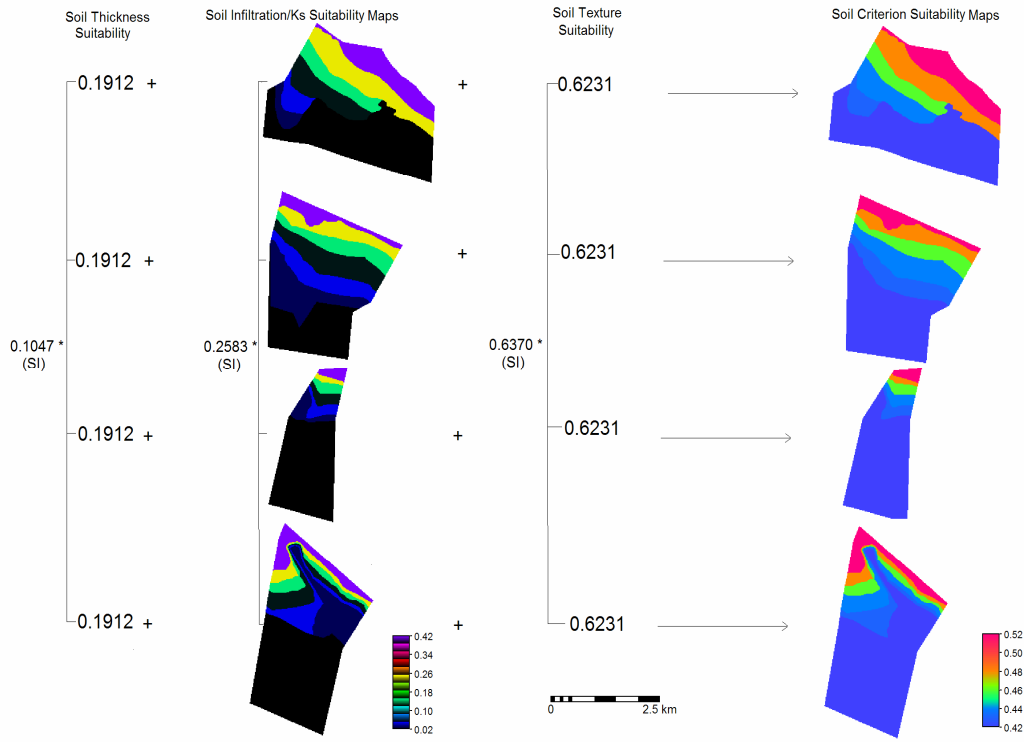

Figure 6.11 Suitability maps for the sub-criterion soil for the four potential floodwater spreading areas. The map on the right is the weighted combination of the three main indicators thickness, infiltration and texture.

Table 6.23 Sub-criterion soil: main indicators and their relative importance

Main Indicators	Texture	Infiltration/Ks	Thickness	Geometric Mean	Relative Importance
Texture	1	3	5	2.4662	0.6370
Infiltration/Ks	1/3	1	3	1	0.2583
Thickness	1/5	1/3	1	0.4055	0.1047

6.3.4 Main criterion infiltration: suitability map

The three major biophysical sub-criteria considered, namely aquifer, topography and soil, were now combined (Figure 6.12). The strongest preference was given to the suitability of the aquifer because the aquifer properties govern the overall feasibility of a floodwater spreading scheme in the first place. The preferences for the topography criterion and for the soil criterion were kept at par (see Table 6.24) because of the interrelations between topography and soil, the expected variation in soil variations in the potential infiltration areas in Iran, and cost considerations related to topography and type of scheme. The relative importance of the sub-criteria was calculated based on expert opinion (Table 6.24).

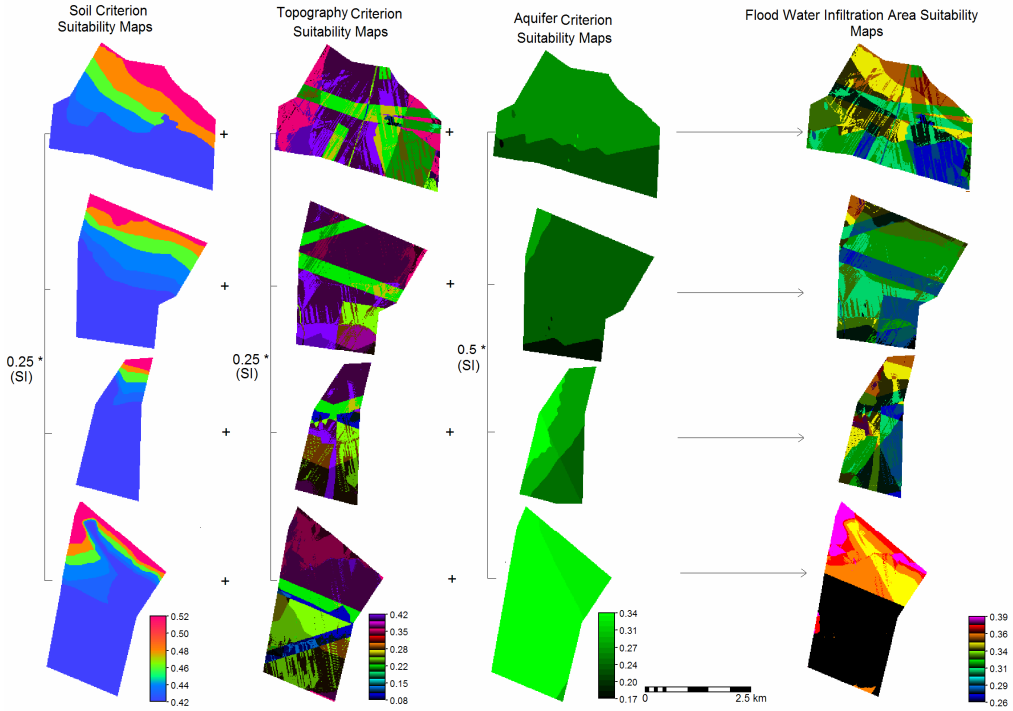

Figure 6.12 Suitability maps for the main criterion infiltration for the four potential floodwater spreading areas. The map on the right is the weighted combination of the three sub-criteria aquifer, soil and topography.

Table 6.24 Main criterion infiltration: sub-criteria and their relative importance

Sub-criteria	Aquifer	Topography	Soil	Geometric Mean	Relative Importance
Aquifer	1	2	2	1.5874	0.5
Topography	1/2	1	1	0.7937	0.25
Soil	1/2	1	1	0.7937	0.25

6.4 Main criterion *water application*

The suitability assessment of water application is determined by suitability assessment of the sub-criteria water demand, social acceptability and environmental acceptability (see Figure 6.13).

6.4.1 Sub-criterion water demand

The value classes of the three distinguished main indicators of the water demand sub-criterion are specified and corresponding relative importance values determined.

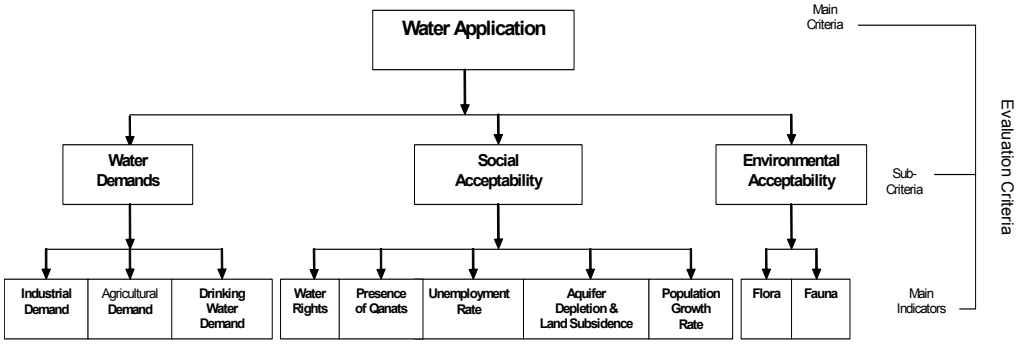

Figure 6.13 Decision tree for the main criterion water application. Sub-criteria and main indicators are shown

Main indicators: industrial demand, agricultural demand, and drinking water demand

These main indicators were estimated based on published data/information (Tehran Province Planning and Management Organization (TPPMO), 2002; Chahardowli, 2003) on the population of the villages/cities, number of industrial units and domestic animals, and surface area of the agricultural lands in the lower parts of the areas. These indicators were classified and the relative importance of each class calculated based on expert opinion, as shown in Table 6.25.

Table 6.25 Main indicators industrial demand, agricultural demand, and drinking water demand: classes and their relative importance

Classes	V.H.	H.	M.	L.	V.L.	Geometric Mean	Relative Importance
Very High	1	5	7	8	9	4.7894	0.5498
High	1/5	1	5	7	8	2.2369	0.2568
Moderate	1/7	1/5	1	6	7	1.0371	0.1190
Low	1/8	1/7	1/6	1	6	0.4471	0.0513
Very Low	1/9	1/8	1/7	1/6	1	0.2013	0.0231

Sub-criterion water demand: suitability value

According to the local people, industrial water and agricultural water have the same value but drinking water is more valuable. Therefore, the related LMP values for the main indicators were assigned and the relative importance of the three main indicators calculated as shown in Table 6.26.

Table 6.26 Sub-criterion water demand: main indicators and their relative importance

Main Indicators	DWD	IWD	AWD	Geometric Mean	Relative Importance
Drinking water demand	1	2	2	1.5874	0.5
Industrial water demand	1/2	1	1	0.7937	0.25
Agricultural water demand	1/2	1	1	0.7937	0.25

6.4.2 Sub-criterion social acceptability

Aquifer depletion/land subsidence damage, presence of qanats, water rights, population growth rate in the lower part villages/cities, and unemployment problems are the main indicators for the social acceptability criterion suitability assessment. The value classes of the five main indicators of the social acceptability sub-criterion are specified and corresponding relative importance values determined.

Main indicators: aquifer depletion/land subsidence damage
The aquifer depletion main indicator rates (according to the local organization there is no land subsidence in the study areas) were estimated and mapped by GIS operations through digitizing two available groundwater table maps of the study areas measured at different dates (March 2000 and September 2001; published by the Iran Ministry of Power) and subtracting the groundwater elevations by using GIS map calculations. Using expert opinion, the aquifer depletion rates were classified and the relative importance of each class calculated as shown in Table 6.27.

Table 6.27 Main indicator aquifer depletion/land subsidence damage: classes and their relative importance

Classes	H.D.	M.D.	L.D.	Geometric Mean	Relative Importance
High Damage	1	5	9	3.5569	0.7352
Moderate Damage	1/5	1	5	1	0.2067
Low Damage	1/9	1/5	1	0.2811	0.0581

Main indicator: presence of qanats
The second main indicator is the presence of qanats in the water application area, because the people value the reactivation of dried qanats, which provide a supply of clean water without high costs. The classes and their relative importance have already been shown in Table 6.15.

Main indicator: water rights
A common issue with regard to floodwater spreading schemes is the ownership of the water placed in underground storage or used for flood irrigation. Iranian law specifies that river floodwater on national land belongs to the public.

However, communities that traditionally use river water and groundwater have water rights for their agricultural lands, irrigation wells, etc. An attempt at a generic approach concerning water rights is shown in Table 6.28. However, according to officials there is no water right problem in the study areas and therefore equal relative importance values have been assigned to all areas.

Main indicator: population growth rate
Population growth rates in the cities/villages of the nominated water application areas is an indicator for water demand in the future, being connected to immigration/migration problems in the study area. The population growth rates in

the study areas were collected from published literature (TPPMO, 2002; Chahardowli, 2003), classified, and the relative importance of each class calculated based on expert opinion (Table 6.29).

Table 6.28 Main indicator water rights: classes and their relative importance

Classes	NP	SP	Se P	Geometric Mean	Relative Importance
No Problem	1	7	9	3.9791	0.7608
Slight Problem	1/7	1	7	1	0.1912
Severe Problem	1/9	1/7	1	0.2513	0.0480

Table 6.29 Main indicator population growth rate: classes and their relative importance

Classes	High	<=0	Moderate-	Low	Geometric Mean	Relative Importance
High (>3) %	1	1	5	7	2.4323	0.4204
<= 0	1	1	5	7	2.4323	0.4204
Moderate (1 to 2%)	1/5	1/5	1	5	0.6687	0.1156
Low (<1%)	1/7	1/7	1/5	1	0.2528	0.0437

Main indicator: unemployment problem

The last main indicator for the social acceptability criterion is the unemployment problem index (R), defined as R = (AJ/JR)*100), where AJ is available jobs and JR is the number of job requirements in the application sub-areas. In the study areas, smaller numbers of R received more priority. The necessary information was collected from published literature (TPPMO, 2002) and, based on expert opinion, classified and weighted as shown in Table 6.30.

Table 6.30 Main indicator unemployment problem: classes and their relative importance

R Index Classes	0 to 25	25 to 50	50 to 100	>100	Geometric Mean	Relative Importance
0 to 25	1	5	7	9	4.2129	0.6174
25 to 50	1/5	1	6	8	1.7602	0.2713
50 to 100	1/7	1/6	1	7	0.6389	0.0936
>100	1/9	1/8	1/7	1	0.2111	0.0309

Sub-criterion social acceptability: suitability map

The suitability maps of the social acceptability criterion for the study areas were generated by the weighted combination of the above main indicators and are shown in Figure 6.14. The relative importance of the main indicators was compared based on expert opinion and is shown in Table 6.31.

Table 6.31 Sub-criterion social acceptability: main indicators and their relative importance

Main Indicators	ADLS	PQ	WR	PGR	RI	Geometric Mean	Relative Importance
Aquifer depletion/land subsidence	1	2	3	5	7	2.9137	0.4443
Presence of qanats	1/2	1	2	3	5	1.7188	0.2621
Water rights	1/3	1/2	1	2	3	1	0.1525
Population growth rate	1/5	1/3	1/2	1	2	0.5818	0.0887
R index	1/7	1/5	1/3	1/2	1	0.3432	0.0523

6.4.3 Sub-criterion environmental acceptability

Floodwater spreading schemes should not create problems for the flora or fauna that could be affected by a reduction in inflow of floodwater because of the construction of a scheme. The main indicators representing the impacts of schemes on flora and fauna are assessed and compared.

Main indicators: flora and fauna damage
The main indicators flora and fauna damage were classified and the relative importance of each class calculated based on expert opinion (see Table 6.32).

Table 6.32 Main indicator flora and fauna damage: classes and their relative importance

Classes	No P.	S.P.	Se. P.	Geometric Mean	Relative Importance
No Problem	1	7	9	3.9791	0.7608
Slight Problem	1/7	1	7	1	0.1912
Severe Problem	1/9	1/7	1	0.2513	0.0480

Sub-criterion environmental acceptability: suitability value
In the study areas there are no specific environmental aspects to be considered. The flora consists of overgrazed rangelands and the fauna holds no special interest because of proximity to settlements and industry, while marshy areas are absent. Therefore, equal suitability values were assigned to the study areas, as shown in Figure 6.14. The relative importance of the flora and fauna main indicators is shown in Table 6.33.

Table 6.33 Sub-criterion environmental acceptability: main indicators and their relative importance

Main Indicators	Fauna	Flora	Geometric Mean	Relative Importance
Fauna	1	1	1	0.5
Flora	1	1	1	0.5

6.4.4 Main criterion water application: suitability maps

The suitability value maps of the main criterion water application for all the alternatives are generated based on weighted combination of its three sub-criteria, suitability values and maps (Figure 6.14). The LMP values were assigned to the sub-criteria based on expert opinion and their relative importance calculated (Table 6.34).

Table 6.34 Main criterion water application: sub-criteria and their relative importance

Sub-criteria	WD	SA	EA	Geometric Mean	Relative Importance
Water Demand	1	1	3	1.4422	0.4286
Social Acceptability	1	1	3	1.4422	0.4286
Environmental Acceptability	1/3	1/3	1	0.4807	0.1428

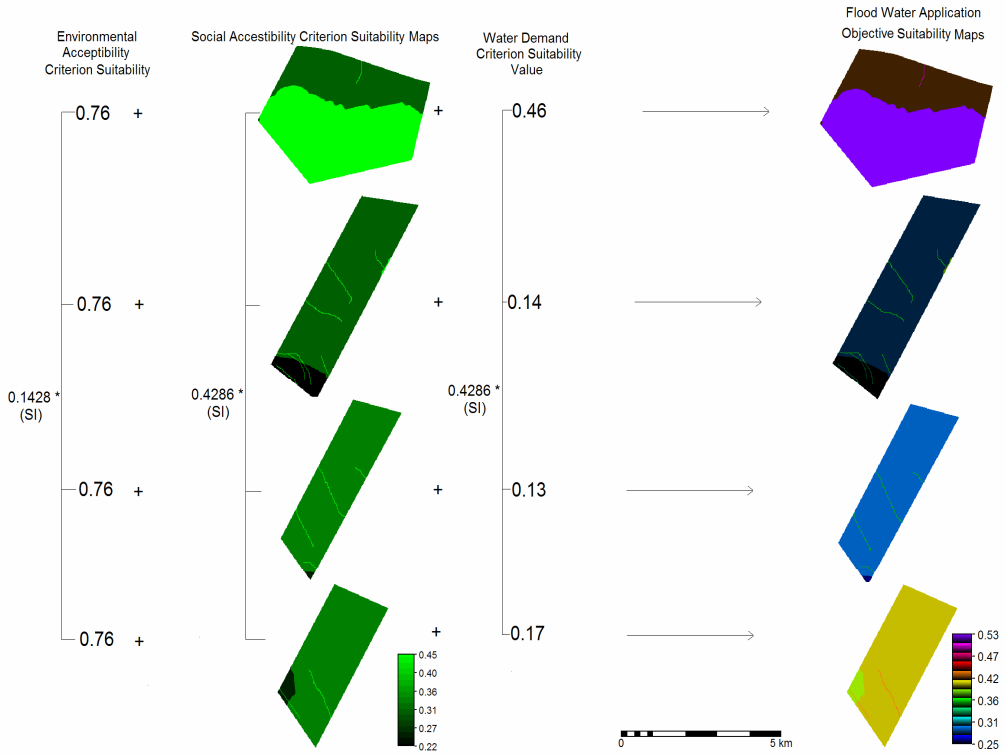

Figure 6.14 Suitability maps for the main criterion water application for the four potential floodwater spreading areas. The map on the right is the weighted combination of the three sub-criteria water demands, and social and environmental acceptability

6.5 Main criterion flood damage

The suitability assessment of flood damage is determined by suitability assessment of the main indicators loss of life, agricultural damage and infrastructure/industrial damage (see Figure 6.15).

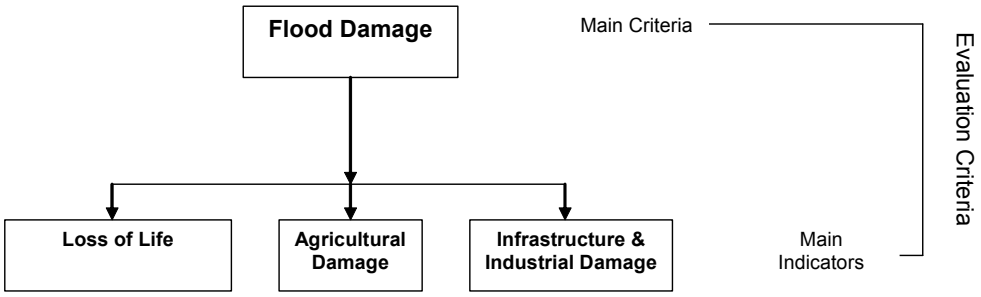

Figure 6.15 Decision tree for the main criterion flood damage, showing main indicators

Main indicators: loss of life, agricultural damage, and infrastructure/industrial damage

Three main indicators in the study areas were estimated using published sources (TPPMO, 2002; Chahardowli, 2003; Khalilpour, 2003), and classified and compared based on expert opinion, as shown in Tables 6.35 and 6.36.

Table 6.35 Main indicator loss of life: classes and their relative importance

Classes	LL	No D	Geometric Mean	Relative Importance
Loss of Life	1	9	3	0.9
No Damage	1/9	1	0.3334	0.1

Table 6.36 Main indicators industrial and agricultural damage: classes and their relative importance

Classes	H	M	L	No D	Geometric Mean	Relative Importance
High	1	5	7	9	4.2129	0.6174
Moderate	1/5	1	6	8	1.7602	0.2580
Low	1/7	1/6	1	7	0.6389	0.0936
No Damage	1/9	1/8	1/7	1	0.2111	0.0309

6.5.1 Main criterion flood damage: suitability maps

The relative importance of the indicators is shown in Table 6.37. The suitability concerning the main criterion flood damage for the study areas was derived by weighted combination of the three above main indicators, as shown in Table 6.38.

Table 6.37 Main criterion flood damage: main indicators and their relative importance

Main Indicators	LF	IID	AD	Geometric Mean	Relative Importance
Loss of Life	1	8	9	4.1602	0.8058
Industrial and Infrastructure Damage	1/9	1	2	0.6057	0.1173
Agricultural Damage	1/8	1/2	1	0.3968	0.0769

Table 6.38 The overall suitability index of potential areas, considering the flood damage

Alternatives	LF	IID	AD	Suitability Value
Alternative 1 (Chandab area)	0.1	0.6174	0.6174	0.2
Alternative 2 (Koliack area)	0.1	0.6174	0.6174	0.2
Alternative 3 (Latshor area)	0.1	0.2580	0.2580	0.13
Alternative 4 (Siahcheshmeh area)	0.1	0.6174	0.6174	0.2

6.6 Scenario analysis and evaluation

The relative importance of the main criteria for suitable floodwater spreading area selection was based partly on the opinion of the different decision makers/experts. Because the procedure is not free from subjectivity and because differences of opinion were noted, five scenarios are presented in which the relative importance of the four main criteria varies.

6.6.1 Scenario (I)

Scenario I reflects the opinion of some experts who believe that the main criterion infiltration has absolute preference (LMP) with respect to the other three criteria. The relative importance for the four main criteria of scenario I and the suitability

maps for all alternatives areas are shown in Table 6.39 (column 2) and Figure 6.16 respectively.

Table 6.39 The relative importance of the main criteria for the all scenarios

Main Criterion	Relative Importance Scenario I	Relative Importance Scenario II	Relative Importance Scenario III	Relative Importance Scenario IV	Relative Importance Scenario V
Infiltration	0.7500	0.0833	0.0833	0.0833	0.25
Water application	0.0833	0.7500	0.0833	0.0833	0.25
Floodwater	0.0833	0.0833	0.0833	0.7500	0.25
Flood damage	0.0833	0.0833	0.7500	0.0833	0.25

In order to achieve the final suitability of the alternative areas, the weighted sum of the utilities was computed, as shown in Table 6.40.

Table 6.40 Final suitability results for scenario I

Alternatives	Sum of utilities
Alt1	0.9141
Alt2	0.8303
Alt3	0.8468
Alt4	0.9418

According to the evaluation, alternative 4 (Siahcheshmeh area) is the suitable area, with the sum of the utilities being a value of 0.9418.

6.6.2 Scenario (II)

Scenario II is based on the opinion that the main criterion water application has absolute preference relative to the other objectives because the water demands and socio-economic problems of the cities/villages located in the lower parts of the areas are more important than other aspects. The relative importance weights for the four main criteria of scenario II and the calculated sum of the utilities for the four alternatives are shown in Table 6.39 (column 3) and Table 6.41 respectively. The resulting value maps for all alternative areas are shown in Figure 6.17.

Table 6.41 Final suitability results for scenario II

Alternatives	Sum of utilities
Alt1	0.9910
Alt2	0.6434
Alt3	0.6304
Alt4	0.6878

According to the evaluation, alternative 1 (Chandab area) is the suitable area, with the sum of the utilities being a value of 0.9910.

6.6.3 Scenario (III)

Scenario III concerns the opinion that control of flood damage in an area is the prime determinant criterion for floodwater spreading area selection. Therefore,

absolute preference is given to the objective criterion flood damage relative to the other three objective criteria. The relative importance weights for the objective criterion of scenario III and the calculated sum of the utilities for the four alternatives are shown in Table 6.39 (column 4) and Table 6.42 respectively. The resulting maps for all alternative areas are shown in Figure 6.18.

Table 6.42 Final suitability results for scenario III

Alternatives	Preference Index
Alt1	0.9910
Alt2	0.9178
Alt3	0.8259
Alt4	0.9418

According to the evaluation, alternative 1 (Chandab area) is the suitable area, with the sum of the utilities being a value of 0.9910.

6.6.4 Scenario (IV)

This scenario emphasizes the amount of floodwater with good chemical water quality and low amount of fine-grained sediment as prime determinants for the floodwater spreading area selection. Therefore in scenario IV absolute preference is assigned to the main criterion floodwater. The relative importance weights for the four main criteria of scenario IV and the calculated sum of the utilities for the four alternatives are shown in Table 6.39 (column 5) and Table 6.43 respectively. The resulting maps for all alternative areas are shown in Figure 6.19.

Table 6.43 Final suitability results for scenario IV

Alternatives	Preference Index
Alt1	0.9910
Alt2	0.5807
Alt3	0.5069
Alt4	0.7013

According to the evaluation, alternative 1 (Chandab area) is the most suitable area, with the sum of the utilities being a value of 0.9910.

6.6.5 Scenario (V)

Scenario V is based on the assumption that four objective criteria have the same preference (Table 6.39, column 6). The calculated sums of the utilities for the four alternatives of scenario V are shown in Table 6.44. The resulting maps for all alternative areas are shown in Figure 6.20.

Table 6.44 Final suitability results for scenario V

Alternatives	Preference Index
Alt1	0.9718
Alt2	0.7431
Alt3	0.7025
Alt4	0.8182

According to the evaluation, alternative 1 (Chandab area) is the suitable area, with the sum of the utilities being a value of 0.9718 (see Figure 6.16).

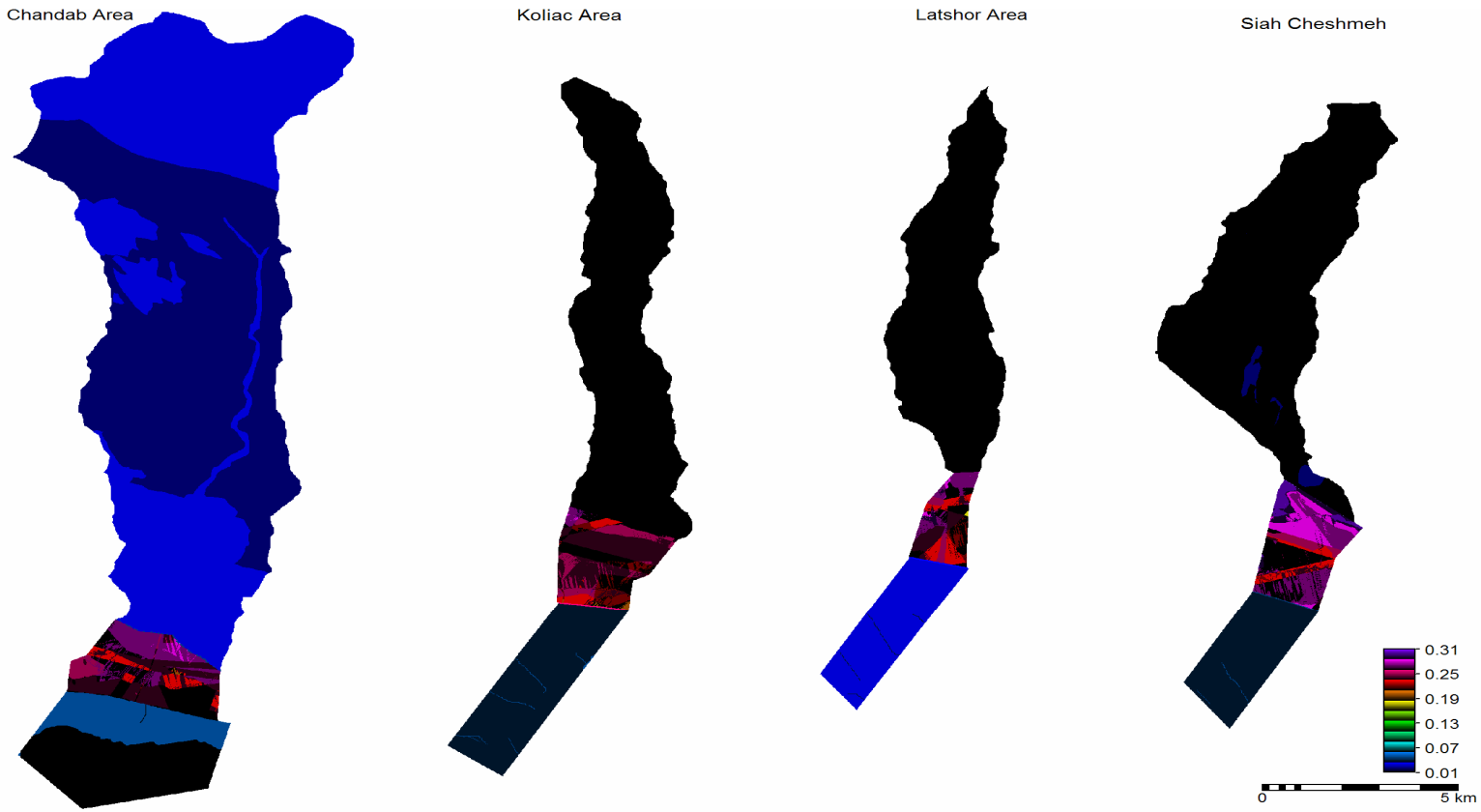

Figure 6.16 The suitability maps of scenario I, where the main criterion infiltration has absolute (LMP) priority

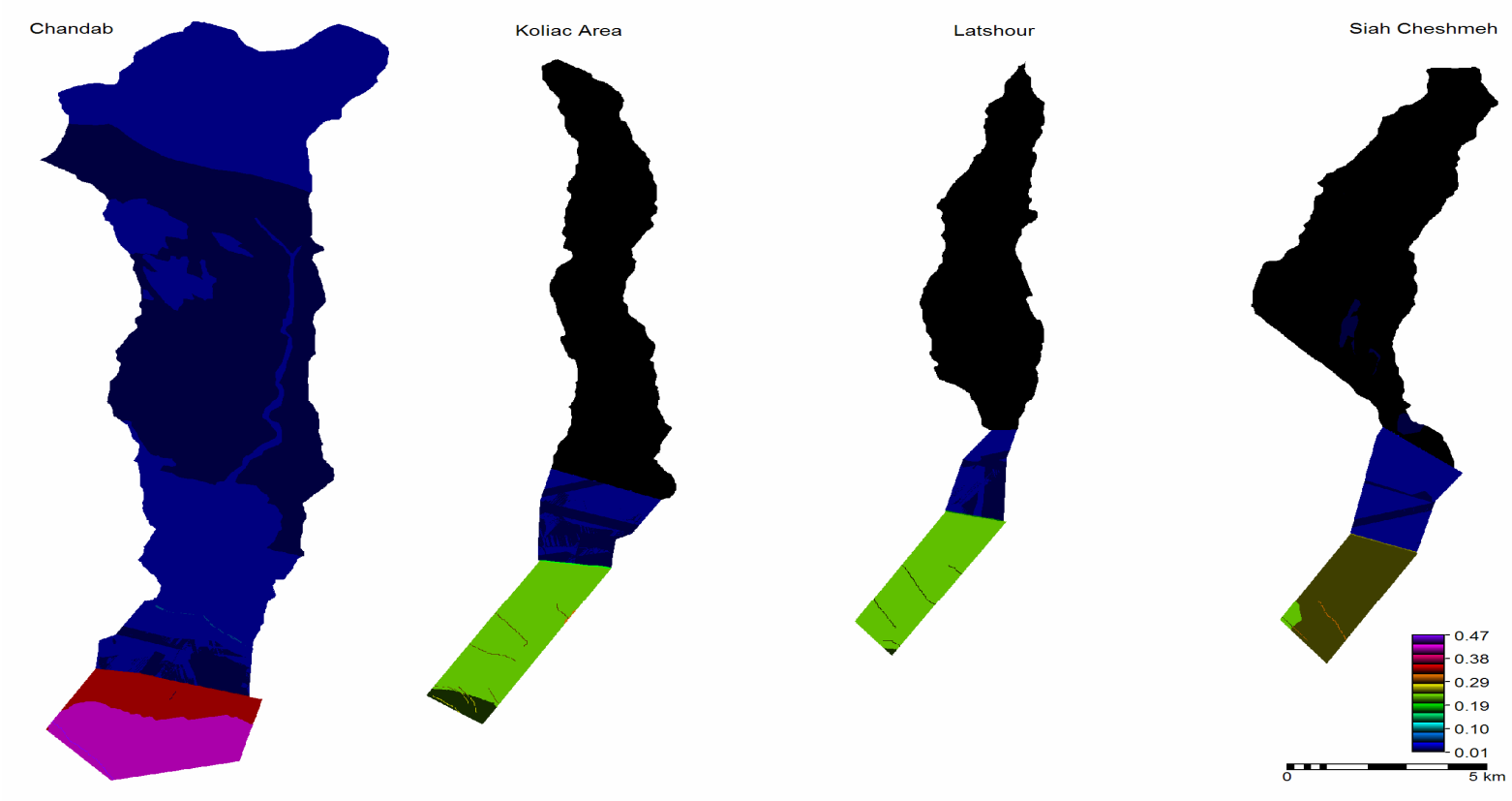

Figure 6.17The suitability maps of scenario II, where the main criterion water application has absolute (LMP) priority

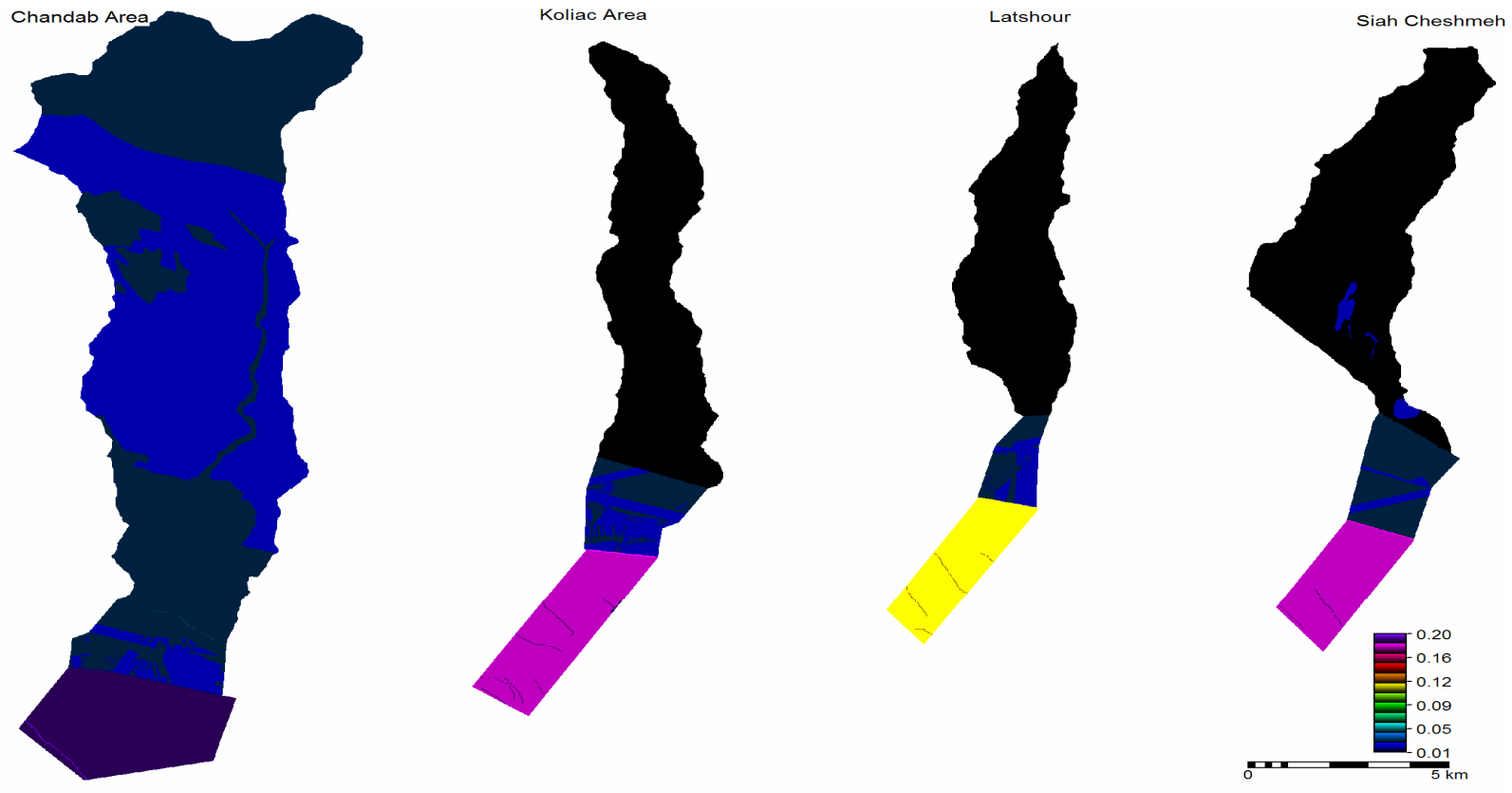

Figure 6.18 The suitability maps of scenario III, where the main criterion flood damage has absolute (LMP) priority

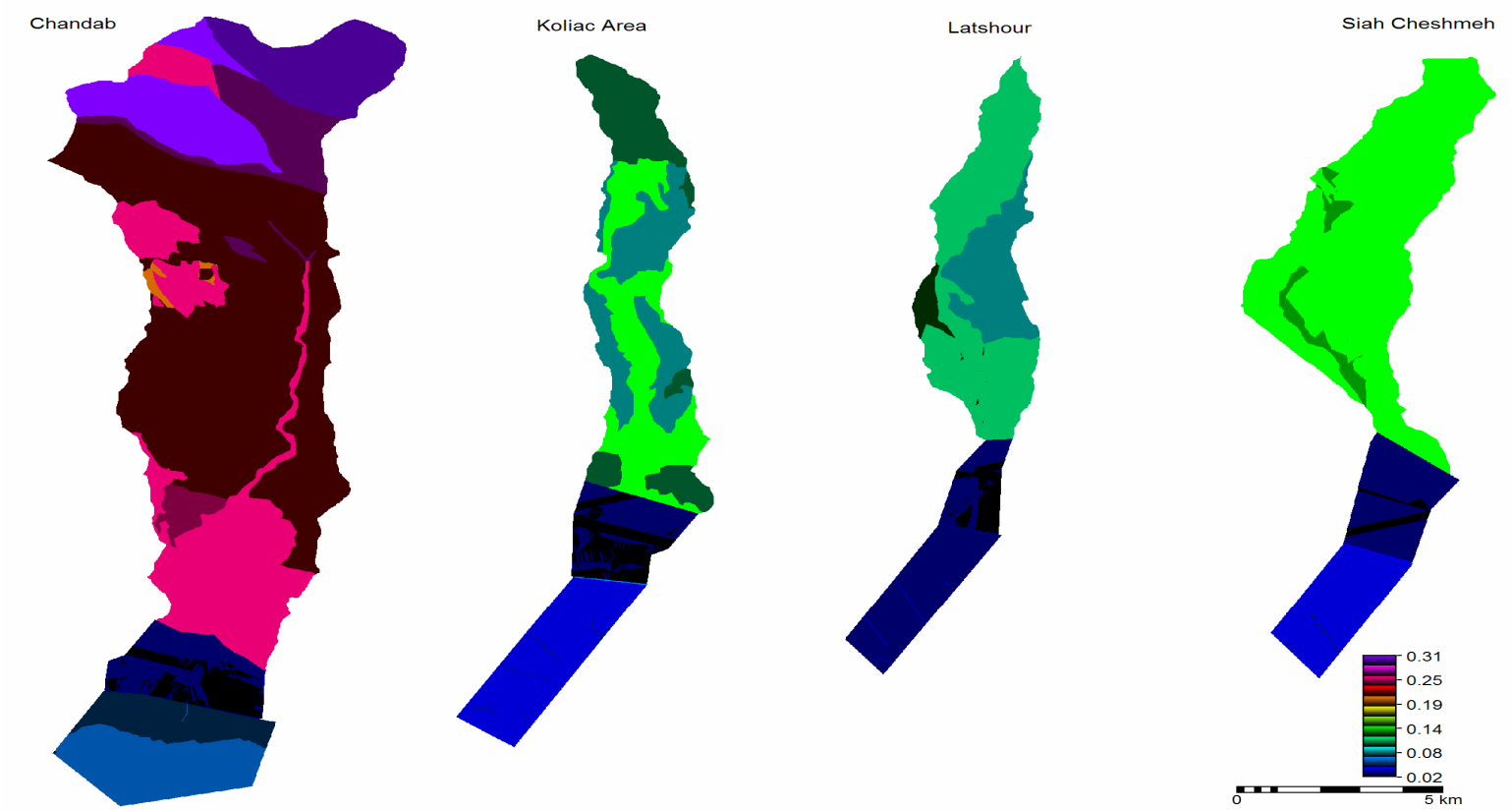

Figure 6.19The suitability maps of scenario IV, where the main criterion floodwater has absolute (LMP) priority

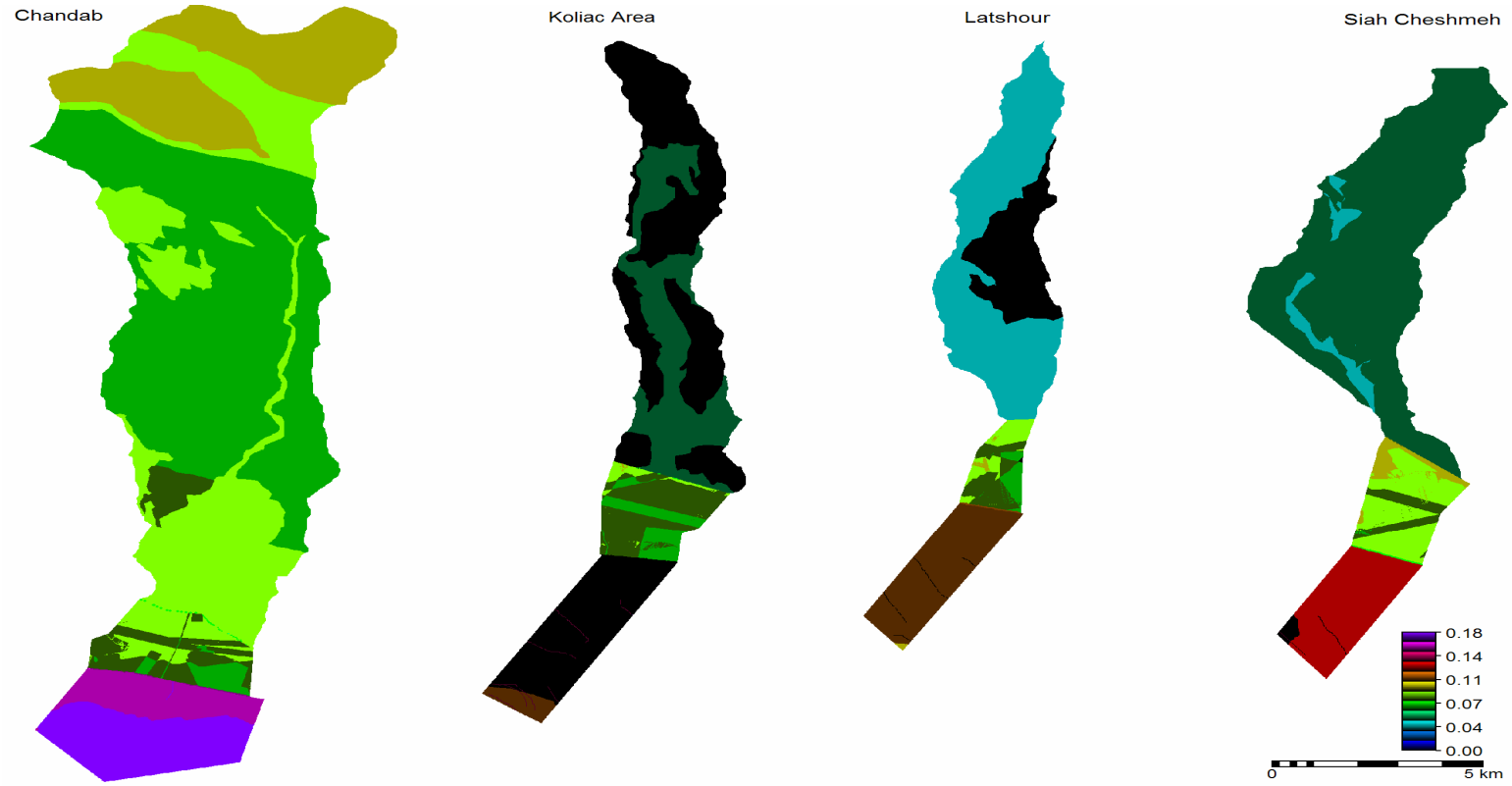

Figure 6.20 The suitability maps of scenario V, where all main criteria have the same priority

6.7 Discussion and conclusions

In this chapter, by considering a multitude of factors of diverse nature that influence decisions, a procedure has been developed and applied to select the most attractive area of a zone fromamong the alternatives pre-selected at reconnaissance scale for a floodwater spreading scheme. In other words, the procedure should weigh and combine arguments that may be heard for or against the selection of a particular area from a group of persons of different (scientific) backgrounds, working out where the 'suitable' area for investing in a floodwater spreading scheme actually is.

Four main criteria are considered: floodwater, infiltration or recharge, the use of the recharged water (in the water application area), and flood damage. Each of the main criteria is evaluated on the basis of sub-criteria or indicators at a lower level, and the four main criteria can be combined in a sum of utilities. Thus, the alternative areas in a zone can be ranked according to this index.

It turned out that the multicriteria evaluation method used in a spatial context (AHP) could be applied. The difficulty in the application was to develop and specify the preferences that are the basis of the relative importance values for all the decision criteria involved at different levels. For some of the physical criteria, such as amount of available floodwater, and sediment type and amount in the alternative areas, established empirical hydrological methods could be used for specification, classification and facilitation purposes. For others, such as those pertaining to the social acceptance criterion, preferences for the indicators had to be based solely on the opinion of experts or stakeholders and on proxy data, such as the unemployment problem index.

The use of the linguistic measures of preference (LMPs) in the pairwise comparison made it possible to implement the full procedure. That would have been difficult, considering the lack of quantified data of good quality and consistency.

In the spatial approach, the various geographical units or sub-units had to be delineated and captured in the GIS, and then the attribute values had to be transformed, such as rock type into sediment type. After that, preferences had to be assigned for each of the three areas, namely the catchment from which the floodwaters and the sediment are derived, the infiltration area in which the scheme will be located, and the downstream application area that will benefit from the scheme. In the evaluation at higher hierarchical level, the suitability values attached to the sub-units at lower level are considered. By doing so, a decrease in sensitivity is avoided that would be caused by lumping the evaluation results for each of the three areas. The sensitivity of the evaluations is an issue because a change in LMP and thus relative importance of, for example, a main indicator (such as sediment type) does not result in much change in the result at the highest evaluation level.

The attempts made in setting up the tables containing the LMPs are subject to improvement, as experience with the approach followed for the subject matter discussed here is only slender.

In spatial AHP, all decision criteria are clearly defined prior to the selection of an actual site. This point is important because the expertise concerning all the various aspects that play a role is not easily found in a single body, and,

furthermore, it enhances the objectivity of the decision process. The latter is certainly of relevance when land and water issues are involved and stakeholders or local officials have different influences and weights in the decision process.

Because of the multidisciplinary nature of the decision process, various points of view as to the preferences or importance of the main criteria are likely to emerge – as turned out to be the case in the interviews conducted for this study. Therefore, five different scenarios were formulated, four emphasizing one each of the four main criteria and the last scenario evaluating the four. It was found that one particular area (Chandab) had a high sum of utilities for three of the four objectives and the highest in the combined scenario. Consequently, that area was selected for developing and applying the method for the last step of the procedure, namely selecting the design type and site (discussed in Chapter 7).

CHAPTER 7
Site and design selection for floodwater spreading schemes

7.1 Introduction

Suitable site selection is coupled with design. If there is a design where the balance between costs and benefits is acceptable to policy makers, this proves that a site is suitable. Therefore this chapter deals with the evaluation of the expected costs and benefits of harvested (recharged) water.

The suitable site selection methodology (Chapter 2) is implemented and evaluated for Chandab, one of the selected areas in the Varamin zone (Chapter 5). Although many schemes have been constructed in Iran, no accessible literature could be found that deals with the comparison of design type and costs in relation to groundwater gained. No doubt such considerations have been investigated but, as with many engineering works, the results of the deliberations have not been made explicit. Yet the issue is of importance if decision makers are to be offered options from which they can choose.

In this chapter, two types of scheme are presented. These are relevant because of the terrain conditions in the selected Chandab area and because these two types are widely used in Iran. The approach could also, with adjustments, be used for another type or for hybrid design types. Use has been made of engineering design principles and rules laid down in handbooks (Ministry of Jihad for Construction, 1986), as well as the guidelines that reflect the accumulated experience with designing floodwater spreading schemes of the Soil Conservation and Watershed Management Research Institute of Iran.

The procedure for designing the channel and basin type of scheme started with considering the critical elements. The first element was the maximum capacity of the uppermost channel, which depends on total possible length, with appropriate dimensioning to keep within the permissible velocity limits. Then the intake was designed in such a manner that no more than the maximum capacity for the uppermost channel would be diverted, taking into account that peak flows in the rivers with different return periods would safely pass the intake.

In working out the total size of the scheme (i.e. the number of spreading channels and basins in the downstream direction), the discharges were considered and a hydromodule was based on infiltration. A spreadsheet model, coupled to a GIS, was developed to facilitate calculations and allow for iterations in order to arrive at a balance between design tolerances and to provide system safety. During such iterations, it was decided to work out options for sub-schemes with more than one intake, aiming to maximize capacity and lifetime. The system design incorporates safety for major flood events that last longer and have larger volumes of diverted water than the average event. The performance and lifetime of the scheme assumed annual desilting of the spreading channels only, not of the ponding areas of the infiltration basins, of which the upper ones are gradually filled. The

recharge efficiency was estimated by taking into account the effects of this silting up.

Evaluations of recharge and total costs (i.e. construction and maintenance costs) were first made on the basis of single events of different magnitude in the designed scheme and its alternatives. This was done to gain general insight into the recharge of different runoff events less or equal to the average runoff, and at what cost, in the design type of scheme. It should be understood that events of greater magnitude will not affect the recharge much because the intake allows only a given amount to be diverted.

The total amount of water gained during the lifetimes of the schemes and the total costs under different scenarios were estimated, and finally a simple method is offered to assist the decision maker in making a choice.

7.2 Study area

The main objective of this phase (large scale) is the development and implementation of a GIS-MCEM-supported model for suitable floodwater spreading site(s) and design type selection that is technically feasible and economically acceptable.

7.2.1 Land use

Since the main aspects of the area have been evaluated as being suitable (Chapter 6), the first step is to study the land use and ownership of the potential floodwater infiltration sub-area (shown in Figure 7.1) to locate the sites that have few or no restrictions. As can be seen on the map, on the eastern side of the access road the proportion of rangelands is limited and most of the area is occupied by private industrial land. Rangelands with poor vegetal cover are found on the western side of the road, while diversion of floodwaters will protect the road and reduce flood damage further downstream. However, if it is found that the western site alone cannot achieve the objective of the scheme, expansion into the eastern part can be considered.

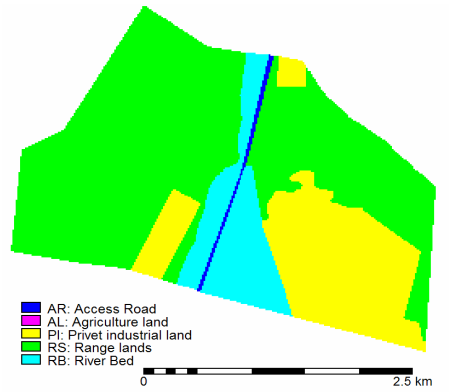

Figure 7.1 The land use map of the floodwater infiltration part of the selected Chandab area

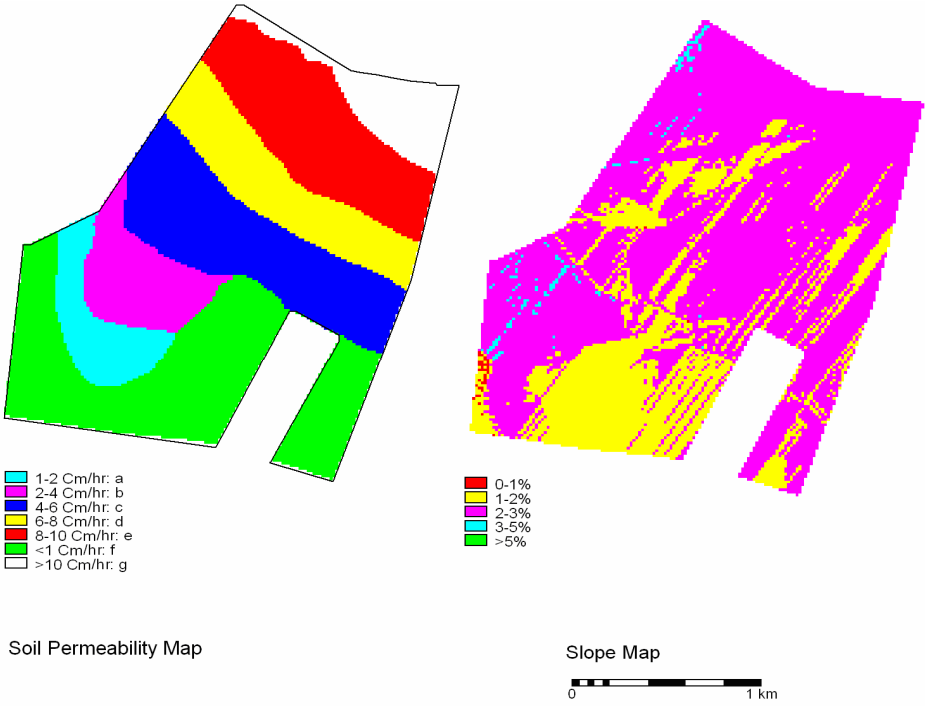

Figure 7.2 Soil permeability and slope maps of the study potential site

Figure 7.2 shows the soil permeability and the slope steepness of the land on the western site that is available for a scheme. As mentioned in the previous chapter, the transmissivity of the aquifer is more than adequate.

After having identified the potential site area(s), the runoff and sediment characteristics of the upstream catchment have to be known or estimated in order to match type of scheme with infiltration acreage available. For the ephemeral rivers of the smaller catchments, the required data can be obtained by current hydrological methods as a follow-up to the hydrological estimation made earlier for evaluating the best areas. The results, which are of an approximate nature, need to be compared with hydrological information obtained in the field. Such information may consist of estimated peak flows, preferably based on the measurement of actual flow depths and velocities but if they are not available on estimates using the slope area method. Interviews with local inhabitants concerning the number of flow occurrences, the duration of flows, and observations of sedimentation on the active parts of the middle and lower alluvial fan help in compiling the data set.

For the selected Chandab area, daily rainfall data of several stations with different lengths of records were available, and observations were made of runoff events over a period of six years and some instantaneous suspended load sampling was carried out. Best use was made of the hydrological data observed in the field but, in view of the intended long lifetime of a scheme, considerations of frequencies or recurrence intervals made it necessary to use rainfall records, being the only source of long-term data.

7.2.2 Rainfall

The daily rainfall of four stations (listed in Table 7.1) was used to calculate the catchment rainfall by using the Thiessen method, after testing the station data for homogeneity. The location of the stations is such that the altitude-rainfall relationships are captured. The average mean annual rainfall based on a period of 24 years worked out to be 207.5 mm.

Ephemeral flash flows are associated with high rainfall intensities over the catchment. In order to have some values for design, first the maximum probable 24-hour rainfall for specific return periods was calculated for the stations, using a fitted Pearson Type III distribution. The result is shown in Table 7.1. It should be understood that the values are approximate because the duration of the records of the stations varied from 11 to 22 years. It was assumed that maximum runoff would occur when the maximum intensity covered the full catchment area. This assumption implies that the catchment rainfall with maximum intensity (Table 7.2) will be too high because it is not likely that the maximum rainfall of a given return period will happen on the same day at all stations.

Table 7.1 Maximum probable 24-hour rainfall for the study stations calculated using Pearson Type III distribution

Station	Return Periods (year)					
	2	5	10	25	50	100
Gandab	9.33	28.44	34.78	42.93	48.90	54.74
Haman-e-Absard	16.66	40.02	45.44	51.68	55.97	58.87
Sharif abad	9.46	34.04	40.96	49.29	55.21	60.91
Varamin	11.16	29.87	35.38	42.05	46.81	51.41
Mamlo	16.65	34.42	40.33	47.71	53.09	58.36

The time of concentration in the catchment was estimated to be 1.82 hrs, using the Chow et al. (1988) formula. With the aid of FAO equation (Alizadeh, 1995), Equation 7.1

$$I = (P/24)\,(24/t)^{0.6} \qquad [7.1]$$

the 10-year maximum 24-hour rainfall intensity (I, mm hr^{-1}) for the concentration time (t, hr) and the maximum 24-hour rainfall with a 10-year return period (P) can be estimated. The maximum 1.82-hour rainfall intensity for other return periods was derived from the 10-year intensity using Bell equation (Alizadeh, 1995), Equation 7.2

$$P^t_T / P^t_{10} = 0.21 \ln T + 0.52 \quad 2 \leq T \leq 100 \qquad [7.2]$$

where P^t_T is the rainfall height for the specific t (minutes) time with T years return period. P^t_{10} is the rainfall height for the specific t (minutes) time with a 10-year return period. The results are shown in Table 7.3.

7.2.3 Runoff

Although flood peaks and flood volumes were observed (see later section), these observations pertain to a limited period. Therefore, the peak flow discharges (Qp) for the different flood return periods were calculated using the curve number (CN) and dimensionless unit hydrograph of the SCS (1972) method. In order to do so, the Qp of the unit hydrograph for 1 mm net rainfall were calculated. Then using the SCS dimensionless unit hydrograph, the characteristics of the unit hydrograph were determined (illustrated in Figure 7.3). The peak discharges for the different return periods were computed using the resulting Qp and calculated runoff depths for different return periods. The results are shown in Table 7.4.

Using the SCS dimensionless unit hydrograph, the resulting Tp (time to peak) and peak discharges (Qp), the catchment hydrographs for different return periods were estimated. The catchment flood volumes for different return periods are equal to the measured surfaces below the hydrograph curves. The results are shown in Table 7.4.

Table 7.2 Weighted mean rainfall (mm) for the region using Thiessen method

Station	**A_i (area covered by the station) (km^2)**	**$A_i * I_t$ (Rainfall with T years return period)**					
		$A_i * I_2$	**$A_i * I_5$**	**$A_i * I_{10}$**	**$A_i * I_{25}$**	**$A_i * I_{50}$**	**$A_i * I_{100}$**
Hamand-e-Abesard	32	533.12	1280.64	1454.08	1653.73	1791.04	1833.84
Mamloo	32.41	539.63	1177.51	1307.09	1546.28	1720.65	1891.44
Sharifabad	34.15	323.06	1162.47	1398.78	1683.25	1885.42	2080.1
Gandab	83.95	783.25	2387.54	2919.78	3603.97	4105.16	4595.42
Total	182.53	2179.6	6006.16	7079.73	8487.23	9502.27	10313.99
Weighted Mean		11.94	32.91	38.77	46.49	52.06	56.5

Table 7.3 Rainfall intensities (mm hr-1) for the catchment time of concentration with different return periods for the Chandab catchment area

Catchment Name	**Catchment Time of Concentration (hrs)**	**Return Period (years)**					
		2	**5**	**10**	**25**	**50**	**100**
Chandab	**1.82**	5.1	6.1	7.6	9.1	10.2	11.3

Table 7.4 Peak flow discharges (Qp, m3 s-1) and floodwater volume (m3) for the Chandab catchment for different return periods, using SCS method

Catchment Chandab	**Return Periods (years)**					
	2	**5**	**10**	**25**	**50**	**100**
Qp	13	67	100	167	221	280
Volume	75,000	388,200	587,700	975,000	1,291,300	1,630,000

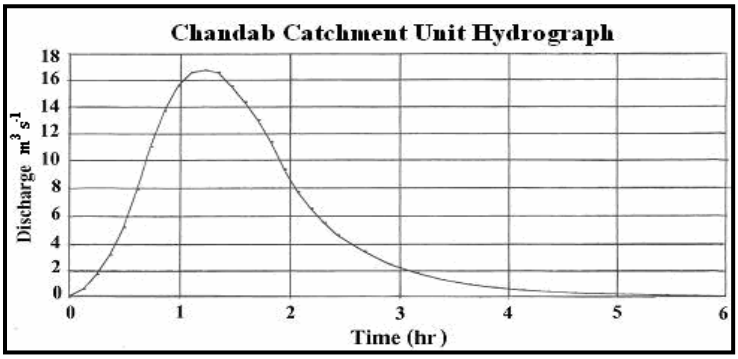

Figure 7.3 Unit hydrograph of the Chandab catchment

The results of the above-described method are approximate and therefore it is useful to inspect the 21 observations of flood events in the Chandab river made from end 1997 to 2003 by Khalilpour et al. (2003) (see Figure 7.4). It should be mentioned that the observations were based on measured depth and velocity by float readings every hour in a stable cross section.

Although these observed data are not accurate, they were used for frequency analysis. It was found that the Log Pearson Type III distribution had the best fit for both annual maximum peak flow and flood volume. However, as can be seen in Figure 7.5, there is a discrepancy between the fitted distribution and the observed values for the longer return periods. The fit for the flood volume distribution was closer, as is shown in Figure 7.6. Possibly, the event with a Weibull plotting position of seven years represents an event with an actual longer return period.

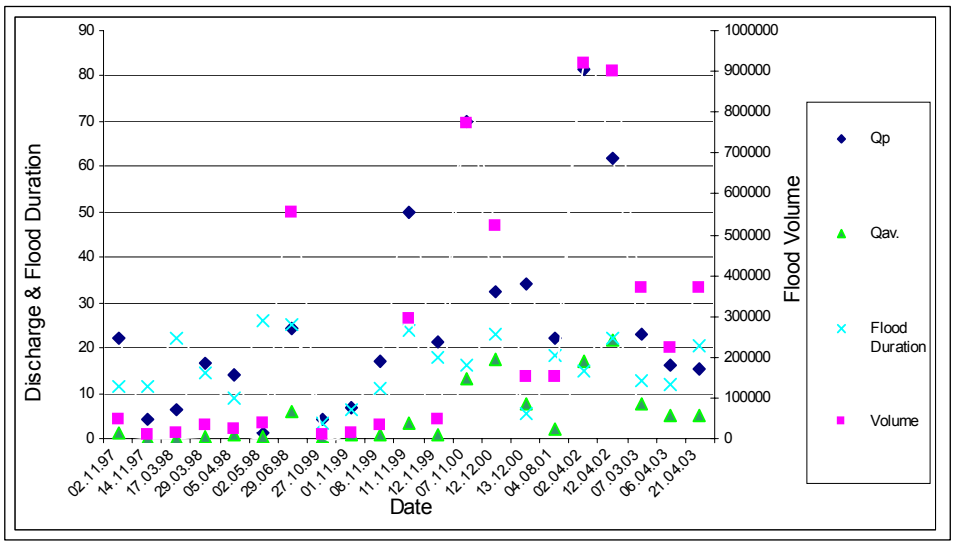

Figure 7.4 Relationship between peak discharges (Qp, m3 s-1), average discharge (Qav, m3 s-1), flood duration (hrs) and flood volume (m3) for the 21 measured flood events in the Chandab area

The comparison between calculated peak discharges using the unit hygrograph (Table 7.4), observed peak discharges for seven years, and observed data based on Log Pearson Type III distribution (Figure 7.5) are shown in Table 7.5.

Table 7.5 Calculated peak discharges (m3 s-1) for Chandab river

Calculation Method	Return Periods (years)					
	2	5	10	25	50	100
Calculated Using Unit Hydrograph (SCS)	13	67	100	167	221	280
Observed Actual Data	24	62	81	-	-	-
Log Pearson Type III Distribution Based on Observed Data	27	45	68	120	183	284

Table 7.5 shows values derived by the SCS method to be much higher than the observed ones, on account of the overestimate of the catchment rainfall for events up to a 10-year return period. The peak flows for longer return periods show only agreement for the longest period of 100 years. The values estimated with the SCS method were adopted for the design of the scheme, to include a safety factor.

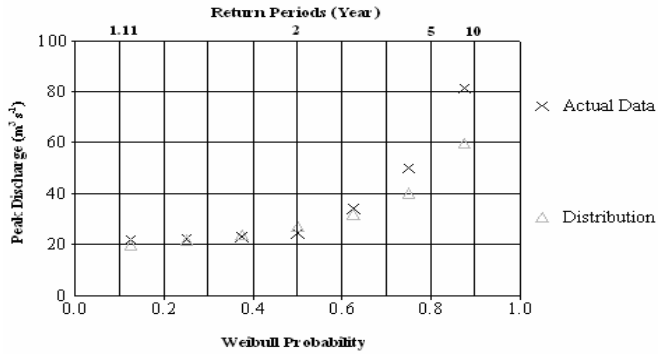

Figure 7.5 Chandab river return periods for peak discharges, based on actual data and calculated Log Pearson Type III distribution

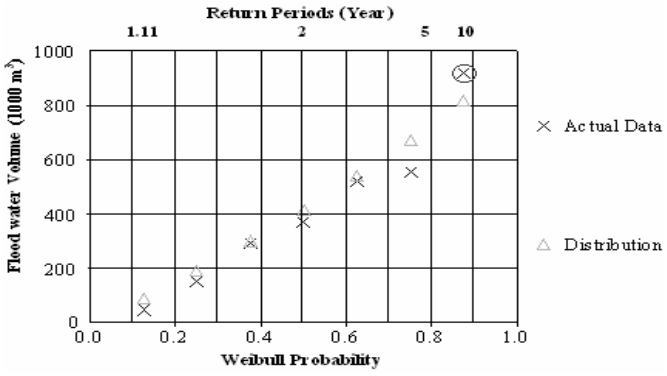

Figure 7.6 Chandab river return periods for floodwater volume based on actual data and calculated Log Pearson Type III distribution

The floodwater volume calculated using the unit hygrographs and the observed floodwater volume for seven years and observed data based on Log Pearson Type III distribution (Figure 7.6) are compared (Table 7.6).

Table 7.6 Calculated floodwater volume (1000 m3) for Chandab river

Calculation Method	Return Periods (years)					
	2	5	10	25	50	100
Calculated Using Unit Hydrograph	75	388	588	975	1291	1630
Observed Actual Data	369	522	918	-	-	-
Log Pearson Type III Distribution	416	729	849	926	951	960

The calculated (SCS method; Table 7.6) flood volumes are much lower than the observed ones for return periods ≤10 years. The SCS values could be adjusted by changing the curve numbers, but this has the consequence that the estimation for longer return periods will deviate even more from the fitted distribution. For the design of the scheme, the observed values for return periods ≤10 years were adopted, and for the longer periods the SCS ones, knowing that the latter are only approximate.

7.2.4 Sediment load

As discussed in Chapter 3, sedimentation (especially heavy texture sediments) in the infiltration basins decreases the efficiency of the recharge. In addition, sedimentation in the water supply and spreading channels decreases the volume of the diverted water, causes damage to the system and increases design and maintenance costs. As no other sources are available, in order to estimate the sediment amount of the correspondent flood events in the study area, the relationship between peak flows (Qp), floodwater volume, sediment concentration and sediment volume of the observed 21 flood events in the Chandab river (Khalilpour et al., 2003) were studied. The result (see Figure 7.7) shows the large year-to-year variation of the quantities involved.

With the aid of regression, the relationships between the variables were analysed. No relationship was found either for the flood peak and sediment concentration, or for the flood volume and sediment concentration (R^2s of 0.0006 and 0.007 respectively). This makes it difficult to obtain a reliable estimate for the sediment yield, and thus the expected amount of sedimentation in the floodwater spreading scheme, by using the standard rating curve procedure. However, several suspended load samples were taken during each runoff event. By taking the average and multiplying it by the volume of discharge, the sediment volume per event was estimated.

The comparison of the number of flood occurrences, floodwater volume and sediment volume for the observed 21 flood events with different return periods in the Chandab river is shown in Figure 7.8. As Figure 7.8 shows, 67% of the total number of observed flood events had a frequency of less than two years. These events generated 20% and 19% of the total floodwater and corresponding sediment volume respectively. Although, the floods with return periods of $2 \leq T \leq 5$ years occurred three times (14%) during the studied seven years, they generated 23% and

18% of the total floodwater and sediment volumes respectively. More than half (57%) of the total floodwater volume was generated by flood events with 5<T≤10 return periods which occurred four times (19%) during the studied period. But these events generated 63% of the total sediment volume.

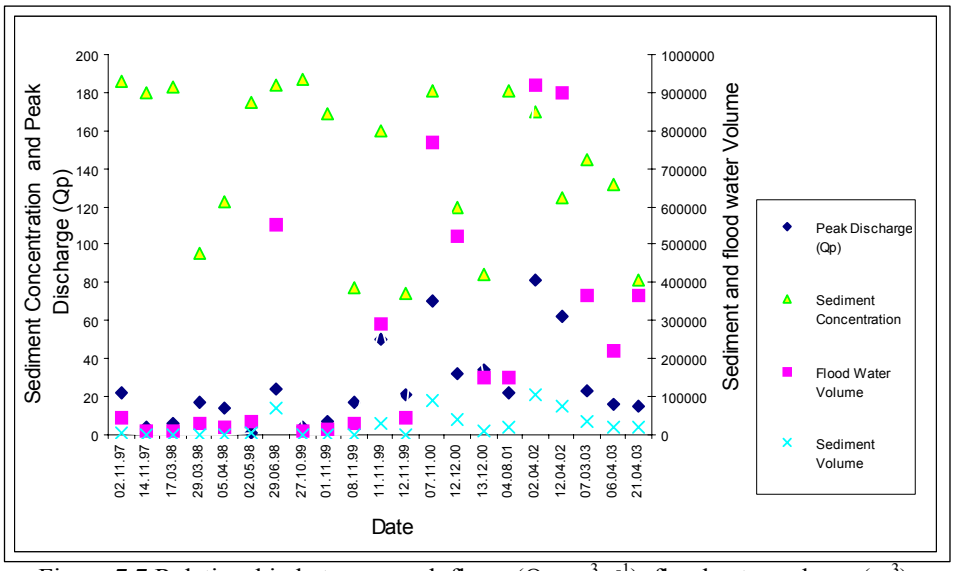

Figure 7.7 Relationship between peak flows (Qp, $m^3 s^{-1}$), floodwater volume (m^3), sediment concentration (gr l^{-1}) and sediment volume (m^3) for the observed 21 flood events in the Chandab river

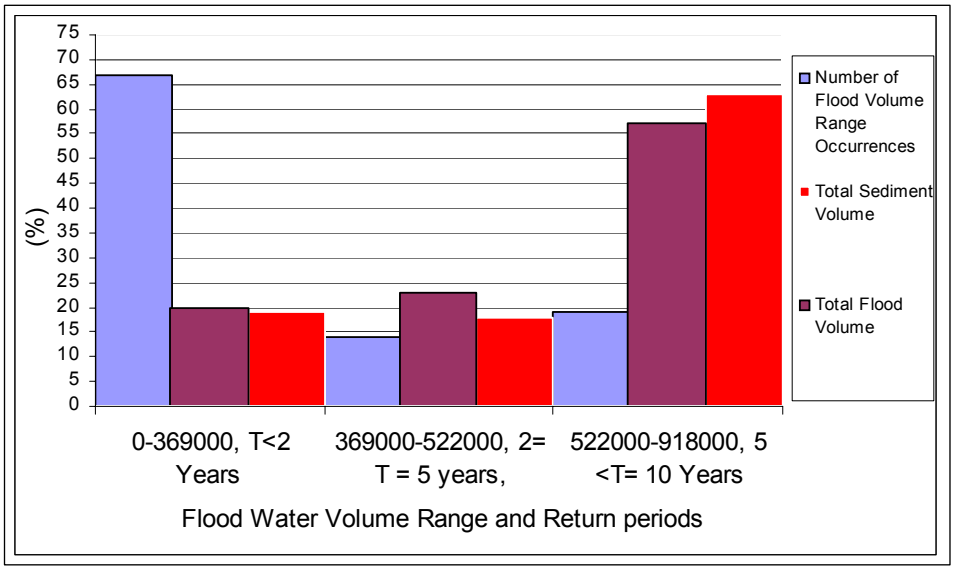

Figure 7.8 Comparison of the number of flood occurrences, floodwater volume range (m^3) and sediment volume for the observed 21 flood events with different return periods in the Chandab river (all expressed as a percentage of total)

7.3 Design considerations

7.3.1 Types of design

As already mentioned (Chapter 2, Section 2.2.3), three main types of design for floodwater spreading schemes have generally been used in Iran:

- schemes with a deep basin
- schemes with canal and basin
- schemes with a long dike

Usually, the deep recharge basin types are designed for artificial groundwater recharge and flood control. The water diverted from the river flows in the deep basins. Each basin is equipped with an inter-basin control structure (such as concrete spillways or control pipes (see Figure 7.9)) that is located at specific elevations to regulate the overflow of water into the next basin. An example of this type of design was discussed in Chapter 4 (Sorkhehesar scheme, Varamin Plain, Tehran, Iran), and the study shows that the recharge efficiency of the system is very high. The advantages of this type are the deep inundation depths, which enhance infiltration and percolation and the relative ease of desilting operations.

The second design type is more adjusted to nature. The floodwater is diverted through the water supply channel to the supply-spreading channel. The supply-spreading channels and the spreading channels are made parallel or nearly so with the contours. One side of the channel acts as a spillway to allow the overflow of a thin layer of water on the land between the spreading channel and the downslope dikes (see Figure 7.10). Each dike is equipped with some spillways, located at specific distances, which transfer water to the lower spreading channel, and the procedure is repeated again. Usually the spillways are constructed with stones, gabions (stone and iron net) or sacks full of soil and some cement.

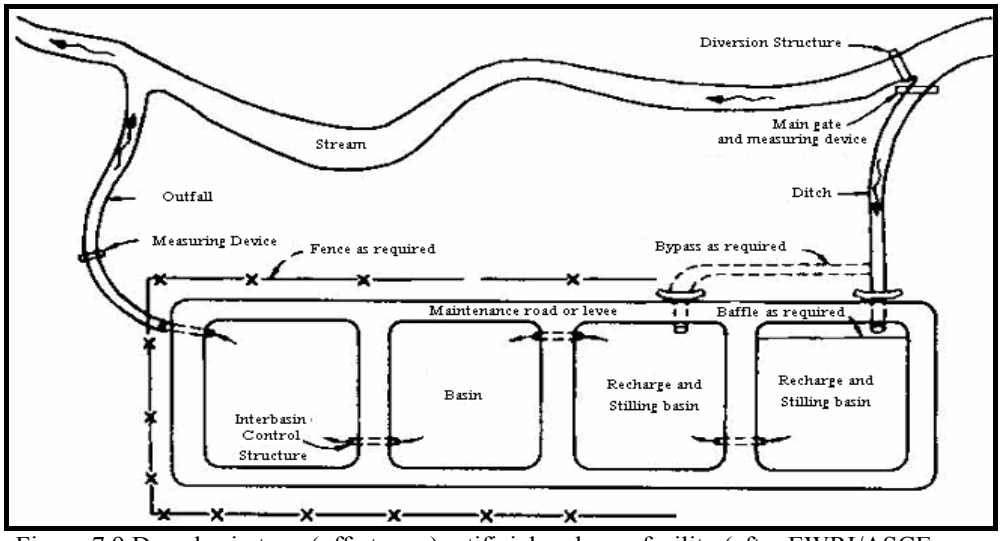

Figure 7.9 Deep basin type (off-stream) artificial recharge facility (after EWRI/ASCE, 2001)

Between the spreading channel and the retention dike is the infiltration area, which is composed of a part where overland flow takes place and a part where ponding occurs. The overflow lasts a few to several hours only; depths are limited and not uniform because of the micro-topography. Therefore, infiltrated water wets only the upper soil, except for some by-pass flow, and that water is lost through evaporation during dry spells after the flood event – as the SWAP simulations indicate. The area and depth of ponding depend on the slope of the terrain and the height of the spillways in the dikes (as indicated in Figure 7.10). The ponding areas, as well as the spreading channels, are the most effective parts for recharge in this type of scheme, but the ponding depths are less than those of the deep basin type of scheme. Heavy textured sediments will be accumulated in the ponding areas and in the spreading canals if they are made level. Desilting operations are expensive because a large surface area will have to be excavated, while use of machinery will compact soil and reduce infiltration.

The third type of design (Figure 7.11) uses very long dikes (e.g. 15 to 16 km) parallel to the contour lines on the alluvial fan in order to capture all the floodwater from the upper part basin. Each dike is equipped with some spillways located at specific distances. This type is recommended if river stability is very low and water intake from the alluvial fan river is not possible or is very expensive and highly risky. In addition, the concentration of flood flow in parts of the canals that are liable to shifts makes the design of the upper dikes and spillways difficult and construction expensive if maintenance costs are to be kept low. Hybrid forms of these types of design also exist, as well as other types.

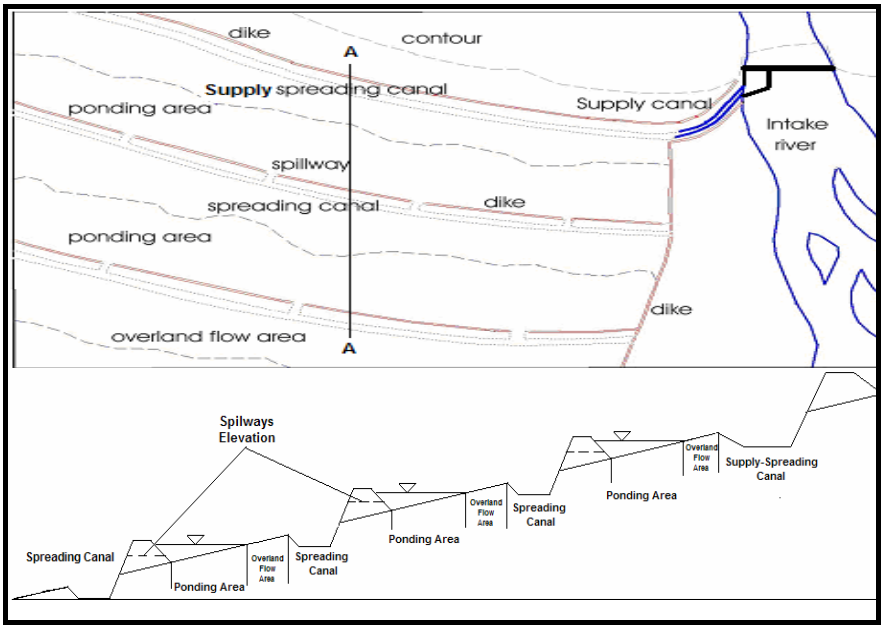

Figure 7.10 Schematic plan and cross section (A-A) of canal and basin type of floodwater scheme

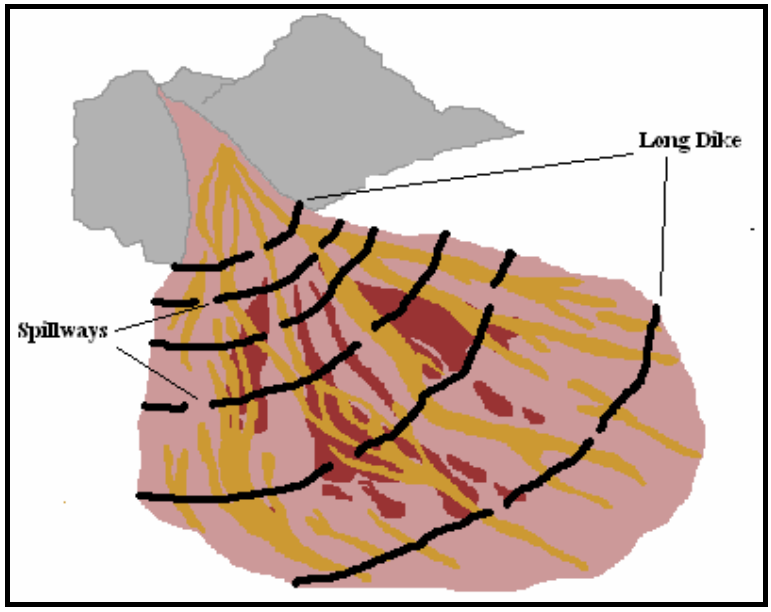

Figure 7.11 Schematic overview of long dike type of floodwater spreading scheme

7.3.2 Design flood

In order to design the scheme(s), three return periods – T≤5 years (short-term period), 5<T≤25 years (medium-term period) and 25<T≤50 years (long-term period) – for the flood and sediment characteristics were selected. As the studied 21 flood events show (Figure 7.8), 81% of the observed flood events had return periods of T≤5 years, while they generated 43% and 37% of the total floodwater and sediment respectively. The rest was generated by flood events with T>5 years.

The Weibull formula for frequency limits the return period of the maximum observed event to the length of record years plus one. However, it is likely that within the six-year period of observation used here, the true but unknown return period of the maximum event was more than seven years. This could be the case for the event annotated with a circle in the frequency plot of Figure 7.6. It was judged that the peak flows obtained by the SCS method were preferable for the design rather than the peak flows obtained by the fitted Log Pearson Type III distribution for return periods of ≥5 years – hence for both the medium-term and long-term design periods. For periods of <5 years, the observed data were used.

For the sediment volume, the averaged sediment concentration for runoff volume of similar observed events was multiplied to find the total weight of the sediment, then using the specific weight of the sediments changed to volume and used.

The comparison of three flood design characteristics is shown in Figure 7.12.

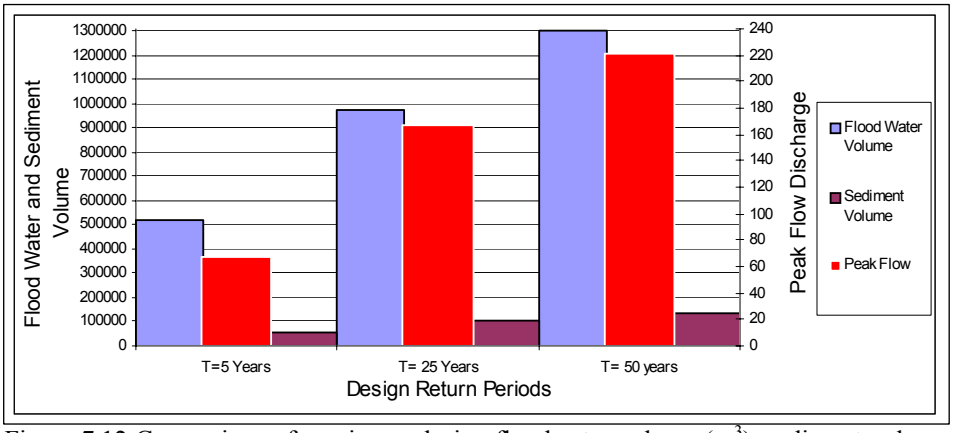

Figure 7.12 Comparison of maximum design floodwater volume (m^3), sediment volume (m^3) and peak discharge ($m^3\ s^{-1}$) rates for three selected return periods

7.3.3 Number of floods

In order to calculate the total harvested water during the lifetime of the project for each of the alternative schemes, the number of flood occurrences and their volumes should be estimated. In this study, as there is no long-term record of flood characteristics, the above observed data and the relationship between rainfall, runoff occurrence and floodwater volume estimated using the SCS method (CN number) were used. To do so, the 20 years of daily rainfall of the Mamloo rainfall station was split into six classes and the floodwater volume for the mean of each class was calculated using the SCS method. The relationship between rainfall, runoff volume and number of flood occurrences is shown in Figure 7.13.

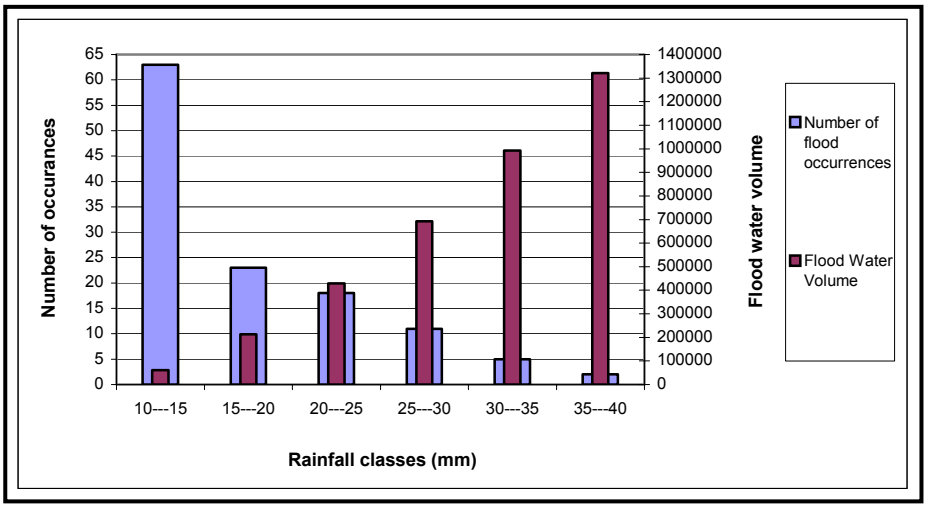

Figure 7.13 Relationship between rainfall, number of flood occurrences and floodwater volume (m^3), estimated using the SCS method

During the 20-year period the total number of events was 122, hence on average about six a year. The probability of occurrences in the various classes is shown in Table 7.7. These data were used to estimate the total volume during a 50-year period.

Table 7.7 The probability of occurrences in the various rainfall and corresponding floodwater volume classes

Rainfall Class (mm)	**1 10-15**	**2 15-20**	**3 20-25**	**4 25-30**	**5 30-35**	**6 35-40**
Floodwater Volume (m^3)	61227	213051	429351	693145	992935	1320656
Probability of Occurrence	0.5083	0.1883	0.1483	0.09	0.417	0.025

7.4 Alternative designs for Chandab

In this phase, the schemes are designed based on two major design types: (1) canal and basin, and (2) deep basin types. In order to evaluate and select the suitable site and design, the costs and benefit criteria for each alternative scheme are estimated.

7.4.1 Canal and basin type

The procedure starts by considering the total area that is available and has suitable properties, which was evaluated earlier (Chapter 6), in order to maximize the potential volume of recharge. A spreadsheet program was developed for the calculations of estimated recharge and costs of construction and maintenance. The program handles single events of different magnitude and takes into account the progressive spreading of water over the scheme for events of larger magnitude. In fact, because of the dynamics of flood spreading, the full representation of what happens is a complex matter. The objective is not to work out a full design but to make a realistic estimate for comparing the costs and benefits of the options open to the decision makers, so simplifications have been made.

The surface of the nominated area (see Figure 7.14) for the scheme design is 253 ha, consisting of two different sites with surface areas of 86 ha and 167 ha respectively. The sites are selected based on different weighted average infiltration rates. Water is diverted to Site I from two intakes (intakes 1 and 2, Figure 7.14), whereas Site II has one intake. The intake locations were selected based on field checks, topography and river conditions/limitations. Based on hydraulic calculations, the intakes were designed in such a way that for the peak flows with 5-year (67 $m^3 s^{-1}$), 25-year (167 $m^3 s^{-1}$) and 50-year (221 $m^3 s^{-1}$) return periods the diverted water to the supply channels remains at the design discharge capacity for each site.

The diverted water from the intake passes through the water supply channel to the supply-spreading channel. The supply-spreading channels are made parallel with contour lines (dead end), which on one side of the channel act as a spillway for overflow to the ponding area. Based on the slope of the site, an elevation difference of 1.2 m between dikes was adopted. The earth dikes are 1 m in height and the height of the spillways in the dikes is 0.5 m above the original land surface. The number and capacity of the spillways are determined in order to ensure a freeboard of 0.2 m during maximum events. With these figures, the overflow area is 34% of

the total area – a fairly large percentage in order to provide safety to the system during prolonged runoff events. Because of the micro-topography, it is assumed that only half of the overflow area (i.e. 17%) is an effective recharge area. The ponding area (see Figure 7.10) and canal areas are 66% of the total area of the site, and the remaining 5% consists of areas occupied by dikes. Thus, the total recharge area is equal to 78%. The calculation procedure is repeated for the successive systems of spreading canal, overflow and ponding that are fed through the spillways in the dikes, using the data contained in the GIS model of the scheme (Figure 7.14).

Infiltration

As mentioned before (Chapter 6), the infiltration rates of the Chandab area (floodwater infiltration sub-part) were measured in the field, and mapped (GIS map) and classified as shown in Figure 7.2. Based on the infiltration map, the weighted average infiltration rates are 80 mm hr^{-1} and 25 mm hr^{-1} for Site I and Site II respectively.

It is useful to note that the infiltration rates are required for designing canals and intakes and the size of the scheme in relation to the maximum volume of intake of river water, and should not be confused with recharge, which is evaluated separately in the various components of the system.

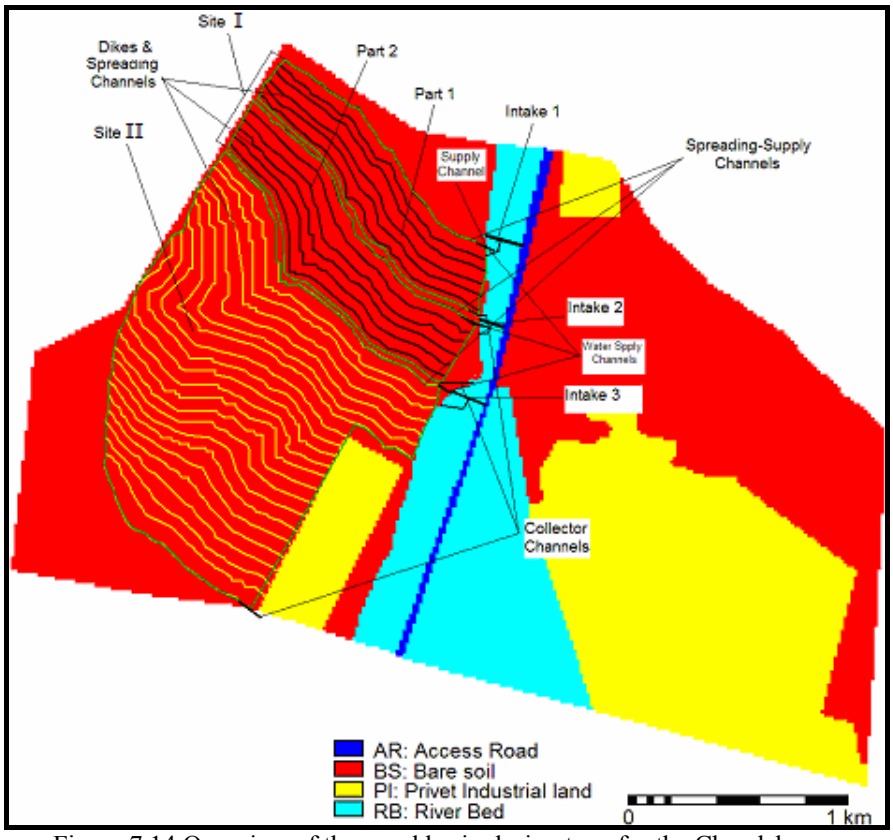

Figure 7.14 Overview of the canal basin design type for the Chandab area

Hydromodule

Based on the infiltration rates, the hydromodules (the term 'hydromodule' is the reciprocal of 'water duty' and thus has units of l s^{-1} ha^{-1}) for the two sites are calculated as follows:

HM_{siteI}= 80 mm hr^{-1}*10^{-3}*(1/3600) *1000*10000=222.22 l s^{-1} ha^{-1}
HM_{siteII}= 25 mm hr^{-1}*10^{-3}*(1/3600) *1000*10000=69.44 l s^{-1} ha^{-1}

As mentioned above, because of the slope between dikes and spreading channels 78% of the land is effective area and acts as a recharge basin. Therefore, the effective area for Sites I and II are 67 ha (0.78*86=67) and 130 ha (0.78*167=130) respectively, and the design (diversion) discharges (Q) for the study sites are equal to:

Q_{siteI} =222.22 l s^{-1} ha^{-1} * 67/1000 ≈ 15 m^3 s^{-1}
Q_{siteII} = 69.44 l s^{-1} ha^{-1} * 130/1000 ≈ 9 m^3 s^{-1}

Water supply channel design for Site I and Site II

The supply channel transfers water from the intake location to the water supply-spreading channel. As mentioned above, the discharge design for Site I is 15 m3s-1. Water will be diverted to the system from two different intakes (Figure 7.15, intakes 1 and 2, each 7.5 m3 s-1) instead of one intake because of the limited length of the water supply-spreading channel, soil characteristics, topography conditions and maximum permissible velocity in the water spreading edge of the water supply-spreading channel.

For Site II the water is diverted to the system from intake 3 (Figure 7.15) with 9 m^3 s^{-1} discharge. The characteristics of the trapezoidal supply channels for Site I and Site II are shown in Table 7.8.

Table 7.8 The characteristics of the supply channels of Site I and Site II

Channel	Q (m^3 s^{-1})	Slope	Side Walls Slope (Z)	Bed Width (m)	Depth (m)	Channel Length (m)	Manning Coefficient (n)
Site I, Part1	7.5	0.001	2.5	8	0.74	246	0.0225
Site I, Part2	7.5	0.001	2.5	8	0.74	170	0.0225
Site II	9	0.001	2.5	9	0.78	160	0.0225

Water supply-spreading channel design for Site I and Site II

The first, most upslope, channel is called the water supply-spreading channel and has a larger width and depth than the other spreading channels in the scheme. It should be noted that the dimensioning of this channel has hydraulic limitations. The maximum discharge capacity adopted for Site I was 7.5 m3s-1 and for Site II 9 m3s-1 because of the greater length of the supply-spreading channel, and these capacities are reflected in the design of the intakes.

These channels are parallel to the contour line and receive the water from first and second supply channels, spreading it to the two parts of Site I. The slope of

the first part of these channels is 0.003% for 85% of its length and the rest is 0%. This type of channel has a dead end and also acts as a stilling and recharge basin. The characteristics of the trapezoidal supply-spreading channels are shown in Table 7.9.

It should be considered that for the design of the supply-spreading channel the flow velocity at the edge of the spreading side should be less than permissible velocity, otherwise the soil between channels will be eroded. According to the lengths of the supply-spreading channels, inflow discharges (7.5 and 9 $m^3 s^{-1}$) and hydraulic calculations, the flow velocity at the edges of the spreading sides are less than the permissible velocity.

Table 7.9 The characteristics of the supply-spreading channels of Site I

Channel	Q ($m^3 s^{-1}$)	Slope	Side Walls Slope (Z)	Bed Width (m)	Depth (m)	Channel Length (m)	Manning Coefficient (n)
Site I, Part 1	7.5	0.003	2.5	8	1.05	1314	0.0225
Site I, Part 2	7.5	0.003	2.5	8	1.05	1489	0.0225
Site II	9	0.003	2.5	9	1.05	1594	0.0225

Spreading channel design for Site I and Site II

These channels are developed on the contour lines with 1.2 m elevation difference and zero slopes. Both sides of the channels have dead ends and are located just below the soil dike of each basin. The hydraulic characteristics of the spreading channels of Site I (Part 1 and Part 2) and Site II are shown in Tables 7.10, 7.11 and 7.12 respectively.

It should be considered that for the spreading channels in the lower parts a lesser width could have been selected. However, because of operational problems and more safety (after some flooding events the capacity of the channels and the infiltration rates decrease) the larger bed width of the spreading channels is to be preferred.

Table 7.10 The hydraulic characteristics of the spreading channels of Part 1

Channel Type	Depth (m)	Length (m)	Basin Effective Area Size (ha)	Channel Area Size (ha)	Bed Width (m)	Inflow ($m^3 s^{-1}$)	Infiltrated Water through the Channel ($m^3 s^{-1}$)	Infiltrated Water through the Basin ($m^3 s^{-1}$)	Outflow ($m^3 s^{-1}$)
Supply-Spreading	1.05	1314	4.65	1.79	8	7.5	0.4	1.03	6.07
Spreading 1	0.5	1341	4.75	0.9	4	6.07	0.2	1.06	4.81
2	0.5	1375	4.98	0.92	4	4.81	0.204	1.11	3.5
3	0.5	1388	5.11	0.93	4	3.5	0.21	1.14	2.15
4	0.5	1430	5.12	0.96	4	2.15	0.21	1.14	0.8
5	0.5	1476	5.26	0.99	4	0.8	0.22	0.58	0

Table 7.11 The hydraulic characteristics of the spreading channels of Part 2

Channel Type	Depth (m)	Length (m)	Basin Effective Area Size (ha)	Channel Area Size (ha)	Bed Width (m)	Inflow ($m^3 s^{-1}$)	Infiltrated Water through the Channel ($m^3 s^{-1}$)	Infiltrated Water through the Basin ($m^3 s^{-1}$)	Outflow ($m^3 s^{-1}$)
Supply-Spreading	1.05	1489	3.39	2.03	8	7.5	0.45	0.75	6.3
Spreading 1	0.5	1483	5	0.99	4	6.3	0.22	1.11	4.97
2	0.5	1501	5.17	1	4	4.97	0.22	1.15	3.60
3	0.5	1507	5.29	1	4	3.60	0.22	1.18	2.20
4	0.5	1541	5.33	1.03	4	2.20	0.23	1.18	0.79
5	0.5	1551	5.36	1.04	4	0.79	0.23	0.56	0

Table 7.12 The hydraulic characteristics of the spreading channels of Site II

Channel Type	Depth (m)	Length (m)	Basin Effective Area Size (ha)	Channel Area Size (ha)	Bed Width (m)	Inflow ($m^3 s^{-1}$)	Infiltrated Water through the Channel ($m^3 s^{-1}$)	Infiltrated Water through the Basin ($m^3 s^{-1}$)	Outflow ($m^3 s^{-1}$)
Supply-Spreading	1.05	1594	3.48	2.34	9	9	0.16	0.24	8.6
Spreading 1	0.5	1641	5.49	1.1	4	8.6	0.08	0.38	8.14
2	0.5	1682	5.54	1.13	4	8.14	0.08	0.38	7.68
3	0.5	1681	6.07	1.13	4	7.68	0.08	0.42	7.18
4	0.5	1752	6.21	1.17	4	7.18	0.08	0.43	6.67
5	0.5	1835	6.5	1.23	4	6.67	0.09	0.45	6.13
6	0.5	1873	6.53	1.25	4	6.13	0.09	0.45	5.59
7	0.5	1561	6.36	1.04	4	5.59	0.07	0.44	5.08
8	0.5	1572	5.74	1.05	4	5.08	0.07	0.40	4.60
9	0.5	1648	5.03	1.10	4	4.60	0.08	0.35	4.18
10	0.5	1280	4.56	0.86	4	4.18	0.06	0.32	3.80
11	0.5	1304	4.67	0.87	4	3.80	0.06	0.32	3.42
12	0.5	1276	4.33	0.85	4	3.42	0.06	0.30	3.06
13	0.5	1304	4.30	0.87	4	3.06	0.06	0.30	2.70
14	0.5	1161	4.34	0.78	4	2.70	0.05	0.30	2.34
15	0.5	1193	4.33	0.80	4	2.34	0.06	0.30	1.99
16	0.5	1115	4.36	0.75	4	1.99	0.05	0.30	1.63
17	0.5	1072	4.44	0.72	4	1.63	0.05	0.31	1.27
18	0.5	1059	4.47	0.71	4	1.27	0.05	0.31	0.92
19	0.5	1029	4.46	0.69	4	0.92	0.05	0.31	0.56
20	0.5	1027	7.34	0.69	4	0.56	0.05	0.51	0.00

Spillways design for Site I and Site II

As mentioned before, each dike of the spreading channels is equipped with some spillways located at specific distances, which transfer the ponded water from the upper part basin behind the dike to its lower spreading channel. Based on hydraulic calculations and the topographical conditions of the areas, the characteristics of the spillways for Part 1, Part 2 (Site I) and Site II are shown in Tables 7.13, 7.14 and 7.15 respectively.

Table 7.13 The characteristics of the spillways located on the dikes of Part 1 (Site I)

Spreading Channel No.	Number of Spillways	Total Inflow ($m^3 s^{-1}$)	Outflow of Each Spillway ($m^3 s^{-1}$)	Distance of Spillways (m)
1	9+1	6.07	0.61	130
2	8+1	4.81	0.56	150
3	9+1	3.5	0.36	150
4	7+1	2.15	0.27	200
5	6	0.8	0.13	250

Table 7.14 The characteristics of the spillways located on the dikes of Part 2 (Site I)

Spreading Channel No.	Number of Spillways	Total Inflow ($m^3 s^{-1}$)	Outflow of Each Spillway ($m^3 s^{-1}$)	Distance of Spillways (m)
1	10	6.3	0.61	150
2	8+1	4.97	0.56	170
3	10	3.60	0.36	140
4	8	2.20	0.27	180
5	6	0.79	0.13	260

Table 7.15 The characteristics of the spillways located on the dikes of Site II

Spreading Channel No.	Number of Spillways	Total Inflow ($m^3 s^{-1}$)	Outflow of Each Spillway ($m^3 s^{-1}$)	Distance of Spillways (m)
1	12	8.6	0.72	140
2	11+1	8.14	0.72	140
3	12+1	7.68	0.61	130
4	11+1	7.18	0.61	150
5	11+1	6.67	0.56	150
6	10+1	6.13	0.56	170
7	9+1	5.59	0.56	160
8	9	5.08	0.56	175
9	10+1	4.60	0.43	150
10	9+1	4.18	0.43	130
11	10+1	3.80	0.36	120
12	9+1	3.42	0.36	130
13	8+1	3.06	0.36	150
14	9+1	2.70	0.29	120
15	8	2.34	0.29	150
16	6+1	1.99	0.29	160
17	9	1.63	0.18	120
18	7	1.27	0.18	150
19	7	0.92	0.13	150
20	4+1	0.56	0.13	200

7.4.2 Deep basin type

The most common design for the deep basin type consists of more or less rectangular basins that are excavated in a cascade, such as the Sokhehesar scheme discussed earlier. However, the slope of the Chandab site prohibits such a design because of the staggering costs of earth movement, and therefore the design used here consists of relatively high dikes along contours in order to make best use of the most permeable part of the area available and the enhanced recharge under deep ponding.

The design is based on the maximum floodwater volume with a 50-year return period (1,400,000 m^3 with about 10% safety because of short period data). The average flooding duration based on observed data is about 15 hrs. Therefore,

the design discharge is equal to 1,400,000/(15*3600) = 26 m^3 s-1. The water is diverted from one intake. The intake was designed in such a way that for the flood peak flows with return periods 5, 25 and 50 years the diverted water to the scheme remains the same.

The characteristics of the basins and dikes

Based on the topography and slope of the area, the deep dikes of the scheme are designed parallel to the contour lines with 3 m elevation difference. The maximum water depth (H_{max}) is 2 m behind the lower part dike of each basin. According to the calculations, the average depth (H_{ave}) of the basins should be half of the H_{max}, in order to store the volume difference (basin volume, V_B) between the total volume calculated based on diversion discharge (Q_d) and flood duration (T_{FD}) and infiltrated water volume (V_R) calculated based on hydromodules of the basins. An overview of the dike characteristics and the location of the soil cut/fill are shown in Figure 7.15.

Calculation of the surface area of the scheme

In order to calculate the design surface area for the scheme, the hydromodule of the area is used. The surface area of this type is divided to two parts: the first part consists of stilling-recharge (S-R) basins and the second part consists of recharge basins (R). The sediments of the diverted water are settled in the stilling-recharge basins and the clean water overflows to the recharge basins. For this study, it is supposed that the shares of each part are equal to 50%. The infiltration rate of the stilling-recharge basins will be decreased because of sedimentation. Because of the high capacity of the basins, removal of the sediment from the stilling-recharge basins takes place after a few years. It is supposed that after sedimentation the infiltration rate of the stilling-recharge basin decreases by 50%. Therefore, the surface area of the scheme is calculated as follows:

HM_R =80 mm hr^{-1}*10^{-3}*(1/3600) *1000*10000=222.22 l s^{-1} ha^{-1}
HM_{S-R} =40 mm hr^{-1}*10^{-3}*(1/3600) *1000*10000=111.11 l s^{-1} ha^{-1}
QR=0.5*A*HMs/1000+0.5*A*HM_R/1000
QR=0.5*A*(111.11)/1000+ 0.5*A*222.22/1000=0.17A m^3 s^{-1}
VR=TFD* QR→VR= 15hr*3600 s hr^{-1} *0.17A m^3 s^{-1}=9180A m^3
Q_d=26 m3 s^{-1}, TFD =15 hr, V_d= Q_d * TFD =26 m^3 s^{-1}*15hr*3600 s hr^{-1} =1404000 m3
VB= Vd-VR=1404000 m^3 - 9180A m^3
H_{ave}= VB/A=(1404000 m^3 - 9180A m^3)/(A ha*10000 m^2 ha^{-1})
If H_{max}=2.0 m, H_{ave}=H_{max}/2=1.0 m→1.0=(1404000- 9180A)/10000 A→ A=74 ha

Based on the height of the dikes and maximum permissible water depth behind the dikes, 66% of the area between dikes acts as an effective recharge basin and 34% is active during flooding events when the spillways are working, and half of that (17%) was considered as effective or recharge area. The dikes will cover on average 10% of the total surface area. As a result, the total recharge or effective

area between dikes is equal to 73% (66-10+17) of the surface area. Considering the calculated effective percentage, the design scheme surface area is equal to 102 ha. Because of topographical conditions, the area is set at 110 ha and the design discharge selected is 30 m^3 s^{-1} instead of 26 m^3 s^{-1}. An overview of the scheme is shown in Figure 7.16.

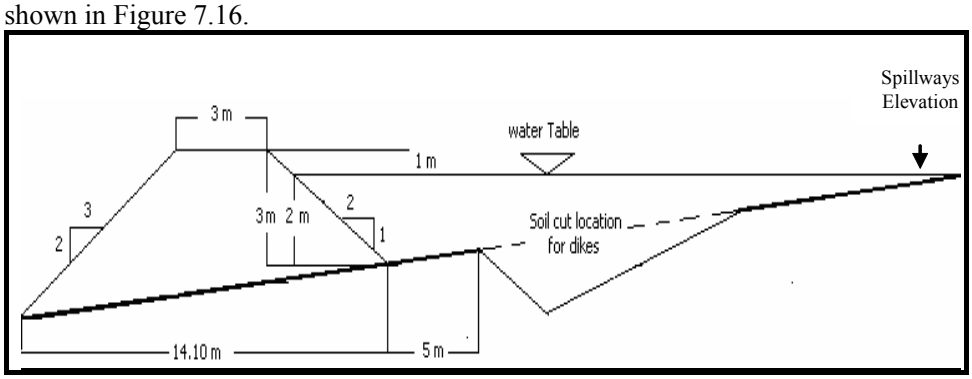

Figure 7.15 Overview of the designed dikes for the scheme (scale is not correct)

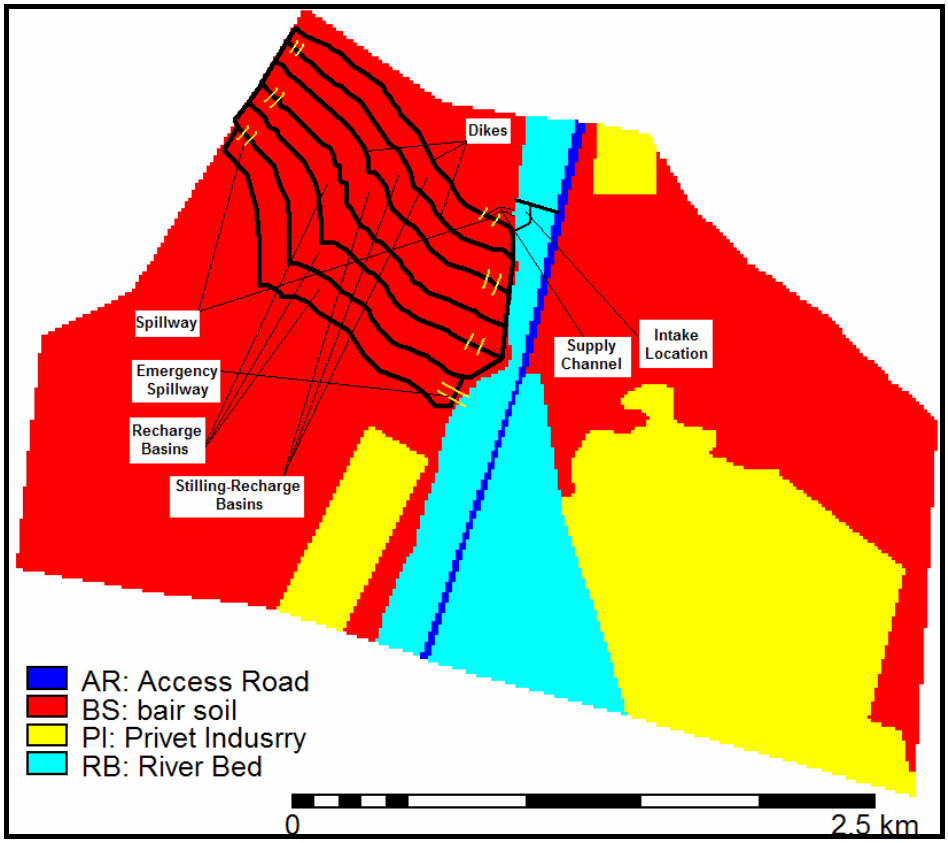

Figure 7.16 Overview of deep basin type design

Water supply channel design for the scheme

The supply channel transfers water from the intake location to the first recharge-stilling basin. As mentioned above, the discharge design for the scheme is 30 m^3s^{-1}. The hydraulic characteristics of the concrete supply channel are shown in Table 7.16.

Table 7.16 The characteristics of the main water supply channel

Channel	Q (m^3 s^{-1})	Slope	Side Walls Slope	Bed Width (m)	Depth (m)	Channel Length (m)	Manning Coefficient (n)
Supply	30	0.001	2.5	10	1	246	0.011

Spillway design for the scheme

The lower dike of each basin is equipped with one spillway, which allows overflow of water to a lower basin. The location of the spillways and the hydraulic characteristics of the spillways and basins are shown in Figure 7.16 and Table 7.17 respectively.

Table 7.17 The hydraulic characteristics of the scheme spillways and basins

Dike No.	Dike Length (m)	Average Dike Volume (m^3)	Average Width of Basin	Basin Effective Area Size (m^2)	Inflow Volume (m^3) (for 15 hr flood duration)	Basin Storage Volume (m^2)	Basin Recharged Discharge (m^3 s^{-1})	Outflow Volume (m^3)	Inflow Discharge (m^3 s^{-1})	Outflow Discharge Concrete Spillway Capacity (m^3 s^{-1})
1	1321	8838	-	-	-	-	-	-	30	30
2	1393	38405.01	110	14.9175	1620000	153252	1.66	1377244	30	28.3
3	1474	40638.18	95	13.6756	1377244	151201	1.52	1152207	28.34	26.8
4	1591	43863.87	120	18.442	1152207	192503	4.10	783663	26.82	22.7
5	1657	45683.49	99	16.0639	783663	174830	3.57	485732	22.72	19.2
6	1629	44911.53	114	18.7598	485732	231302	4.17	148719	19.16	15.0
7	1666	45931.62	112	18.5285	148719	230007	4.12	0	15.00	0.0

7.5 Costs and benefits

Although there are different benefits such as job creation, immigration control, and so on, in this study the benefit criteria for the alternative schemes are estimated based on the total recharged/harvested water and on the benefits resulting from flood damage mitigation. The decision criteria structure for evaluating the alternative schemes is shown in Figure 7.17. The suitability of the alternative schemes is evaluated based on cost and benefit criteria. The cost criterion is estimated based on construction and maintenance cost indicators and the benefit criterion is estimated based on the indicators flood mitigation/control and volume of harvested water.

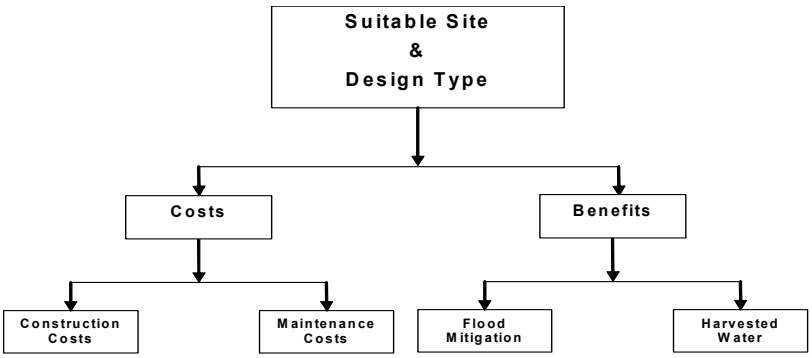

Figure 7.17 The decision criteria structure for suitable site and design type selection

7.5.1 Construction costs

The costs were calculated for the various options and magnitudes of events. For the channel and basin type, gabions for the intake were considered, earth channels only and simple spillways in the dikes. Total lengths, volumes and number of channels and spillways were determined using the GIS data for the scheme and its alternatives and the spreadsheet model. For the deep basin type, larger and heavier gabions were adopted and a concrete supply channel with distribution box and concrete spillways between the infiltration basins. For the maintenance costs, only desilting operations and repairs were included, no personnel and administrative costs. Prices were based on current rates in Iranian currency and converted to euros. The basic data are shown in Table 7.18.

The amount of recharge water and the associated costs for events of different magnitude are shown in Figure 7.18. Although there is a common minimum expenditure for the intake and supply channel, the lowest cost per unit of water is obtained when only Site I, Part 1 is used, but the total amount of recharge that this part of the scheme can accept is less than 300,000 m^3 because of the size limitation of the area. The costs for the full channel and basin type of scheme per unit of water are higher because three intakes are required, but the system has a capacity that allows some 800,000 m^3 of water. Minor breaks in the slope of the curve are related to activation of the successive parts for larger volumes. The deep basin type has much higher minimum costs because of the more expensive intake, and the breaks in the slope of the curve reflect the increasing number of basins when inflow volumes increase. This type of scheme has the largest capacity, a capacity of about 1,400,000 m^3 of water.

Table 7.18 The construction and maintenance costs of the alternative schemes for an event with 67 $m^3 s^{-1}$ discharge and 15-hour flood duration

Scheme		Diverted Discharge ($m^3 s^{-1}$)	Diverted Water Volume (m^3)	Recharged Water Volume (m^3)	Construction and maintenance costs												Total Costs (€)
					Intake (1000 m^3)		Supply Channel (1000 m^3)		Channels (1000 m^3)		Dikes and Access Road (1000 m^3)		Spillways (number)		Removing Sediments and Repair Structures (1000 m^3)		
					Amount	Price per unit (€)	Amount	Price per unit (€)	Amount	Price per unit (€)	Amount	Price per unit (€)	Amount	Price per unit (€)	Amount	Price per unit (€)	
Site I Canal and Basin	Part 1	7.5	405000	263013	860	4	1793	2	32866	1.5	37113	1.5	43	50	40266	1	154411
	Part 2	7.5	405000	267948	713	4	1239	2	32577	1.5	44914	1.5	43	50	40599	1	164318
	Part 1 + Part 2	15	810000	530961	1573	4	2520	2	65444	1.5	82028	1.5	86	50	80865	1	317704
Site II		9	486000	297117	577	4	1281	2	79873	1.5	89948	1.5	151	50	48977	1	316128
SiteI+SiteII		24	1296000	828078	2150	4	4314	2	145316	1.5	171976	1.5	237	50	129842	1	634857
Deep Basin		30	1620000	1308512	1125	4	3325	15	0	1.5	304180	3	7	2000	159503	1	1140420

Water diverted by the intake was determined as a function of the various river discharges, which have been expressed as an average discharge (i.e. volume/ duration), followed by estimation of the recharge in the scheme and calculation of the cost per cubic metre of water recharged. Calculations were made up to 67 $m^3 s^1$, which is the peak flow discharge with five-year return period; larger discharges in the river do not affect the intake capacities, which have set maxima.

The results, split up for the various components of the scheme (or options) in Figure 7.19, show high costs per unit of water gained when small amounts of water are diverted. Costs decrease rapidly for the larger amounts of water diverted, up to about 30 $m^3 s^{-1}$, and tend to stabilize for the largest volumes, demonstrating the economy of scale effect. On an event basis, Site I has the lowest cost per unit of water, and the deep basin type takes an intermediate position when the costs of Site II are considered.

7.5.2 Lifetime and maintenance

The lifetimes of the alternative schemes were calculated based on the sedimentation in the infiltration basins. Different sediment samples of the Chandab river and laboratory tests indicate that about 40% of the sediment consists of clay. In this study, it is supposed that 60% of the clay materials are settled in the spreading channels and the rest are spread in the infiltration basins. Although simulation results did show some recharge for 30 cm of clay under deeper ponding, the fact that the clays in Chadab have montmorillonite – and as a conservative estimate – it is assumed that when much clay has accumulated in the infiltration basins of the canal and basin type of scheme, no recharge takes place.

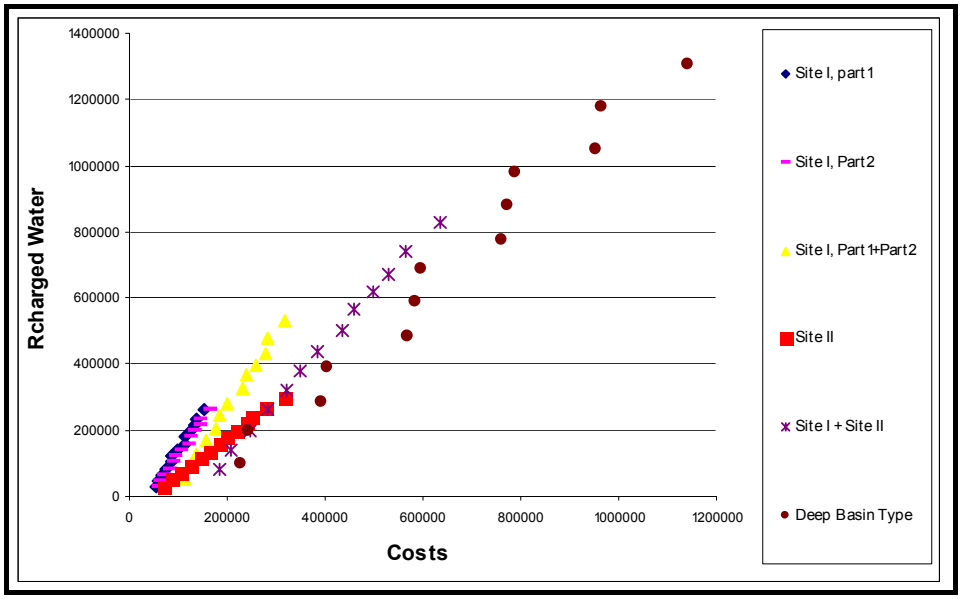

Figure 7.18 Relationship between cost (euro) and recharged water volume (m3) for the alternative schemes per event

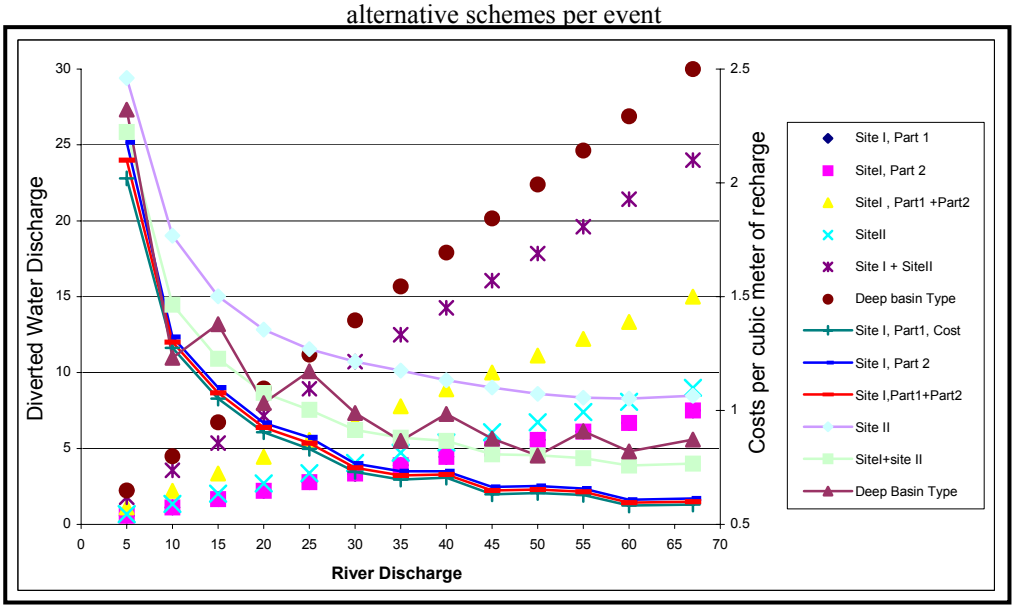

Figure 7.19 Relationship between river discharges ($m^3 s^{-1}$), diverted water discharges ($m^3 s^{-1}$) and cost (euro) per cubic metre recharged water for the alternative schemes

The adopted maintenance for this type of scheme consists of annual desilting of the supply channels, the supply-spreading channel and the spreading channels only, because of the large cost of desilting the infiltration basins, which would be accompanied by compaction. Therefore, the lifetime of these schemes was

calculated based on the time it takes for the successive silting up of the effective area (ponding area) of all the infiltration basins by clay.

For the deep basin type scheme, maintenance is not yearly. After the silting up of the stilling-recharge basins (in this case about 12 years), the maintenance is started and the stilling-recharge and recharge basins are desilted. The lifetime of this type of scheme is very long and depends on the lifetime of the hydraulic structures, which in this case is at least 50 years.

7.5.3 Volume of harvested water

Using the spreadsheet model with simplified dynamics of the successive spreading of water over both types of scheme and the corresponding water depths, the recharge and evaporation are estimated using the MG PTF for the soil textures in the Chandab site. It may be remembered that these functions performed best in the evaluation of the nearby Sorkhehesar scheme.

The relationship between river discharge (m^3 s^{-1}), recharged water volume (m^3) and recharge efficiency for the alternative schemes (15-hour flood duration and single event) is shown in Figure 7.20. Figure 7.20 shows that the deep basin type has the largest total water capacity of the scheme and highest recharge efficiency. The recharge efficiency rate of Site II (see Figure 7.14) is the lowest. The total harvested water for the scheme life period depends on the number of flood occurrences per year. The number of flood occurrences in the study area (six times a year) and the probability of occurrences of each rainfall/runoff class were discussed in Section 7.3.3. In order to estimate the total harvested floodwater volume, average river discharge (m^3 s^{-1}) for each class of the calculated floodwater volumes using the SCS method (Table 7.7) were estimated based on average flood duration of the observed flood events (15 hrs), as shown in Table 7.19. With that data and by taking six yearly flood events during the lifetime of each alternative scheme, the total volume of water entering the schemes was estimated. By considering the information on the lifetime of the infiltration/recharge-stilling basins, the knowledge of recharge efficiency (Chapter 4 and Chapter 3) and the yearly amount of recharged water, finally the total harvested water during the lifetime of each alternative scheme was estimated.

Table 7.19 Average discharges and probability of occurrence for the rainfall/runoff calculated using SCS method in the Chandab area

Rainfall Class (mm)	**1 10-15**	**2 15-20**	**3 20-25**	**4 25-30**	**5 30-35**	**6 35-40**
Floodwater Volume (m^3)	61227	213051	429351	693145	992935	1320656
Probability of Occurrence	0.5083	0.1883	0.1483	0.09	0.417	0.025
Average Discharge (m^3 s^{-1})	1.14	4	8	13	19	25

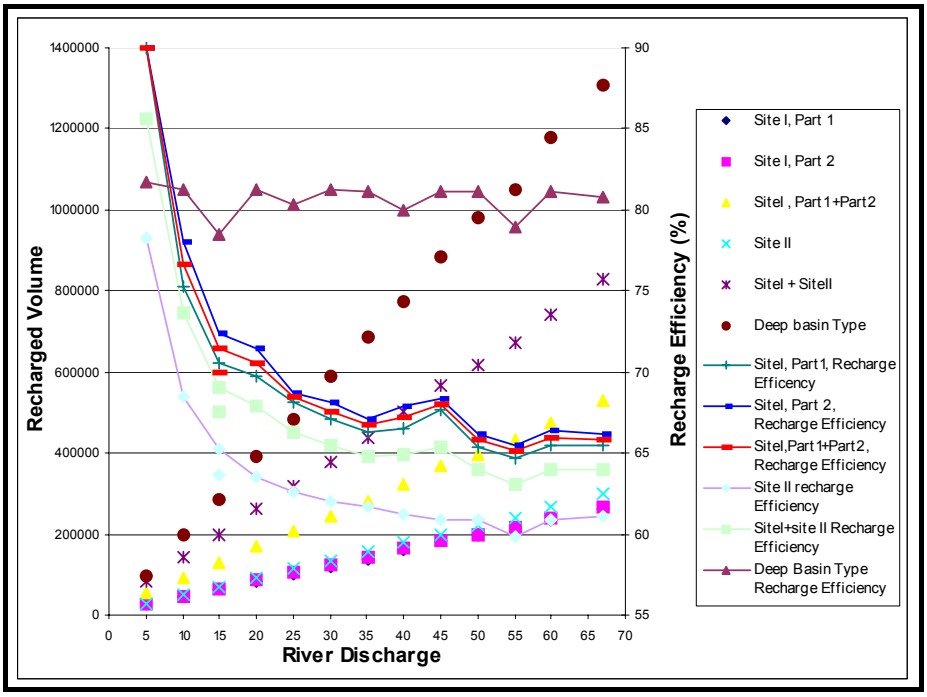

Figure 7.20 Relationship between river discharge (m^3 s^{-1}), recharged water volume (Q_R, m^3) and recharge efficiency for the alternative schemes for single events of different magnitude

7.5.4 Flood mitigation

The available information on damage (Khalilpour et al., 2003) attributable to the Chandab river flood events, as related to specific floodwater volumes and peak discharges, is shown in Table 7.20.

Table 7.20 Flood damage expressed as annual values for different flood event categories in the Chandab area

Observed Peak Discharge (m^3 s^{-1})	Observed Floodwater Volume (1000 m^3)	Observed Damage (€1000; annual average)			
		Agricultural Lands	Houses	Infrastructures	Total
>111	≥1000	70	12	84	166
82-111	700≥V<1000	22	3	51	76
70-81.4	500 >V<700	21	-	45	66

As the content of Table 7.20 shows, the flood events with peak discharge less than 70 m^3 s^{-1} and flood volume less than 500,000 m^3 do not create flood damage.

For a first estimate of the benefit of flood reduction, it was considered how much attenuation of flood peaks and flood volumes was achieved by the scheme alternatives and the information of Table 7.20.

As will be discussed below, the effect of flood damage mitigation is substantial when the overall costs and benefits are compared.

7.6 Results and discussion

The global benefits and costs of the various design options for a floodwater spreading scheme in the Chandab area have been worked out, with the above-mentioned assumptions and limitations concerning estimated recharge, construction and maintenance. Costs have been expressed in euros per m3 of recharge water. The results for a lifetime of about 50 years – a more precise time depends on the scheme alternative – are shown in Table 7.21. Table 7.21 shows the choices that can be made by decision makers. If the choice is made for maximizing the amount of recharge, the deep basin type should be selected, but at the highest total cost if the benefits of flood mitigation are not considered. An alternative is the Site I + II option, with lower costs but also less recharged water. In the case where expenditure has to be kept as low as possible, option Site I, Part 1 could be selected, but the total volume of water gained is limited.

When savings are made through flood mitigation, the situation changes. In the last table column, negative values are listed because the benefits exceed the costs. It should be remembered that the estimate of the benefit of flood mitigation is a rough one.

Although the content of Table 7.21 speaks for itself, so to say, making a choice is perhaps not that simple, considering the various factors involved, which could be expanded by more alternatives offered by hybrid schemes, and by more economic values. Therefore, a weighting procedure may be used, placing emphasis on what a decision maker may consider the most important aspect or main suitability. This procedure consists of the suitability value estimation (see [7.3] below: simply a summation of weights or preference given multiplied by the quantity involved, after standardization, for the main criteria total cost and total benefit, or for the four sub-criteria construction costs (Co), maintenance costs (Ma), volume of recharged or harvested water (Ha), and savings made by flood mitigation (FM).

$$SV = \Sigma (W*q_s) \qquad [7.3]$$

Where, SV = suitability value, W= weight, and qs=standardized quantity. For the sake of simplicity, equal weights were assigned (0.5 and 0.5) or a preference was given a double weight (0.67 counterbalanced by a weight of 0.33 because the sum of weights has to be unity). The following combinations can be made, whereby changing the weights will increase the range of suitability values, but not the highest rank.

Table 7.21 Costs and benefits estimation for all the alternative schemes

Scheme Type		Main Criterion		Total Costs	Main Criterion		Life-time (year)	Costs per m^3 Water (€)	
		Costs (€1000)			Benefits				
Canal and Basin	Deep Basin Type Site	Sub-criterion	Sub-criterion		Sub-criterion	Sub-criterion		Without Flood Mitigation Benefit	Considering Flood Mitigation Benefit
		Construction	Maintenance[6]		Harvested Water ($1000m^3$)	Flood Mitigation (€1000)			
Site I, Part 1		114	394	508	6321	0	45	0.0803	0.0803
Site I, Part 2		124	381	505	5087	0	37	0.0993	0.0993
Site II		267	1004	1272	10227	0	50	0.1244	0.1244
Site I, Part 1 + Part 2		238	775	1013	11408	1254	37-45	0.0888	-0.0211[7]
Site I + Site II		505	1780	2285	21635	2312	37-50	0.1056	-0.0012
	Deep Basin Scheme	981	2032	3013	28606	3922	50>	0.1053	-0.0318

Equal weights only for sub-criteria

The suitability values on a scale of 0 to 1 for equal preferences for all sub-criteria but different weights for the main criteria are shown in Table 7.22. The deep basin scheme has the highest suitability value (0.7176) if benefits weigh most heavily, and Site I, Part 1 or Site I, Part 1+Part 2 if the costs are a main consideration. Suitability values for other combinations take an intermediate position, as shown in the table.

Table 7.22 Estimated suitability values (SV) for the alternative schemes

Scheme	Weight		Weight		Weight	
	Cost	Benefit	Cost	Benefit	Cost	Benefit
	0.5	**0.5**	**0.33**	**0.67**	**0.67**	**0.33**
Site I, Part1	0.5536		0.4056		0.7016	
Site I, Part 2	0.5419		0.3906		0.6932	
Site II	0.4737		0.3752		0.5723	
Site I, Part 1+Part 2	0.5996		0.5193		0.6798	
Site I+Site II	0.5647		0.6008		0.5285	
Deep Basin Scheme	0.5759		0.7176		0.4323	

[6] The maintenance costs include mainly desiltation of the channels (for both types) and basins (deep basin type only).

[7] The negative costs mean that the total benefits of flood mitigation are more than the total costs.

Equal weights only for main criteria

When costs and benefits are considered of equal preference, but not the sub-criteria, as indicated in Tables 7.23 and 7.24, the range of variation in the suitability values is less than in the above case. The highest suitability is obtained for Site I, Part 1+Part 2 if preference is given to volume of harvested water and initial costs for construction are considered to be more of a problem than maintenance costs.

More weight to the main cost criterion

When the main criterion cost is weighted twice as much as the criterion benefit, suitability values vary with permutations of weightings of the sub-criteria, as shown in Tables 7.25 and 7.26. Obviously, the relatively cheap Site I, Part 1 has the highest suitability, but little water is recharged. The deep basin type now has the lowest suitability values.

Table 7.23 Estimated suitability values for the alternative schemes

Scheme	Weight				Weight				Weight				Weight			
	Cost		Benefit		Cost		Benefit		Cost		Benefit		Cost		Benefit	
	0.5		0.5		0.5		0.5		0.5		0.5		0.5		0.5	
	Co.	Ma.	Ha.	FM	Co.	Ma.	Ha.	FM	Co.	Ma.	Ha.	FM	Co.	Ma.	Ha.	FM
	0.33	0.67	0.5	0.5	0.67	0.33	0.5	0.5	0.5	0.5	0.33	0.67	0.5	0.5	0.67	0.33
Site I, Part 1	0.5531				0.5542				0.5352				0.5521			
Site I, Part 2	0.5428				0.5411				0.5271				0.5567			
Site II	0.4612				0.4863				0.4439				0.5036			
Site I, Part 1+Part 2	0.5939				0.6052				0.593				0.6062			
Site I+Site II	0.5405				0.5889				0.5507				0.5786			
Deep Basin Scheme	0.5819				0.57				0.5759				0.5759			

Table 7.24 Estimated suitability values for the alternative schemes

Scheme	Weight				Weight				Weight				Weight			
	Cost		Benefit		Cost		Benefit		Cost		Benefit		Cost		Benefit	
	0.5		0.5		0.5		0.5		0.5		0.5		0.5		0.5	
	Co.	Ma.	Ha.	FM	Co.	Ma.	Ha.	FM	Co.	Ma.	Ha.	FM	Co.	Ma.	Ha.	FM
	0.33	0.67	0.33	0.67	0.67	0.33	0.67	0.33	0.67	0.33	0.33	0.67	0.33	0.67	0.67	0.33
Site I, Part 1	0.5346				0.5726				0.5367				0.5716			
Site I, Part 2	0.5279				0.5559				0.5262				0.5576			
Site II	0.4318				0.5162				0.4565				0.4910			
Site I, Part 1+Part 2	0.5873				0.6118				0.5986				0.6005			
Site I+Site II	0.5265				0.6028				0.5750				0.5544			
Deep Basin Scheme	0.5819				0.57				0.57				0.5819			

Table 7.25 Estimated suitability values for the alternative schemes

Scheme	Weight				Weight				Weight				Weight			
	Cost		Benefit		Cost		Benefit		Cost		Benefit		Cost		Benefit	
	0.67		0.33		0.67		0.33		0.67		0.33		0.67		0.33	
	Co.	Ma.	Ha.	FM	Co.	Ma.	Ha.	FM	Co.	Ma.	Ha.	FM	Co.	Ma.	Ha.	FM
	0.33	0.67	0.5	0.5	0.67	0.33	0.5	0.5	0.5	0.5	0.33	0.67	0.5	0.5	0.67	0.33
Site I, Part 1	0.701				0.702				0.689				0.714			
Site I, Part 2	0.694				0.692				0.683				0.703			
Site II	0.555				0.589				0.552				0.592			
Site I, Part 1+Part 2	0.672				0.687				0.675				0.684			
Site I+Site II	0.496				0.561				0.519				0.538			
Deep Basin Scheme	0.442				0.426				0.474				0.434			

Table 7.26 Estimated suitability values for the alternative schemes

Scheme	Weight				Weight				Weight				Weight			
	Cost		Benefit		Cost		Benefit		Cost		Benefit		Cost		Benefit	
	0.67		0.33		0.67		0.33		0.67		0.33		0.67		0.33	
	Co.	Ma.	Ha.	FM	Co.	Ma.	Ha.	FM	Co.	Ma.	Ha.	FM	Co.	Ma.	Ha.	FM
	0.33	0.67	0.33	0.67	0.67	0.33	0.67	0.33	0.67	0.33	0.33	0.67	0.33	0.67	0.67	0.33
Site I, Part 1	0.689				0.715				0.690				0.713			
Site I, Part 2	0.684				0.709				0.586				0.704			
Site II	0.536				0.602				0.569				0.575			
Site I, Part 1+Part 2	0.668				0.692				0.683				0.677			
Site I+Site II	0.487				0.570				0.552				0.506			
Deep Basin Scheme	0.442				0.426				0.426				0.442			

More weight to the main benefit criterion

Noting the results of the overview (Table 7.21), it is no surprise that, when the main benefit is given double preference over cost, the deep basin type has the highest suitability values, as is shown in Tables 7.27 and 7.28.

Table 7.27 Estimated suitability values for the alternative schemes

Scheme	Weight				Weight				Weight				Weight			
	Cost		Benefit		Cost		Benefit		Cost		Benefit		Cost		Benefit	
	0.33		0.67		0.33		0.67		0.33		0.67		0.33		0.67	
	Co.	Ma.	Ha.	FM	Co.	Ma.	Ha.	FM	Co.	Ma.	Ha.	FM	Co.	Ma.	Ha.	FM
	0.33	0.67	0.5	0.5	0.67	0.33	0.5	0.5	0.5	0.5	0.33	0.67	0.5	0.5	0.67	0.33
Site I, Part 1	0.405				0.406				0.381				0.430			
Site I, Part2	0.391				0.39				0.371				0.410			
Site II	0.367				0.384				0.335				0.415			
Site I, Part 1+Part 2	0.513				0.523				0.510				0.528			
Site I+Site II	0.585				0.617				0.572				0.619			
Deep Basin Scheme	0.722				0.714				0.718				0.718			

Table 7.28 Estimated suitability values for the alternative schemes

Scheme	Weight				Weight				Weight				Weight			
	Cost		Benefit		Cost		Benefit		Cost		Benefit		Cost		Benefit	
	0.33		0.67		0.33		0.67		0.33		0.67		0.33		0.67	
	Co.	Ma.	Ha.	FM	Co.	Ma.	Ha.	FM	Co.	Ma.	Ha.	FM	Co.	Ma.	Ha.	FM
	0.33	0.67	0.33	0.67	0.67	0.33	0.67	0.33	0.67	0.33	0.33	0.67	0.33	0.67	0.67	0.33
Site I, Part1	0.381				0.431				0.381				0.430			
Site I, Part 2	0.371				0.410				0.370				0.411			
Site II	0.327				0.423				0.344				0.407			
Site I, Part 1+Part 2	0.507				0.532				0.514				0.524			
Site I+Site II	0.566				0.636				0.598				0.603			
Deep Basin Scheme	0.722				0.714				0.714				0.722			

Final remarks[8]

Together with the presentation of the global costs and benefits, the selection of the desired floodwater spreading scheme also needs to take a position on which aspects weigh heavily in the decision making. This point was recognized and did play a role in deciding on the existing schemes in Iran, but to our knowledge no formal

[8] In this chapter, particular reference has been made to work of EWRI/ASCE (2001) and the Ministry of Jihad for Construction (1986).

procedure existed where the costs of various alternative schemes, all based on the characteristics of the particular site, and their benefits were estimated.

The lifetime delivery costs per m^3 of water harvested (i.e. amount of recharge) were estimated in the range of 8 to 12 euro cents, and this is less than the costs of 15 to 18 euro cents mentioned by Gleick (1993) for artificial groundwater storage.

The evaluation made here is a global one. It is therefore likely that before the final decision is made, more precise estimates of costs and benefits are judged necessary, and this is particularly true for the estimation of the reduction in flood damage after the implementation of a scheme. The estimate for construction costs is fairly accurate, thanks to the GIS model coupled with a spreadsheet model and the known prices per unit of construction. The accuracy of the estimate of the volume of recharge is less, because the true performance may be different from what is assumed using transfer functions and imperfect knowledge of the progress of sedimentation type and behaviour of the clays in a proposed scheme. Of course, the amount of recharge affects the cost of recharged water directly, and the estimate here is a conservative one, assuming no recharge when infiltration basins are filled with clay.

It is to be hoped that more reliable data will be collected from existing schemes in Iran, for example, in the manner performed for the Sorkhehesar scheme in this study, but preferably with good groundwater data, in order to improve *a priori* estimation of the recharge.

It is reasonable to state that the value of water will increase in Iran and other semi-arid regions, and a proper economic evaluation using more information will be required to work out the benefits and costs. However, this is considered to be beyond the scope of this study, which has focused on the physical and engineering aspects.

With the presentation of design alternatives with global costs and benefits to decision makers, the full process of selecting sites, first on a qualititative basis using remote sensing and general data, then by zooming in on promising sites and using a multicriteria analysis for selecting the most promising one, has been explained and discussed.

CHAPTER 8
Conclusions and Recommendations

8.1 Conclusions

The complexity of floodwater spreading schemes using flash flows of ephemeral rivers in semi-arid regions became evident during the task of selecting, defining and structuring criteria for the selection of suitable areas and sites for a scheme. Complexity is due, on the one hand, to biophysical factors, such as the spasmodic and erratic occurrences of flash flows, usually with high sediment loads that have to be diverted to areas overlying aquifers with suitable properties; and, on the other hand, to socio-economic factors, such as the benefit for irrigated agriculture, the mitigation of flood damage, and possibly environmental aspects. The last three factors may even dominate the outcome of the selection process for suitable areas and sites because of political preferences.

A decision support system (DSS) for the selection of suitable areas and sites – the topic of this thesis – has to recognize that the procedure is therefore not a straightforward deterministic process considering biophysical criteria only. A crucial aspect was to find and apply a multicriteria evaluation method that allows comparison and weighting criteria of highly diverse nature in the presence of data of differing consistency, quality and detail.

After studying various theoretical approaches/methods for planning and decision making, a value-focused compensatory approach based on Saaty's analytical hierarchy process (AHP) method was selected. In its application, the method honours results obtained by deterministic modelling in the biophysical domain, but also results of relative, qualitative nature are used, through the expression of preferences with a pairwise comparison technique.

Like most DSS for complex problems, the one developed in this thesis is a composite one, which follows from the definition and structuring of the criteria that dominate a decision for a flood spreading scheme.

The leading element of the DSS described in this thesis is the procedure to narrow the search progressively in three scales or steps. The procedure starts with the screening for zones with potentially suitable areas. This screening has to be efficient in terms of time and data acquisition, because a large number of possible areas within the zones have to be considered. The next step, area selection, is the evaluation of the potentially suitable areas to select the one that in the terminology of the MADM-adopted paradigm is called the 'satisfying' because of the presence of uncertainty and the limited number of alternatives. The AHP aggregation method implemented in a spatial (GIS) domain was used for this selection. The last step, site selection, consists of working out the alternatives to be offered to the decision maker(s) for feasible designs according to the estimated benefits and costs. In each step, the DSS progressively involves more data with more detail and passes from a small to large cartographic scale.

Various hydrological simulation or estimation models form part of the DSS to supply the required data. Of importance is the *a priori* estimation of the recharge

efficiency of a scheme or, in other words, of the amount of water diverted from an ephemeral river that will reach the groundwater table, bearing in mind the soil texture of the infiltration area and the expected sedimentation within the scheme. One-dimensional soil moisture modelling (SWAP) was applied to obtain insight into the effects of soil texture and inundation depth on recharge efficiency, using soil texture and different PTFs to obtain hydraulic parameters. It was found that results differed considerably for soils containing clay and silt, but less for coarser-grained soils.

Since nearly all schemes in semi-arid regions will suffer from sedimentation by clays and silts, a study was made of an existing complex scheme (the Sorkhehesar scheme) to determine which PTF gave the best results. This was the case for the Mualem-Van Genuchten function.

Current hydrological methods such as the SCS method for estimating runoff from rainfall and a method for estimating sediment yield were used. A problem is that such methods give results of approximate accuracy, as was evident when estimation results were compared with observed runoff and sediment concentration data for one of the selected catchments. However, at the area selection stage, the effect of error in estimating runoff and sediment – in fact, uncertainty – is lessened by the aggregation procedure of the AHP method, which takes into account other criteria as well.

GIS procedures coupled to spreadsheet programs were used and developed for the multicriteria evaluation of the 'satisfying' area selection, for the assessment of the most appropriate PTF, and for working out and preparing the options during the last stage. Use of such programs proved to be very efficient, partly because iterations were possible, allowing feedback mechanisms.

Zone selection

The screening for zones with potential was based on qualitative results achieved using the interpretation of remotely sensed images, supplemented by generally available additional sources of information, such as geological and topographical maps. By interpreting these data and using criteria such as catchment size, presence of aquifer, water quality, excessive sediment yield, high transmission losses, lack of space for schemes in suitable infiltration areas, and so on, it was possible to obtain sufficient evidence to exclude areas that seemed potentially suitable at first glance. It was found that zones with potentially suitable areas to be retained for further scrutiny consisted of catchments of medium size (a few tens to hundreds of square kilometres in size) with rivers that formed alluvial fans.

The interpretation of the collected data also resulted, before ending the screening, in specifying the nature of the field data required and in giving specific points of attention for the next stage of evaluation, such as the presence of a salinity hazard.

By coupling groundwater-level fluctuations in wells close to active rivers or active sedimentation on alluvial fans, the importance of river recharge or transmission loss could be demonstrated. The type of image processing technique to highlight such areas was mentioned.

To arrive at results, the interpretation required a holistic approach, supported by field knowledge of various regions of Iran. The geological setting and dynamic geomorphology had to be assessed first to estimate relative runoff and sediment yield, as well as probable gross nature and depth of aquifers. In many parts of Iran, it was found that neotectonics played a role in the erosion and deposition. Using images to study details of the fluvial geomorphology gave information on the general feasibility of a scheme, considering transmission losses and the main type of scheme possible in view of suitable sites for intakes for a diversion scheme.

Because of the age-old use of groundwater in Iran, interpreted land cover information allowed conclusions to be drawn on the presence of aquifers, the suitability of soils for irrigation and possible increase in acreage using artificially recharged water, saline water, and space for floodwater spreading schemes (also in relation to land acquisition).

Because of the interrelationships that, owing to cause-and-effect relationships, often exist between the terrain features of relevance for the selection of areas for floodwater spreading schemes, it can be concluded that the interpretation results could be regarded as being more than the sum of separate 'interpretation' layers: i.e. geology, geomorphology, land use. The interpreter has to have a firm footing in earth science.

The end product of the screening was the identification of potentially suitable areas within a zone, grouped according to a relative qualification, leaving options open for the selection of the most suitable areas when considering the size of possible scheme.

Area selection

Because the number of criteria of diverse nature has expanded, as well as the level of detail of the required information, for the selection of the most suitable area use should be made of a method that handles multicriteria in a formal evaluation approach for decision making. It was found that Saaty's AHP method was well suited to arrive at that selection, once the criteria and sub-criteria had been identified and structured. One difficulty was to be sure that appropriate linguistic measures of preference (LMP) values, inherent in the method, were assigned to the various criteria and sub-criteria. It is therefore important that the method compensates for flaws in the assignment. For example, the low performance of one of the alternative areas (Chandab) as regards the infiltration criterion was compensated for by a high performance as regards the floodwater criterion.

In the adopted AHP method, criteria can be easily expanded to include other public concerns and engineering needs. Because of the spatial feature of the approach, every cell of land in the study areas is considered. The advantage is that data and information can be passed on to a next stage (i.e. site selection). This is not practical using manual or conventional means. An important aspect in this approach is that the focus is on what is desired, rather than on the evaluation of alternatives. The LMPs for the comparison of criteria must be chosen carefully. Decision makers/experts must be able to define these choices. It should be considered that a

high rate of inconsistency (more than acceptable) does not automatically mean the wrong judgment of what we already know.

Based on the interviews conducted for this study and considering the multidisciplinary nature of the decision process, five different scenarios were generated: four emphasizing one each of the four main criteria and the last scenario with equal preference. It was found that one particular area (Chandab) had the highest sum of utilities for three of the four main criteria and the last scenario. For that reason, that area was selected for developing and applying the method for the last step: site and scheme selection.

Site and scheme selection

Each infiltration area identified as a suitable site has constraints but also possibilities for alternatives. The latter is important for giving decision makers options as to the type of scheme and the associated global investment they want to select by considering the political or social aspects and the capital available weighed against the estimated desired effect of the scheme. This can be done by designing a limited number of layouts of schemes of various sizes, and working out the estimated benefits and costs of the alternative scheme designs.

The program developed in this thesis consisted of a spreadsheet coupled to a GIS, and proved to be an essential tool because the consequences of adjustments to particular site characteristics, such as slope, infiltration, infrastructure and land availability, can be assessed in an efficient manner. The program also enables maintenance costs during the scheme lifetime, consisting mainly of desilting costs, to be calculated.

The alternative designs thus obtained can be regarded as suitable options for the particular site with given conditions of runoff and sediment. They resulted after several iterations using feedback in the form of benefits and costs. In fact, this working out of alternatives may be regarded as a kind of optimisation.

Estimating the costs is quite a straightforward procedure once the components of the scheme are known, such as the length of dikes, canals and intake(s). However, this is not the case for working out the benefits. The main benefits used in this study are the amount of recharged water expressed in cubic metres, the cost per cubic metre of recharged water, and the estimated reduction of flood damage.

The estimated amount of recharged water with different inundation depths depending on type of scheme has a margin of error because of the inaccuracy of an estimation based on soil textures only, but this margin is considered to be acceptable at this stage.

The estimated reduction of flood damage was based on surveys made of past damage caused by floods of different magnitudes, but no attempt was made to consider this benefit during the lifetime of the alternative schemes, assuming further development of the infrastructure downstream of the scheme. Other socio-economic benefits, such as job creation, have been included, but only in a cursory fashion.

The benefit of flood damage mitigation proved to be major factor in the cost per unit of recharged water in the Chandab area and showed the economy-of-scale effect in the presentation of the alternative scheme types.

Compared with worldwide figures, the costs of water harvesting in the Chandab area proved to be less, which reflects the lower cost of earth moving and construction in Iran.

To our knowledge, this is the first time that a study presents information on the costs and benefits of a floodwater spreading scheme in Iran in a structured manner.

Final conclusion

The DSS described in this thesis, with its three stages of increasing focus and associated data requirements and with an evaluation approach using a multitude of criteria of diverse nature, has proven to be an efficient tool for selecting the most appropriate alternatives when making a choice for investment in a floodwater spreading scheme. Although the emphasis has been on Iranian conditions, the DSS is essentially of generic nature and may be applied – *mutatis mutandis* – to other semi-arid regions.

8.2 Recommendations

The selection of an area suitable for a floodwater spreading scheme and the type of scheme is strongly influenced by social and economic considerations, but during the investigation it was noticed that decision makers are not sufficiently aware that these issues play an important role. Often, a floodwater spreading scheme is regarded as a mere engineering effort that is supposed to be beneficial for augmenting groundwater and flood damage mitigation.

As socio-economic priorities or issues vary from region to region and from province to province, it is recommended that, when the DSS described here is used in a given region, the decision makers are first consulted as to the weight or relative importance they want to give to the issues. These will influence all three stages of the procedure, particularly the last stage when alternative designs are produced.

The cost-benefit analysis of course affects the decision whether or not a scheme should be accepted, and it is expected that this analysis will play a greater role in reaching a decision than has been the case in the past in Iran. More attention should be placed on evaluating the benefits, with agronomists and economists involved in assessing the benefit of additional irrigation water for food production, damage assessment during the lifetime of a scheme, job creation, and so on.

The holistic or comprehensive interpretation using terrain features as observed on remotely sensed images, based on reasoning and analysis of their possible mutual connections, proved to be an efficient method for the screening. It is recommended that the capacity for in-depth interpretation be maintained, if not revived, because of the absence of relevant spatial thematic data for many potentially suitable areas.

In this thesis, a number of references have been made to existing schemes, some unsuccessful owing to poor recharge efficiency. Because of the unknown accuracy of an *a priori* estimation of that efficiency, more schemes should be analysed, using one-dimensional soil and water simulation with different soil textures and PTFs. This may require hydrometry, now usually lacking, to be

improved. Availability of such data sets will place the estimation on a firmer footing.

There is a paucity of accessible results of hydrological analysis – water and sediment – for the semi-arid regions of Iran. Often one has to resort to empirical methods with unknown accuracy when applied to a given catchment.

There is a lack of regionalization studies based on hydrometric data from ephemeral rivers in small and medium-sized catchments, such as areal rainfall duration and depth, probable flood frequencies, and long-term sediment yields. A start could be made with the hydrometric data available. It is evident that improved information will benefit the accuracy of the evaluation contained in the DSS described here.

Summary

Problem Statement

Most aquifers of semi-arid Iran suffer from over-exploitation of groundwater for irrigation. It is therefore important to augment the groundwater resource by artificial recharge, using floodwaters that flow into salt lakes or into the sea. Generally, the recharge schemes consist of diverting part of the flood discharges of ephemeral rivers in small to medium-sized catchments into infiltration basins. Apart from recharging groundwater, and supporting food production and drinking water supplies, the schemes have other benefits, such as the mitigation of flood damage and the 'greening of the desert'. Many governments, including the one of Iran, now place great emphasis on increasing the number of floodwater spreading schemes.

The construction of many floodwater spreading schemes with a relatively low initial investment forms a diversion from past development in Iran, where the emphasis was on building large dams to store water, which incurred high initial capital costs. Groundwater storage has the advantages of buffering, operational flexibility and reliability, but, compared with the large dams, scores lower on adequacy because of the limited volume of water stored during the lifetime of schemes. Because the infrastructure for delivering water to the fields by pumping or by qanats is usually in place, the conveyance costs for recharge projects are low or non-existent compared with the conveyance costs in the case of dams. The increased awareness of the environmental impacts of large dams tends to increase their costs, and makes the artificial recharge schemes more cost-effective.

The complexity of floodwater spreading schemes using flash flows of ephemeral rivers in semi-arid regions became evident during the task of selecting, defining and structuring criteria for the selection of suitable areas and sites for a scheme. Complexity is due to a large number of factors that play a role in the selection of the most suitable sites for deciding on investment in a scheme. These factors pertain to earth science (geology, geomorphology, soils), to hydrology (runoff and sediment yield, infiltration and groundwater conditions) and to socio-economic aspects (irrigated agriculture, flood damage mitigation, environment, job creation and so on). Hence, the decision depends on criteria of diverse nature.

This thesis deals with developing a decision support system (DSS) to assist decisions as to where suitable catchments and associated infiltration areas are located and to work out options for types of schemes, which are adjusted to the characteristics of the selected infiltration area (the site available). The DSS developed relies on the combined use of remotely sensed information, geographical information system (GIS) techniques and a spatial multicriteria evaluation model (SMCE).

Chapter 1: Introduction

The biophysical setting for floodwater spreading schemes is discussed in this introductory chapter, highlighting some specific aspects of ephemeral rivers and alluvial fan aquifers.

Chapter 2: Decision Support Systems (DSS)

Suitable approaches for developing a DSS for the problem at hand are discussed. Like most DSS' for complex problems, the one developed in this thesis is a composite system, which follows from the definition and structuring of the criteria that dominate a decision on a floodwater spreading scheme.

The leading element of the DSS described in this thesis is the procedure to progressively narrow the search in three scales or steps: (i) small scale (cartographic) for identifying and selecting potential zones, (ii) medium scale for area(s) suitability evaluation, and (iii) large scale for evaluating the suitability of site and type of design.

At the small scale, potentially suitable zones are screened with the assistance of remotely sensed data, field knowledge and expert knowledge. This screening has to be efficient in terms of time and data acquisition, because a large number of possible areas within the zones have to be considered.

The next step, area selection, is the evaluation of the potentially suitable areas in order to select the one that is – in the terminology of the adopted multi-attribute decision making (MADM) paradigm – 'satisfying', because of the presence of uncertainty and the limited number of alternatives. The analytical hierarchy process (AHP) aggregation method, implemented in a spatial (GIS) domain, was used for this selection.

The last step, site selection, consists of elaborating the alternatives offered to the decision maker(s) into feasible designs, according to their estimated benefits and costs.

In each step, the DSS progressively involves more data with more detail and passes from a small cartographic scale to a large scale. Various common hydrological simulation or estimation models form part of the DSS in order to supply required data.

Chapter 3: Water recharge assessment using a numerical model

Of key importance, of course, is the expected infiltration of the floodwater diverted. In other words, knowing the soil texture of the infiltration area and the expected sedimentation within the scheme, how much of the water diverted from an ephemeral river will reach the groundwater table? In this chapter, the effects of soil textures in a soil column on infiltration and percolation are estimated, as well as the effects of clay and sand sedimentation in a scheme, and the effects of inundation depth and flooding frequency. One-dimensional soil and water modelling was carried out with the physically based numerical model SWAP (Soil-Water-Atmosphere-Plant), using two pedo-transfer functions (PTFs) for the hydraulic parameters based on textures. It was found that for coarsely textured soils there was reasonable agreement between the functions used, but quite a few differences were found for the soils containing clay and silt. From this part of the study, it was concluded that saturated hydraulic conductivity (Ks) and recharge were not correlated, except for light soil textures when the soil hydraulic parameters are

calculated using the Mualem-Van Genuchten transfer function (MG). The Campbell function (CA) was the other one used.

As expected, recharge efficiency was positively affected by inundation depth and by rapid succession of inundations. It is interesting to note that the largest increase due to inundation depth occurred in the simulations with a clay layer on top. It is recommended that scheme design should aim at deep inundation and that water should be diverted in as short a time span as possible. Therefore, catchments with rainfall-runoff events clustered in time are preferred, all other factors being equal.

As computer simulations using various PTFs may not represent the true field conditions, they need to be verified by field studies, particularly by using existing schemes where significant sedimentation of clay has taken place. This is done in the next chapter.

Chapter 4: Modelling groundwater recharge in Varamin Plain, Iran

The main objective of this chapter was to explore whether upscaling the results of the numerical modelling has practical significance when used to simulate recharge of a complete scheme. The recharge of the complex and large Sorkhehesar scheme was analysed by developing a spreadsheet program to work out water depths, inundation areas and duration of inundation, as to match observed loss of water by infiltration with simulated estimates.

It was noted that SWAP simulations gave realistic results when applied to the Sorkhehesar case provided ponding depths were included.

The saturated hydraulic conductivities (Ks) calculated using the MG method gave the most accurate results. The result calculated using the aggregation of the MG and CA methods did not show much difference from the observed field data but the aggregation was not as accurate as the MG method. Using laboratory-measured (Ks) values and ignoring ponding depths in the scheme with sedimentation resulted in recharge efficiencies that were too low. Simulation results using the CA method differed much from the observed field data.

Statistical analysis suggests that water ponding depth has an important effect on recharge, as well as sediment depth and saturated hydraulic conductivity (according to the computed Beta value).

The study confirmed that permeability is a prime factor in the selection of suitable areas and sites. If the subsoil is less permeable and the sediment has bad hydraulic properties (e.g. clay with much montmorillonite), the recharge efficiency is likely to be much less than the efficiency of the Sorkhehesar scheme.

In this chapter, it is recommended that the design of a scheme should consider both a long scheme lifetime, and the inflow of much sediment. Large sediment loads are typical of runoff in semi-arid regions, while a few major events may carry a large proportion of the total long-term sediment load. This makes it hazardous to rely on suspended load measurements obtained during relatively short periods of time.

Although simplifying assumptions were made in the spreadsheet model developed, such as averaging Ks values and the sediment thickness in each basin without mapping the soil textures and depths in detail, such an approach is recommended for evaluating more floodwater spreading schemes. The results can be checked by simple measurement of water depths and inundation limits in the basins. Data becoming available in this manner would be welcome in order to validate simulation modelling results and determine the most effective factors in the recharge process.

Chapter 5: Zone Selection for Floodwater Schemes

Given the large number of ephemeral rivers draining hilly catchments and passing through alluvial areas, it is necessary to first use a rapid screening method to identify zones to which the main criteria are applicable. The objective of this chapter is to develop and evaluate a method for screening zones containing feasible or potentially suitable areas, as a component of the DSS.

The screening was done at a small scale and the criteria were judged qualitatively to select the suitable zones containing potential areas for floodwater spreading. The screening was based on the interpretation of remotely sensed images supplemented by generally available additional sources of information, such as geological and topographical maps. Remotely sensed images have the advantage that various aspects are presented in a synoptic spatial view.

The interpretation has to be firmly rooted in earth science because of the mutual relationships between terrain features; it is not desirable to do the interpretation of the various aspects in an isolated manner. Estimation of relative runoff and sediment transport makes use of the lithology and geomorphology, while the dimensions of the riverbeds and the transmission losses are related to runoff and sediment delivery and sediment transport. In a wider time-perspective aquifer properties and salinity hazard are related to the geology and geomorphology of the catchment and the tectonism. It should be realized that most aquifers occur in deposits of alluvial fans and the fans reflect the supply of sediment from the catchment.In addition, land use and infrastructure were rapidly assessed with the images. It was concluded that the interpretation results could be regarded as being more than the sum of separate interpretation layers, i.e. geology, geomorphology and land use.

The study has shown that image interpretation facilitated by field visits and by the presence of hydrogeological data allows empirical knowledge to be accumulated for understanding interrelationships of features on the images and for extrapolation purposes. This enables potentially suitable areas to be identified and areas with little or no promise to be excluded by using criteria such as catchment size, presence of aquifer, water quality, excessive sediment yield, high transmission losses, lack of space for schemes in suitable infiltration areas, and so on. A number of examples from Iran are described in this chapter, highlighting the importance of transmission losses. The interpretation also leads to the formulation of certain field observations that are required before a final evaluation can be made at the screening level.

The end product of the screening was the identification of possible suitable areas within a zone, grouped according to a relative qualification, leaving options open for the selection of the most suitable areas according to the size of the possible scheme.

Chapter 6: Area(s) Selection for Floodwater Spreading

The objective of this chapter is to develop and evaluate a multicriteria evaluation model (MCEM) as a second component of the DSS for finding the 'suitable area' within a zone.

The multi-attribute decision making (MADM) paradigm based on the value-focused approach using the compensatory analytical hierarchy process (AHP) method was selected. An important aspect in this approach is that the focus is on what is desired, rather than on the evaluation of alternatives. The method was considered to be appropriate for the problem at hand and use was made of the spatial extension of this approach in a GIS environment, after structuring all the major criteria for a floodwater spreading scheme.

In order to select the most suitable of the promising areas, the spatial AHP, incorporating a multitude of criteria, was applied in the Varamin zone. Once the various factors had been estimated, the difficulty was to specify and determine the preferences that form the base of the relative importance values for all the decision criteria involved at different levels. For some physical criteria, established empirical hydrological methods were used for specification, classification and facilitation purposes. For others, such as those pertaining to the social acceptance criterion, preferences for the criteria had to be based solely on the opinion of experts or stakeholders and on proxy data.

The use of the linguistic measures of preferences in the pairwise comparisons made it possible to implement the full procedure, even though data differed much in nature, consistency and quality.

Considering the multidisciplinary nature of the decision process, five different scenarios were generated, four emphasizing one each of the main criteria and the last scenario with equal preference. In the Varamin zone, the Chandab catchment and infiltration area emerged as the 'satisfying' area. It had the highest sum of utilities for three of the four main criteria and the highest score in a combination scenario. For that reason, this area was selected for developing and applying the method for the last step of DSS: site and scheme selection.

Chapter 7: Site and design Selection for Floodwater Spreading Schemes

The objective of the procedure at the large scale was, as the last component of the DSS, to work out a method to arrive at options for decision makers with regard to type and size of scheme that honoured the site-specific characteristics of the 'suitable area'. When a suitable area had been selected (Chandab area), the floodwater infiltration sub-area part was evaluated as a potential site for developing a floodwater spreading scheme. In this last phase or step the hydraulic-technical

design type with the precise site delineation is made, using the most detailed hydrological data available.

For the Chandab infiltration site, a spreadsheet model coupled to a GIS was developed to work out various options with regard to the type (shallow basin or deep basin type) and size of scheme resulting in the expected volumes of recharge during the lifetime of the scheme, assuming desilting operations. Of the additional benefits, flood damage mitigation could be expressed in monetary terms – and this benefit has a profound effect on the cost per unit volume of recharge water if one opts for the two large-sized scheme designs.

Cost estimation was a relatively straightforward procedure once the components of the scheme were known, such as the length of dikes, canals and intake(s). However, this was not the case when working out benefits. The main benefits used in this study were the amount of recharged water (expressed in cubic metres, and cost per cubic metre of recharged water), and the estimated reduction in flood damage.

The benefit of flood damage mitigation proved to be a major factor in the cost per unit of recharge water in the Chandab area and showed the economy-of-scale effect in the presentation of alternative scheme types.

Compared with worldwide figures, the cost of water harvesting in the Chandab area proved to be less, which reflects the lower costs of earth moving and construction in Iran.

To our knowledge, this is the first time that a study presents information on costs and benefits of a floodwater spreading scheme in Iran in a structured manner, with various designs adjusted to a particular site.

Chapter 8: Conclusions and Recommendations

In conclusion, this chapter states that the DSS described here, with its three stages of increasing focus and associated data requirements, and an evaluation approach using a multitude of criteria of diverse nature, has proven to be an applicable and efficient tool for selecting the most appropriate alternatives for making investment decisions regarding floodwater spreading schemes. Although the emphasis has been on Iranian conditions, the DSS is essentially of a generic nature and may be applied – *mutatis mutandis* – to other semi-arid regions.

Samenvatting

Beschrijving van het probleem

De meeste aquifers in het semi-ariede Iran hebben te lijden van overmatige onttrekking van grondwater voor irrigatie. Het is daarom belangrijk de grondwatervoorraad kunstmatig te voeden met water van vloeden dat nu in zoutmeren of in de zee vloeit. In het algemeen bestaan de bouwwerken voor de kunstmatige grondwatervoeding uit het afleiden en uitspreiden van een gedeelte van de vloedafvoer van episodische rivieren in middelgrote tot kleine stroomgebieden naar infiltratiebekkens (hier vloedspreidingswerk genoemd). Behalve de voeding van grondwater voor de ondersteuning van irrigatie en drinkwatervoorziening, hebben de vloedspreidingswerk en ook nog andere voordelen, zoals het verminderen van de schade door overstromingen en het vestigen van groene vegetatie in de woestijn of steppe. Veel regeringen, inclusief die van Iran, geven nu veel belang aan het vermeerderen van het aantal vloedspreidingswerken.

Met de aanleg van de bouwwerken voor de kunstmatige grondwatervoeding, met een relatief lage initiële investering, wordt een andere weg ingeslagen dan in het verleden het geval was, namelijk het bouwen van grote stuwdammen voor wateropslag, verbonden met hoge initiële financiële kosten. Het opslaan van grondwater heeft voordelen, zoals vormen van een buffervoorraad, flexibiliteit in beheer en betrouwbaarheid, maar in vergelijking met de grote dammen is het minder adequaat vanwege het beperkte volume opgeslagen water gedurende de levensduur van de vloedspreidingswerken. Omdat de infrastructuur voor het afleveren van water aan de velden door middel van pompinstallaties of qanats meestal aanwezig is, zijn deze kosten laag of afwezig vergeleken met die van dammen. Het toegenomen besef van de milieu effecten van grote dammen werkt kostenverhogend en dit is ten voordele van de bouwwerken voor kunstmatige grondwatervoeding.

De complexiteit van werken voor spreiding en infiltratie door het afleiden van episodische vloedafvoeren in semi-ariede streken werd duidelijk tijdens het selecteren, definiëren en structureren van criteria voor het selecteren van de geschikte gebieden en plaatsen voor bouwwerken voor vloedspreiding en infiltratie. De complexiteit wordt veroorzaakt door het grote aantal factoren die een rol spelen in het bepalen van de meest geschikte plaats om te beslissen over de investering. Deze factoren zijn van aardkundige aard (geologie, geomorfologie, bodemkunde) van hydrologische aard (afvoer, sediment last, infiltratie en grondwater condities) en ook van socio-economisch karakter (geïrrigeerde landbouw, beperking van overstromingsschade, milieu, werkgelegenheid enz.). De besluitvorming hangt dus af van criteria van diverse aard.

Dit proefschrift behandelt de ontwikkeling van een beslissings-ondersteunend systeem (DSS) ter ondersteuning van de besluitvorming over welke vanggebieden en de daarmee geassocieerde infiltratie gebieden geschikt zijn en tevens het uitwerken van opties betreffende verschillende types van vloedspreidingswerken, die aangepast zijn aan de eigenschappen van de geselecteerde infiltratiegebieden (de beschikbare locatie). Het DSS stoelt op een

gecombineerd gebruik van teledetectie, technieken met een Geografische Informatie Systeem (GIS) en een ruimtelijk multi-criteria evaluatie model (SMCE).

Hoofdstuk 1: Introductie

De elementen van bio-fysische aard van belang voor vloedspreiding en infiltratie worden geïntroduceerd in dit eerste hoofdstuk, enkele specifieke aspecten van episodische rivieren en alluviale puinwaaiers worden naar voren gehaald.

Hoofdstuk 2: Beslissings-ondersteunde Systemen (DSS)

Een discussie is gewijd aan geschikte benaderingen voor het ontwikkelen van een DSS voor het voorliggende probleem. Zoals de meeste DSSen voor complexe problemen, is degene ontwikkeld in dit proefschrift een samengesteld systeem, als gevolg van de definitie en structurering van de criteria die de beslissing over een vloedspreidingswerk en infiltratie domineren.

Een leidraad van de DSS hier beschreven is de procedure om de zoektocht met een voortgaande vernauwing te doen op drie schalen of stappen: (i) kleine (kartografische) schaal voor de identificatie en selectie van potentiële zones, (ii) middenschaal voor de beoordeling van de geschiktheid van gebieden en (iii) de evaluatie van de plaats en type ontwerp op gedetailleerde, grote, schaal.

Bij de eerstgenoemde schaal worden potentiële gebieden gescheiden van andere met behulp van gegevens verkregen door middel van teledetectie, veldkennis en expertise. Deze scheiding moet efficiënt zijn in termen van tijd en het verzamelen van gegevens vanwege het grote aantal van mogelijk geschikte gebieden binnen de zones die beschouwd worden.

De volgende stap, het selecteren van het gebied, bestaat uit de evaluatie van potentieel geschikte gebieden, teneinde het gebied te selecteren die –in de terminologie van de geadopteerde 'meervoudige attributen besluitvorming'(MADM)- "voldoening" geeft (satisficing), vanwege de aanwezigheid van onzekerheid en het beperkt aantal alternatieven. De selectie is gebaseerd op aggregatie met het "Analytische Hiërarchische Proces" (AHP), dat geïmplementeerd is in een ruimtelijk (GIS) domein.

De laatste stap, de selectie van de locatie of plaats, bestaat uit het uitwerken van alternatieven betreffende haalbare ontwerpen met hun geschatte kosten en opbrengsten, aangeboden aan diegene die besluiten nemen. Van de ene naar de volgende stap van het DSS neemt hoeveelheid en detaillering van gegevens toe, daarbij tevens van kleine naar grote schaal gaand. Verscheidene gebruikelijke hydrologische simulatie of schattingsmodellen vormen een onderdeel van de DSS om over de benodigde gegevens te beschikken.

Hoofdstuk 3: Bepaling van de voeding met water met behulp van een numeriek model

Van wezenlijk belang is natuurlijk de verwachte hoeveelheid infiltratie van het afgeleide water. In andere woorden, als de bodemtextuur in het infiltratie gebied en de verwachte hoeveelheid sedimentatie in het vloedspreidingswerk bekend zijn, hoeveel van het water dat van de episodische rivier is afgeleid zal het grondwater

bereiken? In dit hoofdstuk worden de effecten van bodemtextuur in een kolom op de infiltratie en percolatie geschat, alsmede de effecten van sedimentatie van zand en klei in een vloedspreidingswerk en de effecten van water diepte en frequentie van de inundatie. Eén-dimensionele modellering van de vochtbeweging in bodems werd gedaan met het numerieke fysische SWAP model (Soil-Water-Atmosphere-Plant), met gebruikmaking van twee pedo-transfer functies voor hydraulische parameters gebaseerd op textuur. Voor de grove texturen werd een redelijke overeenkomst gevonden tussen de functies, maar nogal wat verschillen werden geconstateerd als de bodem klei of leem bevatte. Dit onderdeel van de studie toonde aan dat de verzadigde hydraulische geleidbaarheid (Ks) en de voeding niet gecorreleerd waren, behalve voor de lichtere bodemtexturen als de hydraulische parameters met de Mualem-van Genuchten (MG) transfer functie werden berekend. De andere gebruikte functie was die van Campbell (CA).

Zoals verwacht had de efficiëntie van de voeding een direct verband met de inundatiediepte en met een snelle opeenvolging van inundaties. Het is interessant om op te merken dat de grootste toename als gevolg van grotere dieptes optrad wanneer een kleilaag bovenop de bodem aanwezig was. Het is daarom aanbevolen dat het ontwerp van een vloedspreidingswerk gericht is op diepe inundatie en zoveel mogelijk water in een korte tijdsspanne wordt afgeleid. De voorkeur hebben daarom vanggebieden die een clustering van regenval-afvoer gebeurtenissen hebben, als alle andere factoren hetzelfde zijn.

Aangezien de computersimulaties met verscheidene PTF's niet de werkelijke veldomstandigheden hoeven weer te geven, moeten ze geverifieerd worden met veldstudies, met name in bestaande werken waar reeds een beduidende hoeveelheid sedimentatie van klei heeft plaatsgevonden.

Hoofdstuk 4: Modelleren van de grondwatervoeding in de Varamin vlakte, Iran

Dit hoofdstuk heeft als hoofddoel na te gaan of het opschalen van de resultaten van de numerieke modellering praktische betekenis heeft voor de simulatie van de voeding van een volledig vloedspreidingswerk. De grondwatervoeding van het complexe en grote Sorkhehesar bouwwerk werd geanalyseerd door het opstellen van een spreadsheet programma om de waterdiepte, geïnundeerde oppervlakte en duur van de inundatie te bepalen, teneinde de geobserveerde hoeveelheid geïnfiltreerd water te vergelijken met de gesimuleerde hoeveelheid.

Opgemerkt kan worden dat SWAP simulaties een realistisch resultaat gaven, toegepast op het Sorkhehesar bouwwerk, mits de inundatiediepten werden meegenomen.

Het beste resultaat werd bereikt door de MG functie te nemen voor de verzadigde hydraulische geleidbaarheid. Als de MG en CA methode werden geaggregeerd, week de simulatie niet veel af van de veldwaarneming, maar was niet zo nauwkeurig als de simulatie met de MG methode. De efficiëntie van de grondwatervoeding was te laag indien berekend met Ks waarden bepaald in het laboratorium en onder verwaarlozing van inundatiediepte in het

vloedspreidingswerk met sedimentatie. Simulatieresultaten met de CA methode verschilden veel met de veldstudie.

Statistische analyse duidt erop dat waterdiepte een belangrijk effect heeft op de grondwatervoeding en hetzelfde geldt voor dikte van sedimentatie en verzadigde hydraulische geleidbaarheid (volgens de berekende Beta-waarde)

De studie bevestigt dat doorlatendheid een hoofdfactor is in de selectie van geschikte gebieden en plaatsen. Als de diepere bodem ondoorlatend is en het sediment slechte hydraulische eigenschappen heeft (b.v. klei met veel montmorilloniet) dan zal de efficiëntie van de grondwatervoeding beduidend lager zijn dan die van het Sorkhehesar bouwwerk.

In dit hoofdstuk wordt aanbevolen dat het ontwerp voor een vloedspreidingswerk met volledige capaciteit gericht moet zijn op een lange levensduur en het instromen van veel sediment. Een grote last aan sediment is karakteristiek voor de rivierafvoer in semi-ariede gebieden, terwijl een groot gedeelte van de totale lange termijn hoeveelheid door maar een paar grote afvoeren getransporteerd wordt. Men kan daarom niet afgaan op metingen van het sedimenttransport in suspensie gedaan gedurende een relatief korte periode.

Hoewel vereenvoudiging van aannames voor het spreadsheetmodel werd gedaan, zoals middelen van Ks waarden en sediment dikte in ieder bassin, zonder detail opnamen van de texturen en diktes, wordt deze benadering aanbevolen voor het evalueren van meerdere werken voor vloedspreiding en infiltratie. De resultaten kunnen worden gecontroleerd door eenvoudige meting van waterdieptes en inundatieoppervlaktes in de bassins. Gegevens die hiermee worden verkregen zijn een welkome bijdrage om simulatie modellering te valideren en om de meest effectieve factoren in het proces van grondwatervoeding te vinden.

Hoofdstuk 5: Selectie van de Zone voor vloedspreidings-werken

Gegeven de vele episodische rivieren, die heuvelachtige vanggebieden ontwateren en door alluviale gebieden stromen, is het noodzakelijk om eerst een methode voor een snelle zifting (screening) te maken, waarmee zones kunnen worden geïdentificeerd waar de hoofdcriteria van toepassing zijn. Het doel van dit hoofdstuk is om zulk een methode te ontwikkelen en te beproeven, als onderdeel van de DSS, om zones te vinden met geschikte gebieden voor haalbare vloedspreidingswerken.

De zifting wordt uitgevoerd op kleine schaal en de criteria werden kwalitatief beoordeeld om de geschikte zones met daarin potentiële gebieden voor vloedspreidings-werken te vinden. De zifting was gebaseerd op de interpretatie van teledetectiebeelden, aangevuld met algemeen aanwezige bronnen van informatie, zoals geologische en topografische kaarten. Teledetectiebeelden hebben het voordeel dat verscheidene aspecten getoond worden in een ruimtelijk synoptische beeld.

De interpretatie moet stevig geworteld zijn in de aardwetenschappen vanwege de onderlinge relaties tussen de terrein verschijnselen; het is niet wenselijk de interpretatie van de verscheidene aspecten op geïsoleerde manier te doen.

Schatting van relatieve afvoer en sediment transport maakt gebruik van de lithologische voorkomens en geomorfologie, terwijl de dimensies van de beddingen en transmissieverliezen weer gerelateerd zijn aan de afvoer en aanlevering en transport van sediment. In een ruimer tijdsverband geplaatst, zijn ook de aquifer eigenschappen en gevoeligheid voor salinisatie, verbonden met de geologie en geomorfologie van het stroomgebied en de tektoniek. Bedacht moet worden dat de meeste aquifers voorkomen in de afzettingen van alluviale puinwaaiers en de puinwaaiers reflecteren de aanvoer van sediment uit het vanggebied. Geconcludeerd werd dat het resultaat van de interpretatie meer was als de som van afzonderlijke interpretatielagen, i.e. de geologie, de geomorfologie en het landgebruik.

De studie heeft aangetoond dat de beeldinterpretatie vergemakkelijkt werd door veldbezoek en de aanwezigheid van hydrogeologische gegevens leidde tot de opbouw van empirische kennis om de onderlinge relaties tussen terreinverschijnselen te begrijpen zolas weergegeven op de beelden en om extrapolaties te kunnen doen. Hierdoor werd het mogelijk om potentiële geschikte gebieden te identificeren en gebieden met weinig of geen belofte uit te sluiten, door gebruik te maken van criteria zoals grootte van het vanggebied, aanwezigheid van een aquifer, kwaliteit van het water, excessieve aanlevering van sediment, grote transmissieverliezen, ruimtegebrek voor vloedspreidingswerken in geschikte infiltratie gebieden, enzovoorts. Een paar voorbeelden uit Iran worden in dit hoofdstuk beschreven om de aandacht te vestigen op het belang van de transmissieverliezen. De interpretatie leidt tevens tot het formuleren van bepaalde veldgegevens die noodzakelijk zijn voordat de uiteindelijke evaluatie gedaan kan worden op het niveau van de zifting.

Het eindproduct van de zifting was de identificatie van mogelijk geschikte gebieden in een zone, gegroepeerd volgens een relatieve kwalificatie, waarbij de keuze voor de grootte van een mogelijk vloedspreidingswerk vooralsnog open wordt gelaten.

Hoofdstuk 6: Selectie van het meest geschikte gebied voor en vloedspreidingswerk

Het doel van dit hoofdstuk is om een multicriteria evaluatie model (MCEM) te ontwikkelen en te evalueren als een tweede component van de DSS voor het vinden van het meest geschikte gebied in een zone.

Geselecteerd werd het paradigma betreffende de besluitvorming op basis van meerdere attributen (het z.g. multi-attribute decision making, MADM), gebaseerd op toespitsing op waarden (value-focussed approach) gebruikmakend van de methode van het ‘gecompenseerde analytisch hiërarchische proces’ (compensatory analytical hierarchy process, AHP). Een belangrijk aspect van deze benadering is dat deze zich richt op wat wenselijk is en niet op de evaluatie van alternatieven. De methode werd geacht geschikt te zijn voor het probleem van deze studie en er werd gebruik gemaakt van een ruimtelijke uitbreiding van deze benadering in een GIS omgeving, nadat alle hoofdcriteria voor een vloedspreidingswerk waren gestructureerd.

Om het meest geschikte van de veelbelovende gebieden te selecteren werd het ruimtelijke AHP toegepast, met inachtneming van vele criteria, in de Varamin zone. Nadat de verscheidene factoren waren ingeschat was de moeilijkheid om de voorkeuren te specificeren en te bepalen. De voorkeuren zijn de basis voor de waarden voor het relatieve belang (relative importance value) voor alle beslissingscriteria op verschillende niveaus. Voor sommige fysische criteria werden welbekende hydrologische methodes gebruikt voor specificatie, classificatie en vereenvoudiging. Voor andere, zoals die verband houdend met het criterium van sociale acceptatie, moest de preferentie uitsluitend worden gebaseerd op de mening van deskundigen, belanghebbenden en op vervangende gegevens.

Het gebruik van de 'taalkundige preferentiële maat' (linguistic measure of preference) in de paarsgewijze vergelijkingen maakte mogelijk om de volledige procedure te implementeren, zelfs bij gegevens van zeer verscheiden aard, consistentie en kwaliteit.

Gelet op het multidisciplinaire aard van het beslissingsproces, werden vijf verschillende scenario's gemaakt, vier daarvan spitsen zich toe op elk der hoofdcriteria en het laatste scenario gaf gelijk belang aan de hoofdcriteria. In de Varamin zone kwam het Chandab vanggebied en infiltratiegebied naar boven als de 'satisficing area'. Het had de grootste som van de gebruikerskenmerken voor drie van de vier hoofdcriteria en de hoogste score in de combinatiescenario. Daarom werd dit gebied geselecteerd om de methode voor de laatste stap van de DSS, namelijk selectie van plaats en type, te ontwikkelen.

Hoofdstuk 7: Selectie van de plaats voor en type van een vloedspreidingswerk

Het doel van de procedure op grote schaal, als de laatste component van de DSS, was het uitwerken van een methode om tot opties te komen voor diegenen die het besluit nemen betreffende het type en grootte van een werk, dat de plaatsgebonden karakteristieken van het 'geschikte gebied' eer aan doet. Toen een geschikt gebied werd geselecteerd (het Chandab gebied) werd het infiltratie sub-gebied reeds geëvalueerd als potentiële plaats voor het maken van een vloedspreidingswerk. In deze laatste fase of stap wordt het hydraulisch-technisch ontwerp type gemaakt met de precieze omlijning van de plaats op basis van de meest gedetailleerde voorhanden zijnde hydrologische gegevens.

Een spreadsheetmodel, gekoppeld aan een GIS werd ontwikkeld voor het Chandab gebied om de diverse opties uit te werken met betrekking tot het type (ondiepe bassins of diepe bassins) en de grootte van het ontwerp met de daarmee verbonden volumes van grondwatervoeding gedurende de levensduur, onder aanname dat het sediment verwijderd zou worden. Van de additionele voordelen kon de vermindering van overstromingsschade in geldeenheden worden uitgedrukt – en dit voordeel heeft een belangrijk effect op de kosten per eenheid grondwatervoeding, als men kiest voor de twee ontwerpen met het grootste oppervlak

Het schatten van kosten was een relatief recht toe rechtaan procedure als eenmaal de componenten van het ontwerp bekend waren, zoals lengten van dijken,

kanalen en inlaten. Echter, dit was niet het geval bij het uitwerken van de voordelen. De hoofdvoordelen gebruikt in deze studie waren de hoeveelheid grondwatervoeding (uitgedrukt in kubieke meters en kosten per kubieke meter) en de geschatte afname van de overstromingsschade.

Het voordeel van vermindering van overstromingsschade kwam uit als een hoofdfactor in de kosten per eenheid grondwatervoeding in het Chandab gebied en daaruit bleek het voordeel van een groots opgezet ontwerp in de presentatie van de alternatieve ontwerpen.

De kosten van de kunstmatige grondwatervoeding in het Chandab gebied zijn minder dan die bekend uit andere delen van de wereld, hetgeen de lagere kosten van het verplaatsen van aarde en van constructie in Iran weerspiegelt.

Voor zover ons bekend is dit de eerste keer dat in een studie informatie wordt verschaft over de kosten en baten van vloedspreidingswerken in Iran op een gestructureerde manier met verscheidene ontwerpen die aangepast zijn aan een bepaalde plaats.

Hoofdstuk 8: Conclusies and aanbevelingen

Dit hoofdstuk bevat de conclusie dat gebleken is dat de beschreven DSS, met haar drie stadia van toenemende toespitsing en geassocieerde gegevensbenodigdheden, alsmede een benadering voor evaluatie waarbij vele criteria van diverse aard gebruikt worden, een toepasbaar en efficiënt middel is om de meest geschikte alternatieven te selecteren voor het maken van een beslissing om te investeren in een vloedspreidingswerk. Ofschoon de aandacht was gericht op de Iraanse situatie, is de DSS van algemene aard en kan – mutatis mutandis - elders in semi-ariede gebieden worden toegepast.

References

Alizadeh, A.1995. Principle of Applied hydrology. Ferdosi University of Mashhad Pub. Mashhad, Iran.

Anselin, L. and Getis, A. 1992. Spatial statistical analysis and geographic information systems. In: Fisher, M. and Nijkamp, P., Geographic Information Systems, Spatial Modeling and Policy Evaluation. Springer-Verlag, Berlin.

Bani Hashemi, S.A.R. 1994. Hydrogeological study of eastern part of Zanjanrud catchment in Zanjan Province, northwest Iran. MSc thesis, ITC, Enschede, The Netherlands, 120 pp.

Bastiaanssen, W.G.M. and Menenti, M. 1989. Mapping groundwater losses in the Western Desert of Egypt with satellite measurements of surface reflectance and surface temperature, in (ed.) J.C. Hooghart, Water Management and Remote Sensing, TNO Committee on Hydrological Research, proceedings and information no. 42: 61-89

Bastiaanssen, W.G.M., Singh, R., Kumar, S., Schakel, J.K. and Jhorar, R.J. 1996. Analysis and recommendations for improved on-farm water management in Harayana, India: a model approach. Report 118, DLO-Winand Staring Centre, Wageningen, The Netherlands, 152 pp.

Beekma, J.H., Kelleners, T.J., Chaudhry, M.R., Boers, Th.M. and Van Dam, J.C. 1997. Recharge from irrigated lands. In: Simmers, I. (ed.), Recharge of Phreatic Aquifers in (Semi-)Arid Areas. International Association of Hydrologists, Pub. 19.

Belmans, C., Wesseling, J.G. and Feddes, R.A. 1983. Simulation model of the water balance of a cropped soil: SWATRE. Journal of Hydrology 63 (3-4): 271-286.

Bouwer, H. 2002. Artificial recharge of groundwater: hydrogeology and engineering. Hydrology Journal. 10:121-142.

Brooks, R.H. and Corey, A.T. 1964. Hydraulic properties of porous media. Hydrology Paper 3, Colorado State University, Fort Collins.

Campbell, G.S. 1974. A simple method for determining unsaturated conductivity from moisture retention data. Soil Science 117: 311-314.

Campbell, G.S. 1985. Soil physics with basic. Department of Agronomy and Soils, Washington State University, Pullman WA.

Carsel, R.F. and Parrish, R.S. 1988. Development joint probability distributions of soil water characteristics. Water Resources 24: 755-769.

Chahardowli, H. 2003. Economical evaluation of the Chandab flood water spreading scheme in Tehran province. In: 3rd Conference on Aquifer Management, 15-16 December, Tehran, Iran.

Chankong, V. and Haimes, Y.Y. 1983. Multiobjective decision making: theory and methodology. Amsterdam, North Holland.

Chow, V.T., Maidment, D.R. and Mays, L.W. 1988. Applied Hydrology. McGraw-Hill.

Christiaens, K. and Feyen, J. 2001. Analysis of uncertainties associated with different methods to determine soil hydraulic properties and their propagation in the distributed hydrological MIKE SHE model. Journal of Hydrology 246 (1-4): 63-81.

Clapp, R.B. and Hornberger, G.M. 1978. Empirical equations for some soil hydraulic properties. Water Resources Research 14 (4): 601-604.

Colson, G. and Bruyn, C. 1989. Models and methods in multiple objectives decision making. Mathematical/Computer Modelling 12: 1201-1211.

Conyers, D. and Hill, P. 1989. An introduction to development planning in the Third World. John Wiley and Sons, New York.

Cooke R.U., Brunsden D., Doornkamp J.C. and Jones, D.K.C. 1982. Urban geomorphology in drylands. Oxford University Press, UK.

Cortez, R. 2004. Recharge assessment and groundwater modeling of the Pisoes aquifer (Beja_Portugal). MSc thesis, ITC, Enschede, The Netherlands, 81 pp.

Crerar, S., Fry, R.G., Slater, P.M., van Langenhove, G. and Wheeler, D. 1987. An unexpected factor affecting recharge from ephemeral river flows in SWA/Namibia. In: Simmers, I. (ed.), Estimation of Natural Recharge, NATO ASI Series, Series C, Vol. 222: 11-28. John Wiley and Sons, New York.

De Ridder, N.A. and Erez, A. 1977. Optimum use of water resources. International Institute for Land Reclamation and Land Improvement (ILRI), Wageningen, The Netherlands.

Dirksen, C. 1991. Unsaturated hydraulic conductivity. In: Smith, K.A. and Mullins, C.E. (eds), Soil Analysis, Physical Methods. Marcel Dekker, New York: 209-269.

Droogers, P., Bastiaanssen, W.G.M., Beyazgül, M., Kayam, Y., Kite, G.W. and Murray-Rust, H. 2000. Distributed agro-hydrological modeling of an irrigation system in western Turkey. Agricultural Water Management 43 (2): 183-202.

Drury, S.A. 1987. Image interpretation in geology. Chapman and Hall, London.

Eftekhari, A. 2000. Erosion and sediment yield assessment using remote sensing and geographic information system: a case study in the A2 sub-catchment of Zayandeh Rud basin, Isfahan Province. MSc thesis, ITC, Enschede, The Netherlands.

Entin, J.K., Robock, A., Vinnikov, K.Y., Hollinger, S.E., Liu, S. and Namkhai, A. 2000. Temporal and spatial scales of observed soil moisture variations in the extra tropics. Journal of Geophysical Research 105 (D9): 11865-11877.

EWRI/ASCE. 2001. Standard guidelines for artificial recharge of ground water. Environmental and Water Resources Institute, American Society of Civil Engineers, USA.

FAO/AGL, 2000. Water Harvesting. http://www.fao.org/ag/agl/aglw/wharv.htm

Fatehi-Marj, A. 1994. Evaluation of artificial recharge using numerical models: a case study in Gareh Baygan plain, Fasa, Fars Province, Iran. MSc thesis, ITC, Enschede, The Netherlands, 111 pp.

Feddes, R.A., Kowalick, P.J. and Zarandy, H. 1978. Simulation of field water use and crop yield. Simulation Monographs, PUDOC, Wageningen, The Netherlands, 189 pp.

Fennemore, G.G., Davis, A., Goss, L. and Warrick, A.W. 2001. A rapid screening-level method to optimise location of infiltration ponds. Groundwater 39 (2): 230-238.

Forman, E. 1999. Decision By Objectives (How to convince others that you are right). George Washington University, Mary Ann Selly, Expert Choice Inc.

Freeze, R.A. and Cherr, J.A. 1979. Groundwater. Prentice Hall, NJ, USA.

Gardner,W.R., Hillel, D. and Benyamini, Y. 1970a. Post-irrigation movement of water: I. Redistribution. Water Resources Research 6:851-861.

Gardner, W.R., Hillel, D. and Benyamini, Y. 1970b. Post-irrigation movement of water: II. Simultaneous redistribution and evaporation. Water Resources Research 6 (4):1148-1153.

Gleick, P. 1993. Water in crisis: a guide to the world's fresh water resources. Oxford University Press, Oxford, UK.

Gorry, G.A. and Morton, S.M.S. 1971. A framework for management information systems. Sloan Management Review 13: 56-70.

Gregory, K.J. and Walling, D.E. 1973. Drainage basin, form and process: a geomorphological approach. Edward Arnold, London.

Guber, A.K., Rawls, W.J, Shein, E.V. and Pachepsky, Y.A. 2003. Effect of soil aggregate size distribution on water retention. Soil Science 168: 223-233.

Gupta, S.C. and Larson, W.E. 1979. Estimating soil water retention characteristics from particle size distribution, organic matter content, and bulk density. Water Resources Research 15: 1633-1635.

Gusev, Y.M. and Nasonova, O.N. 2003. The simulation of heat and water exchange in the boreal spruce forest by the land-surface model SWAP. Journal of Hydrology 280 (1-4): 162-191.

Hadley, R.F., Lal, R., Onstad, C.A., Walling, D.E. and Yair, A. 1985. Recent developments in erosion and sediment yield studies. IHP-UNESCO Technical Documents in Hydrology. UNESCO, Paris.

Haimerl, G. 2001. Talsperren zur Grundwasseranreicherung in ariden Gebieten-Bewirtschaftungsstrategien und Optimierungsmöglichkeiten. Report of the Institute of Hydraulic and Water Resources Engineering. Technical University, Munich, Germany.

Hakimi, M. 2003. Potentials and constraints for expansion of alfalfa cultivation in Varamin. MSc thesis, ITC, Enschede, The Netherlands.

Heusch B. 1971. Estimate and control of hydrous erosion. Ploughshare Sci. Nat. Phys. Morocco, C. R., 37: 41-54.orest in Morocco 12: 9-176.

Hillel, D. 1980. Fundamentals of soil physics. Academic Press, San Diego, 412 pp**.**

Hionidi M., Panagopoulos A., Koumantakis J. and Voudouris K. 2002. Groundwater quality considerations related to artificial recharge application in the aquifer of the Korinthos Prefecture, Greece, In: Proc.3th Int. Conf. Groundwater Quality 2001, Sheffield, United Kingdom.

Hossainipoor, H.K. 2000. Water quality analysis of the Sarchahan Plain aquifer, Hormozgan, Iran. MSc thesis, ITC, Enschede, The Netherlands.

Hughes, D.A. and Sami, K. 1992. Transmission losses to alluvium and assicated moisture dynamics in a semiarid ephemeral channel system in Southern Africa. Hydrological Processes 6: 45-53.

Huyakorn, P.S. et al. 1984. Techniques for making finite element competitive in modeling flow in variably-saturated porous media. Water Resources Research 20 (8): 1099-1115.

Huyakorn, P.S. et al., 1985. Finite element matrix and mass balance computational schemes for transport in variably-saturated porous media. Water Resources Research 21 (3): 346-358.

ILWIS 3.0 Academic: User's Guide, 2001.The Integrated Land and Water Information System, Budde, P.E., Nijmeijer, R.G., Dost, R.J.J., Haas, A.de.

Inbar, M. 1972. A geomorphic analysis of a catastrophic flood in a Mediterranean basaltic watershed. 22nd International Geographical Congress, Montreal, Canada.

Jankowski, P. 1995. Integrating geographical information systems and multiple criteria decision making methods. International Journal Geographic Information Systems 9 (3): 251-273.

Jansson, M.A. 1988. Global survey of sediment yield. Geografiska Annaler 70 (Ser. A 1-2): 81-98.

Janssen, R. 1992. Multi-objective decision support for environmental management. Environment and Management. Vol. 2. Kluwer Academic Publisher, Dordrecht, The Netherlands.

Kearns, A.K. and Hendrickx, J.M.H. 1998. Temporal variability of diffuse groundwater recharge. New Mexico Water Resources Research Institute in cooperation with the Department of Earth and Environmental Science and the Geophysical Research Center and New Mexico Institute of Mining and Technology. Technical Report 1345676-77.

Keeney, R.L. 1992. Value focused thinking. Harvard University Press, London.

Keller, A., Sakthivadivel, R. and Seckler, D. 2000. Water scarcity and the role of storage in development. Research Report 39. International Water Management Institute, Colombo, Sri Lanka.

Kennett-Smith, A., Cook, P.G. and Walker, G.R. 1994. Factors affecting groundwater recharge following clearing in the southwestern Murray Basin. Journal of Hydrology 154: 85-105.

Khalilpour, A., Golbabaei, H. and Atapourfard, A. 2003. Effects of the floodwater schemes development on flood mitigation and their economical values. Case study Shahid Hadi Ahamadi station. In: 3rd Conference on Aquifer Management, 15-16 December, Tehran, Iran.

Khosheghbal, M.Z. 1999. Sedimentology and study of infiltration changes in the Varamin floodwater spreading scheme. MSc thesis, Shahid Beheshti University, Tehran, Iran.

Klosterman, R.E. 1995. Planning support systems. In: Wyatt, R. and Hossain, H. (eds), Proceedings of 4th International Conference on Computers in Urban Planning and Management, Vol. 1: 19-36, University of Melbourne, Melbourne.

Klosterman, R.E. 1997. Planning support system: a new perspective on computer-aided planning. Journal of Planning Education and Research 17: 45-54.

Kowsar, A. 1982. Water harvesting for afforestation: III. Dependence of tree growth on amount and distribution of precipitation. Soil Science Society of America Journal 49: 20-25.

Kowsar, A. 1992. Desertification control floodwater spreading in Iran. In: Unasylva 168, Arid Zone Forestry.

Kowsar, A. 1995. Introduction to floods mitigation and optimum utilization. Book, Pb. no. 1374-150. Ranges and Forests Research institute, Ministry of Jahad-e-Sazandegi, 524 pp.

Langbein, W.B. and Schumm, S.A. 1958. Yield of sediment in relation to mean annual precipitation. Transactions American Geophysical Union 39 (6): 1076-1084.

Leij, F.J., Alves, W.J., van Genuchten, M.Th. and Williams, J.R. 1996. Unsaturated soil hydraulic database (UNSODA): user's manual, version 1.0. EPA/600/R-96/095, National Risk Management Laboratory, Office of Research and Development, U.S. Environmental Protection Agency, Cincinnati, OH, 103 pp.

McCuen, R.H., Rawls, R.J. and Brakensiek, D.L. 1981. Statistical analyses of the Brooks-Corey and the Green-Ampt parameters across soil textures. Water Resources Research 17:1005-1013.

Meijerink, A.M.J. 1985. Estimates of peak runoff from hilly terrain with varied lithology. Journal of Hydrology 77: 227-236.

Meijerink, A.M.J. 1996. Remote sensing applications to hydrology: groundwater. Hydrological Sciences Journal 41 (4): 549-561.

Meijerink, A.M.J., Valenzuela, C.R. and Stewart, A. (eds). 1988. ILWIS: the integrated land and watershed management information system: scientific status report on the project geo-information system for land use zoning and watershed management. ITC Publication 7, Enschede, The Netherlands.

Meirovich, L., Ben-Svi, A., Shentsis, L. and Yanovich, E. 1998. Frequency and magnitude of runoff events in the arid Negev of Israel. Journal of Hydrology 207: 204-219.

Menenti, M., Feddes, R.A., Kabat, P. and Bastiaanssen, W.G.M. 1993. Is large-scale inverse modelling of unsaturated flow with areal average evaporation and surface soil moisture as estimated from remote sensing feasible? Journal of Hydrology 143 (1-2): 125-152.

Miller, V.C. and Miller, C.F. 1961. Photogeology. MacGraw Hill, New York.

Ministry of Energy, 2002. Study of water resources in Varamin Plain. Water Affairs Deputy, Tehran province water organization, Tehran province water affairs office, Varamin plain water affairs division.

Ministry of Jihad for Construction. 1986. Handbook of gabion structures design. Ministry of Jihad for Construction, Water Affairs Deputy.

Mintzberg, H., Raisinghani, D. and Theoret, A. 1976. The structure of 'Unstructured Decision Processes'. Administrative Science Quarterly 21: 246-275.

Mobarakian, S.M. 1998. Erosion assessment using remote sensing and geographic information system in the Nojian catchment, Lorestan Province, Iran. MSc thesis, ITC, Enschede, The Netherlands.

Monteith, J.L. 1965. Evaporation and environment. Symposia of Society Experimental Biology 19: 205-234.

Mualem, Y. 1976. A new model for predicting the hydraulic conductivity of unsaturated porous media. Water Resources Research 12: 513–522.

Munevar, A. and Marino, M.A. 1999. Modeling analysis of groundwater recharge potential on alluvial fans using limited data. Groundwater 37(5): 649-659.

Nijkamp, P., Rietveld P. and Voogd, H. 1990. Multicriteria evaluation in physical planning. Amsterdam, North Holland.

Olive, W.W., Chleborad, A.F., Frahme, C.W., Schlocker, J., Schneider, R.R. and Shuster, R.L. 1989. Swelling clays map of the conterminous United States. U.S. Geological Survey publication.

Oroumieh, M. 1994. Sediment production of the Bisheh Zard watershed and assessment of the sedimentation in the floodwater spreading scheme: a study in Fars province, south Iran. MSc Thesis, ITC Enschede, The Netherlands.

Pacific Southwestern Inter-Agency Committee (PSIAC). 1968. Report of the water management subcommittee on factors affecting sediment yield in the Pacific southwest area. USDA Forest Service.

Pettijohn, F.J. 1957. Sedimentary rocks. Harper and Row, New York.

Peyrovan, H. 1995. Effects of geological formation on surface water quality. Soil Conservation and Watershed Management Research Institute Publication (in Persian).

Pishkar, A. 2003. Analysis of the relationship between soil salinity dynamics and geopedologic properties: a case study of the Goorband area, Iran. MSc thesis, ITC, Enschede, The Netherlands.

Power, D.J. 1999. A brief history of decision support systems. DSS Resources, World Wide Web, http://dss.cba.uni.edu/dss/dsshistory.html.

Prinz, D. 2002. The role of water harvesting in alleviating water scarcity in arid areas. Keynote lecture, Proceedings, International Conference on Water Resources Management in Arid Regions, 23-27 March, Kuwait Institute for Scientific Research, Kuwait (Vol. III: 107-122).

Raeisi Nafchi, H.A. 1998. A study of the sediment yield in Gorgak watershed, Chahar Mahal and Bakhtiary Province, Iran. MSc thesis, ITC, Enschede, The Netherlands.

Rawls, W.J., Brakensiek, D.L. and Saxton, K.E. 1982. Estimation of soil water properties. Transactions American Society of Agricultural Engineers 25:1316-1320.

Rodier, J.A. 1975. Evaluation de l'écoulement annuel dans le Sahel tropical Africain. Travaux et Documents de l' ORSTOM, no. 46. Bondy, France.

Rogowski, A.S. 1971. Watershed physics: model of the soil moisture characteristic. Water Resources Research 17: 1575-1582.

Saaty, T.L. 1980. The analytic hierarchy process. McGraw-Hill, New York.

Saaty, T.L. 1994. How to make a decision: the analytical hierarchy process. Interfaces 24 (6, S): 19-43.

Sarlak, A. 1994. Analysis of factors influencing flood characteristics: a case study in the Gareh-Agaj watershed, Fars Province, Iran. MSc thesis, ITC, Enschede, The Netherlands.

Saxton, K.E., Rawls, W.J., Romberger, J.S. and Papendick, R.I. 1985. Contributions from Agricultural Research Service, USDA, in cooperation with the College of Agriculture and Home Economics, Agricultural Research Center, Washington State University, Pullman, WA. Scientific Paper 6911.

Schuh, W.M. 1990. Seasonal-Variation of Clogging of an Artificial Recharge Basin in a Northern Climate. Journal of Hydrology. 121(1-4): p. 193-215.

Schumm, S.A. 1972. Benchmark papers in geology: river morphology. Dowden, Hutchinson and Ross, Stroudsburg, Pennsylvania.

Schwartz, B.E., Chappell, C.F., Togstad, W.E., Zhong, X. 1990: The Minneapolis flash flood: meteorological analysis and operational response. Wea. Forecasting, 5, 3-21.

Seckler, D., Amarasinghe U., Molden D., de Silva R. and Barker R. 1998. World water demand and supply, 1990 to 2025: scenarios and issues. Research Report 19. International Water Management Institute, Colombo, Sri Lanka.

Shafique, M.S. and Skogerboe, G.V. 1983. Impact of seasonal infiltration function variation on furrow irrigation performance. In: Advances in Infiltration, Proceedings National Conference on Advances in Infiltration: 292-301, American Society of Agricultural Engineers, St Joseph.

Sharifi, M.A. and Herwijnen, M. van, (2003). Spatial Decision Support Systems. International Institute for Geoinformation Science and Earth Observation (ITC) Enschede, pp. 174.

Sharifi, M.A. and Retsios V. 2003. Site selection for waste disposal through spatial multiple criteria decision analysis. In: Proceedings 3rd International Conference on Decision Support for Telecommunications and Information Society, 4-6 September, Warsaw, Poland: 15 pp.

Sharifi, M.A. and Rodriguez, E. 2002. Design and development of a planning support system for policy formulation in water resource rehabilitation. Journal of Hydroinformatics 4 (3), IWA Publishing.

Sharifi, M.A., Shamsudin K. and Boerboom, L. 2004. Evaluating rail network options using multiple criteria decision analysis (MCDA): case study Klang Valley, Malaysia.

Sharifi, M.A., van den Toorn, W.H., Rico, A. and Emmanuel, M. 2003. Application of GIS and multicriteria evaluation in locating sustainable boundary between the Tunari national park and Cochabamba city, Bolivia. In: Journal of Multi-criteria Decision Analysis, 11(2003)3, pp. 151-164

Shentsis, I., Meirovich, L., Den-Zvi, A. and Rosenthal, E. 1999. Assessment of transmission loss and groundwater recharge from runoff events in a wadi under shortage of data on lateral inflow, Negev, Israel. Hydrological Processes 13: 1949-1663.

Shirazi, M.A. and Boersma, L. 1984. A unifying quantitative analysis of soil texture. Soil Science Society of America Journal 48 (1): 142-147.

Siddiqui, M.Z., Everett, J.W. and Vieux, B.E. 1996. Landfill siting using geographic information systems: a demonstration. Journal of Environmental Engineering, June: 515-523.

Simon, H.A. 1960. The new science of management decisions. Harper and Brother, New York, 54 pp.

Simunek, J., Vogel, T and van Genuchten, M.T. 1994. The SWMS 2D code for simulating water flow and solute transport in two dimensional variably saturated media. Version 1.21. Research Report 132. U.S. Salinity Laboratory, U.S. Dept. of Agricultural Research Service.

Singh, R. 2004. Simulations on direct and cyclic use of saline waters for sustaining cotton-wheat in a semi-arid area of north-west India. Agricultural Water Management 66 (2): 153-162.

Soil Conservation Service. 1972. National Engineering Handbook: Section 4, Hydrology. U.S. Dept. of Agriculture (available from U.S. Government Printing Office, Washington DC).

Sorman, A.U. and Abdulrazzak, M.J. 1993. Infiltration through wadi beds in arid regions. *Hydrol. Sci. J.* 38i3 i; 173-186.

Sprague, R.H. and Watson, H.J. 1986. Decision support system: putting theory into practice. Prentice-Hall, Englewood Cliffs, NJ, USA.

Stokes, C.M., F.D. Larson, and C.K. Pearse.1954. Range improvement through water spreading . Foreign Operations Administration, Washington, D.C. 36p.

Stolte, J., Freijer, J.I., Bouten, W., Dirksen, C., Halbertsms, J.M., van Dam, J.C., van den Berg, J.A., Veerman, G.J. and Wösten, J.H.M. 1994. Comparison of six methods to determine unsaturated soil hydraulic conductivity. Soil Science Society of America Journal 58: 1596-1603.

Stuth, J.W. and Lyons, B.G.D. 1993. Decision support systems for the management of grazing lands. UNESCO, Man and Biosphere Series, Vol. II, Paris, France, 301 pp.

Tedeschi A. and Menenti, M. 2002. Simulation studies of long-term saline water use: model validation and evaluation of schedules. Agricultural Water Management 54 (2): 123-157.

Tehran Province Planning and Management Organization. 2002. Tehran Province Statistics, Publication 82/22.

Tkach, R.J. and Simonovic, S.P. 1997. A new approach to multi-criteria decision making in water resources. Journal of Geographic Information and Decision Analysis 1 (1): 25-43.

Todd, D.K. 1980. Groundwater hydrology. John Wiley and Sons, New York.

Topcu,Y.I. 1999. Analysing the problem. http://www.isl.itu.edu.tr/ya/decision7.ppt.

Tosomeen, C.A.S. 1991. Modeling the effects of depression focusing on groundwater recharge. MSc thesis, Dept. of Agricultural Engineering, University of Minnesota.

Turban, E. 1995. Decision support and expert system: management support system. Macmillan Publishing Company, New York.

UNDP/FAO. 1987. Spate irrigation. Proceedings Subregional Expert Consultation on Wadi Development for Agriculture in the Natural Yemen, 6-10 December, Aden, PDR Yemen: 180 pp.

Utset, A., Farr**é,** I., Martínez-Cob, A. and Cavero, J. 2004. Comparing Penman-Monteith and Priestley-Taylor approaches as reference: evapotranspiration inputs

for modelling maize water-use under Mediterranean conditions. Agricultural Water Management 66 (3): 205-219.

Vallentine, J.F.1971. Range development and improvements, 2nd ed. Brigham Young Univ Press, Provo, Utah, 545 pp.

Van Arst, A. 1987. Flood protection works and low cost diversion structures. In: UNDP/FAO. Spate irrigation. Proceeding of sub regional expert consulting on wadi development for agriculture for natural Yemen.6-10 Dec. 1987. p. 118-127.

Van Dam, J. C., Huygen, J., Wesseling, J. G., Feddes, R. A., Kabat, P., van Walsum, P. E. V., Groenendijk, P., van Diepen, C. A., 1997. Theory of SWAP version 2.0. Report 71. Technical Document 45, Wageningen, 167 pp.

Van Genuchten, M.Th. 1980. Predicting the hydraulic conductivity of unsaturated soils. Soil Science Society of America Proceedings 44 (5): 892-898.

Van Genuchten, M.Th., Leij, F.J. and Yates, S.R. 1991. The RETC code for quantifying the hydraulic functions of unsaturated soils. USDA, U.S. Salinity Laboratory, Riverside, California, EPA document EPA/600/2-91/065.

Van Herwijnen, M. 1999. Spatial decision support for environmental management. Free Unversity, Amsterdam.

Verstappen, H.Th. 1977. Remote sensing in geomorphology. Elsevier, Amsterdam: 214 pp.

Vogel, J.R., Garbrecht, J. and Brown, G.O. 2000. Spatial and temporal variability of infiltration, bulk density, and soil composition in dryland winter wheat and native warm season grass. Paper 002141 presented at July 2000 ASAE International Meeting, Milwaukee, WI.

Walters, G.A. and Tan, J.B. "Assessing storm water flood levels in tide-locked river basins", in eds. Y. Iwasa and T. Sueishi Drainage Systems and Runoff Reduction, Proceedings of Fifth International Conference on Urban Storm Drainage, Vol.2, pp.633-8, Osaka, Japan, July 1990.

Warrence, N.J., Bauder, J.W. and Pearson, K.E**.** 2002. Basics of salinity and sodicity effects on soil physical properties. Land Resources and Environmental Sciences Department, Montana State University, 29 pp.

Way, D.S. 1978. Terrain analysis (2nd ed.). Dowden Hutchinson and Ross, Stroudburg, USA.

Williams, J., Prebble, R.E., Williams, W.T. and Hignett, C.T. 1983. The influence of texture, structure, and clay mineralogy on the soil moisture characteristic. Australian Journal Soil Research 21: 15-32.

Wischmeier, W.H. and Smith, D.D. 1978. Predicting rainfall erosion losses: a guide to conservation planning. Agricultural Handbook 537, U.S. Government Print Office, Washington, DC.

Withers, B. and Vipond, S. 1988. Irrigation: Design and Practice. Anchor Press Ltd, Tiptress Essex for B.T. Batsford Ltd 4 Fitzhardinge Street, London WIH OAH.

Wood E.F., Sivapalam M., Beven, K. and Band, L. 1988. Effects of spatial variability and scale with implications to hydrologic modelling. Journal of Hydrology 102: 29-47.

Wösten, J.H.M., Veerman, G.H. and Stolte, J. 1994. Water retention and hydraulic conductivity functions of top- and subsoil in the Netherlands. The Staring Series. Technical Document 18, Wind Staring Center, Wageningen, The Netherlands, 66 pp (in Dutch).

Yates, S.R., M.Th. van Genuchten, A.W. Warrick, and F.J. Leij. 1992. Analysis of measured, predicted, and estimated hydraulic conductivity using the RETC computer program. Soil Sci. Soc. Am. J. 56:347–354.

Zanakis, S.H. et al. 1998. Multi-attribute decision making: a simulation comparison of select methods. European Journal of Operational Research 107.

List of Abbreviations

AHP	Analytical hierarchy process
AI	Artificial Intelligence
ANOVA	Analysis of Variance
ASCE	American Society of Civil Engineers
ASM	Antecedent Soil Moisture
ASTER	Advanced Spaceborne Thermal Emission and Reflection Radiometer
BAS	Basin Area Size
BD	Basin Depth
CA	Campbell PTF
DA	Decision analysts
DSC	Dead Water Storage Capacity
DSS	Decision Support System
EWRI	Environmental & Water Resources Institute
FAO	Food and Agriculture Organisation
FAS	Flooded Area Size
FCC	False Colour Composite
FH	Flooding Height
Ks	Saturated Hydraulic Conductivity
LMP	Linguistic Measures of Preference
MADM	Multi-Attribute Decision Making
MCDA	Multiple Criteria Decision Analysis
MCDM	Multiple Criteria Decision Method
MCEM	Multiple Criteria Evaluation Model
MG	Mualem-Van Genuchten PTF
MODM	Multi-Objective Decision Making
MPSIAC	Modified Pacific Southwest Interagency Committee
OR	Operation research
PC	Principle Component
PCA	Principle Component Analysis
PSIAC	Pacific Southwest Interagency Committee
PSS	Planning Support System
PTF	Pedo Transfer Function
Qin	Inflow discharge
Qremain	Dead Water Body
RECT	Retention Curve Computer Code
REo	Recharge Efficiency of Original Soil Coulmn
REs	Recharge Efficiency of Soil Coulmn with Sediment Layer
RI	Relative Importance
RR	Recharge Reduction
SCS	Soil Conservation Service
SCWMRI	Soil Conservation and Watershed Management Research Institute
SD	Sediment Depth
SI	Suitability Index
SMCE	Spatial Multi Criteria Evaluation
SWACROP	Soil Water and CROP production model

SWAP	Soil-Water-Atmosphere-Plant
SWATRE	Soil-Water-Crop-Atmosphere
T	Transmissivity
TDS	Total Dissolved Solids
TM	Thematic Mapper
TMU	Terrain Mapping Unit
TPPMO	Tehran Province Planning and Management Organization
UNDP	United Nation Development Program
USDA	U.S. Department of Agriculturer
USLE	Universal Soil Loss Equation
VAM2D	Variably-Saturated Analysis Model in Two (2) Dimensions

Appendices

Appendix 1

Main indicator "surface area feature": Classes, LMP values and relative importance of its sub-indicators.

Sub-indicator land use: classes and their relative importance

Classes	RBS	Af L	Ag L	FL	IL	SL	Geometric mean	Relative Importance
Rangeland & Bare soil	1	7	8	8	9	9	5.7539	0.6011
Afforested land	1/7	1	2	2	3	3	1.3138	0.1373
Agricultural land	1/8	1/2	1	1	2	2	0.7937	0.0829
Classification Forested land	1/8	1/2	1	1	2	2	0.7937	0.0829
Industrial land	1/9	1/3	1/2	1/2	1	1	0.4582	0.0479
Settlement land	1/9	1/3	1/2	1/2	1	1	0.4582	0.0479

Sub-indicator evenness of the surface area:
classes and their relative importance

Classes	Even and flat	Moderate flat	Uneven	Geometric mean	Relative Importance
Even and flat	1	5	9	3.5569	0.7352
Moderate flat	1/5	1	5	1	0.2067
Uneven	1/9	1/5	1	0.2811	0.05810

Sub-indicator presence of infrastructures in the area:
classes and their relative importance

Classes	Infrastructure	No Infrastructure	Geometric mean	Relative Importance
Infrastructure	1	9	3	0.9
No Infrastructure	1/9	1	0.3334	0.1

Sub-ndicator shortest distance to the main river:
classes and their relative importance

Classes	0-1000 m	1000-2000 m	>2000 m	Geometric mean	Relative Importance
0-1000 m	1	5	9	3.5569	0.7352
1000-2000 m	1/5	1	5	1	0.2067
>2000 m	1/9	1/5	1	0.2811	0.05810

Sub-indicator presence of access road in the area:
classes and their relative importance

Classes	Access road	No Access road	Geometric mean	Relative Importance
Access road	1	9	3	0.9
No Access road	1/9	1	0.3334	0.1

Appendix 2

Main indicator “unsaturated zone”: Classes, LMP values and relative importance of its sub-indicators.

Sub-indicator thickness: classes and their relative importance

Classes	Tick 80-120m	Moderate 40-80m	Very Tick >120m	Shallow <40m	Geometric mean	Relative Importance
Tick 80-120m	1	5	8	9	4.3559	0.6497
Moderate 40-80m	1/5	1	5	6	1.5651	0.2335
Very Tick >120m	1/8	1/5	1	2	0.4729	0.0705
Shallow <40m	1/9	1/6	1/2	1	0.3102	0.0463

Sub-indicator horizontal hydraulic conductivity: classes and their relative importance

Classes	Very High	High	Moderate	Low	Very Low	Geometric mean	Relative Importance
Very High	1	5	7	8	9	4.7894	0.5422
High	1/5	1	5	7	9	2.2902	0.2593
Moderate	1/7	1/5	1	7	9	1.1247	0.1273
Low	1/8	1/7	1/7	1	7	0.4471	0.0506
Very Low	1/9	1/9	1/9	1/7	1	0.1813	0.0205

Appendix 3

Main indicator "saturated zone": Classes, LMP values and relative importance of its sub-indicators.

Sub-indicator transmisivity: classes and their relative importance

Classes	Very High >5000	High 3000-5000	Moderate 1000-3000	Low 500-1000	Very Low 0-500	Geometric mean	Relative Importance
Very High >5000	1	5	7	8	9	4.7894	0.5422
High 3000-5000	1/5	1	5	7	9	2.2902	0.2593
Moderate 1000-3000	1/7	1/5	1	7	9	1.1247	0.1273
Low 500-1000	1/8	1/7	1/7	1	7	0.4471	0.0506
Very Low 0-500	1/9	1/9	1/9	1/7	1	0.1813	0.0205

Sub-indicator groundwater quality: classes and their relative importance

Classes	Very Good	Good	Moderate	Just acceptable	Geometric mean	Relative Importance
Very Good	1	3	5	9	3.4087	0.5651
Good	1/3	1	3	7	1.6266	0.2696
Moderate	1/5	1/3	1	5	0.7598	0.1260
Just acceptable	1/9	1/7	1/5	1	0.2374	0.0394

Sub-indicator hydraulic gradient: classes and their relative importance

Classes	4-5%	3-4%	2-3%	1-2%	0-1%	Geometric Mean	Relative Importance
4-5%	1	2	3	4	5	2.6052	0.4174
3-4%	1/2	1	2	3	4	1.6438	0.2634
2-3%	1/3	1/2	1	2	3	1	0.1602
1-2%	1/4	1/3	1/2	1	2	0.6084	0.0975
0-1%	1/5	1/4	1/3	1/2	1	0.3839	0.0615

ITC Dissertation List

1. **Akinyede** (1990), Highway cost modelling and route selection using a geotechnical information system
2. **Pan He Ping** (1990), 90-9003-757-8, Spatial structure theory in machine vision and applications to structural and textural analysis of remotely sensed images
3. **Bocco Verdinelli, G. (1990), Gully erosion analysis using remote sensing and** geographic information systems: a case study in Central Mexico
4. **Sharif, M**. (1991), Composite sampling optimization for DTM in the context of GIS
5. **Drummond, J.** (1991), Determining and processing quality parameters in geographic information systems
6. **Groten, S.** (1991), Satellite monitoring of agro-ecosystems in the Sahel
7. **Sharifi, A.** (1991), 90-6164-074-1, Development of an appropriate resource information system to support agricultural management at farm enterprise level
8. **Zee, D. van der** (1991), 90-6164-075-X, Recreation studied from above: Air photo interpretation as input into land evaluation for recreation
9. **Mannaerts, C.** (1991), 90-6164-085-7, Assessment of the transferability of laboratory rainfall-runoff and rainfall - soil loss relationships to field and catchment scales: a study in the Cape Verde Islands
10. **Ze Shen Wang** (1991), 90-393-0333-9, An expert system for cartographic symbol design
11. **Zhou Yunxian** (1991), 90-6164-081-4, Application of Radon transforms to the processing of airborne geophysical data
12. **Zuviria, M. de** (1992), 90-6164-077-6, Mapping agro-topoclimates by integrating topographic, meteorological and land ecological data in a geographic information system: a case study of the Lom Sak area, North Central Thailand
13. **Westen, C. van** (1993), 90-6164-078-4, Application of Geographic Information Systems to landslide hazard zonation
14. **Shi Wenzhong** (1994), 90-6164-099-7, Modelling positional and thematic uncertainties in integration of remote sensing and geographic information systems
15. **Javelosa, R.** (1994), 90-6164-086-5, Active Quaternary environments in the Philippine mobile belt
16. **Lo King-Chang** (1994), 90-9006526-1, High Quality Automatic DEM, Digital Elevation Model Generation from Multiple Imagery
17. **Wokabi, S.** (1994), 90-6164-102-0, Quantified land evaluation for maize yield gap analysis at three sites on the eastern slope of Mt. Kenya
18. **Rodriguez, O.** (1995), Land Use conflicts and planning strategies in urban fringes: a case study of Western Caracas, Venezuela
19. **Meer, F. van der** (1995), 90-5485-385-9, Imaging spectrometry & the Ronda peridotites

20. **Kufoniyi, O.** (1995), 90-6164-105-5, Spatial coincidence: automated database updating and data consistency in vector GIS
21. **Zambezi, P.** (1995), Geochemistry of the Nkombwa Hill carbonatite complex of Isoka District, north-east Zambia, with special emphasis on economic minerals
22. **Woldai, T.** (1995), The application of remote sensing to the study of the geology and structure of the Carboniferous in the Calañas area, pyrite belt, SW Spain
23. **Verweij, P.** (1995), 90-6164-109-8, Spatial and temporal modelling of vegetation patterns: burning and grazing in the Paramo of Los Nevados National Park, Colombia
24. **Pohl, C.** (1996), 90-6164-121-7, Geometric Aspects of Multisensor Image Fusion for Topographic Map Updating in the Humid Tropics
25. **Jiang Bin** (1996), 90-6266-128-9, Fuzzy overlay analysis and visualization in GIS
26. **Metternicht, G.** (1996), 90-6164-118-7, Detecting and monitoring land degradation features and processes in the Cochabamba Valleys, Bolivia. A synergistic approach
27. **Hoanh Chu Thai** (1996), 90-6164-120-9, Development of a Computerized Aid to Integrated Land Use Planning (CAILUP) at regional level in irrigated areas: a case study for the Quan Lo Phung Hiep region in the Mekong Delta, Vietnam
28. **Roshannejad, A.** (1996), 90-9009284-6, The management of spatio-temporal data in a national geographic information system
29. **Terlien, M.** (1996), 90-6164-115-2, Modelling Spatial and Temporal Variations in Rainfall-Triggered Landslides: the integration of hydrologic models, slope stability models and GIS for the hazard zonation of rainfall-triggered landslides with examples from Manizales, Colombia
30. **Mahavir, J.** (1996), 90-6164-117-9, Modelling settlement patterns for metropolitan regions: inputs from remote sensing
31. **Al-Amir, S.** (1996), 90-6164-116-0, Modern spatial planning practice as supported by the multi-applicable tools of remote sensing and GIS: the Syrian case
32. **Pilouk, M.** (1996), 90-6164-122-5, Integrated modelling for 3D GIS
33. **Duan Zengshan** (1996), 90-6164-123-3, Optimization modelling of a river-aquifer system with technical interventions: a case study for the Huangshui river and the coastal aquifer, Shandong, China
34. **Man, W.H. de** (1996), 90-9009-775-9, Surveys: informatie als norm: een verkenning van de institutionalisering van dorp - surveys in Thailand en op de Filippijnen
35. **Vekerdy, Z.** (1996), 90-6164-119-5, GIS-based hydrological modelling of alluvial regions: using the example of the Kisaföld, Hungary
36. **Pereira, Luisa** (1996), 90-407-1385-5, A Robust and Adaptive Matching Procedure for Automatic Modelling of Terrain Relief

37. **Fandino Lozano, M.**, 1996, 90-6164-129-2, A Framework of Ecological Evaluation oriented at the Establishment and Management of Protected Areas: a case study of the Santuario de Iguaque, Colombia
38. **Toxopeus, B.** (1996), 90-6164-126-8, ISM: an Interactive Spatial and temporal Modelling system as a tool in ecosystem management: with two case studies: Cibodas biosphere reserve, West Java Indonesia: Amboseli biosphere reserve, Kajiado district, Central Southern Kenya
39. **Wang Yiman** (1997), 90-6164-131-4, Satellite SAR imagery for topographic mapping of tidal flat areas in the Dutch Wadden Sea
40. **Saldana-Lopez, Asunción** (1997), 90-6164-133-0, Complexity of soils and Soilscape patterns on the southern slopes of the Ayllon Range, central Spain: a GIS assisted modelling approach
41. **Ceccarelli, T.** (1997), 90-6164-135-7, Towards a planning support system for communal areas in the Zambezi valley, Zimbabwe; a multi-criteria evaluation linking farm household analysis, land evaluation and geographic information systems
42. **Peng Wanning** (1997), 90-6164-134-9, Automated generalization in GIS
43. **Lawas, C.** (1997), 90-6164-137-3, The Resource Users' Knowledge, the neglected input in Land resource management: the case of the Kankanaey farmers in Benguet, Philippines
44. **Bijker, W.** (1997), 90-6164-139-X, Radar for rain forest: A monitoring system for land cover Change in the Colombian Amazon
45. **Farshad, A.** (1997), 90-6164-142-X, Analysis of integrated land and water management practices within different agricultural systems under semi-arid conditions of Iran and evaluation of their sustainability
46. **Orlic, B.** (1997), 90-6164-140-3, Predicting subsurface conditions for geotechnical modelling
47. **Bishr, Y.** (1997), 90-6164-141-1, Semantic Aspects of Interoperable GIS
48. **Zhang Xiangmin** (1998), 90-6164-144-6, Coal fires in Northwest China: detection, monitoring and prediction using remote sensing data
49. **Gens, R.** (1998), 90-6164-155-1, Quality assessment of SAR interferometric data
50. **Turkstra, J.** (1998), 90-6164-147-0, Urban development and geographical information: spatial and temporal patterns of urban development and land values using integrated geo-data, Villaviciencia, Colombia
51. **Cassells, C.** (1998), Thermal modelling of underground coal fires in northern China
52. **Naseri, M.** (1998), 90-6164-195-0, Characterization of Salt-affected Soils for Modelling Sustainable Land Management in Semi-arid Environment: a case study in the Gorgan Region, Northeast, Iran
53. **Gorte B.G.H.** (1998), 90-6164-157-8, Probabilistic Segmentation of Remotely Sensed Images
54. **Tegaye, Tenalem Ayenew** (1998), 90-6164-158-6, The hydrological system of the lake district basin, central main Ethiopian rift
55. **Wang Donggen** (1998), 90-6864-551-7, Conjoint approaches to developing activity-based models

56. **Bastidas de Calderon, M.** (1998), 90-6164-193-4, Environmental fragility and vulnerability of Amazonian landscapes and ecosystems in the middle Orinoco river basin, Venezuela
57. **Moameni, A.** (1999), Soil quality changes under long-term wheat cultivation in the Marvdasht plain, South-Central Iran
58. **Groenigen, J.W. van** (1999), 90-6164-156-X, Constrained optimisation of spatial sampling: a geostatistical approach
59. **Cheng Tao** (1999), 90-6164-164-0, A process-oriented data model for fuzzy spatial objects
60. **Wolski, Piotr** (1999), 90-6164-165-9, Application of reservoir modelling to hydrotopes identified by remote sensing
61. **Acharya, B.** (1999), 90-6164-168-3, Forest biodiversity assessment: A spatial analysis of tree species diversity in Nepal
62. **Akbar Abkar, Ali** (1999), 90-6164-169-1, Likelihood-based segmentation and classification of remotely sensed images
63. **Yanuariadi, T.** (1999), 90-5808-082-X, Sustainable Land Allocation: GIS-based decision support for industrial forest plantation development in Indonesia
64. **Abu Bakr**, **Mohamed** (1999), 90-6164-170-5, An Integrated Agro-Economic and Agro-Ecological Framework for Land Use Planning and Policy Analysis
65. **Eleveld, M.** (1999), 90-6461-166-7, Exploring coastal morphodynamics of Ameland (The Netherlands) with remote sensing monitoring techniques and dynamic modelling in GIS
66. **Yang Hong** (1999), 90-6164-172-1, Imaging Spectrometry for Hydrocarbon Microseepage
67. **Mainam, Félix** (1999), 90-6164-179-9, Modelling soil erodibility in the semiarid zone of Cameroon
68. **Bakr, Mahmoud** (2000), 90-6164-176-4, A Stochastic Inverse-Management Approach to Groundwater Quality
69. **Zlatanova, Z.** (2000), 90-6164-178-0, 3D GIS for Urban Development
70. **Ottichilo, Wilber K.** (2000), 90-5808-197-4, Wildlife Dynamics: An Analysis of Change in the Masai Mara Ecosystem
71. **Kaymakci, Nuri** (2000), 90-6164-181-0, Tectono-stratigraphical Evolution of the Cankori Basin (Central Anatolia, Turkey)
72. **Gonzalez, Rhodora** (2000), 90-5808-246-6, Platforms and Terraces: Bridging participation and GIS in joint-learning for watershed management with the Ifugaos of the Philippines
73. **Schetselaar, Ernst** (2000), 90-6164-180-2, Integrated analyses of granite-gneiss terrain from field and multisource remotely sensed data. A case study from the Canadian Shield
74. **Mesgari, Saadi** (2000), 90-3651-511-4, Topological Cell-Tuple Structure for Three-Dimensional Spatial Data
75. **Bie, Cees A.J.M. de** (2000), 90-5808-253-9, Comparative Performance Analysis of Agro-Ecosystems

76. **Khaemba, Wilson M**. (2000), 90-5808-280-6, Spatial Statistics for Natural Resource Management
77. **Shrestha, Dhruba** (2000), 90-6164-189-6, Aspects of erosion and sedimentation in the Nepalese Himalaya: highland-lowland relations
78. **Asadi Haroni, Hooshang** (2000), 90-6164-185-3, The Zarshuran Gold Deposit Model Applied in a Mineral Exploration GIS in Iran
79. **Raza, Ale** (2001), 90-3651-540-8, Object-oriented Temporal GIS for Urban Applications
80. **Farah, Hussein** (2001), 90-5808-331-4, Estimation of regional evaporation under different weather conditions from satellite and meteorological data. A case study in the Naivasha Basin, Kenya
81. **Zheng**, **Ding** (2001), 90-6164-190-X, A Neural - Fuzzy Approach to Linguistic Knowledge Acquisition and Assessment in Spatial Decision Making
82. **Sahu, B.K.** (2001), Aeromagnetics of continental areas flanking the Indian Ocean; with implications for geological correlation and reassembly of Central Gondwana
83. **Alfestawi, Y.** (2001), 90-6164-198-5, The structural, paleogeographical and hydrocarbon systems analysis of the Ghadamis and Murzuq Basins, West Libya, with emphasis on their relation to the intervening Al Qarqaf Arch
84. **Liu, Xuehua** (2001), 90-5808-496-5, Mapping and Modelling the Habitat of Giant Pandas in Foping Nature Reserve, China
85. **Oindo, Boniface Oluoch** (2001), 90-5808-495-7, Spatial Patterns of Species Diversity in Kenya
86. **Carranza, Emmanuel John** (2002), 90-6164-203-5, Geologically-constrained Mineral Potential Mapping
87. **Rugege, Denis** (2002), 90-5808-584-8, Regional Analysis of Maize-Based Land Use Systems for Early Warning Applications
88. **Liu, Yaolin** (2002), 90-5808-648-8, Categorical Database Generalization in GIS
89. **Ogao, Patrick** (2002), 90-6164-206-X, Exploratory Visualization of Temporal Geospatial Data using Animation
90. **Abadi, Abdulbaset M.** (2002), 90-6164-205-1, Tectonics of the Sirt Basin – Inferences from tectonic subsidence analysis, stress inversion and gravity modelling
91. **Geneletti, Davide** (2002), 90-5383-831-7, Ecological Evaluation for Environmental Impact Assessment
92. **Sedogo, Laurent G.** (2002), 90-5808-751-4, Integration of Participatory Local and Regional Planning for Resources Management using Remote Sensing and GIS
93. **Montoya, Lorena** (2002), 90-6164-208-6, Urban Disaster Management: a case study of earthquake risk assessment in Carthago, Costa Rica
94. **Ahmad, Mobin-ud-Din** (2002), 90-5808-761-1, Estimation of Net Groundwater Use in Irrigated River Basins using Geo-information Techniques: A case study in Rechna Doab, Pakistan

95. **Said, Mohammed Yahya** (2003), 90-5808-794-8, Multiscale perspectives of species richness in East Africa
96. **Schmidt, Karin** (2003), 90-5808-830-8, Hyperspectral Remote Sensing of Vegetation Species Distribution in a Saltmarsh
97. **Lopez Binnquist, Citlalli** (2003), 90-3651-900-4, The Endurance of Mexican Amate Paper: Exploring Additional Dimensions to the Sustainable Development Concept
98. **Huang, Zhengdong** (2003), 90-6164-211-6, Data Integration for Urban Transport Planning
99. **Cheng, Jianquan** (2003), 90-6164-212-4, Modelling Spatial and Temporal Urban Growth
100. **Campos dos Santos, Jose Laurindo** (2003), 90-6164-214-0, A Biodiversity Information System in an Open Data/Metadatabase Architecture
101. **Hengl, Tomislav** (2003), 90-5808-896-0, PEDOMETRIC MAPPING, Bridging the gaps between conventional and pedometric approaches
102. **Barrera Bassols, Narciso (**2003), 90-6164-217-5, Symbolism, Knowledge and management of Soil and Land Resources in Indigenous Communities: Ethnopedology at Global, Regional and Local Scales
103. **Zhan, Qingming** (2003), 90-5808-917-7, A Hierarchical Object-Based Approach for Urban Land-Use Classification from Remote Sensing Data
104. **Daag, Arturo S.** (2003), 90-6164-218-3, Modelling the Erosion of Pyroclastic Flow Deposits and the Occurrences of Lahars at Mt. Pinatubo, Philippines
105. **Bacic, Ivan** (2003), 90-5808-902-9, Demand-driven Land Evaluation with case studies in Santa Catarina, Brazil
106. **Murwira, Amon** (2003), 90-5808-951-7, Scale matters! A new approach to quantify spatial heterogeneity for predicting the distribution of wildlife
107. **Mazvimavi, Dominic** (2003), 90-5808-950-9, Estimation of Flow Characteristics of Ungauged Catchments. A case study in Zimbabwe
108. **Tang, Xinming** (2004), 90-6164-220-5, Spatial Object Modelling in Fuzzy Topological Spaces with Applications to Land Cover Change
109. **Kariuki, Patrick** (2004), 90-6164-221-3, Spectroscopy and Swelling Soils; an integrated approach
110. **Morales, Javier** (2004), 90-6164-222-1, Model Driven Methodology for the Design of Geo-information Services
111. **Mutanga, Onisimo** (2004), 90-5808-981-9, Hyperspectral Remote Sensing of Tropical Grass Quality and Quantity
112. **Šliužas, Ričardas V.** (2004), 90-6164-223-X, Managing Informal Settlements: a study using geo-information in Dar es Salaam, Tanzania
113. **Lucieer, Arko** (2004), 90-6164-225-6, Uncertainties in Segmentation and their Visualisation
114. **Corsi, Fabio** (2004), 90-8504-090-6, Applications of existing biodiversity information: Capacity to support decision-making
115. **Tuladhar, Arbind** (2004), 90-6164-224-8, Parcel-based Geo-information System: Concepts and Guidelines

116. **Elzakker, Corné van** (2004), 90-6809-365-7, The use of maps in the exploration of geographic data
117. **Nidumolu, Uday Bhaskar** (2004), 90-8504-138-4, Integrating Geo-information models with participatory approaches: applications in land use analysis
118. **Koua, Etien L.** (2005), 90-6164-229-9, Computational and Visual Support for Exploratory Geovisualization and Knowledge Construction
119. **Blok, Connie A.** (2005), Dynamic visualization variables in animation to support monitoring of spatial phenomena
120. **Meratnia, Nirvana** (2005), 90-365-2152-1, Towards Database Support for Moving Object Data
121. **Yemefack, Martin** (2005),), 90-6164-233-7, Modelling and monitoring Soil and Land Use Dynamics within Shifting Agricultural Landscape Mosaic Systems